Electrospinning of Polyesters

S.Schweizer¹, A. Taubert²

¹Departement of Chemistry, University of Basel, Klingelbergstrasse 80, 4056 Basel, Switzerlan.
²Institute of Chemistry, University of Potsdam, Karl-Liebknecht-Str. 24-25, Building 26, Room 2.64, 14476 Golm. Germany.

INTRODUCTION: Electrospinning is a unique procedure using electrostatic forces to make fine fibers with diameters in the range of nanometers to a few microns from solutions or melts. These fibers may act as highly porous scaffolds for tissue engineering, among others. So far, we have spun some poly(ε-caprolactone) (PCL)- fibers by variation of several parameters using a self constructed apparatus. Subsequently we want to spin PCL and other polyesters as scaffolds for Calcium Phosphate mineralization.

METHODS: The apparatus used for electrospinning consists of a high voltage electric source with positive or negative polarity, a syringe pump with capillaries or tubes to carry the solution from the syringe to the capillary, and a conducting collector like aluminium (Figure 1). The final fibrous structure can be tailored by altering the concentration of the polymer solution, the weight and molecular-weight distribution, the applied voltage, the solution flow rate and the distance between the capillary and collector. The effects of the preparation conditions on the fiber diameter were observed by optical microscopy and scanning electron microscopy (SEM).



Fig. 1: Configuration of our Electrospinning apparatus.

RESULTS: Most effective parameter variations are polymer concentration and flow rates of the polymer solutions. If the flow rate is low, the capillary may plug. On the other hand, no continuous jet will form when the flow rate is too

high. Spinning with different polymer concentrations leads to different fiber diameters, nonfibrous structure, and bead-rich scaffolds. Another very important parameter is the distance between needle and collector plate. For fine and uniform fibers, the interspace has to be as wide as possible. But for a constant flow and formation of fibers, one needs a minimal distance.

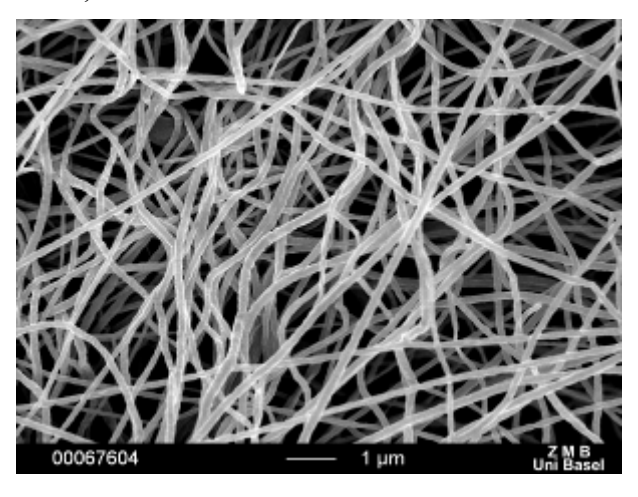


Fig. 2: Scanning Electron Microscope Image from 7 % wt PCL (80kDa) in Dichloromethane at 20 kV with 0.7 ml/h solution flow and a needle to collector distance of 9 cm.

IGF-I time-concentration profiles can modulate the early stage differentiation of human mesenchymal stem cells: application to ligament or cartilage engineering

Marcos Garcia-Fuentes, Lorenz Meinel, Hans P. Merkle

Drug formulation and delivery group, Department of Chemistry and Applied Biosciences, ETH Zurich, CH-8093 Zurich, Switzerland

INTRODUCTION: Traumatic injuries of musculoskeletal tissues pose a significant problem to current medicinal practise. Mesenchymal stem cells (MSCs) are self-replicating multipotent cells with the capacity to regenerate structural and connective tissues of the body when in the presence of suitable environmental cues [1]. Nevertheless, the biochemical pathways that regulate MSC differentiation are mostly unknown, and, therefore, engineered grafts cannot yet match the properties of native tissues. In this work we hypothesized that insulin-like growth factor-I (IGF-I) is an important signal in MSC differentiation, and that commitment of MSCs to specific cell lineages can depend on the concentration of this cytokine present at different stages of cell differentiation.

METHODS: Silk fibroin was purified and porous scaffolds from this biomaterial were prepared as previously described [2]. MSCs were seeded onto the scaffolds and cultured in DMEM supplemented with fetal bovine serum, ascorbic acid, nonessential amino acids, dexamethasone (10 nM) and TGF-\(\beta\)1 (1 ng/ml) (control medium). Total culture time was 3 weeks and medium was changed every other day. IGF-I was added to the control medium in three regimens: 0 ng/ml for the whole experiment (regimen 0, control), 50 ng/ml for the whole experiment (regimen 1), and 100 ng/ml for first week and 25 ng/ml for the two further ones (regimen 2); thus regimens 1 and 2 had the same total amount of IGF-I supplemented during the whole culture time. Cell medium for the test samples was also changed every other day during the experiment, but IGF-I was supplemented every day. Tissues were analyzed for differences in cell proliferation (DNA measurement), glycoaminoglycan content, gene expression (Real Time RT-PCR) histology (hematoxylin-eosin and staining).

RESULTS: All engineered tissues displayed an structured fibrous structure typical for ligament-like grafts. Histological analysis confirmed that culture of MSCs resulted in fibroblastic morphology. IGF-I treated constructs showed

enhanced proliferation and enhanced extracellular matrix formation.

Gene expression analysis of the samples showed that the main structural protein of ligaments (collagen type-I) was up-regulated for all of the experimental groups and controls. We also found that MSCs cultured in the presence of IGF-I can overexpress typical makers of cartilage such as collagen type-II and SOX9, but this occurred for an intermediate stage in cell development only. Intriguingly, by changing the IGF-I dosing regimen, we could also shut down collagen type-II and SOX9 expression. Under the test II dosing regimen (i.e. the one that concentrates most of the IGF-I dose at the initial culture time points). collagen type-II expression remained at levels similar to those of reached by samples without IGF-I.

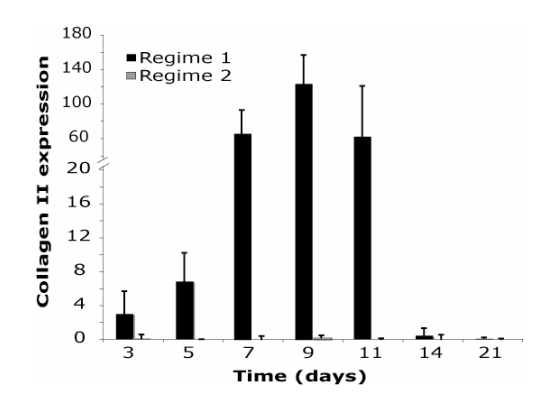


Fig. 2: Gene expression levels of collagen type-II in MSCs cultured over a 21 period (mean \pm SD, n=6). Expression levels were normalized to the housekeeping gene GAPDH and are relative to those of non-cultured MSCs (day 0).

DISCUSSION & CONCLUSIONS: IGF-I appears to be deeply involved in both cartilage and ligament development. Particularly, IGF-I concentration in the first stages of MSC differentiation might be an important regulator in lineage commitment.

REFERENCES: ¹S Hofmann et al., Tissue Eng 2006; ²S Sofia et al., J Biomed Mater Res 2001.

ACKNOWLEDGEMENTS: MGF thanks the European Commission for a Marie-Curie fellowship (MEIF-CT-2005-023633).

ELECTRONICALLY ADDRESSABLE POLYELECTROLYTE COATINGS AND THEIR POTENTIAL FOR CELL SHEET ENGINEERING

O. Guillaume-Gentil¹, Y. Akiyama³, CS. Tang^{1,2}, M. Textor², M. Yamato³, T. Okano³, J. Vörös¹

¹ Laboratory of Biosensors and Bioelectronics. ² Laboratory for Surface Science and Technology, ETH Zurich. ³ Institute of Advanced Biomedical Engineering and Science, TWMU, Japan.

INTRODUCTION: In the field of regenerative medicine, cell sheet based tissue engineering holds great promises for the construction of three dimensional functional tissues. In contrast to the conventional tissue engineering approaches, this technique allows for the fabrication of cell-dense structures with preservation of critical cell surface proteins. The technique has been initially developed using thermo-responsive polymergrafted dishes that enable cell detachment upon temperature reduction. As an alternative, we developed a novel method for cell sheet recovery based on highly tunable, electrochemically addressable surfaces.

METHODS: Biodegradable mono- or multilayer films based on poly(L-lysine), poly(L-glutamic acid) and hyaluronic acid were built on an indium tin oxide semi-conductor substrate by a simple dip and rinse coating process. The layer-by-layer buildup [1] and the dissolution of the polyelectrolyte films upon electrochemical polarization of the substrate [2] were followed by electrochemical optical waveguide light mode spectroscopy [3]. For cell sheet detachment by electrochemical polarization, the electronically surfaces with addressable confluent monolayers were subjected to an external potential. using the indium tin oxide substrate as a working electrode in a three-electrode configuration system.

RESULTS: Various biocompatible polyelectrolyte mono- and multilayers were built up, and optionally bio-functionalized by deposition of fibronectin onto films ending with a positively charged polymer layer or by the adsorption of RGD-modified poly(L-lysine)-graft-(polyethylene glycol) onto films ending with a negatively charged polymer layer. When seeded at high densities onto coatings consisting in 1 to 6 layers of poly(L-lysine) and poly(L-glutamic acid) or hyaluronic acid, confluent osteoblasts fibroblasts detached as cell sheets without the need for any external stimulus. In contrast, the cells grown onto PLL-g-PEG/PEG-RGD monolayers under similar conditions as well as the cells seeded at lower densities did not spontaneously detach. In those cases, the cell sheets could be recovered by

subjecting the substrate to electrochemical polarization (Fig.1).

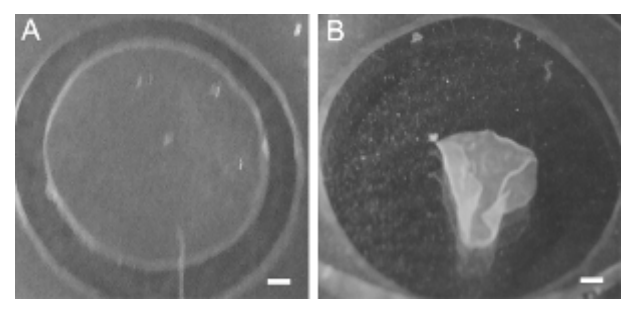


Fig. 1: Cell sheet recovery by electrochemical polarization: monolayer of confluent fibroblasts grown onto ITO-PLL-PGA-PLL-g-PEG/PEG-RGD before (A) and after (B) the application of an external potential. Bars are 1mm.

DISCUSSION & CONCLUSIONS: These biocompatible polyelectrolyte coatings allowed for non-invasive cell sheet harvesting by fine-tuning of the bio-interface or by their use as electronically addressable sacrificial layer. Both strong cell-cell cohesion and weak cell-substrate interactions are probably required for the spontaneous cell sheet detachment. While the cell type and the cell density influence the cell-cell cohesion, the highly tunable properties of polyelectrolyte multilayers allow for a fine control of the cell-substrate interactions. cell sheet recovery In electrochemical polarization, a local pH change leads to the dissolution of the polyelectrolyte coating, and the applied current and the buffer capacity determine the confinement of this pH change. These easy-to-build substrates are applicable to any surface geometry and offer a promising new tool for cell sheet-based tissue engineering.

REFERENCES: ¹ G. Decher, J.D. Hong, et al (1992) *Thin Solid Films* **210/211**:831-835. ² F. Boulmedais et al (2006) *Advanced Functional Materials* **16**: 63-70. ³ J.P. Bearinger et al (2003) *Biotechnology and Bioengineering* **82**:465-473.

ACKNOWLEDGEMENTS: This work was supported by the Roche Research Foundation (Mkl/stm 39-2005) and the Competence Centre for Materials Science and Technology.

Corrosion behavior of Magnesium alloy WE 43 used in Biomedical Applications

studied by electrochemical techniques

N.C. Quach, P. Schmutz

EMPA, Materials Science and Technology, Laboratory for Corrosion and Materials Integrity, 8600 Dübendorf, Switzerland

Metallic materials including stainless steel, titanium alloys, and cobalt-based alloys constitute, due to their high strength, ductibility, and good corrosion resistance, an important class of materials in hard tissue replacement, especially load-bearing implants for the repair or replacement of diseased or damaged bones tissues. But, these metallic materials are not biodegradable in the human body, so a second surgical intervention may be necessary after the tissues have healed. Thus a strong body of research focuses on new biodegradable implants, which dissolves in biological environment after a certain time of functional use. Biodegradable implants constitute an appropriate solution because of cost, convenience and aesthetic reasons favorable to patients. Magnesium is one of the essential elements in the human body and has the advantage to be biodegradable [1]. So its corrosion performance can also be envisaged as potential applications for bioabsorbable stent implant logy for cardiovascular diseases. Although excellent preliminary results have been achieved, absorbable metal stents (AMS) currently under clinical investigation [2] possess degradation kinetics and mechanical characteristics which are far from being completely optimized for all uses and applications.

The purpose of this study is to investigate the corrosion behaviors of pure magnesium and of a standard Mg-Y-RE WE43 alloys (untreated and anodized) in artificial body fluids. Because of potential use of Magnesium alloys and especially the WE43 for different types of implants, two types of physiology solutions were used, Artificial Plasma (AP) with high carbonate content and a buffered Simulated Blood Fluid (SBF). Due to solid-solution strengthening, the presence of yttrium in the WE43 should not only increase the creep resistance properties [3-5] but also the corrosion resistance, in addition to favourable high temperature properties. Then, the influence of the galvanostatic anodization treatment on the surface on the corrosion behavior was documented. Characterization of the oxide film structure and composition for optimized conditions

performed by different electrochemical (EIS), optical, SEM, and Auger Electron Spectroscopy (AES) measurements. The investigations showed that SBF is significantly more aggressive than AP with regard to the untreated WE43 surface. The anodization process led to a formation of a thin hydroxide layer (few hundred nm) which increases the corrosion resistance of the alloy in both physiological solutions, especially in AP.

The final objective is to modify the composition and / or the surface of the alloy with an anodic layer to obtain a suitable material with initial stability for an absorbable implant, followed after a couple of weeks by a full degradation of the implant.

REFERENCES:

- [1]. G. Song, K. Videm, Control of biodegradable Magnesium alloys, Corrosion Science, Vol. 49, Issue4, 1696-1702 (2007).
- [2]. Peters & al., Preliminary results after application of absorbable metals stents in patients with critical limb ischemia. J. of Endovascular Therapy, 2005. 12(1), p1-5
- [3]. Polmear IJ. Magnesium Alloys, in Light Alloys Metallurgy of the Light Metals. London: Edward Arnold; 169-210, 1989.
- [4]. I. Nakatsugawa, S. Kamado, Y. Kojima, R. Ninomiya, K. Kubota. Corrosion reviews, vol.16, N°1-2, 1998.
- [5]. W. Unsworth. Int. J. of Materials and products Technology, 4 (4), 359-378, 1989.

ACKNOWLEDGEMENTS: The authors would like to thank the Competence Centre for Materials Science and Technology for the financial support

Intraoral welding of implants abutments with a prefabricated titanium bar

Marius Leretter¹, Cosmin Sinescu¹, Meda Negrutiu¹, Radu Negru², Nicolae Faur², Mihai Hluscu², Mihai Rominu¹, Mihali Sorin¹

¹"VictorBabes" University of Medicine and Pharmacy, School of Dentistry, Timisoara, Romania.

² University of Politechnica, Timisoara, Romania.

INTRODUCTION: The burden of being edentulous and the functional limitation caused by this phenomenon have been committed to paper since ancient times. The lack of stability and retention especially of the lower denture are responsible for the majority of functional problems complaints. **Problems** associated athrophied mandible have been a challenge for oral and maxillofacial surgeons and prosthodontists for a long time. It is not always possible or advisable to install five to six endosseous implants in the edentulous mandible. Therefore the treatment concept of a removable overdenture anchored to two to four endosseous implants was introduced. The superstructure connecting the implants with the overdenture has been evaluated in several studies.

METHODS: Another technology related to implant-supported prosthodontics is welding mesostructures directly in the oral cavity or on the working cast. Mesostructures obtained by welding efficiently meet the requirements of passivity for supporting implants. It is a fact that mesostructures casting technology obtained by imperfections due to cumulative errors along the technological process. This, many times cast mesostructures are torn apart and the pieces are connected together again on the working cast using laser welding. Nowadays laser welding of mesostructures is a must for obtaining the passivity for a better prognosis. For even a greater precision a new concept was developed, which is the welding of the mesostructure directly in the oral cavity so that errors due to modification of the abutments positions during transportation are avoided. The objective of this article was to introduce a prosthetic concept for an accelerated rigid splinting of multiple implants for same-day immediate loading by utilizing Syncrystallization technique. Titanium implant abutments are welded with the titanium bar in the oral cavity using the Syncrystallization Unit. The welding process is electrical and protected by an argon gas supply (Syncrystallization). equipment allows the welding of metallic elements directly in the mouth. The two elements to be welded are placed between the two electrodes of a

welding clamp. The energy contained in a previously unloaded battery of capacitors is transferred to the electrodes of the welding clamp. Current flowing through the contact points, being in contact with the parts to weld, warms up to the point of fusion, achieving a solid, welded junction.

RESULTS: The advantages of the new technique are: (1) reduction of treatment time for immediate temporization at stage one surgery; (2) predictable fixation and immobility of implants in the early stages of bone healing; and (3) less time spent for repairing provisional restorations as a result of no or less frequent fracture.

DISCUSSION & CONCLUSIONS: In case of immediate loading of implants, adequate stability and immobility of the implants are very important for bone formation at the implant-bone interface. The problems are related to the mesostructure and/or suprastructure design so that surgical stage is not affected. This method can optimize the dental treatment in the considered cases.

REFERENCES: 1. Brånemark PI, Breine U, Adell R, Hanson BO, Linström J, Ohlsson A.(1969) Intraosseous anchorage of dental prosthesis. I. Experimental studies. Scandinavian Journal of Plastic Reconstructive Surgery ;3:81-100. 2. Albrektsson T, Brånemark PI, Hansson HA, Lindstrom J.(1981) Osseointegrated titanium implants. Requirements for ensuring a longlasting, direct bone-to-implant anchorage in man. Acta Orthopaedica Scandinavica;52:155-170. 3. Brånemark PI. (1983) Osseointegration and its theoretical background. Journal of Prosthetic Dentistry;50: 399-410. 4. Donath K, Laass M, Gunzl HJ. (1992) The histopathology of different foreign-body reactions to oral soft tissue and bone tissue. Virchows Archiv A Pathol Anat;420:131-137. 5. Ledermann PD(1988). The New Ledermann Screw (Article in German). Die Quintessenz;5:1-17. 6. Schnitman PA, Wöhrle PS, Rubenstein JE. (1990) Immediate fixed interim prostheses supported by twostage threaded implants: Methodology and results. J Oral Implantol;16:96-105.

CONFORMATION DEPENDENT INTERACTION BETWEEN FIBRONECTIN AND COLLAGEN I IN CELL MEDIATED REMODELING OF ECM

Rada Vukmirovic, Michael L. Smith, Krisopher E. Kubow, Delphine Gourdon, and Viola Vogel Laboratory for Biologically Materials, Materials Department ETH Zurich, Switzerland.

INTRODUCTION: In order to design engineered scaffolds which mimic the structure and function of host tissues, it is necessary to characterize whether molecular conformation of inherent matrix components regulate design criteria necessary for promotion of tissue reconstruction. We investigate ECM protein conformation changes during cell mediated remodelling of ECM. The conformation of fibronectin (Fn), a prevalent component of the ECM of developing or healing tissues, is known to be highly variable. Although Fn binds and crosslinks numerous ECM components, the impact of its molecular conformation on association with other ECM components in native matrix is unknown.

METHODS: Confocal microscopy and intramolecular fluorescence resonance energy transfer (FRET) are used to study if Fn and collagen fibrils interact in a Fn conformation dependent manner and if Fn fibrillar matrix conformation is affected by presence of collagen. Collagen was imaged using immunohistochemistry with a 3rd color which did not affect FRET. The confocal images were then analyzed to determine whether collagen tended to colocalize with Fn fibrils.

RESULTS: The results showed that collagen I production and Fn-collagen co-localization in 3D matrices begins within one day in culture using fibroblasts. Co-localization was dependent on Fn conformation.

DISCUSSION & CONCLUSIONS: These results suggest that Fn conformation either regulates its association with collagen or is stabilized into a specific conformation thought association with collagen. This investigation is a first step towards understanding how cell force dependent conformation changes of Fn may regulate its integration and assembly into multicomponent ECM.

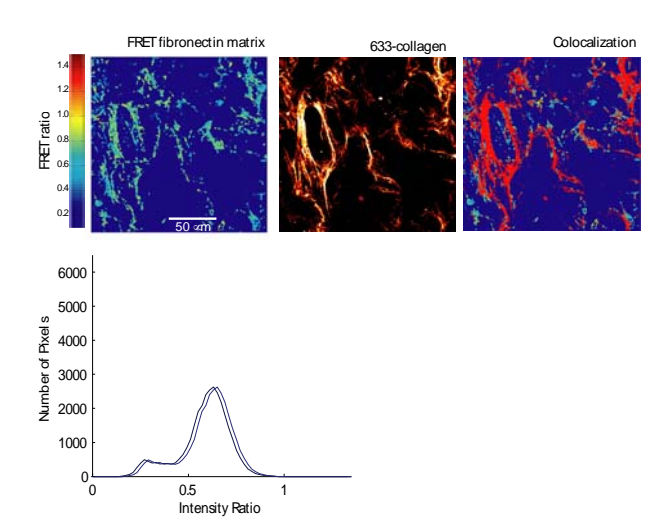


Fig. 1: Collagen I co-localization with Fn is dependent on Fn conformation.

REFERENCES: ¹M.L. Smith, D. Gourdon, W.C. Little, K.E. Kubow, R. A. Eguiluz, S. L. Morris, V. Vogel (2007) *PLoS Biology*, in revision. ² V. Vogel and M. Sheetz (2006) *Nat Rev Mol Cell Biol*. 7(4):265-75. ³ Vogel V. (2006). *Annu Rev Biophys Biomol Struct*.35:459-88. ⁴ G. Baneyx and V. Vogel (1999) *Proc Natl Acad Sci USA*. 96(22):12518-23.

Characterization of a novel biodegradable 3D-scaffold designed for medical applications

V. Milleret, P. Neuenschwander*, A. G. Bittermann[§] and H. Hall

Cells and BioMaterials, Department of Materials, ETH Zurich, Switzerland; * ab medica, Italy; \$ ZMB, Center for Microscopy and Imaging Analysis, University of Zurich, Switzerland

INTRODUCTION: An increasing need for biodegradable 3D-scaffold materials usable as interactive wound dressings or scaffolds in tissue engineering requires characterization of novel materials with respect to their mechanical and chemical properties, their ways of processing to form the requested shape and to adjust their degradation kinetics to the requirements of specific applications. However, prior to any envisioned medical application biocompatibility of implanted material needs to be analyzed. A new family of Degrapol® polymers is aimed to be explored for medical applications. These polymers show essential requirements for materials used for medical applications; namely mechanical properties and degradation rates can independently controlled. The aim of this work was to determine endothelial cell survival and proliferation on Degrapol® polymers.

METHODS: Polylactic acid (PLA) and Degrapol[®] polymer scaffolds were supplied by ab medica, Italy. NIH-3T3 fibroblasts were cultured in DMEM supplemented with 10% NCF. Human Umbilical Vein Endothelial Cells (HUVECs) were cultured in Endothelial Cell Medium (Promocell) supplemented with 2% FCS, 2 mL ECGS/H, 0.1 ng/mL EGF, 1.0 ng/mL bFGF and 1.0 µg/mL hydrocortisone at 37°C at 5% CO₂. Prior to cell seeding, Degrapol® or PLA have been treated in several ways in order to improve cell survival and proliferation. Scaffolds have been: rinsed in water (1, 3 d or more than 7 d), O2-plasma cleaned or decorated with cell adhesive proteins: fibronectin or collagen I. Cellular mitochondrial activity was assessed with Alamar Blue proliferation assay after 0, 4 and 8 d. Cell adhesion on the scaffolds of chemically fixed, dehydrated and critically pointdried samples was observed by SEM.

RESULTS: For both HUVECs and NIH-3T3 fibroblasts, scaffolds treatment affected cell adhesion and cell survival. As shown in Figure 1, pre-treatment of Degrapol® polymers was essential for cell adhesion and proliferation. In the presence of cell adhesive proteins collagen I or fibronectin, cell activity was strongly increased with time on Degrapol® and PLA surfaces as compared to the native polymers.

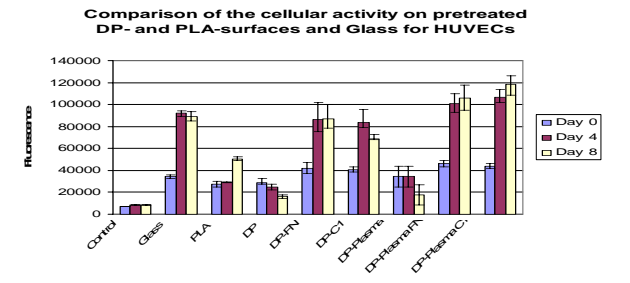


Figure 1: Cell proliferation on Degrapol® and PLA surfaces. 20'000 HUVECs were seeded on 1% PLA or 1% Degrapol®-coated glass surfaces. The surfaces were further treated with O2-plasma and adsorbed with 2 μg/ml collagen I or fibronectin. Cellular activity was measured four hours after seeding (day 0) and at day 4 and 8 by Alamar Blue proliferation assay.

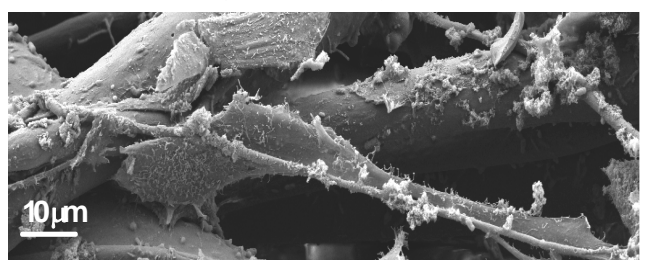


Figure 2: SEM image of NIH-3T3 fibroblasts cultured for 14 days on Degrapol® fibers.

polymers provided biocompatible surfaces that allowed HUVECs and NIH-3T3 fibroblasts to proliferate with time. Pre-treatment with O2-plasma and adsorption of cell adhesive proteins enhanced cell adhesion and proliferation. HUVECs and NIH-3T3 fibroblasts adhered on Degrapol® fibers (Figure 2) and spanned within them. Overall, Degrapol® showed comparable results to PLA, a polymer already used for medical applications and therefore, Degrapol® might be a valuable alternative for the production of medical scaffolds.

REFERENCES: ¹Das S, Hollister S. *Tissue Engineering scaffolds*. Elsevier Ltd. 2003 ²Sperling.C *Design and evaluation of novel blood incubation systems for in vitro hemocompatibility of planar solid surfaces*. Wiley Interscience 2002.

ACKNOWLEDGEMENTS: Viola Vogel's lab is acknowledged for many valuable discussions.

CHARACTERIZATION OF NOVEL PLL-g-PEG-DNA NANOPARTICLES FOR LOCAL AND CONTROLLED DNA RELEASE

M. Rimann, T. Lühmann, M. Textor* and H. Hall

Cells and BioMaterials, Department of Materials, ETH Zurich, Switzerland; *BioInterfaceGroup, Oberflächentechnik / Laboratory for Surface Science and Technology, Department of Materials, ETH Zurich, Switzerland

INTRODUCTION: Deficient angiogenesis is a major clinical incidence and affects wound healing especially in elderly persons and diabetes patients. Many studies and different technologies aim to locally increase blood perfusion and improve the endogenous wound healing capacity and thereby ameliorate the patient's life quality. Since viralbased gene delivery systems are still associated with severe security problems many non-viral gene delivery vehicles were developed Unfortunately, non-viral DNA delivery vehicles often affect cell viability; therefore our project design novel DNA-containingnanoparticles using grafted copolymers of PLL and PEG to increase their biocompatibility and stealth properties.

METHODS: The PLL-g-PEG polymer used in this study was synthesized as described previously [2] and for all experiments a pEGFP-N1-plasmid encoding for green fluorescence protein was used. The DNA-PLL-g-PEG condensates were formed at different P: N ratios and characterized as follows: a) particle size using dynamic light scattering, b) shape and homogeneity using negative staining transmission electron microscopy (TEM), c) *in vitro* transfection efficiency. The PLL-g-PEG-DNA nanoparticles were tested for their *in vitro* gene expression capabilities and cytotoxicity using WST-1 proliferation assay in COS-7 cells.

RESULTS: The PLL-g-PEG-DNA condensates formed particles with a wide range of polymer concentrations (P:N ratios = 1:1 to 1:25), indicating stable particle formation at room temperature. Dynamic light scattering revealed an average hydrodynamic diameter of about 100 nm (Fig. 1) of the PLL-g-PEG-DNA condensates.

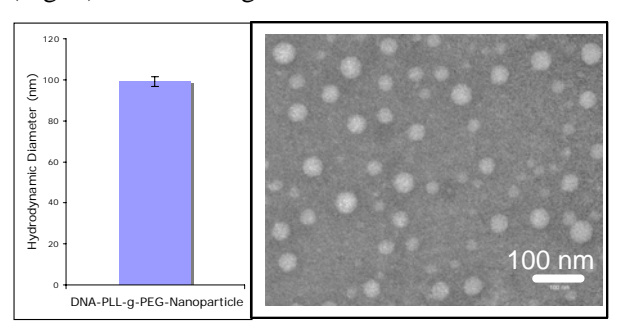


Fig.1: Hydrodynamic diameter of DNA-PLL-g-PEG-nanoparticles obtained by DLS measurement

(left). Negative staining TEM micrograph of the DNA-PLL-g-PEG-nanoparticles (right).

Negative stained TEM micrographs demonstrated that the DNA-PLL-g-PEG nanoparticles have a narrow size distribution and a spherical shape (Fig. 1). Moreover, the DNA-PLL-g-PEG nanoparticles do not aggregate in solution.

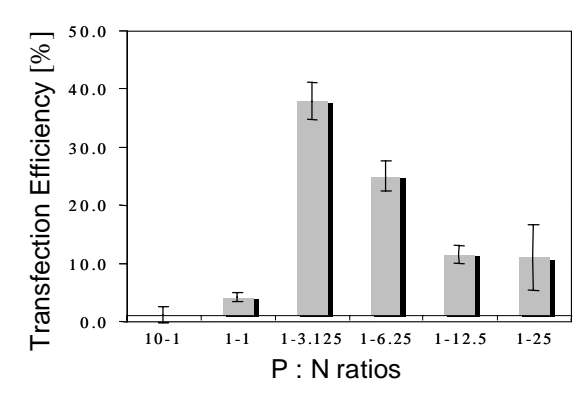


Fig.2: DNA-PLL-g-PEG nanoparticles were formed with different P:N ratios and in vitro transfection efficiency was determined on COS-7 cells after 2 days.

The here used DNA-PLL-g-PEG condensates displayed transfection efficiencies comparable with standard transfection agents (DEAE transfection efficiency is about 50 %, not shown). Cytotoxicity was found to be less than 5 % for DNA-PLL-g-PEG nanoparticles formed with P: N ratios between 10:1 and 1:6.25 (not shown).

DISCUSSION & CONCLUSIONS: These novel DNA-PLL-g-PEG condensates are promising candidates for future local and controlled release studies in the treatment of impaired wound healing. As PLL-g-PEG successfully condensated the plasmid DNA into non-aggregated, nano-sized particles that is suitable for cellular uptake [3]. Additionally, PLL-g-PEG-DNA nanoparticles seem to be biocompatible and stealth. All these features are a prerequisite for future somatic gene therapy.

REFERENCES: ¹ Itaka, et al., (2007) Mol. Ther., June 5 (Epub ahead of print). ² VandeVondele, et al., (2003) Biotechnol. Bioeng. Jun 30; 82(7): 784-90. ³ Tiera, et al., (2006) Curr. Gene Ther. Feb; 6(1):59-71.

ACKNOWLEDGEMENTS: This work was supported by Gebert Rüf Foundation, Switzerland

Engineering and Differentiation of Stem Cell Sheets

OV.Semenov^{1,2}, J.Voeroes², AH.Zisch¹

¹ Department of Obstetrics, University Hospital Zurich, Zurich, Switzerland. ² ETH-Zurich, Institute for Biomedical Engineering, Laboratory of Biosensors and Bioelectronics, Zurich, Switzerland

INTRODUCTION: Cell sheet engineering has emerged as a novel technique for creation of artificial, three-dimensional model tissues without the need for biodegradable scaffolds. Others could show that cell culture on temperature-responsive polymer films allows non-enzymatic harvesting of intact cell sheets, which can be further surgically transplanted for tissue reconstruction [1,2]. We have begun to explore new methodology that builds on the use of electric charge to accomplish non-enzymatic harvest of cell sheets. For this purpose, we developed polymer electrolyte films, and tested whether they would perform as substrates for growth of human stem cells effectively.

METHODS: We explored charge-sensitive arrangements of polyelectrolyte multilayer films (PEMs) that were coated on the conductive surface Indium Tin Oxide (ITO). The PEM layers were obtained by piling up to 8 alternating layers of poly-L-lysine (PLL) and hyaluronic acid (HA). The top layers, either PLL or HA, were coated with fibronectin, or alternatively we used of PLL-PEG-RGD as cell-adhesive surface. The studies were performed with human placenta-derived mesenchymal stem cells (HPMSC) that we isolated from chorionic villi. The cells were seeded at 15000 cells /cm².

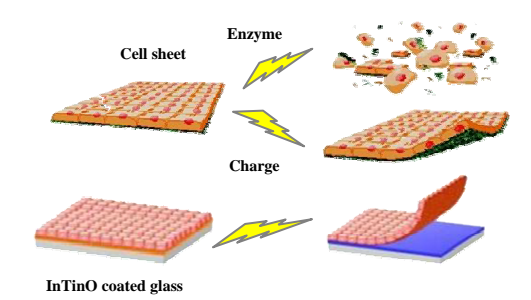


Fig. 1. Working hypothesis

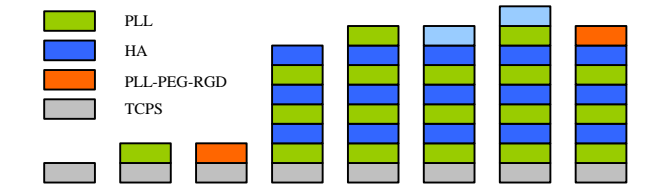
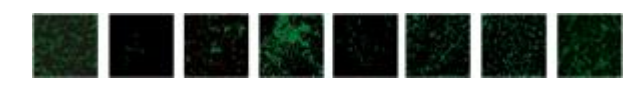


Fig. 2 PEM surfaces under this study

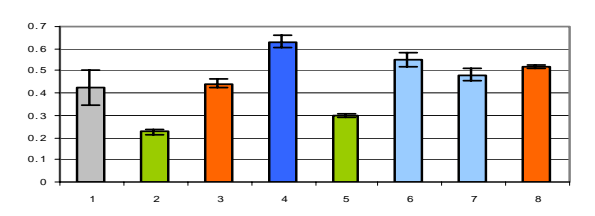
RESULTS: Cells were seeded on PEM films and cultured for 48hrs, then examined for morphology (phase microscopy), viability (life/death stain) and vitality (WST-assay). Stratification of nine different surfaces revealed following principal requirements [I] HPMSC adhered and grew out on [HA] but not on [PLL] surfaces [II] Display of fibronectin of upper layer of [PEM] is necessary to mediate efficient adhesion and outgrowth of HPMSC.



A: Crystal Violet Staining of Cell Sheets



B: Viability - Live/Death Staining



C: Vitality - WST-1 Test

Fig. 3. Representative results of positive and negative outgrowth of HPMSCs on PEM surfaces

DISCUSSION & CONCLUSIONS: We showed that the charge-sensitive arrangements of PEM can serve as a substrates for confluent layers of adult human mesenchymal stem cells. Future directions of this research are to evaluate whether stem cells grown on PEMs can be stimulated to differentiate into chondrocytes, osteocytes or cardiomyocytes *in vitro*, and whether differentiated sheets can be collected in intact form.

REFERENCES: ¹ T. Okano, et al. (2005) Biomaterials **26**: 6415-6422. ² Y. Miyahara, et al. (2006) Nature Medicine 12, (4): 459-465.

ACKNOWLEDGEMENTS: We thank Dr. A. Malek for help with isolation of HPMSCs. OVS is supported by a grant of CCMX-MatLife of the ETH-Board to JV and AHZ.

Enzymaticically formed, Modular designed Biomaterials

M. Ehrbar¹, M.P. Lütolf², A. Sala¹, S.C. Rizzi^{1,3}, J.A. Hubbell², F.E. Weber¹

¹ Bioengineering, Department of Cranio-Maxillofacial Surgery, University Hospital Zurich, Zurich Switzerland

INTRODUCTION: Naturally occurring materials were successfully explored in Tissue engineering approaches¹. However synthetic hydrogels that can be designed for specific applications with respect to mechanical properties, susceptibility to proteolytic activity and biological cues might be good alternatives for cell delivery and tissue regeneration. Here we present poly(ethylene glycol) (PEG)-based hydrogels that are biomimetic in both their synthesis and degradation. This new class of biomaterials enables the formation of matrices and the tethering of multiple engineered bioactive molecules in a simple one step reaction, which is catalyzed by the action of the activated transglutaminase enzyme factor XIIIa. The modular designed of the system allows the almost independent and flexible variation of physical and biological properties by using different building blocks.

METHODS: Hydrogel networks were formed in TBS (50mM TrisHCl, pH7.6; 50mM CaCl2) upon addition of activated FXIII to PEG precursor solutions, which consisted of a stoichiometrically balanced mix of 8arm-PEGs that are functionalized with either Lys-domaine or TG-domaine (two known substrate domains for FXIII)². Cells and/or bioactive molecules were added to the precursor solution prior to gelation. Coupling efficiency and release of RGD-peptides and vascular endothelial growth factor (VEGF) molecules that were modified with a TG-domain were assessed by HPLC and ELISA respectively^{2,3}. Adhesion and migration behavior of cells was followed by fluorescence and time-lapse microscopy. Matrices containing tethered VEGF were grafted on top of the chick chorioallontoic membrane (CAM) at embryonic

day 9 and bioactivity was determined by morphometric analysis.

RESULTS: We show that bioactive molecules, such as peptides and proteins, with concentrations up to $100\mu M$ can be quantitatively and site specifically tethered to the forming hydrogel, without altering the

network`s macroscopic properties. incorporation of the integrin ligand RGD supported cell adhesion on 2D substrates in a dose dependent manner and was indispensable for cell spreading and migration in a 3D environment. The migration behaviour of cells in 3D culture could be modulated by varying concentration polymer and substrate's susceptibility to proteolytic degradation. Incorporated vascular endothelial growth factor (VEGF) was shown to be releases upon cellderived proteolytic degradation of the gels and, due to the precise control over the conformation of the immobilized morphogen, completely retained its bioactivity.

DISCUSSION & **CONCLUSIONS:** In conclusion these novel artificial ECMs, in contrast to materials from natural sources, allow the nearly independent tailoring of properties including matrix stiffness, protease susceptibility and presentation of biological cues and might enable us to rationally control cell behaviour in both in vitro and in vivo contexts. Therefore, these matrices could be useful tools for experimental cell biology as well as for in vivo applications such as therapeutic angiogenesis and bone tissue regeneration.

REFERENCES:

ACKNOWLEDGEMENTS: We thank for support by Inion OY, Tampere, Finland

²Institute of Bioengineering, Ecole Polytechnique Fédéral de Lausanne (EPFL), Switzerland ³Present address: School of Life Sciences, University of Technology (QUT), Brisbane, Australia

¹ Langer, R. and D.A. Tirrell, Nature, 2004. 428(6982): p. 487-92.

² Ehrbar, M., et al., Biomaterials, 2007

³Ehrbar, M., et al., in press

A visible antithrombogenic biosurface for synthetic vascular grafts

H. Perea¹, J. Heverhagen², J. Aigner³, I. Feix¹, S. Repmann³, A. Stemberger³, E. Wintermantel¹

¹ Chair of Biomedical Engineering, TUM, Munich, Germany ²Department of Diagnostic Radiology, University Hospital Marburg, Marburg, Germany ³Institut für experimentelle Onkologie und Therapieforschung, K.r.d. Isar, TUM, Munich, Germany

INTRODUCTION: Synthetic vascular grafts are used with moderate success for the replacement of large diameter blood vessels. Small diameter (<6mm) synthetic vascular grafts are highly prone to thrombotic failure and are not suitable for clinical applications. In native blood vessels the luminal surface is lined by a monolayer of endothelial cells which secrete a variety of antithrombogenic and fibrinolytic factors. In this work we present a new strategy to obtain an antithrombogenic endothelial coating on the luminal surface of synthetic vascular grafts. The cellular coating can be additionally assessed noninvasively on a clinical MRI scanner thus providing a valuable pre- and postoperative diagnostic control[1].

METHODS: Human umbilical vein endothelial cells (HUVECs) were prelabeled with clinically superparamagnetic approved nanoparticles (Resovist®, Schering, Germany). Magnetically labelled cells were delivered with a customised solenoid onto the lumen of a tubular collagen coated graft. The solenoid provides a radial magnetic force which impels the cells towards the luminal surface of the scaffold, fostering a homogenous luminal cell distribution[2]. Upon completion of the seeding process, samples were examined in a clinical 1,5T magnetic resonance imaging (MRI) scanner to demonstrate the integrity of the cellular coating on the graft surface. Constructs were incubated with nonanticoagulated human whole blood for 8 minutes and characterised for blood clots via SEM. Markers of activated coagulation and complement system F1+2 and C3a were analysed by ELISA.

RESULTS: MRI inspection through a T2* sequence using a transversal gradient echo sequence reveals circumferential integrity of the endothelium as a bright layer covering the entire luminal surface of the scaffold. SEM inspection of unseeded samples shows platelet activation and fibrin formation over the entire surface. In contrast endothelialised scaffolds showed no evidence of thrombogenicity after contact with whole blood corroborated by lower levels of the activation markers F1+2 and C3a.

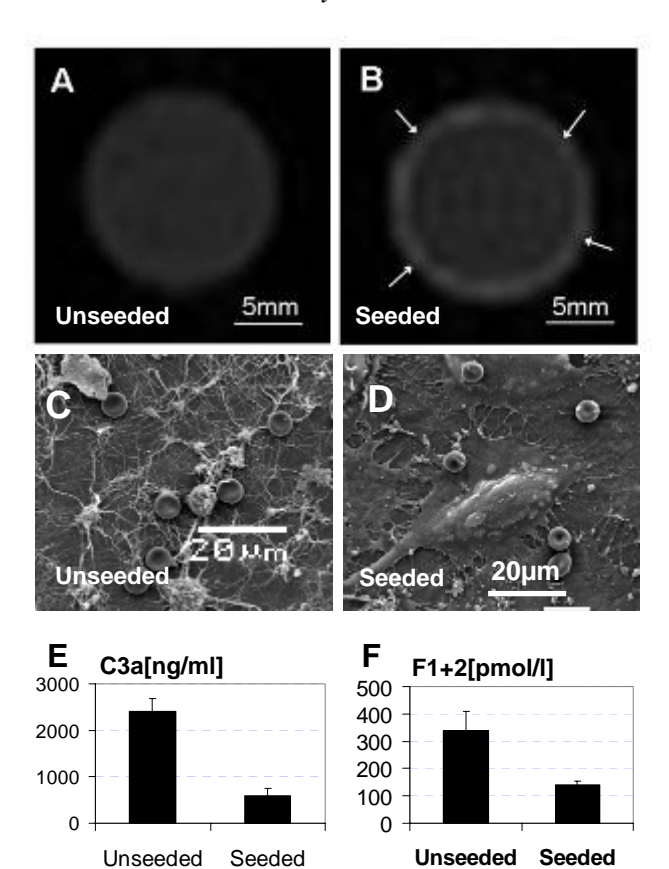


Fig. 1: MRI inspection of unseeded (A) and seeded (B) vascular grafts. The endothelium appears as a bright layer on the lumen of the graft(arrows). Unseeded grafts trigger platelet activation and fibrin formation(C). Endothelialised grafts inhibit coagulation(D). Endothelial cells inhibit the thrombogenic properties of synthetic grafts(E,F).

DISCUSSION & CONCLUSIONS: Magnetic endothelial cell seeding provides an intact antithrombogenic interface which can be assessed non-invasively in a clinical MRI scanner. This technology provides a visible antithrombogenic biosurface for synthetic vascular grafts.

REFERENCES:

- 1. Perea, H., et al., *Vascular tissue engineering* with magnetic nanoparticles: seeing deeper. Journal of Tissue Engineering and Regenerative Medicine, 2007. *In Press*.
- 2. Perea, H., et al., *Direct Magnetic Tubular Cell Seeding: A Novel Approach for Vascular Tissue Engineering*. CTO, 2006. **183**(3): p. 156-165.

Use of a rabbit cornea model for the development of a cell transfer system for limbal epithelial cells

P. Deshpande¹, N. Bullett², M. Notara³, J.T. Daniels³, D. Haddow² and S. MacNeil¹

Department of Engineering Materials, University of Sheffield, Sheffield, S3 7HQ.² CellTran Ltd, Innovation Centre, 217 Portobello, Sheffield, S1 4DP.³ Cells for Sight Transplantation and Research Programme, Ocular Repair and Regeneration Biology Unit, UCL Institute of Ophthalmology, 11-43 Bath Street, London, EC1V 9EL

INTRODUCTION: After cataracts, the major causes of blindness worldwide are diseases affecting the cornea. These diseases in particular have an adverse effect on the limbus: the stem cell factory of the cornea. Procedures have been developed to prevent blindness from occurring by transplantation of donor corneas or by transfer of limbal cells using a carrier, but these methods depend on the availability of the donor cornea and the carrier. Also it has been seen that the results maybe good, but the transparency of the cornea is not completely regained. The aim of this work is to develop a contact lens system for transferring laboratory expanded limbal epithelial cells for treatment of the cornea. The project uses a chemically defined plasma polymer surface which supports both the initial attachment of epithelial cells and their subsequent transfer onto the denuded cornea.

METHODS: A rabbit organ culture model has been established to examine the transfer of cells onto the cornea. Initial studies identified the most appropriate plasma polymer coating for support of epithelial cells. We are also examining the contribution of stromal cells to the survival of epithelial cells under serum-free conditions in this model. First we examined the culture of a human corneal epithelial cell line (HCEC) and primary rabbit limbal epithelial cells on a range of plasma coatings. Acrylic acid (AAc), allyl amine (AAm) and allyl alcohol (AlA) plasma polymer surfaces were synthesised at different powers and flow rates and their surface chemistry examined by XPS analysis. From these, the surface which best supported epithelial cell culture (both human and rabbit cells) was identified. Cells were then cultured on contact lenses coated with this surface. Rabbit corneal organ cultures with the intact epithelium were then denuded of epithelial cells (Fig 1a & b). Lenses with cells were placed onto the cornea and kept in place for 4 days. Transfer of cells from lenses was examined by pre-staining cells with CellTrackerTM Red CMTPX and also by subsequent staining of cells on the cornea with DAPI and phalloidin FITC.

RESULTS: The surface that best supported the epithelial cell culture was acrylic acid. Preliminary results using this model show that the primary rabbit limbal epithelial cells and the human corneal cell line will transfer from the lens onto the cornea (Fig 1c &d).

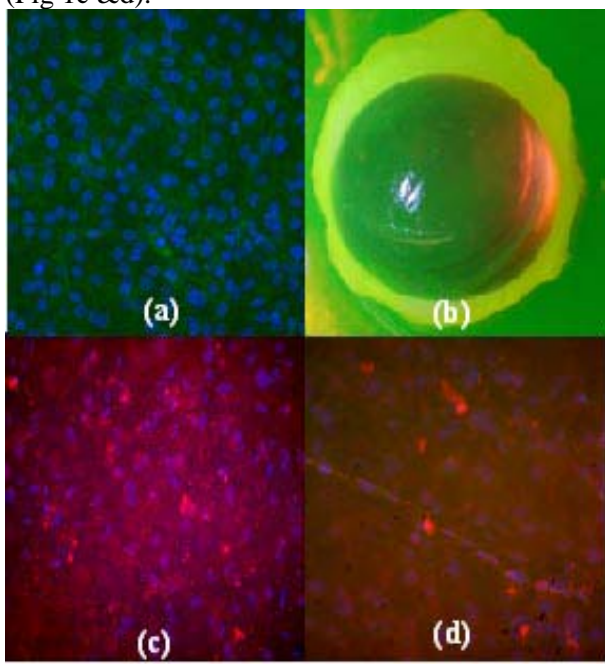


Fig 1: Culture model with (a) intact epithelium (labelled with DAPI and phalloidin FITC), (b) a denuded epithelium (stained with fluorescein), (c) rabbit limbal epithelial cells and (d) human corneal epithelial cell line after transfer from ppAAc coated lens (labelled with CellTrackerTM Red).

CONCLUSIONS: Results show that this model can be used to develop a culture and transfer protocol which we hope to use for future clinical studies.

REFERENCES: Notara M, Bullett NA, Deshpande P, Haddow DB, Macneil S, Daniels JT (2007) Journal of Materials Science: Materials in Medicine, **18** (2): 329-338

ACKNOWLEDEMENTS: We thank BBSRC for funding this work.

Investigation of artificial hip joint lubrication

M. Roba¹, M.H. Naka², B. Gasser³, D. Delfosse⁴, E. Gautier⁵, N.D. Spencer², R. Crockett¹

Nanoscale Materials Science, EMPA, Switzerland. Department of Materials, ETH Zurich, Switzerland. Robert Mathys Foundation, Switzerland. Mathys AG, Switzerland. FMH Chirurgie Orthopedique, hôpital cantonal de Fribourg, Switzerland.

INTRODUCTION: Under physiological conditions, natural hip joints are lubricated by synovial fluid, an aqueous electrolyte solution produced by the synovial membrane and cartilage and containing proteins, lipids and hyaluronic acid. After a hip implant surgery, the synovial membrane eventually reforms, producing a liquid similar to synovial fluid (SF) which lubricates the implanted device [1,2]. The interaction of this fluid, known as pseudo synovial fluid (PSF), with the bearing surfaces of hip implants, is of great importance. Nevertheless this area has so far been scarcely explored. The aim of this work is to investigate the interactions of PSF components, such as proteins and glycoproteins with materials used for hip implants.

METHODS: To analyze if PSF components adsorb on the implant's sliding surfaces, and to which extent they contribute to lubrication, a novel approach based on fluorescence labeling was used. Bovine serum albumin (BSA) and alpha-acid glycoproteins (AGP) were fluorescently labeled and were analyzed for their adsorption and exchange during friction tests onto CoCrMo and Ultra High Molecular Weight Polyethylene (UHMWPE) surfaces. Fluorescence microscopy was used to visualize sample surfaces and to investigate protein adsorption and exchange. As for the tribological analysis, CoCrMo discs and UHMWPE pins were used for friction tests, which were carried out with a pin-on-disc tribometer. BSA, AGP and phosphate buffered saline (PBS) were used as lubricants.

RESULTS: The type of friction tests performed show a dynamic situation, in which BSA and AGP, previously adsorbed onto the bearing surfaces, are replaced during sliding by labelled BSA and AGP present in the lubricant solution. In addition, it was observed that AGP also replaces previously adsorbed BSA. Friction results show that the two proteins have different lubricating behaviours for the tribopair CoCrMo-UHMWPE. The use of an AGP solution as lubricant significantly reduces the friction coefficient in comparison with BSA (Fig.1). The fluorescence labelling method reveals that UHMWPE transfer from the pin to the metal disc is occurring during sliding (Fig.2).

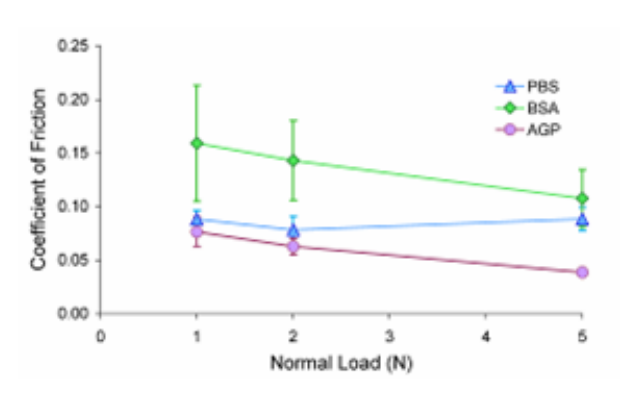
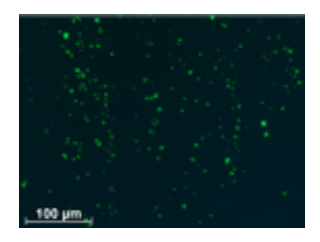


Fig. 1: Friction coefficients for UHMWPE sliding against CoCrMo using BSA, AGP and PBS as lubricants.



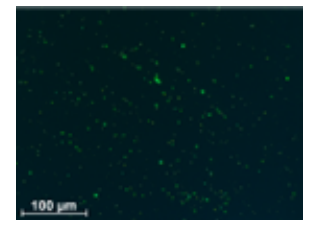


Fig. 2: Fluorescence images showing the wear tracks of CoCrMo discs after pin-on-discs tests carried out using UHMWPE pins and BSA (left) and AGP (right) solutions as lubricant.

DISCUSSION & CONCLUSIONS: Even in the presence of a protein solution, UHMWPE transfer onto the CoCrMo discs occurs during friction tests. In fact, it is possible to visualize labelled proteins on the discs using fluorescence microscopy, since no quenching of fluorophores occurs due to the presence of transferred UHMWPE. As for the lubricating behavior of the investigated proteins, AGP reduces the friction coefficients for UHMWPE-CoCrMo tribopair possibly due to its higher hydrophilicity, thus capability of retaining water improving the lubrication.

REFERENCES: ¹M.P. Heuberger, M.R. Widmer, E. Zobeley, R. Glockshuber, N.D. Spencer (2005) *Biomaterials* **26**:1165-73. ²D. Mazzucco, M. Spector (2004) *Clin Orthop Relat Res* **429**:17-32.

Lubricating Behaviour of Albumin at the Sliding Contacts of Chemically Modified Elastomers

Seunghwan Lee, Nicholas D. Spencer

Laboratory for Surface Science and Technology. Department of Materials, ETH Zurich, Wolfgang-Pauli-Strasse 10, CH-8093, Zurich, Switzerland.

INTRODUCTION: At present, the most widely employed material pairings for artificial articular implants are ceramic/UHMWPE metal/UHMWPE, both of which display "rigid-onrigid" mechanical contacts. Although these pairings have shown many favourable properties and successful performance as articular joint prostheses, their tribological properties demand further improvement, e.g. reduction/control of polymer wear particles, which is known to be responsible for the limitation of lifetime. study was thus inspired by the potential application of elastomeric materials as artificial articular joint implants.^{2,3} Of particular interest is to control the surface chemical properties to probe the lubrication properties of albumin, the most abundant protein in natural cartilage, at an elastomeric interface.

METHODS: Aqueous lubricating properties of human serum albumin (HAS, 1mg/ml, pH 7) at the sliding contact of a self-mated elastomer, PDMS, have been investigated as a function of surface chemical functionality of PDMS: (a) no treatment (-CH₃), (b) air plasma treatment (-OH), (c) PEGylation on hydrophobic PDMS surface (PEO-PPO-PEG-ylation on PEO) (d) plasma-treated, hydrophilic PDMS surface (PLL-g-PEG). A schematic for these surfaces are shown in Figure 1. The adsorption behaviour of HSA onto the PDMS surfaces. either untreated or chemically functionalized, was characterized by means of OWLS.

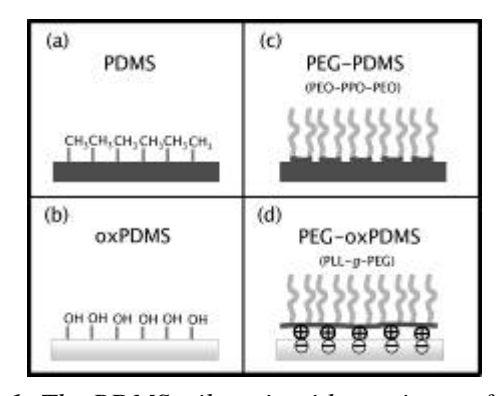


Fig. 1: The PDMS tribopair with varying surface chemical functional groups in this work.

RESULTS:

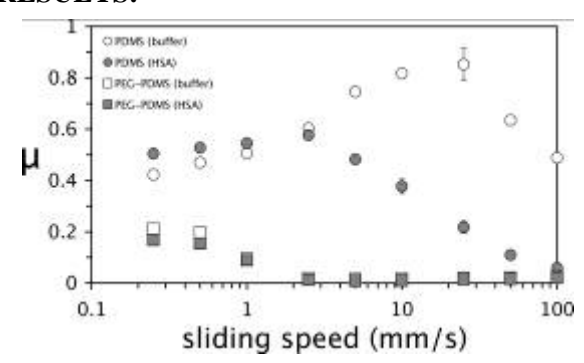


Figure 2. The μ vs. sling speed plots for the PDMS pair and PEG-PDMS pairs with or without HAS.

While an apparent lubricating effect of HSA was observed for the untreated PDMS tribopair, which is attributed to an effective suppression of adhesive hydrophobic interactions between two PDMS surfaces in aqueous environment,⁴ the contribution of HSA to the lubrication of the chemically functionalized PDMS tribopairs was generally negligible (shown in Figure 2 for the PDMS and PEG-PDMS cases only).

DISCUSSION & CONCLUSIONS: It should be noted that the mechanical properties (elasticity modulus) of PDMS employed in this work are similar to those for the natural cartilage system. The results in this study suggest that as long as the surface properties of an elastomeric tribopair can be controlled to remain hydrophilic, an effective aqueous lubricating performance, which is essential for artificial articular joint implants, can be readily achieved without involving HSA.

REFERENCES:

- ¹ M.P. Heuberger, M.R. Widmer, E. Zobeley, R. Glockshuber, and N.D. Spencer (2005) *Biomaterials* **26**:1165-1173.
- ² J.C. Bray, E.W. Merill (1973) *J. Biomed. Mater. Res.* **7**:431-443.
- ³ N.A. Peppas, E.W. Merill (1977) *J. Biomed. Mater. Res.* **11**:423-434.
- ⁴ S. Lee, N.D. Spencer (2005) *Tribology International* **38**:922-930.

NUCLEOTIDE NANOSTRUCTURED SURFACES TO STUDY BACTERIAL ADHESION AND BIOFILM GROWTH

N.Cottenye^{1,2}, J.Razumovitch², K. de França², F. Teixeira Jr. ², W.Meier², C.Vebert², L.Ploux¹

Institut de Chimie des Surfaces et Interfaces, Mulhouse, France.

² Universität Basel, Basel, Switzerland

INTRODUCTION: The understanding of how surface properties influence bacterial adhesion and biofilm growth is of great importance to eventually develop materials which inhibit or stimulate bacterial colonisation. To study the fundamental aspects of biofilm growth, model surfaces are needed, with different but controlled chemical and topographical properties. Using an amphiphilic nucleotide-based diblock copolymer, we developed nanostructured surfaces. A twelve nucleotide-long sequence composed of dCMP cytosine, C, covalently bond to polybutadiene, self-assembles into vesicular structures in dilute aqueous solution. Immobilization of those nucleo-vesicles on a surface modified with the same nucleotide sequence enables the preparation of surfaces with similar chemistry but varied topographies. Bacterial biofilm growth on both flat and nanostructured surfaces was compared, in terms of total number of adherent bacteria and adherent bacteria expressing curli, a proteinic organelle of adhesion.

METHODS: Smooth surfaces were made by grafting DNA sequences onto silicon wafers and characterized as described in another poster [1]. Rough surfaces were obtained by depositing 230 nm large PB-(dCMP)₁₂ nucleo-vesicles self-assembled in PBS buffer (described and characterised in a specific work [2]) on the smooth surface obtained as described above. The properties of the rough surface were characterized by AFM and water wettability measurements.

Microbial experiments were conducted with a wild strain (PHL818) and two mutants of *E. Coli*, which does not produce curli (PHL 847) or expresses GFP when curli are produced (PHL 1273). After incubation between 1 and 168 hours in a selective M63G medium, biofilms were studied by fluorescence microscopy, using Syto9® (Molecular Probes) to label PHL 818 and PHL 1273 bacteria and images were analyzed statistically.

RESULTS: Characterization of the smooth surface shows that the nucleotide sequences were grafted with a brush-like conformation and formed a smooth stable layer in liquid media. Rough surfaces were also stable in aqueous medium, with

homogeneous surface chemistry and a surface density of 1 nucleo-vesicle/µm² (fig.1a).

Adherent PHL 818 and PHL 847 bacteria number increased with time and were similar on smooth, rough and control (glass) surfaces. On the contrary, bacteria number expressing curli was significantly higher on nucleotide-modified surfaces (smooth and rough) compared to control surfaces (fig.1b).

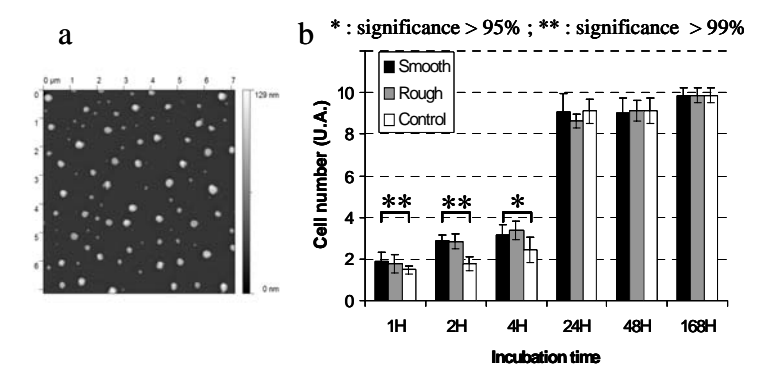


Fig. 1: a) AFM topographic image of 1 vesicle/µm² PB-(dCMP)₁₂ rough surface; b) Quantity of adherent E. Coli PHL 1273 expressing curli.

DISCUSSION & CONCLUSIONS: This work demonstrates the relevance of PB-(dCMP)₁₂ modified surfaces to study bacterial adhesion and biofilm growth. PB-(dCMP)₁₂ -based surfaces are not cytotoxic for Escherichia Coli. Moreover, the results show that grafted nucleotide molecules influence the expression of curli even if the topography of 1 nucleo-vesicle/µm² has no impact on bacterial adhesion and biofilm growth. However, the topography can be varied by modifying the vesicle-size and density. To control surface chemistry, the possibilities combining the four natural nucleotides are specific unlimited. Eventually, nucleotide sequences are expected to lead to specific interactions with some bacterial components.

REFERENCES: ¹see Razumovitch et al. ² see Teixeira et al.

VEGF AND PDGF-BB INCREASE NEOVASCULARISATION INTO A HEPARIN-COATED POLYURETHANE

C. Schmidt^{1,2}, N. Davies¹, D. Bezuidenhout¹, L. Higham¹, P. Zilla¹

¹ Cardiovascular Research Unit, University of Cape Town, South Africa. ² Department of Cardiovascular Surgery and Department of Surgical Research, University Hospital of Zurich, Switzerland.

INTRODUCTION: Spontaneous endothelialisation of a synthetic vascular graft is a prerequisite for long-term patency particularly in peripheral replacements. Transanastomotic endothelialisation is precluded in humans, therefore another source of endothelial cells would be the microvasculature surrounding the graft. As this would require transmural migration of the capillary derived EC's, we have developed a macroporous polyurethane graft. We now report on derivatisation of the surface of this porous polyurethane with proangiogenic Vascular Endothelial Growth Factor (VEGF) and Platelet Derived Growth Factor-BB (PDGF-BB) to stimulate neovascularisation and transmural ingrowth of capillaries.

METHODS: Polyurethane disks (5.4mm diameter, 2mm thick) with well-defined open porosity (82% porosity, 157±1µm pores) were produced by a variation on the phase inversion technique using pre-packed spherical microbeads as porogens. Heparin was subsequently attached covalently to the PU via Acrylic acid-diamine spacers. VEGF₁₆₅ and PDGF-BB were passively adsorbed separately and in combination onto the heparinised surface at 4°C. The optimal loading and period of release was determined by in vitro elution assays using VEGF/PDGF-BB ELISA. Heparinised and non-heparinised discs containing different combinations of growth factors were implanted subcutaneously in Wistar rats for 10 days. Vascular density was assessed on crosssections using image analysis after α-CD31 immunocytochemistry and reported vessels/µm².

RESULTS: VEGF ELISA showed, that a maximum of 1.2 μ g VEGF₁₆₅ (10% of the loading dose) was still adsorbed per disc after 3 washes in PBS and took 48 hrs to elute completely at 37°C. 3.5 μ g PDGF-BB loaded onto PU discs was still adsorbed after 3 washes in PBS and only 5.9% of PDGF-BB was eluted after 7 days. Elution in 1M NaCl/PBS/0.5%BSA confirmed that 91.44% of the loaded PDGF-BB dose was still bound to the PU

discs. Vascular density of the PU discs after 10 days subcutaneous implantation in rats was significantly increased by heparin surface modification versus non-coated control discs $(66.58\pm1.76 \text{vessels/mm}^2 \text{vs.}118.27\pm6.96 \text{vessels/mm}^2; p<0.05)$. There was further a significant increase in vascular density by adding PDGF-BB $3.6\mu \text{g}$ $(138\pm4.77 \text{vessels/mm}^2)$, VEGF $12.5\mu \text{g}$ $(141.12\pm6.49 \text{vessels/mm}^2)$ and VEGF $12.5\mu \text{g}$ plus PDGF-BB $1.8\mu \text{g}$ $(149.31\pm12.29 \text{vessels/mm}^2)$ onto heparin-coated PU discs.

DISCUSSION & CONCLUSIONS: Heparin as a delivery system for the controlled release of growth factors has been reported by passive addition to hydrogel matrices, by non-covalent as well as by covalent immobilization within different matrices [1]. In vivo delivery of VEGF in combination with heparin within a gelatin gel to a graft material has been previously reported by Masuda et al. [2]. VEGF immobilized in a heparin containing collagen matrix was described recently by Steffens et. al [3]. We report for the first time however, to our knowledge, on the direct, covalent attachment of heparin onto the biomaterial polyurethane without the need of an ingrowth matrix. The staged delivery of VEGF and PDGF-BB due to different affinities to the heparin-coated surface might further be a useful tool for future applications in the field of tissue engineering. The positive outcome suggests that this approach may be useful in the endothelialisation of porous synthetic vascular grafts.

REFERENCES: ¹ES.Sakiyama (2000) Development of fibrin derivates for controlled release of heparin-binding growth factors, J Control Release 65:389-402. ²S.Masuda (1997) Vascular endothelial growth factor enhances vascularisation in microporous small calibre polyurethane grafts, ASAIO J, 43:530-34. ³G.Steffens (2004) Modulation of angiogenic potential of collagen matrices by covalent incorporation of heparin and loading with VEGF, Tissue Eng, 10:1502-09.

Polymeric monomolecular magnesium coatings for biomedical applications

Ch. Mayer, V. Zoulalian, S. Tosatti, N. Spencer

Laboratory for Surface Science and Technology, Department of Material Science, ETH Zurich, Switzerland

INTRODUCTION: A novel approach in biomedical implant research is related to metallic biocompatible materials, especially for stents. Materials, such as magnesium alloys, which corrode in an aqueous environment, have been recently developed for these applications [1]. At present the problem is the fast corrosion occurring with available materials. That is the reason why the further degradation behavior of these kinds of alloys has to be fine tuned by e.g. application of an organic overlayer [1].

Moreover, the control over non-specific adsorption of proteins, cells and microorganisms to surfaces is crucial in biomedical implant research, because that can reduce drastically inflammatory reactions, foreign-body responses, failure and rejection of the implants and therefore improve the time performance of the medical device [2].

METHODS: In order to combine both requirements, a novel polymeric coating for magnesium substrates in bio-medical applications has been conceived. The controlled degradation of the substrate as well as the change of interface properties towards a non-fouling surface, preventing non-specific protein adsorption are peculiarities of this novel platform.

RESULTS: A first generation of functional polymers (c.f. Fig.1) has been synthesized by terpolymerization of functional monomers by chain-transfer polymerization to limit the degree of polymerization and propagation [3].

The surface activity has been tested by deposition from aqueous solution onto titanium dioxide as model substrate. Protein resistance has been proven with the aid of XPS and VASE [3].

First deposition experiments have been investigated for WE43 magnesium alloy substrate. Due to the redox degradation of magnesium in contact with aqueous solutions, a new deposition protocol from polar, organic solvents has to be investigated.

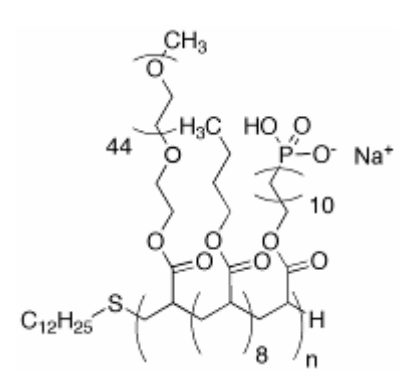


Fig. 1: Structure of poly(alkyl-phosphonates)

Deposition from isopropanol has shown surface activity, but no protein resistance has been obtained yet.

CONCLUSIONS: The polymer of Fig.1 has shown surface activity and protein resistance on titanium dioxide as model substrate. For further surface deposition and characterization on magnesium substrates, a new deposition procedure out of polar, organic solvents has to be developed first.

REFERENCES:

- [1] B. Heublein (2003) Heart 89:651-656
- [2] D.G. Castner (2002) Surface Science 500:28-60
- [3] V. Zoulalian (2006) Journal of Physical Chemistry B 110:25603

ACKNOWLEDGEMENTS: This work has been financially supported by the Materials for the Life Sciences Unit of the Swiss Competence Center for Materials Research and Technology of the ETH Domain

New strategies in polymeric biomaterials functionalisation

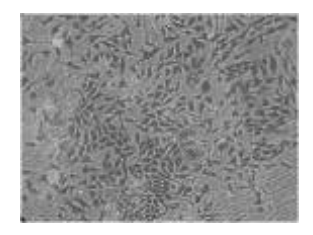
S.Sartori^{1,2}A.Rechichi^{3,2}, G.Ciardelli^{3,2}, A.Caporale⁴, G. Vozzi², L. Mazzucco⁵,

¹ DCCI UNIPI, Pisa, Italy. ²DICCSM UNIPI, Pisa, Italy ³ DIMEC POLITO, Turin, Italy. ⁴ DCS UNIPD, Padua, Italy. ⁵ DCPHTM, SS Antonio and Biagio Hospital, Alessandria, Italy

INTRODUCTION: The development of biodegradable polymers is suitable for a variety of biomedical applications. Polyurethanes (PUs) have been widely employed as elastomeric biomaterials due to their excellent mechanical properties and relatively good biocompatibility¹. A series of polyester-urethanes were synthesised. Furthermore both surface and bulk modification strategies were performed in order to obtain bioactive materials able to elicit specific cellular responses and directing new tissue formation.

METHODS: PUs were synthesised using a two step procedure, as previously described². The building block were: poly(\varepsilon-caprolactone) diol (M_n=1250 or 2000, Sigma-Aldrich); L-lysine ethylester-diisocyanate (Kyowa Hakko Kogyo Co.) or 1,6-diisocyanatohexane (Sigma-Aldrich); the chain extender was 1,4-cyclohexane dimethanol (Aldrich). In the first bulk modification approaches, N-Boc Serinol (1,1-Dimethylethyl [2-(hydroxymethyl)ethyl] hydroxy-1 carbamate Sigma-Aldrich), has been selected as chain extender to introduce amino groups in the PU side chains. The Boc group was then removed after polymerization by treating a polymer solution with trifluoroacetic acid. In order to study the reactivity of functionalised PU versus carboxyl groups of biomolecules, a model reaction with N-Boc phenylalanine was carried out using the carbodiimide chemistry. Another bulk modification involved the employ of a synthetic chain extender, a diammine containing the RGD sequence, synthesised using a phase-solid synthetic approach. The surface modification was carried out by a two-stage method. PU films were first treated with argon RF plasma reactor (Plasma System Junior SN 001/072, Europlasma). After exposure to air and the subsequent deposition of acrylic acid (AA) plasma copolymerization was carried out. Gelatine (Gel, Type A, Sigma) and poly(L-lysine) (PolyLys, Sigma-Aldrich) were immobilized by carbodiimide coupling. The PUs characterization was carried out by Differential Scanning Calorimetry, Size Exclusion several Chromatography and spectroscopy analyses. Preliminary in vitro tests were performed using NIH-3T3, Human Mesenchymal and Fibroblast cells to evaluate PUs biocompatibility.

RESULTS: Concerning the surface modification. the analysis related to the immobilization of Gel and PolyLys confirm the successful grafting. ATR studies shown the presence of amide signals and XPS analysis revealed changing in chemical composition and the presence of amide groups, according to protein bonds. Regarding the bulk modification, spectroscopic studies confirmed the successful functionalisation of PUs with peptides or aminoacids. Cell test demonstrated that PUs and functionalised PUs can be used as valid substrate for tissue engineering. Cell test shown that surface grafting of PolyLys is preferable instead of Gel for the activation of cellular processes (figure 1). Test with Human Mesenchymal performed Fibroblast cells, elucidate that cell adhesion is better on the films functionalised with RGD.



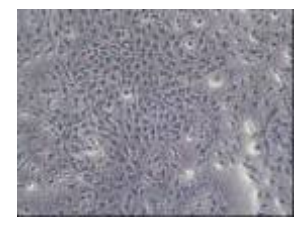


Fig. 1: Optical microscopy pictures of NIH-3T3 mouse fibroblasts cell cultures grown on PU grafted with polylysine (left) and gelatine (right).

DISCUSSION & CONCLUSIONS: A series of PUs and functionalised PUs were synthesised. The results suggest that plasma treatment with AA is an attractive way to introduce carboxylic groups on PU surfaces and immobilise biomolecules. Moreover the introduction of amino groups or peptides in the PU side chains are promising approaches to insert bioactive molecules. This PUs result good candidates in biomedical application.

REFERENCES: ¹N.M.K. Lamba, K.A. Woodhouse, S.L. Cooper (1998) *Polyurethanes in biomedical Application* CRC Press LLC.² Ciardelli G, Rechichi A, Cerrai P, Tricoli M, Barbani N, Giusti P. (2004) *Macromol Symp* **218**:261-71.

ACKNOWLEDGEMENTS: Co-financing by the Italian Ministry of research through the PRIN project2005091572_002, is acknowledged. S. Sartori is grateful to FIRB 2003 RBNE03R78E for scholarship grant.

Material defects investigation in fixed partial dentures using optical coherence tomography method

Cosmin Sinescu¹, Adrian Podoleanu², Meda Negrutiu¹, Carmen Todea¹, Dorin Dodenciu¹, Mihai Rominu¹

¹"VictorBabes" University of Medicine and Pharmacy, School of Dentistry, Timisoara, Romania
² Applied Optics Group, University of Kent, Canterbury.

INTRODUCTION: In odontology, a series of reports first appeared in 1998, with images of both hard and soft oral tissues. This led to several diagnostics of bucal diseases, including periodontal, early carries, among others. Another area in dentistry where OCT can have important findings is in dental restoration imaging. Wang et al. and Fried et al. explored polarization-sensitive OCT to identify dental tissue/restoration interfaces. Up to this date, there is no quantitative method able to perform in vitro or in vivo analysis of dental restoration, particularly from the clinical point of view. Visual inspection and x-ray imaging are not precise enough to diagnose small gaps that result from bad restoration procedures.

METHODS: In this work we used two different OCT systems that were assembled by the Applied Optics Group of the University of Kent. The optical configurations are similar to those presented before in ¹, ² using two single mode directional couplers with a superluminiscent diode as the source. Unlike conventional A-scan based time-domain OCT ³, en-face OCT systems⁴ were used which can deliver B-scans and C-scans from en-face (or T-scan) reflectivity profiles. This is similar to the procedure used in any confocal microscope, where the fast scanning is en-face and the depth scanning (focus change rather than a change in the reference arm length in the case of an OCT) is much slower (at the frame rate). Sequential and rapid switching between the en-face regime and the cross-section regime, specific for the en-face OCT systems developed by us, represents a significant advantage in the noninvasive examination of prostheses. The frame grabber is controlled by signals from the generators driving the X-scanner and the Yscanner. One galvo is driven with a ramp at 500 Hz and the other galvo-scanner with a ramp at 2 Hz. Systems operating at 670 nm, 850 and 1300 nm were used. Both systems have typical working distances of 2 to 3 cm and depth resolutions of 18 to 20 µm (in air).

RESULTS: The gap failure in a restored tooth can be evaluated by the OCT technique, and with a system resolution of $10 \mu m$ we were able to detect

gaps as small as $50~\mu m$, but only those of a few micrometers would be experimentally measurable. Although we demonstrated only gaps that were about 0.5~mm deep, the technique can image the full enamel extension, as demonstrated in earlier work at the same wavelength as used here and verified independently in our laboratory. Therefore, this required performance criteria is satisfied by the technique. The types of restorations that could be imaged by direct and indirect means include gaps wider than the resolution of the system, which could be imaged and spatially quantified.

DISCUSSION & CONCLUSIONS: OCT has numerous advantages which justify its use in the oral cavity in comparison with conventional dental imaging. OCT can achieve the best depth resolution of all known methods (in principle 1 micron if the source exhibits a sufficiently wide spectrum) and is safe. Furthermore, the use of OCT has the advantage of showing the restored region as well as the gap, if it exists, and precisely localizing its position, as demonstrated here.

REFERENCES: 1. B. T. Amaechi, A. Gh. Podoleanu, S.M. Higham, D. Jackson, ;2003, Correlation of Quantitative Light-induced Fluorescence and Optical Coherence Tomography Applied for Detection and Quantification of Early Dental Caries, Journal Biomedical Optics, 8(4); 642-647.

- 2. B. Amaechi, A. Podoleanu, G. Komarov, J. Rogers, S. Higham, D. Jackson, (May 2003) *Application of Optical Coherence Tomography for imaging and assessment of early dental caries lesions*, Laser Physics, Special Issue No.2, Laser Methods in Medicine and Biology, Vol. 13, No. 5,703-710.
- 3. D. Huang, E. A. Swanson, C. P. Lin, J. S. Schuman et al., (2000) Optical coherence tomography, Science 1991 254:1178-1181.
- 4. A. Gh. Podoleanu, J. A. Rogers, D. A. Jackson, S. Dunne "Three dimensional OCT images from retina and skin" Opt. Express, Vol. 7, No. 9, p. 292-298.

Application of the Laser Microspectral Analysis in Dentistry: Mikroleakage evaluation in fixed partial dentures

Meda Negrutiu¹, Cosmin Sinescu¹, Gheorghe Draganescu², Carmen Todea¹, Dorin Dodenciu¹, Mihai Rominu¹, Cezar Clonda¹

¹"VictorBabes" University of Medicine and Pharmacy, School of Dentistry, Timisoara, Romania

² University of Politechnica, Timisoara, Romania.

INTRODUCTION: This method was first introduced in 1962 and was used specially to investigate the surface of the metals. The laser microspectral analysis device consists in an infrared pulsed laser, usually with ruby, or neodimium doped glass as active medium.

METHODS: The laser microspectral analysis device LMA-1 (Carl Zeiss, Jena), equipped with a diffraction spectrometer PGS-2 (Carl Zeiss, Jena). This laser have a resonator with glass doped Nd3+. The output energy of the laser is 0.5-1.2 Joule/pulse λ =1060 nm. The LMA-1 system has mirror lens 40x, used to visualise the explored surface, which can be interchanged with 10 X lens, used to focus the laser pulse. The energy of the pulse was taken so that the diameter of the crater was around $d = 50 \mu m$ and the depth of $h = 35 \mu m$. The corresponding voltage of the flash lamp is around 2 kV. For this, correspond a mass of vapors of around m= 0.1 µg. The voltage on the electrodes can be taken in the interval 0.5 - 3 kV. For the electric discharge it was used two graphite electrodes. The image of the electric discharge was focused on the aperture of the spectrograph using a collimating system. The input aperture of the spectrograph was taken of 10 µm. The energy of the laser pulse can be adjusted by the voltage value of a high voltage pulse generator. For these microanalysis devices there are used lasers operated in the visible and infrared region. The active medium of these lasers is glass doped Nd ions, corresponding to a laser ray wavelength of 1060 nm, and the ruby, corresponding to a wavelength of 694.3 nm. The energy of the lasers used is around 0.5-2 Joule/pulse. Above the crater there are situated two graphite electrodes, connected to a high voltage source. The distance between the electrodes is taken from 1 to few millimeters. For a due distance between the electrodes, the value of high voltage U_E is take so that to be less and closed to breakdown voltage of the air from the vicinity of the probe, in absence of the plasma produced by the pulse. This value can be taken experimentally.

RESULTS: Results that a laser pulse will produce between the electrodes connected to the U_{E} voltage a jet of plasma, which contain the atoms ejected from the crater. This jet of plasma will initiate an electric discharge between the electrodes. This discharge will excite the atoms from the plasma, after which, by transitions from the excited states, it will emit photons, with due wavelengths and intensities. Commonly, there are used graphite The radiation produced by the electrodes. discharge is focused to the input slit of a spectrophotometer, or of a spectrograph. The spectrophotometer will give the emission spectrum of the atoms contained in the plasma. From this spectrum it can be established the content of atoms and their concentration from the crater. This spectrum corresponds to the UV and visible region. In order to made accurate measurements, an accurate delay between the laser pulse and the electric discharge must be taken. This delay is necessary, in order to produce the electric discharge, i.e. the excitation of the atoms, when the jet of plasma which contain the atoms arrive at the electrodes. The data were gathered in various tables of chemical elements showing the quality and the quantity of mikroleakage.

DISCUSSION & CONCLUSIONS: The method of laser microspectral analysis is a method of punctual method of analysis, which permits to investigate small quantity of material, around 0.1 μg.

REFERENCES: 1. Avram NM, Drăgănescu G, Marki I. (1975), The analysis of bonnes with the aid of laser micro-spetrochemical analysis, Studia Biophysica., 51: 69 – 72.; 2. Surmenko EL, Sokolova TN, Tuchin VV. (2001) Microspectral investigation of hair of one girl during six years by laser emission analysis, Diagnostic Optical Spectroscopy in Biomedicine Editors: TG Papazoglou, G A. Wagnieres, SPIE Proceedings. 4432: 253-256

The Quality Of Bracket Bonding Studied By Means Of Oct Investigation. A Preliminary Study

Roxana Otilia Rominu¹, Cosmin Sinescu¹, Adrian Podoleanu², Meda Negrutiu¹, Mihai Rominu¹, Andra Roxana Soicu¹, Cristina Sinescu³

¹"VictorBabes" University of Medicine and Pharmacy, School of Dentistry, Timisoara, Romania.

² Applied Optics Group, University of Kent, Canterbury. ³ Denpasar, Timisoara, Romani.

INTRODUCTION: Bonding brackets is an essential part in most fixed orthodontic treatments. Because of the great diversity of bracket and bonding materials, researchers all over the world have dealt with the various aspects of bonding since the beginning up to the present moments. The aim of our is to initiate an innovative investigation method of the bracket-tooth interface by means of OCT (optical coherent tomography) and to determine whether it is suitable as an orthodontic research tool.

METHODS: 40 extracted noncarious permanent teeth were considered in this study. Prior to the investigation all teeth were cleaned with a nonfluoride polishing paste and a rotary brush. They were divided in two groups of 20 each. One group represented teeth bonded with metallic brackets and the second group contained teeth bonded with ceramic brackets. The bonding protocol for the metallic brackets was performed as follows: 4" aluminablasting, 30" acid etching (38% phosphoric acid), rinsing and gentle but thorough blow-drying, application of an orthodontic bonding agent (Ortho Solo, Kerr), application of bonding on the bracket base followed by gentle blow-drying, application of the composite resin and bonding the bracket on the conditioned tooth surface followed by light curing using a plasma curing unit (Smart Lite, DeTrey Dentsply). For the ceramic bracket bonding our protocol contained the same steps mentioned above. In this work we used two different OCT systems that were assembled by the Applied Optics Group of the University of Kent. The optical configurations are similar to those presented before in ^{1,2} using two single mode directional couplers with a superluminiscent diode as the source. Unlike conventional A-scan based time-domain OCT ³, en-face OCT systems⁴ were used which can deliver B-scans and C-scans from en-face (or T-scan) reflectivity profiles. This is similar to the procedure used in any confocal microscope, where the fast scanning is en-face and the depth scanning (focus change rather than a change in the reference arm length in the case of an OCT) is much slower (at the frame rate). Sequential and rapid switching between the en-face

regime and the cross-section regime, specific for the en-face OCT systems developed by us, represents a significant advantage in the non-invasive examination of prostheses. The frame grabber is controlled by signals from the generators driving the X-scanner and the Y-scanner. One galvo is driven with a ramp at 500 Hz and the other galvo-scanner with a ramp at 2 Hz. Systems operating at 670 nm, 850 and 1300 nm were used. Both systems have typical working distances of 2 to 3 cm and depth resolutions of 18 to 20 μm (in air).

RESULTS: After the OCT investigation several gaps were detected at the bracket base- tooth interface. The largest gap had approximately 0,1 mm in diameter and the smallest one only 250 μ m. In all investigated samples various gaps were found.

DISCUSSION & CONCLUSIONS: OCT helped us perfom a useful noninvasive real-time investigation of the quality of the bracket basetooth interface. Further research is necessary in order to establish a correlation between the number and diameter of the gaps and clinical stability of the bonding procedure.

REFERENCES: 1. B. T. Amaechi, A. Gh. Podoleanu, S.M. Higham, D. Jackson, ;2003, Correlation of Quantitative Light-induced Fluorescence and Optical Coherence Tomography Applied for Detection and Quantification of Early Dental Caries, Journal Biomedical Optics, 8(4); 642-647.

- 2. B. Amaechi, A. Podoleanu, G. Komarov, J. Rogers, S. Higham, D. Jackson, (May 2003) *Application of Optical Coherence Tomography for imaging and assessment of early dental caries lesions*, Laser Physics, Special Issue No.2, Laser Methods in Medicine and Biology, Vol. 13, No. 5,703-710.
- 3. D. Huang, E. A. Swanson, C. P. Lin, J. S. Schuman et al., (2000) Optical coherence tomography, Science 1991 254:1178-1181.4. A. Gh. Podoleanu, J. A. Rogers, D. A. Jackson, S. Dunne "Three dimensional OCT images from retina and skin" Opt. Express, Vol. 7, No. 9, p. 292-298.

FORCE-INDUCED UNFOLDING OF FIBRONECTIN IN THE EXTRACELLULAR MATRIX OF LIVING CELLS¹

Michael L. Smith, Delphine Gourdon, William C. Little, Kristopher E. Kubow, Viola Vogel

Department of Materials, ETH, Zurich, Switzerland.

INTRODUCTION: Whether mechanically unfolded fibronectin (Fn) is present within native extracellular matrix (ECM) fibrils is controversial. Fibronectin extensibility under the influence of cell traction forces has been proposed to originate from either the force-induced lengthening of an initially compact, folded quaternary structure as is found in solution (quaternary structure model where the dimeric arms of Fn cross each other), or from the force-induced unfolding of type III modules (unfolding model). Clarification of this issue is central to our understanding of the structural arrangement of Fn within fibrils, the mechanism of fibrillogenesis, and whether cryptic sites, which are exposed by partial protein unfolding, can be exposed by cell-derived force.

METHODS: In order to differentiate between these two models, two fluorescence resonance energy transfer (FRET) schemes to label plasma Fn were applied, with sensitivity to either compact-to-extended (arm separation) without loss of secondary structure or compact-to-unfolded conformations.

RESULTS: FRET studies revealed that a significant fraction of fibrillar Fn within a three-dimensional human fibroblast matrix is partially unfolded. Complete relaxation of Fn fibrils led to a refolding of Fn. The compactly folded quaternary structure with crossed Fn arms, however, was never detected within ECM fibrils.

DISCUSSION & CONCLUSIONS: We conclude that the resting state of Fn fibrils does not contain Fn molecules with crossed-over arms, and that the several-fold extensibility of Fn fibrils involves the unfolding of type III modules. This could imply that Fn might play a significant role in mechanotransduction processes.

REFERENCES: ¹M. Smith, D. Gourdon, W. Little, K. Kubow, R. Andresen Eguiluz, S. Luna-Morris, V. Vogel (2007) *PLoS Biol*, In Press.

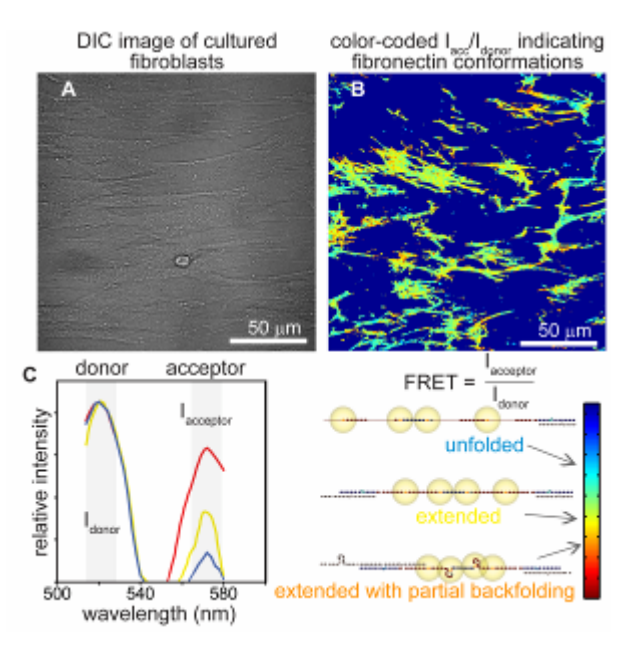


Fig. 1: Fibroblasts in cell culture (A) apply traction forces which lead to dynamic levels of strain within the ECM. Some regions (blue-green fibrils) are significantly unfolded, while other regions contain Fn with intact secondary/tertiary structure (yellow fibrils) and even quaternary structure (orange fibrils; B). Fluorescence Resonance Energy Transfer (FRET) is employed based on the increase in distance of covalently attached donor and acceptor pairs during the stretching of Fn in culture (B) or unfolding in denaturant in solution (C). Increased strain leads to decreased FRET. The proposed conformations of Fn corresponding to different FRET signals are shown (C).

ACKNOWLEDGEMENTS: This work was funded with support from the ETH, the Human Frontier Science Program Organization (MLS), and from the Nanomedicine Development Center (NDC) "Nanotechnology Center for Mechanics in Medicine" Regenerative (NIH grant PN₂ EY016586), that participates in the NIH Nanomedicine Development Center Network (NNDCN).

Evaluation of Anti-Inflammatory and Antimicrobial Resorcinarene-Peptides for Biomaterial Modification

M. Charnley¹, K. Fairfull-Smith², N.H. Williams², C. W. I. Douglas³, S. L. McArthur¹, J.W. Haycock¹.

¹Department of Engineering Materials, Sheffield University, UK. ²Department of Chemistry, University of Sheffield, UK. ³Department of Oral Pathology, University of Sheffield, UK.

INTRODUCTION: There is an increase in the use of implantable medical devices for the repair of soft and hard tissue. Many such devices can initiate acute inflammation, or become infected when implanted, resulting in device failure. α -Melanocyte-stimulating hormone (MSH) is a potent anti-inflammatory hormone¹, which also possesses antimicrobial properties², produced in the body with very short peptide sequences that make it amenable for easy laboratory synthesis. The aim of this work is to immobilise short MSH peptides onto medical device surfaces using molecules called resorcinarenes, which are known to attach to a wide variety of material surfaces. This is being approached by synthesizing MSHresorcinarene molecules with the aim of being able to 'dip and dry' treat medical devices with an antiinflammatory and antimicrobial 'coating'.

METHODS: Surfaces were coated with two compounds, resorcinarene-PEG-OMe, without the peptide moiety, and resorcinarene-PEG-GKP(D)V in varying molar ratios (0% to 100%), and characterised using XPS.

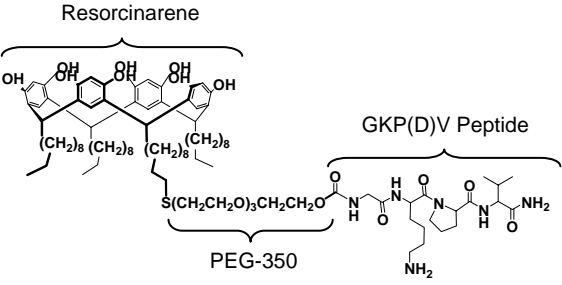


Figure 1: Schematic diagram of the GKP(D)V peptide attached to the resorcinarene compound via a PEG-350 tether, which is then coated onto glass.

The ability of the immobilized peptide to inhibit inflammatory signaling was determined by culturing RN22 Schwann cells upon the treated surfaces and measuring NF-κB/p65 inflammatory transcription factor activation.

RESULTS: *Surface Characterisation*; XPS indicated that the GKP(D)V peptide was immobilized onto the glass surface.

NF-κB Activation: Unstimulated cells exhibited predominately cytoplasmic labelling stimulation of the cells with LPS (100 ngml⁻¹) rapid translocation, and therefore activation, of NF-κB to the nucleus. Culturing cells on resorcinarene-monoPEG-OMe coated surfaces had no effect on NF-κB activity. In contrast resorcinarene-monoPEGculturing cells on GKP(D)V coated surfaces inhibited stimulated NF-κB activation by up to 28.2±4.0% (p<0.001). Levels of inhibition were comparable to those observed when cells were co-stimulated with GKP(D)V at 10^{-9} M and LPS (38.9±3.3%; p<0.001) (Fig 2).

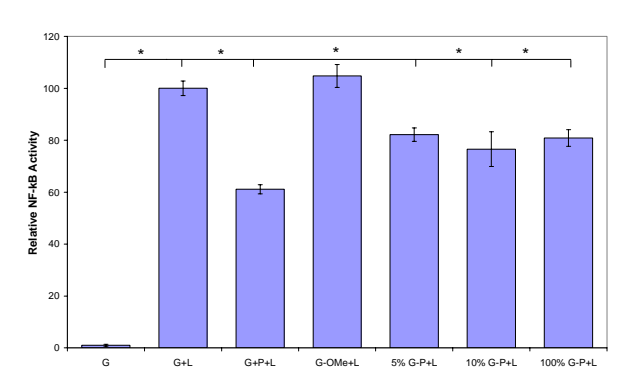


Figure 2: Immobilised GKP(D)V inhibits NF-κB activity. G, glass; L, LPS; P, GKP(D)V peptide; G-OMe, resorcinarene-monoPEG-OMe; G-P, resorcinarene-monoPEG-GKP(D)V; n=3, *p≤0.05

CONCLUSIONS: Results indicate the GKP(D)V peptide has been immobilised onto glass using resorcinarene chemistry and retains anti-inflammatory properties. Future work involves the investigation of the antimicrobial properties of KP(D)V peptide, and related melanocortin peptides, in solution and when immobilised.

REFERENCES: ¹R. P. Hill, S. MacNeil, and J.W. Haycock, (2006) *Peptides* **27**; 421-430. ²M. Cutuli, S. Cristiani, J. M. Lipton, A. Catania, (2000) *J. Leukoc Biol* **67**; 233-239.

ACKNOWLEDGEMENTS: We would like to thank the BBSRC and EPSRC for funding this work.

INFLUENCE OF POTENTIAL ON THE ELECTROCHEMICAL BEHAVIOUR OF Co-Cr-Mo ALLOY IN SIMULATED BODY FLUIDS USING ELECTROCHEMICAL IMPEDANCE SPECTROSCOPY

J.L. Vázquez-Gutiérrez, A. Igual-Muñoz

Departamento de Ingeniería Química y Nuclear. Universidad Politécnica de Valencia. P. O. Box 22012, E-46071 Valencia. Spain. Tel. 34-96 387 96 32, Fax. 34-96-387 76 39, e-mail. anigmu@iqn.upv.es

INTRODUCTION: Co-Cr-Mo alloy is commonly used as implant biomaterial because of its high corrosion resistance, wear resistance, and fatigue strength. The corrosion resistance is imparted by a passive oxide film that forms spontaneously on the alloy surface. In this sense, the potential at which the passive film is formed may play an important role in the electrochemical behavior of the biomaterial.

The purpose of this work was to characterize the corrosion behaviour of a high carbon Co-Cr-Mo alloy depending on the applied potential for a range of 0, 100, 250 and 500 mV within the passive zone during 1 hour using Electrochemical Impedance Spectroscopy (EIS).

METHODS: Open-circuit potential (OCP), potentiostatic tests and AC impedance were measured in a three-electrode vertical cell. An Ag/AgCl, 3-M KCl electrode and a platinum electrode were used as reference and counter electrode, respectively. The experiments were carried out using four different solutions: NaCl, NaCl + albumin, Phosphate Buffered Solution (PBS) and PBS + albumin in order to analyze the influence of phosphates and albumin on the electrochemical behaviour of the biomaterial.

RESULTS: OCP values depend on solution chemistry. Main influence on the OCP was observed in presence of albumin molecules which decreases the OCP values. Applied potential slightly increases the passive current density at 0, 100 and 250 mV after 1 hour of immersion in the simulated body fluids. The influence of the applied potential is more significant at 500 mV and in the phosphate-containing solutions, while albumin slightly decreases the current density values in the whole potential range.

The EIS results agree with the dc results and they show that polarization resistance decreases at 500 mV and this decrease is higher in the presence of phosphates. Albumin mainly affects the capacitive behaviour of the interface.

DISCUSSION & CONCLUSIONS: The results show that there are not significant differences on the passivation kinetics depending on the applied potential, neither on the solution. However, differences were observed in the passive current density values. The increase in the current density at 500 mV was attributed to the breakdown of the passive film due to the displacement to the transpassive zone. This increase at 500 mV is higher in the presence of phosphates, due to the formation of phosphates-chromium ion complexes that activates transpassive dissolution.

These results agree with those obtained using Electrochemical Impedance Spectroscopy (EIS).

Therefore, the influence of applied potential on the electrochemical properties of the interface depends on solution chemistry. There is an interaction between species in the solution and the biomaterial surface depending on the potential and the nature of those species. In this sense, phosphates slightly decrease the resistance of the interface in the whole passive range, mainly at higher potentials, while albumin increases the resistance. Albumin effect disappears when phosphates are present in the solutions due to the competitive adsorption of both species.

ACKNOWLEDGEMENTS: We wish to express our gratitude to the Spanish Government, "Ministerio de Educación y Ciencia" CIT-300100-2007-49 for the economic support.

ELECTROCHEMICAL CHARACTERIZATION OF BIOMEDICAL ALLOYS FOR SURGICAL IMPLANTS IN SIMULATED BODY FLUIDS

C. Valero Vidal, A. Igual Muñoz,

Departamento de Ingeniería Química y Nuclear. E.T.S.I.Industriales. Universidad Politécnica de Valencia. P.O. Box 22012, E-46071 Valencia. Spain

INTRODUCTION: Stainless Steel AISI 316L and Co-based alloys are highly biocompatible biomaterials widely used as orthopaedic implant materials in clinical practice. Biocorrosion has been considered a problem for the long durability of implants into human bodies and the release of metal ions can cause adverse physiological effects, toxicity, carcinogenicity and metal allergy. The purpose of this work is to compare the electrochemical properties of both biomaterials.

METHODS: The electrolytes employed were 0.14M NaCl solution and Phosphate Buffered Solutions (PBS). In order to analyze the protein effect 0.5 g/l of albumin were added to both electrolytes. The temperature of the solutions was kept out 37°C and the solutions were adjusted to pH 7.4 (human body conditions).

The study of the electrochemical behaviour of biomedical materials in simulated body fluids was carried out using open circuit-potential, potentiodynamic polarization curves, potentiostatic measurements at different immersion times and electrochemical impedance spectroscopy (EIS).



Fig. 1: Plate and screws of AISI 316L

RESULTS: The study reveals that OCP values stabilize with time in the two biomaterials due to spontaneous formation of a passive oxide film.

Phosphates act as anodic inhibitor on AISI 316L and CoCrMo, while albumin acts cathodic or anhodic inhibitor depending on solution chemistry and biomaterial.

Furthermore, EIS results for both biomaterials show the resistance of the interface under passive conditions increases in presence of albumin. Moreover, phosphate ions enhance the interface resistance value.

Immersion time decreases the charge transfer resistance of AISI 316L in all solutions, while on CoCrMo alloy charge transfer resistance increases in PBS solutions.





Fig. 2: CoCrMo knee implant (left) CoCrMo hip implant (right)

DISCUSSION & CONCLUSIONS: Influence of Albumin on both biomaterials, depends on the nature of the alloy. It decreases the corrosion resistance of AISI 316L while increases the corrosion resistance of CoCrMo. Although it is known that it adsorbs in both cases, properties of the passive layer modifies the effect of albumin. On the contrary, precipitation of phosphate ions could explain the highest resistance values in the phosphate solutions on both cases.

The study shows that the electrochemical behaviour of CoCrMo shows higher charge transfer resistance and lower capacitance which means thicker passive films than AISI 316L.

ACKNOWLEDGEMENTS: We wish to express our gratitude to the Spanish Government, "Ministerio de Educación y Ciencia" CIT-300100-2007-49 for the economic support.

Amphiphilic Copolymers at the Air-Water Interface for the Preparation of Calcium Phosphate Thin Films

O. Casse¹, A. Taubert²

¹ University of Basel, Basel, Switzerland. ² University of Potsdam, Golm, Germany.

INTRODUCTION: A series of poly(n-butyl acrylate)-block-poly(acrylic acid) in a Langmuir monolayer system is presented as a good template to generate calcium phosphate (CaP) thin films. Those hybrid flexible (later on you say that they are not flexible, see purple text below) films offer controlled thickness and organic-inorganic ratio. As fixed horizontal surfaces offer simpler conditions for study and modeling of processes such as charge interaction, complexation, and crystal nucleation when compared to colloids, those films can be considered as a step towards the coating of organic particles and surfaces.

METHODS: A KSV Langmuir-Blodgett system with moving barriers assigned to surface pressure control and automatic dipping for solid substrates was used to create the films. Subphases consisted of buffered calcium solutions in a Teflon trough. After the polymer was cast on the water surface from a small volume of a chloroform solution, time was left for the calcium to complex with the acrylic acid moieties. The phosphate counter-ion was then added with a syringe at the bottom of the trough through the polymer monolayer.

Optical, transmission/scanning electron and atomic force microscopies were used to characterize the films

RESULTS: Films were obtained only at basic pH, whereas at low pH the polymer monolayer would most of its original elasticity. Organic/inorganic ratio within the films were controlled by 3 parameters: the polymer monolayer stress ("solid" or "liquid" phase of the Langmuir isotherm), the supersaturation of the subphase and the mineralization time. In all cases at basic pH the elastic polymer monolayer was rendered stable over time and compact (unable to extend upon decompression) and brittle when transferred to solid substrates.

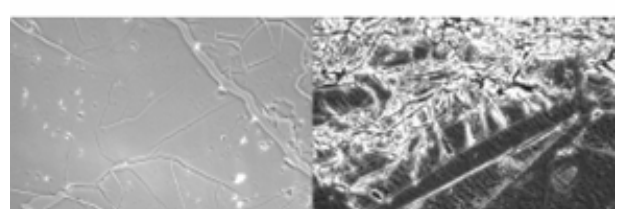


Fig. 1: optical microscopy images of a dried

hybrid CaP-polymer film transfered on glass (left: bright field, right: dark field, wrapped film after collapse), witdh 300µm.

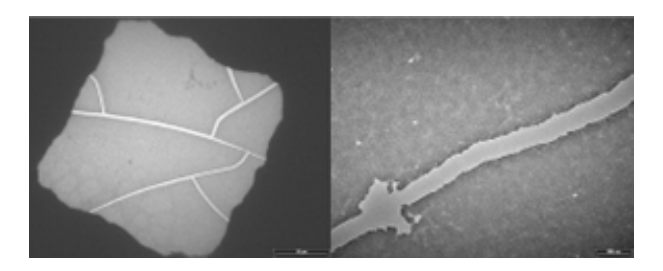


Fig. 2:Transmission electron microscopy images (left width: 60μm, right width: 2μm)

DISCUSSION & CONCLUSIONS: The wide-scale monolayer homogeneity of the films shown above speak in favour of a mechanism of mineralization where the CaP was nucleated by the polymer carboxylic acid moieties (fast with respect to the further growth of CaP). Other mechanisms including nucleation of CaP in solution before aggregation under the polymer monolayer would result in very inhomogeneous mineral layers in terms of thickness and density, non of which has been observed in TEM or optical microscopy.

REFERENCES: ¹ E. DiMassi (2002), Langmuir, Polymer-Controlled Growth Rate of an Amorphous Mineral Film Nucleated at a Fatty Acid Monolayer, **18**, pp 8902-8909. ² E. Eghbali, O. Colombani (2006), Langmuir, Rheology and Phase Behaviour of poly(n-butyl-acrylate)-block-poly(acrylic acid) in aqueous solution, **22**(10), pp 4766-4776.

ACKNOWLEDGEMENTS: We thank Olivier Colombani (University of Le Mans, France) and Axell Müller (University of Bayreuth, Germany) for providing us with the polymers and characterizing the polymer monolayers, and Sandro Erni (University of Basel, Switzerland) for performing mineralization experiments.

Solid Supported Membranes based on Amphiphilic Gramicidin Derivatives

Th. Schuster, Ch. Dittrich, D. de Bruyn Outer, W. Meier

University of Basel, Switzerland.

INTRODUCTION: Gramicidin A (gA) is a 15mer peptide antibiotic, originally derived from the soil living bacterial species *Bacillus brevis*. It consists exclusively of hydrophobic amino acids, alternating in D- and L-conformation, which leads to a rolled-up β -sheet, the so-called β -helix (1). Quaternary structure is manifested in the helical dimer or the double helical form; latter is dominant in lipid bilayers (Figure 1).

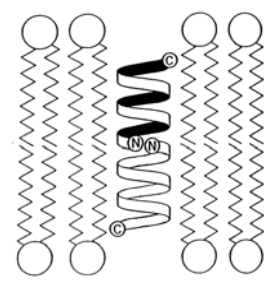


Figure 1: helical dimer in lipid membrane (1)

We attached hydrophilic sequences of oligo-lysine to the N-terminus of Gramicidin and yielded amphiphilic peptides with the ability to self-organize to membranes and vesicular structures in aqueous solution.

METHODS: All peptides were synthesized on solid phase using Fmoc chemistry. Purification was performed by preparative RP-HPLC.

Superstructural analysis was carried out using TEM, SEM, AFM, LS and CD techniques.

RESULTS: In this project, we end-functionalize Trunk-peptides with lipoic acid (2) to immobilize them on gold surfaces (Figure 2).

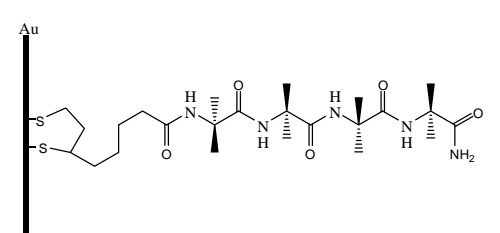


Figure 2: scheme of the chemical adsorption of a thiopeptide

We expect to observe the dimerization kinetics of our peptides by QCM experiments and its response to a variation of solvent and temperature.

Additionally, we anticipate to detect (AFM, ellipsometry and film balance) a regular molecular alignment governed by the interactions responsible

for membrane formation in aqueous bulk solution (3).

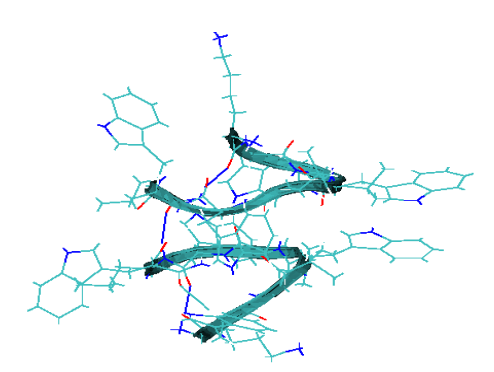


Figure 3: dimer structure of K(WL)₃W

MD calculations of $K(WL)_3W$ were setup with CHARMM (Figure 3) and complemented with NMR measurements to approve the hypothesized membrane structure as well as the role of the tryptophanes within.

DISCUSSION & CONCLUSIONS: The gA sequence is a suitable hydrophobic block to form purely peptidic membranes. Furthermore, we reduced the functional structure to a repetitive sequence of L-tryptophane and D-leucine amino acids. In conclusion, we propose aromatic interactions in addition to the hydrophobic effect to be held responsible for the structural characteristics of our membranes. Surface measurements on gold as well as the computational approach will give important complementary information about the membrane structure.

REFERENCES:

- 1. B. A. Wallace, Journal of Structural Biology 121, 123 (1998).
- 2. E. P. Enriquez et al., Journal of Vacuum Science & Technology, A: Vacuum, Surfaces, and Films 10, 2775 (1992).
- 3. H. Lavoie et al., Biophys J FIELD Full Journal Title:Biophysical journal 83, 3558 (2002).

The Transmission Interference Adsorption Sensor (TInAS)

T. E. Balmer¹, M. Heuberger²

¹ Department of Materials, ETH Zurich, CH-8093 Zurich, Switzerland. ² Empa, Materials Science & Technology, CH-9014 St. Gallen, Switzerland.

INTRODUCTION: The time-resolved measurement of molecular adsorption onto surfaces yields a wealth of valuable information about surface properties, solution properties, and adsorbent properties, adsorption mechanism as well as specific or unspecific adsorbent-surface interactions. Here we describe a novel high-speed adsorption sensor based on thin-film interference at interfaces. This Transmission Interference Adsorption Sensor (TInAS) can be used as standalone instrument or in combination with a direct surface force measurement, which yields a wide range of additional information on molecular interactions on adsorbed films.

METHODS: The TInAS uses white light that is directed through a transparent dielectric multilayer structure, with each layer exhibiting a different refractive index. Partial reflections at these optical interfaces lead to the formation and superposition of multiple beams-giving rise to an interference effect in the reflection- and transmission- spectra. Analysis of such interference fringes can be used to determine small changes of film thickness, as for example, due to molecular adsorption at the sensor surface. The experimental challenges of the described method are an accurate wavelength calibration and an accurate wavelength determination of feeble interference maxima.

The measurement spot size is one micrometer or more and sampling rates >10Hz are readily possible. In contrast to other bio-sensors, the signal baseline has a remarkable long-term stability since the measured signal is virtually independent of refractive index changes in the fluid medium above the sensor surface.

RESULTS: We demonstrate sensor operation for various bio-sensor configurations, including specific protein adsorption onto a functionalized polymer surface from aqueous solution and water adsorption from the gas phase.

In combination with an optical spectral correlation method [1], the classical computer calculations are substituted by an optical calculator and a label-free real-time imaging adsorption sensor is realized. This imaging capability of the new sensor technology is illustrated on a patterned biofunctionalized surface.

DISCUSSION & CONCLUSIONS: The achieved mass resolution of the presented method $(1-10\,ng/cm^2\sqrt{Hz})$ is comparable or better than other modern bio-sensors. The dependence of mass resolution on various factors is presented and demonstrated in a number of relevant examples. The described method is suitable for the implementation of a low-cost bio-sensor with a minimal number of optical elements.

REFERENCES: ¹ T.E. Balmer, M. Heuberger (2007) submitted to *Rev. Sci. Instr.*

Engineered mannose-presenting platform for the study of *E. coli* adhesion under static and dynamic conditions

K. Barth¹, G. Coullerez¹, L. Nilsson², R. Castelli³, M. Textor¹.

¹Biointerfacegroup, Laboratory for Surface Science and Technology, ²Laboratory for Biological Oriented Materials, ³Laboratory for Organic Chemistry, ETH Zurich, Zurich, Switzerland.

INTRODUCTION: Bacterial adhesion to carbohydrates of eukaryotic cell surfaces is involved in a plethora of infections. Often, mannoside-containing N-linked glycoproteins are targeted by the pathogen lectins, though molecular details are not entirely understood. Therefore, the study of bacteria adhesion at the molecular level and their carbohydrate binding fingerprint are believed to contribute to a better understanding of adhesion mechanisms, important for bacterial infections and biofilm formation on medical devices. In the present study, we investigated the specific interactions between surface immobilized mannosides and the bacterium Escherichia coli (E. coli). Synthetic oligomannoside determinants, derived from high-mannose glycoproteins, were conjugated to the polycationic graft copolymer poly-(L-lysine)-graft-poly(ethylene glycol) (PLLg-PEG) and adsorbed on Nb₂O₅-coated surfaces. E. coli adhesion was studied upon the sugar epitope, PEG-carbohydrate density and linker both under static and dynamic conditions.

METHODS: Surfaces were incubated with a genetically modified K-12 *E. coli* strain presenting fully functional type I fimbriae with mannose binding lectin FimH² at 38 °C during 30 min both under stagnant (10⁹ cells/ml) and flow conditions (10⁸ cells/ml). Stable adhered bacteria were observed by phase contrast microscopy and quantified by image analysis. A photolithography based patterning method (MAPL) was used to create bacteria adhesive patterns in a non-interactive background.³

RESULTS: *E. coli* adhered to surfaces via specific interactions with the adhesin FimH to the immobilized mannosides. No adhesion was observed with FimH deficient *E. coli* strains, on pure PLL-g-PEG surface, nor in the presence of high concentration of the inhibitor α-Me-mannose. Although, strong multivalent interactions occurred at all the studied PEG-mannose densities (6.7x10⁴-2.2x10⁵ mannosides/μm²), the number of adherent bacteria varied with the saccharide density. Furthermore, the *E. coli* binding affinity varied with the mannoside epitopes. The highest binding was shown to the branched trimannoside Man

 $(1\rightarrow 3)$ Man $(1\rightarrow 6)$ Man (M3) compared to the monosaccharide (M1) while low affinity was observed to hexa- (M6) and nona-structures (M9) exposing $(1\rightarrow 2)$ -linked mannoses (Figure 1a). Interestingly, it was also shown that a propyl linker stabilized the binding compared to an ethylene glycol chain. As bacterial adhesion in the body often occurs in the presence of fluid flow, E. coli adhesion was also studied under dynamic conditions. It showed that the binding of E. coli to the monosaccharide was enhanced by the shear stress while about no effect was seen for the binding to M3 or reduced as a result of kinetic effect on the initial attachment.⁴ Finally, bacteria micropatterns in a bioinert non-functionalized PLL-g-PEG background were produced (Fig. 1b).

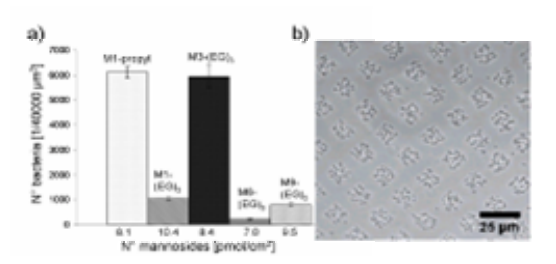


Fig. 1: E. coli adhering to PLL-g-PEG/PEG-mannoside: a) homogeneous surface containing various mannoside epitope at ca. 10 pmol/cm²; b) $10 \times 10 \text{ µm}^2$ patterns of trimannose.

DISCUSSION & CONCLUSIONS: Mannoside functionalized PLL-*g*-PEGs are useful tools mimicking glycoproteins to study *E. coli* adhesion using well defined carbohydrate structures and controlled density. The presented platform can be easily extended for studies of other bacteria strains. Bacteria micropatterns are of interest to study mechanistic aspects of bacteria communication such as quorum sensing and biofilm formation in small and well-defined bacterial colonies.

REFERENCES: ¹N. Sharon (2006) *Biochem Biophys Acta* **1760**, 527-537. ²W. Thomas et al. (2002) *Cell* **109** (7), 913-923. ³D. Falconnet et al. (2004) *Adv Funct Mater* **14**, 749-756. ⁴ L. Nilsson et al. (2006) *J. Biol. Chem.* 281, 16656-16663.

ACKNOWLEDGEMENTS: ETH Research Grant TH-38/04-2: "GlycoSurf" for funding.

Neurons Derived From P19 Embryonic Carcinoma Cells As A Platform For Biosensor Applications

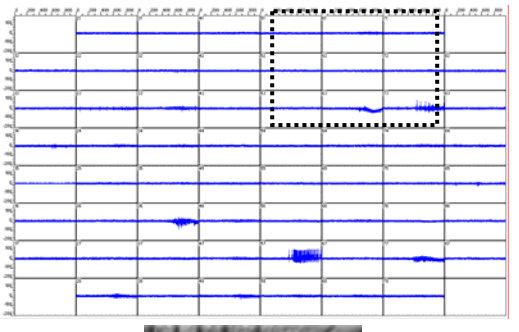
HL. Khor, E. Sinner, W. Knoll

Max Planck Institute for Polymer Research, 55128 Mainz, Germany

INTRODUCTION: P19 is a mouse-derived embryonal carcinoma cell line capable of differentiation toward ectodermal, mesodermal and endodermal lineages. Cell lines offer advantages of reproducibility, unlimited availability, pliability homogeneity and genetic manipulation. A spontaneously active neuronal ensemble derived from differentiated P19 cells cultured on microelectrode array can thus be engineered to sense a variety of chemical compounds with the potential to sensitivity, accuracy and long term on line performance as a biosensor.

METHODS: Microelectrode arrays (MEA) were purchased from MultiChannel Systems. P19 embryonic carcinoma cells were differentiated into neurons by treating with retinoic acid and cultured up to a month on the MEAs. Immunohistology was performed on the P19-derived neurons. The response of the P19-derived neurons to two major neurotransmitters, γ-aminobutyric acid (GABA) and glutamate, and their antagonists was studied. The cells were tested with different concentration of GABA, bicuculline, musimol, glutamate, cyclothiazide, the 2, 3-bezodiazepine derivative, GYKI 52466 to examine their plausibility as a biosensor. Recordings were done with MC rack software and analysed.

RESULTS: Recordings obtained from the cultures showed consistency within the same batch of differentiated P19 cells. Spontaneous neuronal activity was detected after 7 days *in vitro* (Fig. 1). We found that P19-derived neurons developed network activity with synchronised burst activity after 15 days *in vitro* (Fig. 2). Activity could be detected usually in regions where cell clusters were attached to the electrodes. Synchronised firing patterns were observed in electrodes connected together in the same cell cluster network.



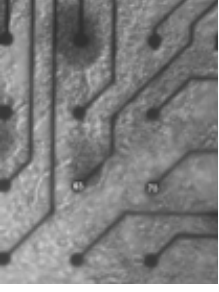


Fig. 1: Intrinsic extracelluar signals of P19-derived neurons after 17 days in vitro. Below: Optical micrographs of the cells at the corresponding electrodes highlighted.

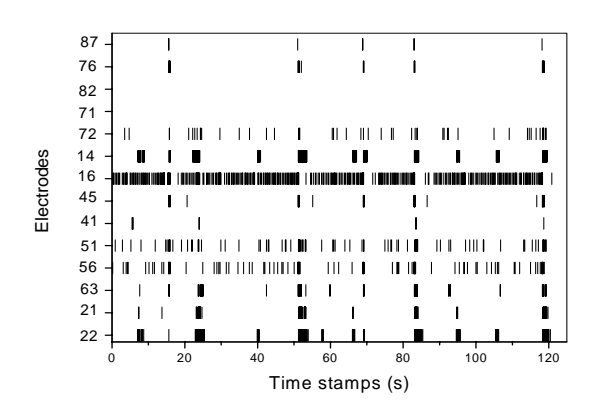


Fig. 2: Raster plots of P19-derived neuronal culture after 23 days in vitro.

DISCUSSION & CONCLUSIONS: P19-derived neurons were able to form network connections displaying network properties. P19-derived neurons appeared to give inhomogenous response to the neurotransmitters exposed. Ongoing work is done at the moment to further analyse their responses.

Controlling Self-Assembled Structures via Different Hydrophobic Amino Acids in Short Peptide Amphiphiles

Martina Baumann¹, Erik Reimhult¹, Marcus Textor¹

INTRODUCTION: Designing and functionalizing structures on the nanoscale is a goal of research fields ranging from materials science to nanomedicine¹. Self-assembly of molecular building blocks presents a promising route towards controlled engineering of functional macromolecular parts. The ability to self-assemble into ordered structures as well as the straight forward production of peptides make them excellent building blocks to design and build biocompatible structures on the nanoscale, with relevant applications in e.g. drug delivery vehicles, engineering scaffolds and templating^{2,3}. To gain control over the formed structures, insight into the physicochemical processes underlying the self-assembly is crucial.

METHODS: We investigate the influence of systematical changes in the amino acid sequence of short amphiphilic peptides on the self-assembled macromolecular structures. Cationic surfactant-like peptides with systematically varied tail and head regions serve in this study as model peptides, phospholipids biological resembling from membranes in dimension and architecture². Two positively charged amino acids comprise the polar head, and the hydrophobic tail is formed by a repetitive sequence of one apolar amino acid. Such peptides are especially of interest for investigating negatively interactions with charged membranes, e.g. for drug delivery applications. The self-assembled structures of Ac-Ile6Lys2-NH2 (I6K2), Ac-Leu6Lys2-NH2 (L6K2) and Ac-Val6Lys2-NH2 (V6K2) were characterized as function of concentration and temperature. The hydrophobic amino acids were chosen to systematically vary the propensity to form an αhelical secondary structure while conserving the hydrophobicity of the overall sequence⁴. Characterizations of the assembled supramolecular structures were made using transmission electron microscopy (TEM) and atomic force microscopy.

RESULTS: For all three peptides distinct macromolecular structures were found with TEM.

I6K2 assembles into flat ribbon-like structures whereas L6K2 and V6K2 assemble into micellar fibres depending on peptide concentration. CD spectroscopy was used to determine the secondary structure. CD data reveals a β -sheet structure for I6K2 peptides in the assemblies and a random coil structure with an α -helical content for L6K2 and V6K2.

propensity can be used to understand the assembled macromolecular structures. Furthermore, the effect of different kinetic pathways, on intermediate states, secondary structure and assembled superstructure are investigated. In particular annealing at higher temperature has shown to yield a pronounced increase in secondary order and stability.

REFERENCES: 1. Santoso, S., et al., Self-assembly of surfactant-like peptides with variable glycine tails to form nanotubes and nanovesicles. Nano Letters, 2002. **2**(7): p. 687-691. 2. von Maltzahn, G., et al., Positively charged surfactant-like peptides self-assemble into nanostructures. Langmuir, 2003. **19**(10): p. 4332-4337. 3. Zhang S., Fabrication of novel biomaterials through molecular self-assembly. Nat Biotechnol. 2003 Oct; **21**(10): p.1171-8. Review. Pace, C. N. Scholtz, J. M., A helix propensity scale based on experimental studies of peptides and proteins. Biophysical Journal 1998, **75**, (1), 422-427

ACKNOWLEDGEMENTS: Swiss National Science Foundation, NCCR project "Nanoscale Science"

¹ Department of Materials, Laboratory for Surface Science and Technology (LSST), ETH Zurich, Switzerland

Focused Ion Beam Treatment of Self-Assembled Monolayers for Protein Patterning

N. Giamblanco, N. Tuccitto, A. Licciardello, G. Marletta¹.

¹ Dip. di Scienze Chimiche- Università degli studi di Catania, A. Doria, 6, 95125, Catania Italy.

INTRODUCTION: Patterning of protein on surfaces is a topic of great interest for many applications including biosensors and bioelectronic devices¹. The formation of protein patterns requires surfaces combining the resistance to unspecific surface adsorption with spatially-resolved specific binding interactions. In this paper we report a new protein patterning method involving the use of Focused Ion Beams (FIB) combined with metal complex-based self-assembled monolayers (SAM).

METHODS SAM of 11-mercapto-1-undecanol (MUO) was prepared on polycrystalline gold. The MUO-SAM was etched with the focused gallium ion beam to produce square regions of bare gold. Such regions were covered with a mixed² component SAM containing terpyridine ligand that upon reaction with an iron (II) salt produces the iron-terpyridine complexes. The patterned substrate was then incubated with Lactoferrin (LF) 10 μg/ml in millipore H₂O. The adsorption behaviour of LF from aqueous solution on the surface-anchored iron complex and for comparison, onto the original SAM as well as onto the MUO-SAM has been studied in situ by means of Quartz Crystal Microbalance with Dissipation Monitoring (QCM-D)⁴. The spatial selectivity of LF adsorption has been demonstrated by using ToF-SIMS chemical imaging.

RESULTS: The QCM-D adsorption curves of LF on the iron-containing SAM were indicative of remarkable and very fast adsorption. On the contrary, a lower but detectable adsorption also occured in the case of LF on MUO and terpyridine based SAM. The ToF-SIMS chemical maps of the patterned surface before (Fig.1a,b) and after (Fig.1c) LF adsorption results are shown in Fig. 1. In particular, Fig. 1b demonstrates that iron has been selectively fixed on the terpyridine-containg areas (the squares in Fig. 1a) whereas the remaining surface, still covered by the MUO-SAM, is iron-free. Fig. 1b shows that stable protein adsorption occurred selectively on the iron-containing patterns.

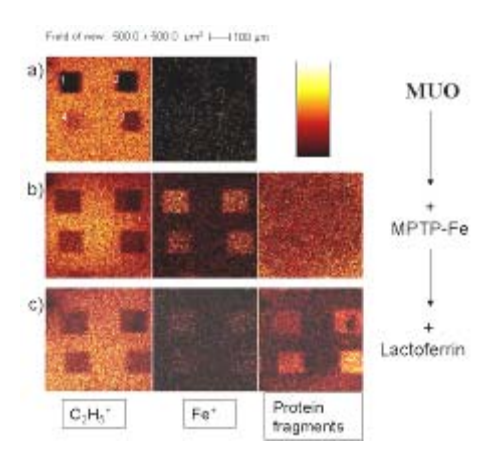


Fig. 1: ToF-SIMS imaging of patterned surface. a) MUO self-assembled monolayer, b) iron complex SAM, c) lactoferrin-treated surface. Numbers in the top-left image indicate ion dose :1>2>3>4.

DISCUSSION & CONCLUSIONS: QCM-D and ToF-SIMS measurements showed that LF monolayers can be selectively and stably adsorbed on the iron-containing areas, but not on the OH-terminated alkanethiol SAM. In conclusion, we developed a bottom-up method for preparing surface patterns of LF by specific non-covalent interactions between the native protein and an iron-terpyridine complex-based SAM.

REFERENCES: ¹ A.S. Blawas, W.M. Reichert (1998) Biomaterials 19: 595-609. ² A. Auditore, N. Tuccitto, G. Marzanni, S. Quici, F. Puntoriero, S. Campagna, A. Licciardello (2003) Chemical .Comunication 19:2494-95. ³ E. Reimhult, C. Larsson, B. Kasemo, F. Hook (2004) Analitycal Chemistry 76:7211-20.

ACKNOWLEDGEMENTS: The authors acknowledge financial support from NationalProject FIRB RBNE01ZB7"MICRAN". The authors wish to thank Dr Silvio Quici (CNR – Milan, Italy) for kindly providing MPTP samples and Genady Zhavnerko (Academy of Science of elarus) for helpful discussions.

Stable planar lipid bilayers in nanopores

A.Studer, L.X.Tiefenauer

Biomolecular Research, Structural Biology, Paul Scherrer Institut, Villigen, Switzerland.

INTRODUCTION: Membrane proteins play a key role in transport, signaling, and energy transduction processes and many of them are potential targets for novel drugs. The requirement of a lipid bilayer for proper function makes the handling of these proteins difficult. Several strategies were pursued to form stable artificial bilavers. Free-standing lipid bilavers nanoporous support offer several advantages: (I) the lipid and electrolyte composition can be defined (II) both sides of the bilayer are accessible and (III) they possess a higher stability than conventional black lipid membranes [1].

METHODS: *Nanopore array chips* (Fig.1) were fabricated as previously reported [2]. The chip (0.6x0.6cm) has a squared silicon nitride membrane (SNM) of 500 μ m width that is 300 nm thick. The $9.6*10^5$ pores with diameters of 200 nm form a total bilayer area of $3.0*10^{-4}cm^2$. The chips were hydrophobically silanized.

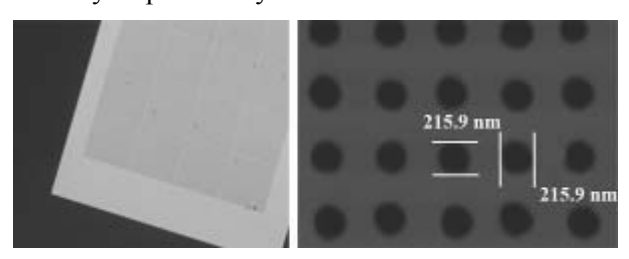


Fig. 1: Micrograph image (left) and SEM image (right) of a silicon nitride membrane

Free-standing lipid bilayers were formed using the Müller-Montal method [3]. The chips were first treated by pentane/hexadecane 9:1 (v/v) before vertically assembled in the measurement cell. 5 μ l of lipid dissolved in pentane (10 mg/ml) was added to the salt solution in both compartments and the level on both compartments were alternatively raised and lowered until the expected increase of impedance was observed.

Electrochemical impedance spectroscopy (EIS) was performed using an Autolab PGSTAT 12 and conducted in the frequency range from 1 MHz to 0.01 Hz at 0 V potential applying the signal amplitude of 10 mV. All experiments were carried out using two platinum wires (1 mm diameter) at room temperature.

RESULTS: The formation of lipid bilayers is clearly recognized as a jump in the impedance value (Fig. 2). From fitting the impedance spectra

using $R_S(R_TC_T)$ as the fitting model for bilayers on SNMs and $R_S(R_{El}C_{El})(R_MC_M)$ for the bare chip, the bilayer resistance and capacitance values are obtained. High membrane resistance values above 1 G Ω were reproducibly achieved. The reported capacitance of lipid bilayers depends on the lipid, the preparation method and the immobilization chemistry and is in the range of 0.4 to 0.9 µF/cm². The specific membrane capacitance of our POPC bilayer preparations in nanopores was 1.6 μF/cm², slightly higher than expected. When the membrane resistance dropped below 1 $G\Omega$ already few bilayers in nanopores may be ruptured. DOPC bilayers have membrane resistance values above this threshold for only 1h whereas POPC bilayers were stable for 5h (n=3). This can be expected since the molecular order parameter of the DOPC with two unsaturated alkyl chains is lower. By reducing the pore diameter from 800 nm to 200 nm we could significantly improve the stability of suspended bilayers [4].

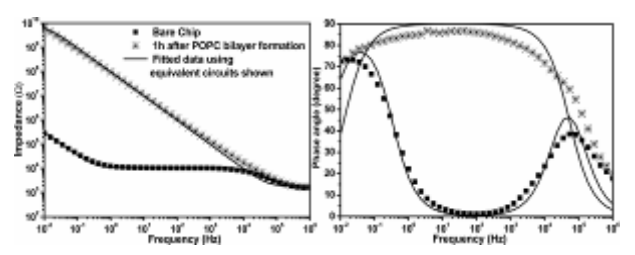


Fig. 2: Impedance spectra measured in 0.5 M KCl before (■) and after (*) POPC bilayer formation. Solid lines represent the fitted data.

CONCLUSIONS: We can form free standing lipid bilayers with commonly occurring lipids which is a requirement to keep mammalian membrane proteins in a functional state. Due to the low aspect ratio of the pores molecular diffusion is free. High bilayer stability and access from both sides allows us now to investigate trans-membrane protein activities.

REFERENCES: ¹W. Römer and C. Steinem (2004) *Biophys. J.* **86**:955-965. ²L.J. Heyderman, et al (2003) *Microelectronic Engin.* **67-8**:208-213 ³M.Montal and P.Müller (1972) *Proc. Natl. Acad. Sci. USA* **69**:3561-3566. ⁴X. Han, et al (2007) *Advanced Materials*, in press.

ACKNOWLEDGEMENTS: The research was partially supported by the Swiss Commission for Technology and Innovation (CTI) grant #7644.2.

Novel surface architectures for biomimetic lipid membranes

E.Reimhult¹, C.Merz¹, Q.Ye¹, R. Konradi¹, M.Textor¹

ETH Zurich, Zurich, Switzerland

INTRODUCTION: Many important biological processes occur at, via or across one of the various lipid membranes present in the cell. Designing and controlling self assembly of model membranes onto sensor substrates thus constitutes an important field of research, enabling applications in e.g. drug screening, dynamic biointerfaces and artificial noses. ¹

We present how mimics of bacterial membranes with applications in antibiotics research can be self-assembled at common biosensor interfaces. Results are also presented on the assembly of poly(L-lysine)-graft-poly(ethylene glycol) (PLL-g-PEG) cushioned lipid membranes for incorporation of large transmembrane proteins on any substrate with negative surface charge.

METHODS: Quartz crystal microbalance with monitoring (QCM-D, dissipation Sweden) and Optical Waveguide Lightmode Spectroscopy (OWLS, MicroVacuum, Hungary) experiments were conducted to follow the adsorption kinetics. The complementary nature of the techniques is used to deduce conformation and conformational changes of the supramolecular assemblies.² To further verify formation of planar supported lipid bilayers (SLB) fluorescence recovery after photobleaching (FRAP) was used. Experiments were performed using bath sonicated large unilamellar lipid vesicles (LUV) and PLL-g-PEG with the PEG functionalized with N⁺-C₁₂H₂₅ "biocide" molecules synthesized in-house.

RESULTS: We show that bacterial lipid membrane mimics of varying degrees of complexity, POPC:POPG (2:1), POPE:POPG (2:1) and E. Coli total lipid extract lipid mixtures (Avanta Polar Lipids, USA), can be self-assembled from LUV onto relevant biosensor materials like TiO₂ and SiO₂ by tuning the concentration of Ca²⁺ ions in a narrow interval up to 2 mM.

We furthermore demonstrate that by tuning the density of "biocide" the capture and deformation of LUV at the interface can be controlled. By adding a trigger step consisting of addition of 30% (v/v) of PEG(8000) the LUV are made to rupture and fuse into a polymer-supported SLB.

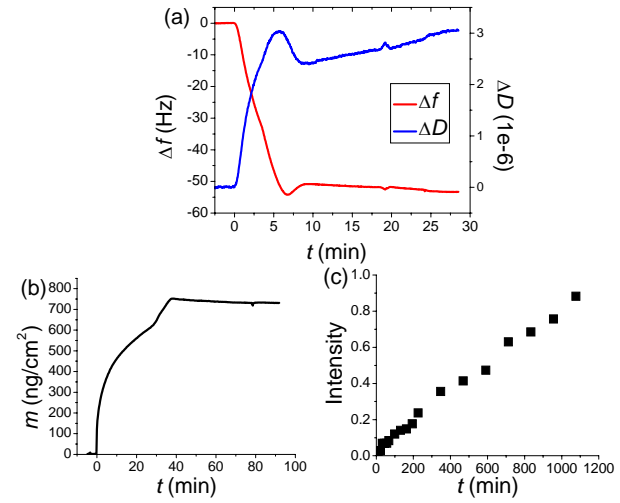


Fig. 1: (a) QCM-D adsorption curve for E. Coli LUV on TiO₂ at 1 mM CaCl₂. (b) OWLS adsorption curve. (c) FRAP recovery data.

DISCUSSION & CONCLUSIONS: While the formation of bacterial mimic SLBs is conclusively demonstrated the results highlight the need for using complementary methods when studying supramolecular assemblies, as demonstrated by the data collected in Fig. 1. A further analysis of e.g. these results indicates formation of an undulating rather than a planar SLB tethered to the surface.

Both the bacterial membrane mimics and the PLL-g-PEG-supported SLB are compatible with a large range of biosensing techniques and through the use of sequential adsorption and rupture steps the PLL-g-PEG-supported SLB is not sensitive to e.g. roughness, charge or other properties of the underlying substrate.

REFERENCES: ¹S. Daniel, F. Albertorio, P.S. Cremer (2006) *MRS Bulletin*, **31**(7):536-540. ²E. Reimhult, B. Kasemo and F. Hook (2004) *Anal Chem*, **76**(24):7211-7220

ACKNOWLEDGEMENTS: Financial support is acknowledged from Competence Center for Materials Science and Technology (CCMX), Switzerland.

Silicone Nanocarpets as Biointerfaces: from Superhydrophobicity to Selective Protein Enrichment

J.Zimmermann, M.Rabe, S.Seeger

Institute of Physical Chemistry, University of Zurich, Zurich, Switzerland.

INTRODUCTION: Surfaces with extreme wetting properties are receiving a lot of attention mainly in regards to fabricating superhydrophobic or superhydrophilic coatings for self cleaning, antifouling or anti-fogging applications. 1 The ability to create a wetting/non wetting contrast on a substrate has expanded the potential of such coatings to areas like liquid handling, micro array technology or open channel microfluidics devices.² We present a simple and versatile procedure to create surfaces with arbitrary superwetting/-nonwetting properties based on a novel, high surface area silicone nanofilament coating.³ Additionally, the coating could be modified to mimic stable, high surface area anionic or cationic exchange resins with specific protein adsorption properties.

METHODS: Details on the preparation of the initial superhydrophobic silicone nanofilament coating can be found in a previous publication.³ To create superhydrophilic/superhydrophobic surface patterns, areas on the coating were selectively activated in an oxygen plasma. The activated areas were chemically modified with 2-(carbomethoxy)ethyltrichlorosilane (CETS) and aminopropyltrichlorosilane (APTES) by standard SAM techniques.

Protein adsorption on the activated, CETS and APTES modified coatings was monitored by fluorescent techniques using dye labelled model proteins β -Lactoglobulin, α -Chymotrypsin, and Lysozyme.

RESULTS: Through plasma activation the initially superhydrophobic silicone nanofilament coating becomes superhydrophilic. In this way a wetting contrast of arbitrary shape and size can be created on a substrate (Figure 1). In a subsequent functionalization step only previously activated areas on the surface are susceptible to chemical modification. This enables a patterning of the surface both with a wetting contrast and a specific chemical functionality. On the charged APTES and CETS modified coating for instance, proteins specifically adsorb according to their electrostatic properties (Figure 2).

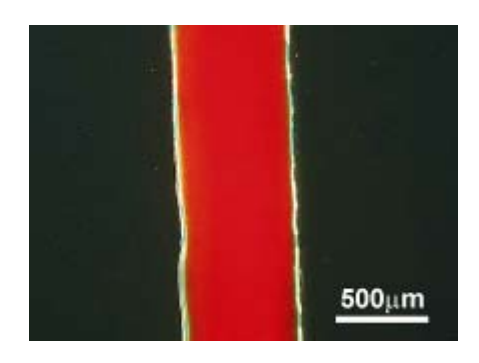


Fig. 1: A superhydrophilic stripe on a superhydrophobic background visualized by fluorescence microscopy.

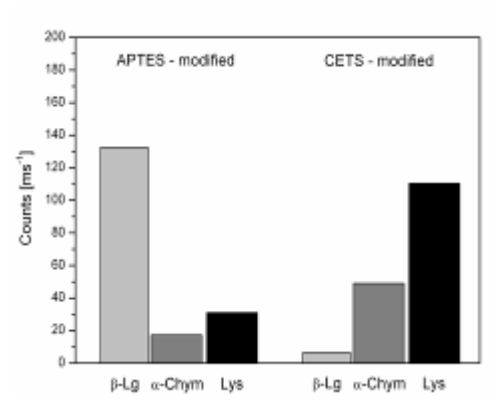


Fig. 2: Equilibrium coverage intensities of fluorescent dye labeled β -Lg, α -Chym and Lys on APTES and CETS modified silicone nanofilaments at pH 6.

DISCUSSION & CONCLUSIONS: The ability to create a diverse wetting and chemical contrast on a single, high surface area substrate will offer many new opportunities in the areas of micro array, micro channel and biosensor applications.

REFERENCES: ¹ Feng, X. J.; Jiang, L. Adv. Mater. 2006, 18, 3063. ² Zhai, L.; Berg, M. C.; Cebeci, F. C.; Kim, Y.; Milwid, J. M.; Rubner, M. F.; Cohen, R. E. Nano Lett. 2006, 6, 1213. ³ Artus, G. R. J.; Jung, S.; Zimmermann, J.; Gautschi, H.-P.; Marquardt, K.; Seeger, S. Adv. Mater. 2006, 18, 2758.

ACKNOWLEDGEMENTS: Financial support was obtained from the Swiss National Foundation (SNF).

Nanogel-based Materials For Drug Delivery System

K. Akiyoshi

¹ Institute of Biomaterials & Bioengineering, Tokyo Medical & Dental University, Tokyo, JAPAN.

² Center of Excellence Program for Frontier Research on Molecular Destruction and Reconstruction of Tooth and Bone, Tokyo Medical & Dental University, Tokyo, JAPAN.

INTRODUCTION: There has been interest in applying nanogels to drug delivery systems, such as protein delivery and gene delivery. In general, chemically cross-linked nanogels are synthesized by microemulsion polymerization or a crosslinking reaction of intra-associated polymer We develop tailor-made functional molecules. nanogels to create novel nanobiomaterials (nanogel engineering) by the self-assembly of functional associating polymers as building blocks¹. In particular, nanogels of cholesteryl group-bearing pullulan (CHP) selectively interact with proteins as a host and are useful as artificial molecular chaperone² and drug carriers such as cancer immune therapy³. Various stimuli-responsive nanogels such as pH, tenperature and light were also obtained by the self-assembly of functional associating polymers. Macrogels with welldefined nanostructures were obtained by using these nanogels as building blocks⁴. The selfassembling method using associating polymers is an efficient and versatile technique for preparing functional nanogels and hydrogels.

We report here recent advances of nanogel engineering for drug delivery system, especially polymerizable nanogels as functional cross-linkers for preparing hybrid hydrogels with nanosize domains for application to tissue engineering.

METHODS: Methacryloyl group - bearing cholesteryl pullulan (CHP) (CHPMA) was prepared by the reaction of CHP ($M_W = 1.0 \times 10^5$) (1.2 cholesteryl groups per 100 glucose units) with glycidyl methacrylate (GMA). For example, the degree of substitution was 6.2 per 100 glucose units (CHPMA6). CHPMA6 formed nanogels (-17nm) by self-assembly in water. The association number of CHPMA6 molecules per nanogel was 4-5 by SEC-MALS. The hybrid hydrogel was prepared by radical polymerization in water with CHPMA nanogel (10-30mg/mL) and MPC (10-30 mg/mL). Acryloyl-group modified (CHPA) molecules, for example, which have 28 acryloyl groups per 100 anhydrous groups, selfassembled to form a relatively monodisperse nanogel with a diameter of 27 nm in water. CHPA nanogel suspension and thiol-group modified poly (ethylene glycol) (PEGSH) solution were mixed as the molar ratio of acryloyl group to thiol group was 1.1

RESULTS: CHPMA nanogels acted effective cross-linkers gelation. **TEM** observation showed that the nanogel structure was retained after gelation and that the nanogels were well dispersed in the hybrid hydrogel. immobilized nanogels retained their ability to encapsulate proteins. addition, the trapped proteins can be released form hydrogel an active form (chaperon like activity).

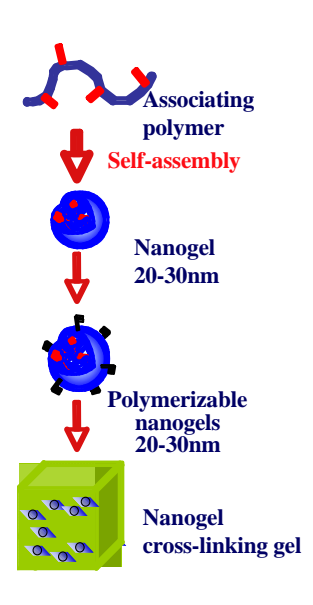


Fig.1 Nanogel engineering

CHPA nanogels were cross-linked with PEGSH to prepare a biodegradable hydrogel (CHP-PEG gel). Galation occurred within 10 minutes when the final concentration of CHPA nanogels was 30 mg/ml in hydorgel. The nanogel structure was maintained after gelation and nanogels distributed homogeneously in the hydrogel. The CHP-PEG hydrogel was an efficient delivery system for bone anabolic agent, PGE_2 and also cytokines.

DISCUSSION & CONCLUSIONS: Nanogel cross-linking hydrogel with chaperon-like activity can be used as a new hydrogel scaffold with isolated binding nanodomain (nanomatrix) of proteins or drugs for tissue engineering.

REFERENCES: ¹N. Morimoto, et al (2006) Nanogel Engineered Designs for Polymeric Drug Delivery in *Polymeric Drug Delivery Volume II* (eds S. Svenson) ACS pp.88-101, ² Y. Nomura, et al (2003) *FEBS Lett.* **553**: 271-276. ³S. Kitano, et al. (2006) *Clinical Cancer Research*, 12:7397-7405. ⁴N. Morimoto, et al (2005) *Biomacromolecules* 6:1829-1834. ⁵N. Kato, et al. (2007) *J. Cell. Biochem.* **101**:1063-1070.

Two-way Interface for Directing the Biological Signals

R.Sklyar

Verchratskogo st. 15-1, Lviv 79010 Ukraine.

INTRODUCTION: Electrical properties of hybrid structures consisting of arrays of nanowire fieldeffect transistors (FETs) integrated with the individual axons and dendrites of live mammalian neurons have been reported. Arrays of nanowirejunctions enable simultaneous neuron measurement of the rate, amplitude, and shape of signals propagating along individual axons and dendrites. Interfacing of nerve cells and FETs is determined by current flow along the electrical resistance of the cell-chip junction. A spectral power density of the junction is $5 \times 10^{-14} \text{ V}^2/\text{Hz}$ and can be interpreted as Nyquist noise of the cell-chip junction with a resistance of 3 MOhm by measuring the fluctuations of extracellular voltage with a low-noise transistor. The thermal noise allows us to elucidate the properties of cell adhesion and it sets a thermodynamical limit for signal-to-noise ratio of neuroelectronic interfacing.

METHODS: Application variety of the novel superconducting, organic and CNT FETs allows us to design transducers of biosignals (BSs) (electronic, nerve, DNA, etc.) that transduce them into different quantities, including electric voltage, density of chemical and biomolecules. On the other hand, the said BSs can be controlled by the applied electrical signals, or bio and chemical mediums [1].

Microdevices with electroplated wire traces were etched with well-defined edges. These devices are implanted in living bodies to connect nerve tissue with electronics to record nerve cell activities or restore lost functions by stimulation of nerve cells. Electroplating of gold meets the requirements for producing neural implants with low-ohmic wire traces, because this technique allows the microfabrication of gold layers with a thickness of several micrometers and lateral dimensions in the same range. Hence the mechanical stability of the electroplated gold is sufficient for chronic implantation of the structures. The implantable microelectrodes for neural applications are based on thin-film polymer foils with embedded microelectrodes for both recording and stimulation.

RESULTS: The peak currents range of BS from 5 to 10 μ A give a maximal output voltage V_{out} on absciss axis -5 to 5V also with the necessity of some its reducing it slightly by changing V_{DS} (bias)

of the FET's channel. A current which elicits an action potential in the neuron is 0.6~nA and will stimulate V_{out} of the transducer equal to 12~mV.

TF of this device will be similar to the previous one:

$$K_{cNW} = \frac{V_{out}}{V_{sup}Q + i} \Longrightarrow \left[\frac{1B}{10^{-7}A}\right] \cong 10^7 \left[\frac{B}{A}\right]$$
 (1)

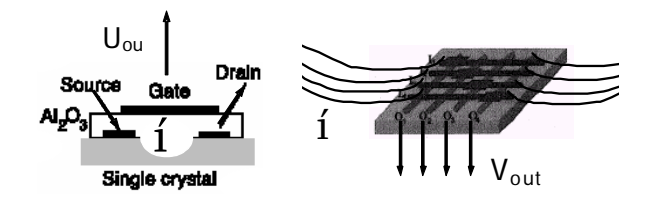


Fig. 1: An organic SuFET device and its electrodes (left); schematic of an interface in the parallel connection (right).

DISCUSSION & **CONCLUSIONS:** described transducers designed on the basis of organic and nano superconducting FETs (SuFETs) are suitable for describing the wide range of BS dynamical parameters. It should be noticeable, that serial connection of the external pickup coils (PCs) allows us to gain some integrated signal, i.e., the whole sensing or control electronic or nerve impulses (NI), which spreads along the number of axons of the nerve fibre; the amount of ions passing through the PCs and the generalized BS passing through one or both spirals of DNA. When SuFET channel(s) of are implanted into the tissue or process we can acquire more precise data about the frequency distribution of NI, volume distribution of ionized molecules and detecting activity of individual nucleoteds [2].

REFERENCES: ¹ R. Sklyar (2003) A SuFET Based Either Implantable or Non-Invasive (Bio)Trans-ducer of Nerve Impulses, 13th International Symposium on Measurement and Control in Robotics - ISMCR'03, Madrid, Spain: 121-6. ² Sklyar R. Superconducting Organic and CNT FETs as a Biochemical Transducer ISMCR 2004: 14th International Symposium on Measurement and Control in Robotics, 16-18 September 2004 - NASA Johnson Space Center, Houston, Texas, IEEE (ISMCR): section 24.

Continuous glucose monitoring in subcutaneous tissue of rats using glucose oxidase based sensors

A Keppler¹, A Feger¹, N Henninger¹, H-M Kloetzer², B Kraenzlin¹, N Gretz¹ and J Pill²

¹Medical Research Center, University Hospital Mannheim, University of Heidelberg, D68167

Mannheim, Germany. ²Roche Diagnostics GmbH, Sandhofer Str. 116, D68305 Mannheim,

Germany

INTRODUCTION: Glucose monitoring is of great importance for the success of complex therapeutic interventions to achieve near normoglycemia in diabetic patients. The substitution of the numerous daily blood glucose measurements by a continuous monitoring system would lead to a considerable progress in the control of the patients' disturbed metabolism.

Aim of our study was to establish an animal model for testing of continuous glucose monitoring systems in normo- as well as hypo- and hyperglycemia. Rats, easy in handling and fast reacting to metabolic changes, were used for verifying the glucose sensor's function.

METHODS: The needle type sensor was composed of a base foil, conduction path, a cover layer for electronic insulation, carbon paste with glucose-oxidase for working electrode silver/silver chloride for the reference electrode. For improving biocompatibility the sensor was covered with MPC (2-methacryloyloxyethyl phosphorylcholine, for details see Woderer et al. 2007). Male SPF Sprague-Dawley rats with a body weight of about 500 g were used for the study. For substance application and blood sampling catheters were inserted into the femoral vein and artery, tunnelled subcutaneously and exteriorized at the back of the neck. The sensors were implanted into the subcutaneous tissue between the scapulae and sutured to the skin. Animals were kept in a rodent work station during the experiment. To achieve hyperglycemia two different kinds of glucose profiles were run: single intravenous injection of glucose (400 mg/kg) and repeated injections (100 mg/kg) every 2 min for a time period of 30 min. After decline to normoglycemia, hypoglycemia was induced by intravenous application of insulin (2U/kg). For reference measurements with an Accu-Check® sensor instrument arterial blood was used.

RESULTS: A close correlation is given between the glucose levels in interstitial fluid (ISF) and the conventional blood glucose readings in hypo- as well as normoglycemia and concentrations up to 300 mg/dL (Fig. 1). Error grid analysis (Table 1) showed the vast majority of data in zone A and B,

demonstrating a good comparability of both methods even over a period of 5 days.

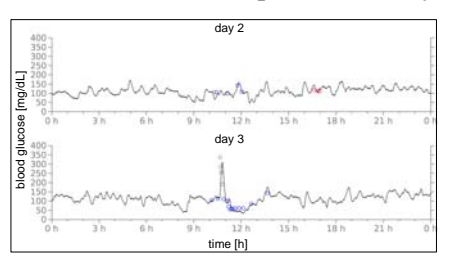


Fig. 1: Continuous glucose monitoring in rat's subcutaneous interstitial fluid (ISF) over a time period of 5 days. Given are the courses of day 2 and 3. Circles indicate spot measurements.

Table 1: Error grid analysis of continuous glucose monitoring in ISF vs. blood glucose (n=3; 5 days)

	error grid zones							
zone	total	A	В	С	D	Е		
absolute	110	71	30	3	6	0		
relative [%]	100	64.5	27.3	2.7	5.5	0		

DISCUSSION & CONCLUSIONS: Good comparability of the sensor readings with the conventional blood glucose measurements in normo- and hypoglycaemic status demonstrates the usefulness of the sensor for in vivo glucose monitoring over at least 5 days. The discrepancy of glucose values above 300 mg/dL may be rather the consequence of fast glucose flux from ISF into cells in metabolically healthy rats than insufficiency of the sensor. Appropriate test systems are essential prerequisites for development and improvement of glucose monitoring systems. Our results demonstrate the rat as a suitable test model for continuous glucose monitoring even over a long time period.

REFERENCES: S. Woderer et al. (2007) Continuous glucose monitoring in interstitial fluid using glucose oxidase-based sensor compared to established blood glucose measurement in rats Analytica Chimica Acta, 581 (1), pp 7-12

ACKNOWLEDGEMENTS: The excellent technical assistance of Viktoria Skude is gratefully acknowledged.

Accu-Check® is a trademark of Roche.

NOVEL SCREENING PROTOCOL FOR UNIVERSAL APPLICABLE ADHESIVE MOLECULES

S.Saxer¹, S.Zürcher¹, S.Tosatti¹, K.Gademann², M.Textor¹

¹ ETH Zurich, Zurich, Switzerland. ² EPF Lausanne, Lausanne, Switzerland.

INTRODUCTION: The arising diversity of biomaterials requires custom-made surfaces that offer application-specific properties. Often surface modification is used to ease an assimilation of the bulk material in different environments and prevent degradation¹. To ensure an adequate surface modification, a firm surface chemistry is needed, which is stable enough to withstand changing conditions over the whole time period. The present work aims on the development of novel binding motifs on the basis of natural adhesives, which shows the extraordinary ability to strongly attach onto various materials^{2,3}. The potential adsorption of single or randomly combined amino acids with different functional groups should be tested under various conditions and surfaces. The high number of experiments requires a novel screening protocol for effective and simultaneous testing. Therefore a multi-well array was designed and verified with a fluorescence-based read out.

METHODS: The verification of the multi-well array is done by the adsorption of poly (L-lysine)-grafted-poly (ethylene glycol) solutions (PLL-g-PEG) in HEPES II buffer. The adsorption is then analyzed by microspot ellipsometry (Sentech SE8500, 350-920nm, spot size; <1mm) and/or by the fluorescence microscope (Zeiss Axioscope 2plus).

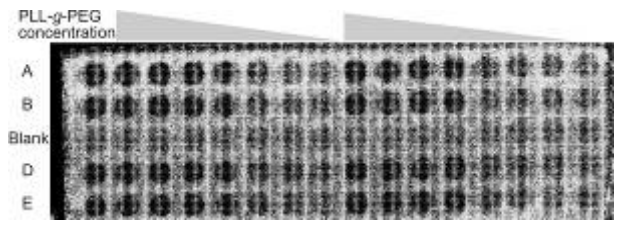
RESULTS: The designed multi-well array is able to perform simultaneously eighty adsorption experiments, each with a volume of $20\mu L$ (Fig. 1).



Fig. 1 Multi-well device

The functionality of the array was tested on glass slides and coated/uncoated silicon wafer, whereas PLL-g-PEG served as an model copolymer, to coat and protect the surface. The quality of this adsorption was then verified with a secondary incubation of FITC-fibrinogen, on top of the PLL-g-PEG layer, followed by measuring the

fluorescence intensity (Fig. 2, top). It shows an increasing FITC-fibrinogen adsorption with decreasing PLL-*g*-PEG layer thickness. Furthermore the adsorption studies were confirmed by microspot ellipsometry (Fig. 2, lower graph).



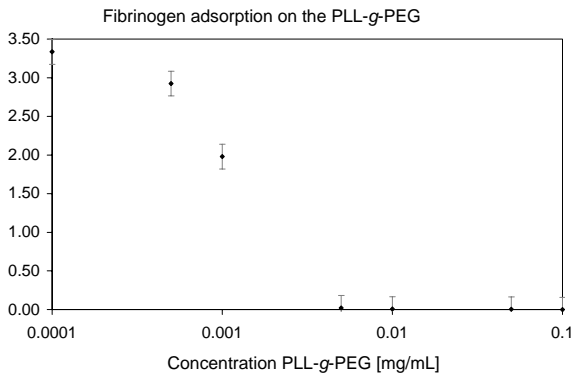


Fig. 2 Fluorescence microscopy & microspot ellipsometry comparison.

DISCUSSION & **CONCLUSIONS:** The fluorescence measurements offer a very fast, semi-quantitative verification of the adsorption properties of different molecules. In addition this data can always be investigated more precisely by microspot ellipsometry, as a secondary method. In the near future new potential adhesive molecules should be linked onto PLL-*g*-PEG and investigated by using the multi-well array.

REFERENCES: ¹Castner, D. G.; Ratner, B. D. (2002) *Surf. Sci.* **500**:28-60. ²Waite, J. H. (2002) *Integr. Comp. Biol.* **42**: 1172-1180. ³Zürcher, S., Wäckerlin, D., Bethuel, Y., Malisova, B., Textor, M., Tosatti, S., Gademann, K. (2006) *J. Am. Chem. Soc.* **128**: 1064-1065

ACKNOWLEDGEMENTS: Thanks to S.Schön, M.Elsener, B.Malisova and the Swiss Nationalfund.

A microarray assay with fluorescent microparticles

Marta Bally, Raghuram Dhumpa, Janos Voeroes

Institute for Biomedical Engineering, Laboratory of Biosensors and Bioelectronics, ETH Zurich, Switzerland

INTRODUCTION: Microarrays make it possible to study thousands of biomolecular interactions in parallel and with high-throughput. While DNA microarrays have already become a standard for the analysis of nucleic acids, protein chips are emerging as a powerful tool for applications in biological research, drug discovery, development and diagnostics. The demand for sensitive assays and further miniaturization requires the optimization of the detection sensitivities. . The aim of this project is to develop a novel bioanalytical assay for the sensitive detection of biomolecular interactions. In this work, microarray assays where performed with fluorescent microparticles coated with capture elements. In order to decrease the background noise, the use of fluidic laminar forces for the discrimination between specific and non-specific bound particles was investigated.

METHODS: Biotinylated bovine serum albumin (BSA-biotin) was spotted onto Ta₂O₅ waveguides coated with dodecylphosphate (Zeptosens, a division of Bayer Schweiz AG, Switzerland). The substrates were blocked by dip-and-rinse with ZeptoMARK Blocking buffer (Zeptosens, Switzerland)). The streptavidin coated fluorescent particles were introduced using a continuous flow. The sample was rinsed with buffer at the same flow rate. Confocal fluorescence microscopy and a ZeptoREADER based on planar waveguide technology were used for imaging.

RESULTS: Microarrays of BSA-biotin were exposed to a continuous flow of streptavidin coated Different flow rates beads. investigated. The ratio of the bead density on the spot to the bead density in the background is shown in Fig 1. The optimal flow rate was found to be situated between 1 µl/min and 2.5µl/min. The lowest concentrations could only be discerned when a flow rate of 2.5 µl/min was applied. However, further reduction led to sedimentation and thus higher background values. The beadbased approach led to a significant increase in spot signal compared to the standard assay performed with fluorescently labeled streptavidin as shown in Fig. 2. While the beads on the spot were clearly visible, the spot incubated with fluorescently labeled streptavidin could not be imaged.

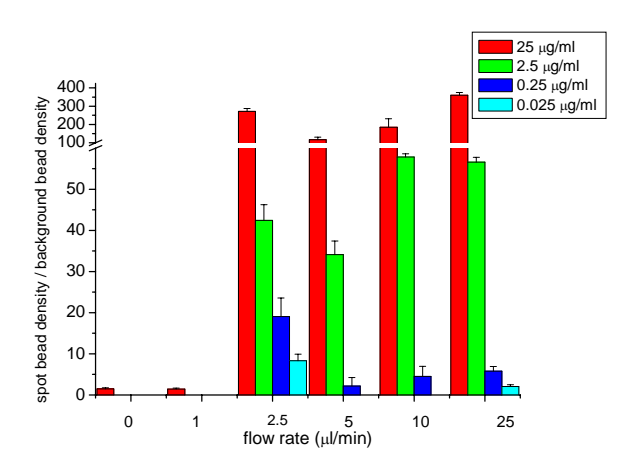


Fig. 1: Ratio of bead density on the spot and bead density in the background for four different BSA-biotin concentrations and different flow rates. The optimal flow rate was $2.5 \mu l/min$.

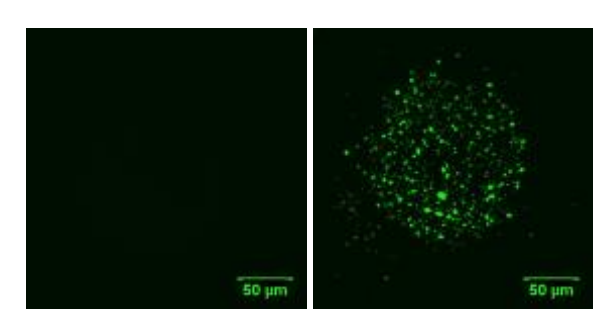


Fig. 2: Microscopy images of a BSA-biotin spot after incubation with streptavidin AlexaFluor488 (left) and streptavidin coated fluorescent beads (right). The same settings were used for both images. The bead-based assay leads to signal amplification.

CONCLUSIONS: We presented a novel approach to perform micoarray assays using fluorescently labeled particles and fluidic flow discrimination. Signal amplification could be achieved when an optimized fluidic force was applied to remove nonspecific bound particles.

ACKNOWLEDGEMENTS: The authors would like to thank Dr. Markus Ehrat and Dr. Ekkehard Kauffmann at Zeptosens for helpful discussions. The CTI (7241.1 NMPP-NM) is acknowledged for financial support.

Binary Nanoparticle Assemblies for Generating Chemical Patterns

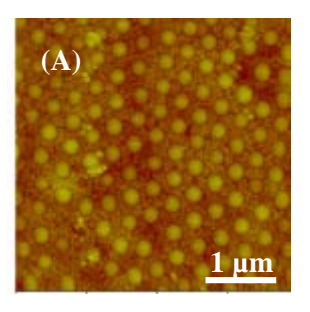
G. Singh, S. Pillai, F. Besenbacher, P. Kingshott
Interdisciplinary Nanoscience Center (iNANO), University of Aarhus, Denmark

INTRODUCTION: Many approaches have focused on preventing protein adsorption aimed at making better medical implants and more sensitive biosensors. These include; grafted polymer layers¹, plasma polymerisation² and oligoethyleneoxide SAMs on gold.³ However, the long term effectiveness of these approaches remain uncertain, therefore alternative methods are of great interest particularly those that can provide a better understanding of protein-surface interactions. Chemical patterning on the nanoscale is one way of generating surface regions with low concentrations of molecules and potentially provides a platform for probing functionality down to the single molecule level. One of the promising ways of generating nanopatterns is by decoration of surfaces with nanoparticles of different size and chemical functionality. Several methods have been developed to grow binary nanoparticle assemblies such as layer-by-layer (LBL) approaches⁴ and onestep assembly. Here, we demonstrate a simple onestep process that generates ordered binary colloidal particles of different surface chemistry assembled on hydrophobic surfaces.

METHODS: The patterns are generated from either diluted or concentrated suspensions of poly(styrene) (PS) nanoparticles of different sizes (diameter = 500nm to 60nm), different size ratios and volume fractions, and different nanoparticle surface chemistry (sulfonated, carboxylated, or aminated). Si wafers and glass are made hydrophobic by modification with OTS (octadecyl tricholorosilane). In addition, adhesive carbon tape is used as a substrate. After preparing nanoparticles suspensions in McIlvaine's buffer with appropriate size ratios and volume fractions, droplets of 25 µl are placed on surface and the assembly process takes place over night under vacuum conditions. We use AFM and SEM to observe the nanoparticles assemblies formed after solvent evaporation.

RESULTS: Figures 1 A and B shows AFM height images of two component patterns formed using 60nm sulphated-PS and 350nm sulphated-PS nanoparticles on carbon tape and OTS modified glass substrate. This pattern consists of a hexagonally packed array of large particles with regularly inter-dispersed with the smaller particles.

The patterns are formed independent of the surface chemistry of the particles (data to be presented).



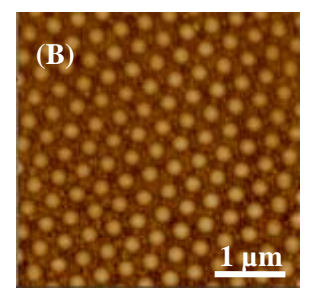


Fig. 1: Two-component patterning using 60nm sulfated-PS NPs and 350 nm sulfated-PS NPs (pH 7) on different substrates. (A) AFM height of a two-component colloid crystal assembled on carbon tape. Peak-to-peak distance was 351 nm. (B) Corresponding height images of hydrophobic glass (OTS-modified) Peak-to-peak distance was 355 nm

DISCUSSION & CONCLUSIONS: The patterns are formed by an entropically driven process upon drying where solvent evaporation increases the particle volume fraction to stage where it is high enough to induce colloid crystal formation. The surface is hydrophobic enough to prevent spreading of solvent. In short, we show that hexagonal structured pattern with twocomponents nanoparticles of varying size and volume fraction can be created by a simple drop-casting process and this provides us with a unique capability to manipulate both surface structure and chemistry at nanoscale level. This is of importance in order to understand and control interfacial phenomena, such as protein adsorption and directed immobilization, cell and bacterial adhesion, and controlled surface wetting in areas of biosensors, medical materials. Future work will involve taking advantage of the surface patterns to perform surface reactions with molecules that have improved functionality.

REFERENCES: 1) N. Nath et al. Surf.,Sci. 2004,570,98. 2) Z. Ademovic et al. Plasma Proc. Polym. 2005,2,53-63. 3) K.L. Prime and G.M. Whitesides. Science 1991,252,1164. 4) X. Hunag et al. Langmuir,2007.

ACKNOWLEDGEMENTS: The Danish research Council for Technology and Production Sciences for an International PhD stipend.

Oriented transfer of proteins for biosensor applications

C. Volcke^{1,2}, R. P. Ghandiraman¹, L. Basabe-Desmonts¹, A. Riaz¹, A. Cafolla¹ and B. McCraith¹

¹ Biomedical Diagnostics Institute, Dublin City University, Dublin, Ireland. ² Laboratoire Lasers et Spectroscopies, University of Namur, Namur, Belgium.

INTRODUCTION: The orientation of antibodies upon their immobilisation on different surfacesis a crucial factor affecting their recognition properties. This phenomenon is strongly dependent on surface properties such as composition, reactivity, wettability, roughness etc. [1-2]. Some polymeric substrates, such as Zeonor, are used in bio-medical or -technological devices, mainly because of their interesting optical properties, low production time cost. However, their surface and modification/functionalisation is more difficult to perform as compared to other widely studied metallic substrates (such as gold or silicon).

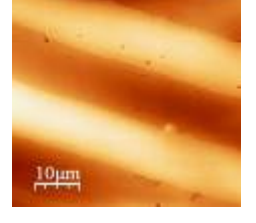
Our objective is to overcome these problems by performing a two-step experiment. The first step uses the advantages of well-known modified metallic/semiconducting substrates (in particular organosilane-modified silicon) for the orientation of antibodies [3-4]. The second step consists of transferring the oriented antibodies onto a second substrate, which may have unfavourable characteristics. This transfer process is based on the template-imprinted nanostructures technique developed by Ratner et al. [5]. In this poster, we focus in particular on the transfer process of proteins from one substrate to the other.

METHODS: The transfer process may be described briefly as follows: a selected protein (fibrinogen, avidin or antibody) is microcontact printed onto a SiO₂ surface, a sugar layer is then spin coated on top of the patterned surface. This is followed by the deposition of a polymer-like layer using a 13.56 MHz RF capacitively coupled plasma in a PECVD reactor. This upper polymerlike layer is then glued to a second substrate. Finally the substrates are separated. microprinted pattern of proteins is therefore transferred to the second substrate. During these experiments, the wettability, film thickness, film morphology were characterised using contact angle measurements (CA), spectroscopic ellipsometry (SE) and atomic force microscopy (AFM), respectively. Fluorescence microscopy was also used to determine the presence of tagged-proteins on the transferred substrate.

RESULTS. We first demonstrate (using AFM) the transfer of microprinted patterns of non oriented

proteins (fibrinogen – Fig. 1 left). We then show that, when using Cy5-labelled anti-human IgG, such patterns are composed of proteins (as revealed by fluorescence microscopy – Figure 1 right). Finally the function of the transferred proteins is investigated using antibodies, which are

recognised by antigens after transfer.



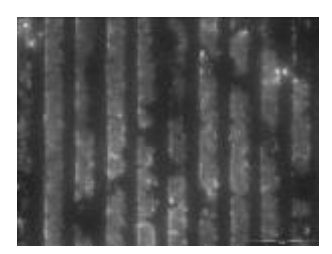


Fig. 1: AFM image (50μm) of fibrinogen microprinted lines after transfer process (left). Fluorescence image of microcontact printed lines of Cy5-labelled anti-human IgG after transfer process (right).

CONCLUSIONS: In this poster, we have demonstrated the transfer of protein from one substrate to another without modifying the protein and its properties. Particularly, the recognition between antigens and antibodies was also proved after transfer of antibodies.

REFERENCES: ¹ A. Sethuraman, M. Han, R.S. Kane et al (2004) *Langmuir* **20**:7779-88. ² L.-C. Xu and C.A. Siedlecki (2007) *Biomaterials* **28**:3273-83. ³ S. Chen, L. Liu, J. Zhou et al (2003) *Langmuir* **19**: 2859-64. ⁴ H. Wang, D.G. Castner, B.D. Ratner et al (2003) *Langmuir* **20**:1877-87. ⁵ H. Shi, W.-B. Tsai, M.D. Garrison et al (1999) *Nature* **398**:593-597.

ACKNOWLEDGEMENTS: C.V. is a postdoctoral researcher of the Belgian National Fund for Scientific Research (F.N.R.S.). Financial support of the Science Fundation Ireland (S.F.I.) is acknowledged.

Surface Functionalization of Single Superparamagnetic Iron Oxide Nanoparticles for Targeted Magnetic Resonance Imaging (MRI)

Esther Amstad¹, Stefan Zurcher¹, Joyce, Y. Wong², Marcus Textor¹, Erik Reimhult¹

¹ Laboratory for Surface Science and Technology, Department of Material Science, ETH Zurich, Switzerland. ² Department of Biomedical Engineering, Boston University, USA.

INTRODUCTION: Magnetic resonance imaging (MRI) is a non-invasive imaging technique often used in clinics for diagnostic purposes. However, its limited spatial resolution prevents the detection of individual cells or even molecules. Targeted MR contrast agents are thought to offer this possibility. Non-targeted ccommercially available negative magnetic resonance (MR) contrast agents such as Feridex often consist of multiple iron oxide cores embedded in a macromolecular matrix such as This results in clusters with a hydrodynamic diameter which is a multiple of the iron oxide core diameter and has a broad size distribution. An alternative to the reversibly binding dextran is PEG-gallol. The latter molecule has a considerably higher binding affinity towards iron oxide nanoparticles compared to dextran, leading to enhanced particle stability and smaller particle diameters.

METHODS: Superparamagnetic iron nanoparticles have been synthesized by aqueous precipitation reaction and were stabilized individually using PEG-gallol. Particle size, thermal stability and magnetic properties of these individually stabilized PEGylated particles have been compared with Feridex. To functionalize the former particles, iron oxide cores were coated with a mixture of biotinylated PEG(3400)-gallol and non-biotinylated PEG(550)-gallol. Neutravidin, a biotin-binding protein, served as a linker between the PEGylated particles bearing biotin sites and biotinylated functional groups. In a first approach, these neutravidin coated PEGylated nanoparticles were targeted against atherosclerotic sites by attaching a custom-synthesized biotinylated peptide sequence known to bind to E-selectin to them¹. E-selectin is a transmembrane protein expressed on inflamed endothelial cells². It thus is an early marker for atherosclerosis.

RESULTS: The high binding affinity of gallol towards iron oxide surfaces results in a high particle stability and a well-controllable interface chemistry. Neutravidin served as an intermediate layer between the biotinylated particles and biotinylated ligands. Specific particle binding was maximized by doing binding studies with the

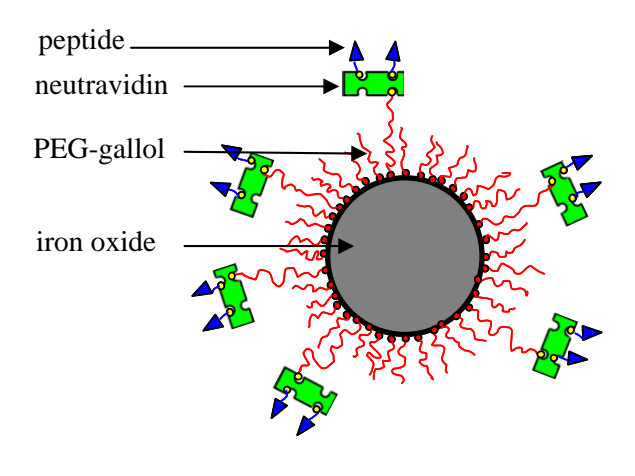


Fig. 1: Cartoon of functionalized superparamagnetic iron oxide nanoparticles. These particles were stabilized with PEG-gallol. To the biotin-bearing PEG chains, neutravidin was added, serving as a linker to attach biotinylated peptides.

quartz crystal microbalance with dissipation monitoring (QCM-D).

DISCUSSION & CONCLUSIONS: Stabilization of single superparamagnetic iron oxide nanoparticles with PEG-gallol results in high particle stability under physiological conditions and allows further functionalization of these negative MR contrast agents. Due to the smaller hydrodynamic diameter, narrower particle size distribution, enhanced particle stability, and similar r₂-values of PEGylated particles compared to Feridex, the former particles are suited as versatile and easy-to-handle research tool for comparing binding efficiencies of ligands immobilized on these negative MR contrast agents.

REFERENCES: ¹ Martens, C.L., et al., Peptides Which Bind to E-Selectin and Block Neutrophil Adhesion. Journal of Biological Chemistry, 1995. 270(36): p. 21129-21136.

² Choudhury, R.P., V. Fuster, and Z.A. Fayad, Molecular, cellular and functional imaging of atherothrombosis. Nature Reviews Drug Discovery, 2004. 3(11): p. 913-925.

Stimuli responsive core-shell silica nanoparticles

Lucy Kind¹, Axel Müller², Uwe Pieles³, Andreas Taubert⁴, Wolfgang Meier¹

¹University of Basel, Basel, Switzerland. ²University of Bayreuth, Bayreuth, Germany. ³University of Life Sciences, Muttenz, Switzerland. ⁴University of Potsdam, Golm, Germany.

INTRODUCTION: Silica nanoparticles gain increasing interest because of their excellent properties such as low density, high specific surface area, adsorption capacity, and the ability for encapsulation. These characteristics can be combined in a hybrid particle with the pH and temperature sensitivity of star shaped polyelectrolytes like poly(*N*,*N*-dimethylaminoethyl methacrylate (poly(DMAEMA)). The polymers form a template for the condensation of tetraethyl orthosilicate (TEOS), which leads to the formation of a silica shell around the polymer molecules.

Here, we investigated the morphology of the silica nanoparticles. The core shell structure of the particles makes them highly interesting for host / guest encapsulation that is relevant for bioimaging or triggered release. Particularly interesting is that the polymer core of the particles shows a pH and temperature dependant solution behavior and ion-specific effects. The associated conformational changes of the polymer create a disruption of the inorganic shells that can be used as a trigger for controlled release.

METHODS: Core-shell silica particles were synthesized proceeding from Poly{[2-(methacryloyloxy)ethyl] trimethylammonium iodide (PMETAI)¹ as templates by condensation reaction of tetraethyl orthosilicate (TEOS) in aqueous solution. The resulting particle size and structure was determined by TEM, SEM and AFM. Host / guest encapsulation and triggered release were detected by Fluorescence Correlation Spectroscopy (FCS) using a Zeiss ConfoCor 2 setup.

RESULTS: Based on various concentrations of silica monomer the particles resulted in different shapes as shown in Fig. 1 and 2.

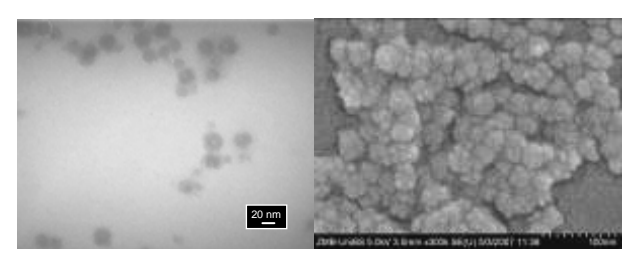


Fig. 1: TEM and SEM from particles obtained with 13.4mM TEOS

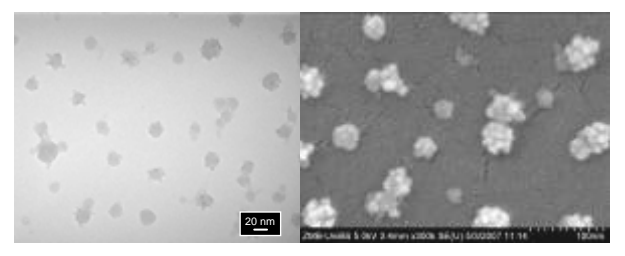


Fig. 2: TEM and SEM from particles obtained with 44.8mM TEOS

A small concentration of TEOS directed to spherically shaped particles with a lower density in the core (Fig.1). Raising the amount of silica monomer leads to blackberry-shaped particles (Fig.2).

FCS showed that an encapsulated dye (Sulforhodamine G) could be released from coreshell silica nanoparticles after changing the pH of the solution (Fig.3).

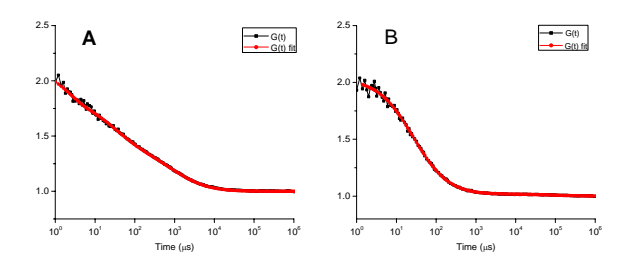


Fig.3: Autocorrelation curves of core-shell silica nanoparticles (in aqueous solution) with encapsulated dye (Sulforhodanine G) at pH6 (Reference) (A) and at pH9 (B).

DISCUSSION & CONCLUSIONS: Concerning these tunable core-shell silica particles there is a potential of encapsulation and following release of applicable substances. Due to the small size and their properties these hybrid particles can play an important role in bioimaging

REFERENCES: ¹F.A. Plamper, A. Walther, Axel H.E. Müller, M. Ballauff (2007) Nano Letters 7 (1):167-171.

ACKNOWLEDGEMENTS: This work is supported by National Center of Competence in Research (NCCR) and Swiss National Science Foundation (SNF).

Fabrication and Visualization of Metal Ion Patterns on Sensing Fluorescent SAMs with AFFM

C. C. Wu^{1,2}, L. Basabe-Desmonts², K. van der Werf¹, C. Otto¹, A. H. Velders², M. Crego-Calama², D. N. Reinhoudt², and V. Subramaniam¹

¹Biophysical Engineering Group, ² Laboratory of Supramolecular Chemistry and Technology, MESA⁺ Institute for Nanotechnology, University of Twente, the Netherlands

INTRODUCTION: Developing miniaturized patterned substrates at μ and sub- μ scale with optical readouts is very important for chemical and biological sensors.[1,2] The combination of optical and scanning probe microscopy and fluorescent self-assembled monolayer technologies will enable the development of sensors of great versatility. In this study, we employed our home-built atomic force fluorescence microscope (AFFM), a combination of atomic force microscope and confocal fluorescent microscope, to write calcium metal ions onto the sensitive fluorescent selfassembled monolayer (SAM) by dip nanolithography (DPN), and visualize modulations of fluorescence intensity resulting from the presence of Ca²⁺ immediately.

METHODS: The sensitive fluorescent SAM, TM1, coated on glass slides was fabricated basically following the protocol published in our group previously except for small modifications [2]. Figure 1 illustrates the procedures of preparing TM1 substrates. The amino terminated SAM were prepared in dry toluene solution of N-[3-(trimethoxysily)propyl]ethylenediamine (TPEDA) first. After that, the fluorophore and binding group, 5-(and-6)-carboxytetramethylrhodamine,

succinimidyl ester (5(6)-TAMRA, SE) and hexanoyl chloride, were immobilized onto the TPEDA SAM randomly to yield the TM1 SAM.

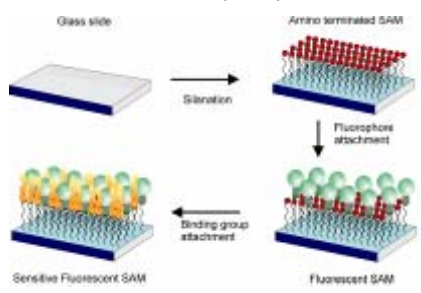
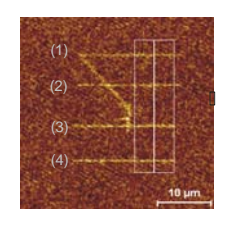


Fig. 1: Schematic representation of the preparation procedures of sensitive fluorescent self-assembled monolayers.

Commercial Si_3N_4 AFM cantilevers with nominal spring constant of 0.05 N/m were used. Right before DPN experiments, cantilevers were rinsed with ethanol and dried under a nitrogen stream gently. The cantilevers were then exposed under UV light for 30 minutes. Subsequently, the cleaned

cantilevers were immersed into the ink solutions (10⁻¹ M ethanol solution of the per-chlorate salts of calcium) for 5 minutes and then dried in air. The DPN experiments were all carried out in contact mode. The load applied by the AFM tip to substrate was kept between 10 and 30 nN to avoid damaging of the SAM.

RESULTS: Figures 2 exhibits four horizontal bright lines of 18 μ m in long generated by deposition of Ca²⁺ ions onto TM1 SAM with a scan rate of 1.8 μ m s⁻¹ for 2, 4, 6 and 8 minutes individually (from (1) to (4)). The width of each line is approximately 0.6 μ m. The line width shown in the image does not correspond to the actual deposited line width because confocal fluorescence microscope has a lateral resolution of the half wavelength value of the excitation beam.



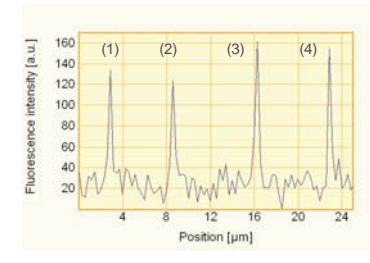


Fig. 2: Fluorescent image of a TM1 SAM acquired from AFFM right after the deposition of Ca²⁺ lines.

DISCUSSION & **CONCLUSIONS:** We demonstrate that it is possible to transfer Ca²⁺ onto TM1 SAMs observing the enhancement of fluorescent intensity instantaneously using AFFM. This study may allow us to explore in more detail the role of different inks, ink diffusion, and other fundamental aspects of DPN.

REFERENCES: ¹R. Kassies, K. O. Van der Werf, et al (2005), *J. Microscopy* **217**: 109-116 ²L. Basabe-Desmonts, J. Beld, et al (2004), *J. Am. Chem. Soc.* **126**: 7293-7299.

ACKNOWLEDGEMENTS: This work was supported by NanoNed and the MESA⁺ Institute for Nanotechnology.

Nanoscale Patterning Of Photosynthetic Light Harvesting Proteins

N. Reynolds¹, S. Janusz¹, C.N. Hunter², G.J. Leggett¹

¹ The Department of Chemistry, The University of Sheffield, UK. ²Molecular Biology and Biotechnology, The University of Sheffield, UK.

INTRODUCTION: Here we present patterning of light harvesting 2 (LH2) complexes from the photosynthetic bacterium Rhodobacter sphaeroides. LH2 complexes consist of circular arrays of bacteriochlorophyll and carotenoid molecules, held together by a cylindrical assembly of polypeptides. As many as 100 LH2 complexes are organized in the membrane to form an interconnected energy transfer network comprising thousands of bacteriochlorophyll molecules that absorb photons, channeling the excitation energy down an energy gradient towards the reaction centre (RC), leading to a charge separation that drives subsequent biosynthetic reactions in the cell. removed from photosynthetic When the membrane, LH2 complexes retain the ability to absorb light, and they emit the energy as fluorescence. This property has been utilized in order to gain insight into the biological functionality of the LH2 after immobilization on to nanoscale patterned surfaces.

METHODS: Alkanethiol SAMs on gold surfaces used in conjunction photolithographic techniques to produce patterned assemblies of LH2. Selective exposure of alkanethiols to UV light (wavelength 244 nm) leads to their photo-oxidation to alkylsulfonates, which may be displaced by a second thiol in a solution-phase process. The adsorption of LH2 onto SAMs with a variety of functional groups has been measured by surface plasmon resonance (SPR) in order to determine which surfaces resist non-specific adsorption. In contrast to plasma proteins, which adsorb strongly to most surfaces, simple patterns consisting of hydrophilic and hydrophobic regions may be used effectively to pattern LH2. Covalent attachment to carboxylic acid groups using carbodiimide activation methods is an effective means of immobilizing LH2 at the surface. Fluorescence spectroscopy measurements of proteins immobilized by attachment to patterned SAMs were used to determine the biological activity of the complexes once immobilized to the surface. Nanoscale chemical patterns have been fabricated using scanning near-field photolithography (SNP), in which a scanning nearfield optical microscope coupled to a UV laser is used to selectively expose regions of a SAM

RESULTS & DISCUSSION: The fluorescent spectroscopy results have confirmed that biological function is retained, leading to the observation of absorption spectra qualitatively identical to those of complexes in solution. Using SNP, lines of carboxylic acid functionalized thiols as small as 70nm have been fabricated in monolayers of perfluoronated thiols and used to form LH2 structures with a width of less than 100nm. Methodologies such as this, that are based on nearfield photolithography offer great promise for the fabrication of functional, nanostructured assemblies of membrane proteins.

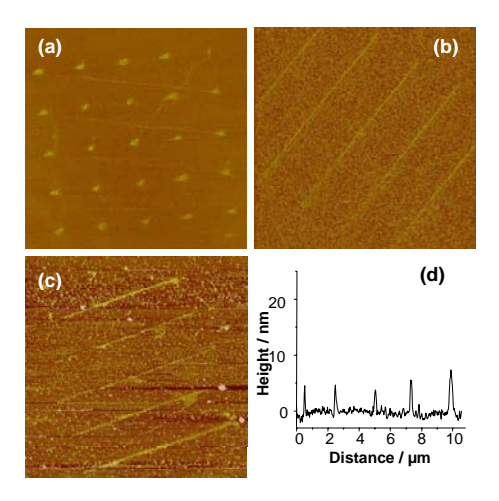


Table 1.: AFM images of nanoscale patterns fabricated by SNP^{1} . (a) $12 \mu m \times 12 \mu m$ FFM image of an array of $C_{10}COOH$ dots in a $C_{2}F_{5}CF_{3}$ monolayer. (b) $15 \mu m \times 15 \mu m$ FFM image of $C_{10}COOH$ lines in a $C_{2}F_{5}CF_{3}$ monolayer. (c) $15 \mu m \times 15 \mu m$ tapping mode image of LH2 immobilised onto $C_{10}COOH$ lines (z-range 0-40 nm). (d) cross-section across the nanolines in (c) with a mean FWHM of 98 nm.

REFERENCES: 1. Reynolds et. al., submitted, 2007

Plasma polymer surfaces for high-throughput microfluidic proteomic analysis

G.J.S.Fowler¹, A.M.Pereira², B.O'Sullivan², G.Mishra¹, P.C.Wright², S.L.McArthur¹

¹ Dept. of Engineering Materials, The Kroto Research Institute, University of Sheffield, UK
² Dept. of Chemical and Process Engineering, University of Sheffield, UK

INTRODUCTION: Proteomics, the identification and quantification of the protein component of parallel biological samples, has at its core the procedures of protein extraction, protein separation, proteolytic cleavage and mass analysis. In order to move on from 2D-gel-based procedures it is necessary to design high-throughput microfluidic gel-free devices. In this study the use of plasma polymerisation allows the introduction of both physical and chemical characteristics microchannels. demonstrate a proteolytic We microreactor as well as microfluidic devices that allow the isolation of subclasses of peptides from a peptide mixture.

METHODS: Plasma polymerisation, absorbance and fluorescence spectroscopy, X-ray photoelectron spectroscopy, LC-MS/MS mass spectrometry, ELISA

RESULTS & DISCUSSION:

Plasma polymers have been used for the covalent immobilisation of various enzymes and as a platform for protein/peptide immobilising transition.metal ions. Plasma polymers are used because they can be introduced onto virtually any substrate to produce coatings of a control thickness and composition.

Trypsin has been covalently immobilised to plasma polymerised poly(acrylic acid) and its activity tested with L-BAPA, epicocconone-labelled proteins (LavaDigest) and mass spectrometry.

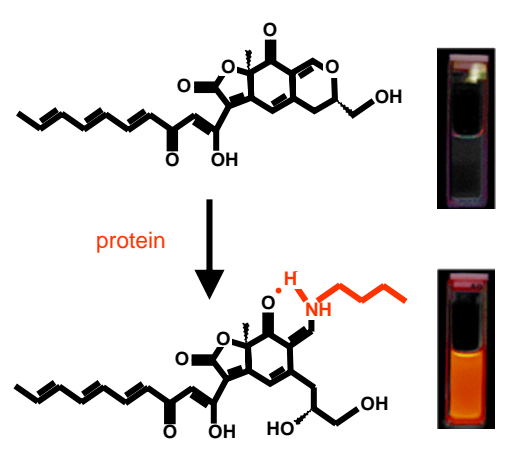


Fig 1: Fluorescent complexes of proteins combined with tryptic peptide identification by MS are used to test effectiveness of proteolytic surfaces.

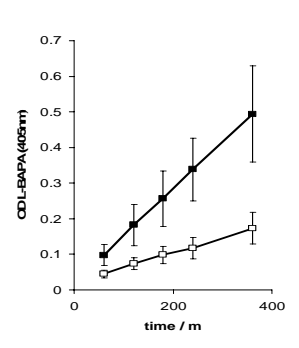


Fig 2. Activity of trypsin EDC/NHS-preimmobilised onto polyacrylic acid plasma polymer surfaces under static conditions as assessed using colorimetric agent L-BAPA. (Trypsin concentration in PBS solution during immobilisation; ■ 0.5mg/ml, □ 0.1mg/ml).

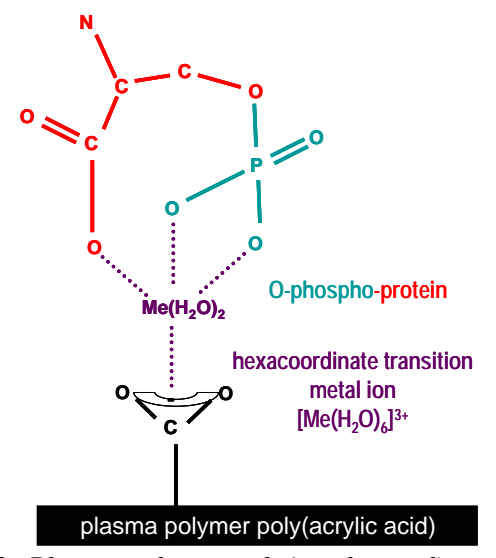


Fig 3: Plasma polymer poly(acrylic acid) used as a platform for immobilised metal ion affinity chromatography (IMAC) The phosphorylated protein O-phospho-L-serine-BSA (see above) has been isolated from solution using transition metal-treated plasma polymer surfaces, and the process assessed using anti-phospho-antibody ELISA and spectroscopy.

CONCLUSIONS: We have demonstrated that plasma polymers can be used both to immobilise proteins and peptide-selective metal ions. In this way we can produce microfluidic components for high-through-put gel-free proteomic analysis.

Patterning of Plasma Polymers for Bioarrays

G. Mishra, S. L. McArthur

Department of Engineering Materials, University of Sheffield, UK

INTRODUCTION: Modern day technological advancements have allowed us to overcome critical challenges posed in proteomic research. As a direct result of developments in miniaturization and automation, the current market has seen ever growing numbers and varieties of high density arraying slides being used for proteome research and application. Needless to say that these developments have been matched with state of art instrumentation and data analysis packages to achieve true automated multiplex analysis. Yet, issues like non-specific adsorption of biomolecules to solid substrate and control over the orientation during immobilization need addressing. Key to these issues could be the precise control over surface modification and patterning. Plasma polymerisation presents a versatile approach to surface modification of these devices. The range of monomers available for plasma polymerisation makes this manufacturing approach even more suitable for use in systems where multiple coatings with specific properties are required for a single device. The ability to spatially define reactive regions to reduce non-specific background adsorption is integral to this project.

METHODS: Characterisation of Plasma polymers, X-ray photoelectron spectroscopy (XPS), Time-of-Flight Static Secondary Ion Mass Spectroscopy (ToF-SSIMS), ATR Fourier Transform Infrared Spectroscopy (FTIR), fluorescence microscopy

RESULTS & DISCUSSION: In this study we use plasma polymerisation technique to functionalise a surface for physical and covalent attachment of biomolecule in a controlled fashion. Various patterning techniques including photolithography and physical masks have been used to compare the pattern resolution and functionality using XPS, ToF-SIMS and AFM. Plasma polymerisation has been used in conjugation with photolithography thus allowing us to simultaneously obtain high spatial and chemical resolution. Multivariate analysis of ToF-SIMS spectral and image data has allowed us to not only optimise the system to retain maximum chemical functional groups but also to critically study and address issues associated with the chemical specificity and spatial resolution of the multilayer patterning approach. Our results suggest that complex multilayer plasma coatings can be produced without compromising the chemical properties of the deposited polymer layers.

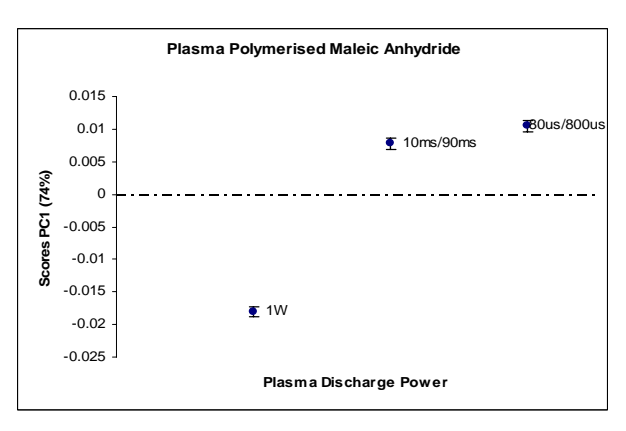


Figure 1: Scores for the first PC of positive ion ToF-SIMS spectra of maleic anhydride plasma polymer showing higher functional group retention under μs pulse plasma discharge condition.

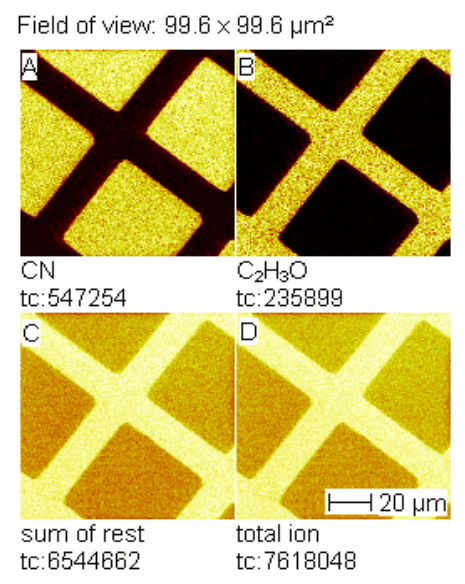


Figure 2: Negative ion ToF-SSIMS image showing regions of (a) plasma polymerised allylamine surrounded by background region of (b) plasma polymerised tetraglyme. Photolithography was used as a patterning technique in this case.

CONCLUSIONS: We have demonstrated that photolithography can be adapted to pattern plasma polymers for bioarray applications. High chemical and spatial pattern resolution can be achieved by using this technique.

Design of a Flow Chamber to Study Shear Stress Induced Endothelial Cell Orientation On/Within Different Modified 3D- Fibrin Matrices

B. Koelsch, M. Rimann and H. Hall

Cells and BioMaterials, Department of Materials, ETH, Zurich, Switzerland.

INTRODUCTION: All tissues require sufficient blood perfusion in order to function properly, as deficient perfusion often lead to loss of function. In hopes of returning sufficient perfusion to ischemic tissues, therapeutic angiogenesis attempts to stimulate the body's endogenous ability to develop new blood vessels. One approach is to stimulate wound healing and tissue regeneration with 3Dfibrin hydrogel matrices that present specific adhesion sequences for integrin attachment. Here we explore the integration of the sixth Ig-like domain of L1 (L1Ig6) into a fibrin matrix, which interacts with the $\alpha_{\nu}\beta_{3}$ integrin present on endothelial cells. It has previously been shown that in vivo interaction between L1Ig6 and $\alpha_{v}\beta_{3}$ stimulates angiogenesis [1].

Under physiological conditions, endothelial cells are exposed to a wide range of mechanical shear stresses from blood flow, resulting in gene regulation and cellular rearrangements [2]. To date, however, the effects of shear stress on endothelial cells in/on L1Ig6-modified 3D-fibrin hydrogel matrices have not been investigated.

The aim of this project was to develop a flow chamber to study HUVECs cultured on/within 3D-3D-fibrin hydrogel matrices and characterize different flow characteristics.

METHODS: Parallel plate flow channels have become the standard in researching cellular responses to shear flow. Therefore, an adapted version was designed that allowed cell culturing in 3D-fibrin matrices. PDMS was used as chamber material as it is gas permeable. For optimal analysis of the cells in the flow device, the overall dimensions of the chamber are limited to that of a standard microscope slide (76 x 26 mm).

Important in the development of parallel plate flow chambers are the dimensions. For laminar flow, the Reynolds numbers must lie below 2000. The ratio height/width for most flow chambers lies below 0.015 [3]. Given the assigned range for these two parameters, flow can be assumed to be within an infinite parallel plate. This gives the following shear stress (τ) and entrance length (l_e) formulas:

$$\tau = (6\mu \text{ O}) / (h^2 \text{w})$$
 (1)

$$l_e = Re(0.08 h)$$
 (2)

RESULTS: The newly designed flow chamber is seen in Figure 1. The reservoir for 3D-matrices and cell culture is located in the middle of the channel to ensure a homogeneous shear stress over it that is neither influenced by entrance or wall effects. Both at the entrance and at the exit fluid reservoirs have been placed, which both facilitate tube attachment and even fluid flow.

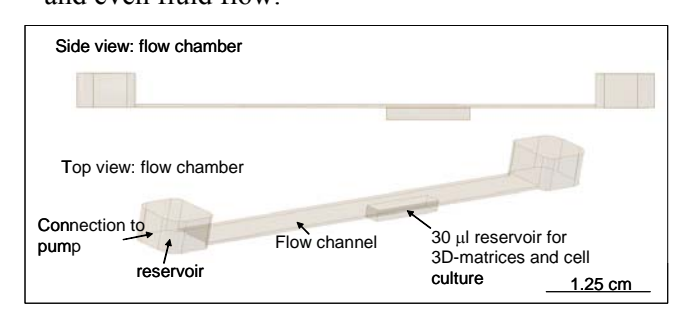
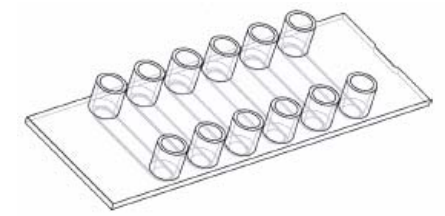


Fig. 1: Schematic of the designed flow chamber.



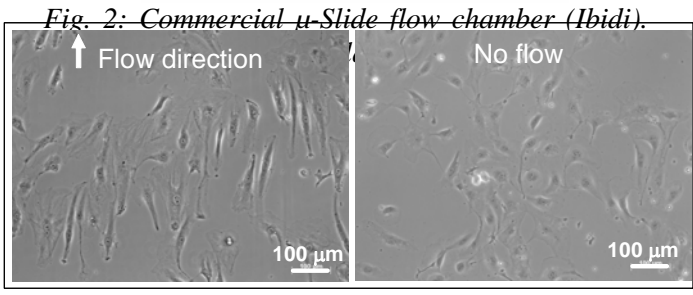


Fig. 3: HUVECs cultured on commercial μ -Slide flow chambers orient along the direction of flow.

DISCUSSION & CONCLUSIONS: The 3D-fibrin matrices will be inserted into the novel designed flow chamber and cellular behavior over characteristic physiological shear stresses will be analyzed. Cellular behavior will be compared between cells cultured in 3D-matrices and on 2D-surfaces.

REFERENCES: ¹Hall, et al. (2004) Angiogenesis **7**:213-223. ² Risau (1997) Nature **386**:671-674. ³Chung (2003) Computers and Structures **81**:535-546.

CONTROL OVER PROTEIN ADSORPTION WITH THERMOSENSITIVE STIMULI-RESPONSIVE COATINGS

M.A.Cole¹, M.Jasieniak¹, N.H.Voelcker², H.Thissen³, H.J.Griesser¹

¹ Ian Wark Research Institute, University of South Australia, Adelaide, Australia. ² School of Chemistry, Physics and Earth Sciences, Flinders University, Adelaide, Australia. ³ CSIRO Molecular and Health Technologies, Melbourne, Australia.

INTRODUCTION: Control over the interactions between biological components and synthetic interfaces is one of the most important goals in biomedical research. This goal is shared by a range of disciplines including biomaterials and tissue engineering as well as biochips and diagnostic devices. Modification of surfaces with thin polymer coatings is commonly employed to control interfacial biological interactions for applications in biosensors, microarrays, cell sheet engineering and 'lab on a chip' devices.

Advances in these applications are expected from the development and integration of stimuli-responsive or switchable coatings that can provide attractive functional properties to manipulate specific biological responses such as adsorption/desorption of biomolecules. Switchable coatings show considerable promise for the realisation of spatial and temporal control over interactions with biomolecules such as proteins and DNA, as well as with cells and bacteria.

METHODS: As part of ongoing research in our lab we report here our findings on stimulimediated protein adsorption to thermosensitive poly(N-isopropylacrylamide) (pNIPAM) coatings in hydrated and collapsed states.

Coatings of pNIPAM were prepared on silicon substrates which had first been functionalised with an alkoxy-silane bearing Silicon methacrylate wafers groups. functionalised with surface polymerisable groups were then grafted with pNIPAM via radical polymerisation. Surface analysis was carried out using X-ray photoelectron spectroscopy (XPS), atomic force microscopy (AFM) and time of flight secondary ion mass spectrometry (ToF SIMS).

Adsorption of the proteins lysozyme (Lys) and bovine serum albumin (BSA) was investigated using TOF SIMS, AFM and XPS.

RESULTS: Surface characterisation of pNIPAM coatings by XPS showed elemental ratios matching values expected from the theoretical bulk polymer composition. The absence of Si in XPS survey

spectra indicated that the dry coatings were thicker than the XPS sampling depth of ${\sim}10$ nm. In colloid probe (CP) AFM experiments, steric repulsion was observed at 4 times greater distance at T $^{\circ}C < LCST$ than for T $^{\circ}C > LCST$, indicating the swelling/deswelling nature of the coating. Furthermore, CP-AFM experiments with protein-functionalised tips allowed the forces between pNIPAM coatings and proteins to be recorded over a range of temperatures.

Analysis by ToF SIMS following protein adsorption experiments demonstrated that pNIPAM coatings showed no measurable fouling at 20 °C whilst they were protein retentive at 37 °C.

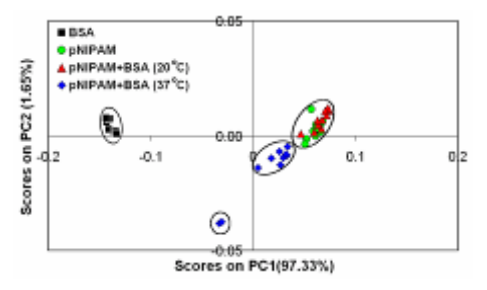


Fig. 1: Principal component analysis of positive ion ToF SIMS data. Score plot of PC1 vs PC2 for BSA, pNIPAM, pNIPAM +BSA (20 °C) and pNIPAM +BSA (37 °C) samples.

DISCUSSION & CONCLUSIONS: Surface coatings of pNIPAM were demonstrated to retain the polymer's inherent temperature-induced phase transition which was used to alter surface properties over modest temperature changes. Protein adsorption studies showed that pNIPAM coatings can be switched between nonfouling and fouling states in order to control protein immobilisation via small temperature changes. Protein could be adsorbed and desorbed reversibly.

The present study is expected to assist the development of switchable coatings for biomedical and biotechnological applications.

ACKNOWLEDGEMENTS: The authors gratefully acknowledge funding from the Australian Government via the ARC Special Research Centre for Particle and Material Interfaces.

Ni²⁺-NTA functionalized amphiphilic diblock-co-polymer vesicles

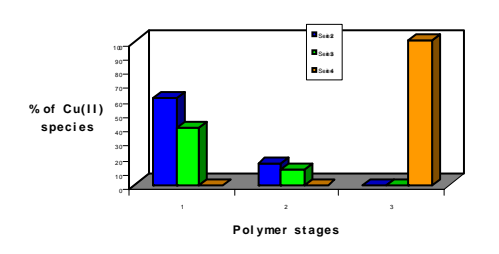
R. Nehring¹, C.G. Palivan¹, W. Meier¹

¹ Chemistry Department, Basel University, Klingelbergstr. 80, 4056 Basel, Switzerland

INTRODUCTION: The amphiphilic systems which connect the worlds of synthetic polymers and natural systems are especially interesting to study the interactions between functionalized polymers and proteins in order to get new hybrid materials. The resulting molecular chimeras of polymer and protein carry the promise to interface the technical world with biological systems. Consequently, a number of experiments on these systems has already been described in the literature, such as the formation of polymer polybutadiene-block-poly(Lvesicles by glutamate)s in aqueous media. In the present work we propose a new system of specifically functionalized nanovesicles for biological applications, such as crystallisation of proteins.

METHODS: Polybutadiene-blockpolyethylenoxide copolymers were synthesized via anionic polymerization and subsequently quenched with molecules bearing active moieties, in an onestep procedure. The chemically active end groups offer various options for further functionalisation. The amphiphilic block copolymers were connected N,N-Bis[(tert-butyloxycarbonyl)methyl]-Llysine tert-Butylester (NTA.p). De-protection of the Carboxyl-groups (NTA.d) and complexation with Ni(II)/Cu(II) (NTA.d-Ni/Cu) results in a specific protein linker. The polymers were characterized by NMR, IR and SEC, while the presence of the functional groups was established by NMR and EPR. The attachment of HIS-tagged proteins to the metal-NTA-linker was studied by FCS.

RESULTS: The block copolymers (PB-PEO-NTA.d) have been complexed with Ni/Cu in order to form active metal regions, able to link His-tag proteins. In order to study if the metal attachment is directed to the NTA moiety we performed EPR measurements of the three stages in the copolymer system assembly: PB-PEO-OH, PB-PEO-NTA.p, PB-PEO-NTA.d. Both paramagnetic species are formed when the copolymer system is not functionalised with NTA (Graph 1.1), are still present when NTA is protected (Graph 1.2), but they are not anymore present when NTA is deprotected. A new paramagnetic is formed in this case (Graph 1.3).



Graph. 1: Cu(II) paramagnetic species formed by addition of Cu(OTf)₂ to: PB-PEO-OH (1), PB-PEO-NTA.p (2), and PB-PEO-NTA.d (3).

In order to link His-tag proteins to the metal coordination sphere we produced nanovesicles, by electroformation as shown in Figure 1.



Fig. 1: Electroformation: vesicles of PB-PEO37-SA-NTA.d. Microscope: Transmission Microscope Leica DMIRE2, magnification: 20x10 Pol.1 media: aqua bidest.

The attachment of His-tag protein to the NTA-polymer linker was studied by FCS. By adding His₆-EGFP to the vesicles-Ni solution, two population were simultaneously present: one formed by the free EGFP ($\tau_D = 54~\mu s$), and an other one with much bigger diffusion times (>5.4ms).

DISCUSSION & CONCLUSIONS: The diblock copolymer Polybutadiene-co-polyethyleneoxide was synthesized and functionalized in an one-step procedure. EPR is indicating that the metal is coordinated only by the NTA moiety which acts as a linking region for His-tag proteins. FCS shows that His-tag proteins attach specifically to NTA.d-Ni functionalized nanovesicles.

REFERENCES: ¹Kukula, H.; Schlaad, H.; Antonietti, M.; Förster, S. *J. Am. Chem. Soc.* **2002**, 8, 124

ACKNOWLEDGEMENTS: The group of W. Meier and the friends of Bill & Bob are gratefully acknowledged. Financial support was given by BioPolySurf and Basel University.

Protein Self-Assembly on Micro-Contact Printed Surface Patterns

L. Iversen, N. Cherouati, D. Stamou, K.L. Martinez

Bio-Nanotechnology Laboratory - Nano-Science Center & Dpt of Neuroscience and Pharmacology University of Copenhagen, Denmark.

INTRODUCTION: Functional protein arrays have a major potential in basic research, drug discovery, drug target identification and the development of novel pharmaceutical therapies. They contain proteins in their native state and are submitted to the analysis of a wide range of biochemical activities.

Micro-contact printing (µCP) has been used to pattern proteins both by direct placement, using the protein solution as the ink¹, or indirectly by selective protein adsorption to a pre-patterned surface. Such self-assembly of proteins to surfaces aims at positioning the protein of interest on a prestamped template pattern via affinity tags allowing a both gentle and specific immobilization of proteins, as well as a controlled and uniform protein orientation at the surface. The recently developed SNAP-tag technology² has been shown to be suitable for surface immobilization of proteins³. The SNAP-tag protein, a mutant of the human DNA repair protein O⁶-alkylguanine-DNAalkyltransferase covalently transfers its substrate (Benzyl Guanine (BG)) onto itself. In this study, we have combined the SNAP-tag technology with μCP in order to achieve high-resolution parallel patterning of protein, combined with a gentle, specific, oriented and versatile immobilization method, applicable to any soluble protein fused to a SNAP-tag.

METHODS: As a model protein we use a non-fluorescent SNAP-FLAG-His10 fusion construct, which enables us to purify the protein via the decahistidine tag, test the array compatibility with standard immunofluorescent staining, using a Cy3-labeled anti-FLAG antibody, and immobilize the protein to surfaces via the SNAP tag. Protein patterns were done by μ CP, according to Stamou *et al.*⁴. Samples were characterized by confocal fluorescence microscopy.

RESULTS & DISCUSSION: The model protein SNAP-FLAG was not directly stamped to the surface but meant to self-assemble via the SNAP tag to streptavidin surfaces, via a biotinylated BG substrate. Two options of self-assembly to the surface are compared: (a) the "standard" biotinylation strategy, where the SNAP-tag moiety is biotinylated by pre-incubation with BG-biotin.

The biotin tag directs the immobilization to prepatterned fluorescently labeled streptavidin on the surface; (b) the "in situ" strategy where the surface is pre-patterned with fluorescently labeled streptavidin preincubated with BG-biotin. The SNAP-tag moiety directs in this case the immobilization by recognizing the BG group from solution. We show that both approaches performed on different kinds of streptavidin surfaces were successful for specific positioning of the protein to the streptavidin layer and its correct orientation, as revealed by subsequent binding of a fluorescent Anti FLAG antibody.

The versatility of the SNAP-tag technology appears to be suitable for successive immobilization of distinct proteins on a single surface, without need of engineering the distinct proteins with various tags.

REFERENCES: ¹ A. Bernard, J.P. Renault, B. Michel, H.R. Bosshard, E. Delamarche, E. (2000) *Advanced Materials* **12:** 1067-1070; ² A. Keppler, S. Gendreizig, T. Gronemeyer, H. Pick, H. Vogel, K. Johnsson, (2003) *Nature Biotechnology* **21:** 86-89; ³ M. Kindermann, N. George, N. Johnsson, K. Johnsson (2003) *J. Am. Chem. Soc.* **125:** 7810-7811. ⁴ D. Stamou, C. Duschl, E. Delamarche, H. Vogel, (2003) *Angew. Chem. Int. Ed Engl.* **42:** 5580-5583.

ACKNOWLEDGEMENTS: The authors thank Covalys (www.covalys.com) for kindly providing reagents and knowledge regarding the SNAP tag technology, as well as E. Delamarche, K. Johnsson and A. Brecht for fruitful discussions.

Characterisation of the structure of PEG-supported lipid bilayers

S.Kaufmann¹, K.Kumar¹, M.Textor¹, E.Reimhult¹

1ETH Zurich, Zurich, Switzerland.

INTRODUCTION: Supported lipid bilayers (SLB) provide a basis for biotechnological applications as they constitute a simple model of cell membranes. They are of particular interest as components of future generations of biosensors based on transmembrane proteins. Two of the current limitations of supported lipid bilayers in biosensor applications are their sensitivity to air exposure and the limited aqueous space between the sensor substrate and the membrane available for large membrane proteins.

Supported membranes resting on a hydrophilic polymer spacer decouples the membrane from the surface and provides increased aqueous space, but are generally more complicated to assemble than supported lipid membranes resting on an inorganic support.1 Recently it has been shown that poly(ethylene glycol) (PEG) can be incorporated into the membrane of liposomes through lipid molecules end-functionalized with a PEG chain and spontaneously fused to supported PEG-lipid bilayers (PEG-SLB) on glass.² These membranes have been shown to posses a remarkable stability in air and would based on the length of the PEGchains provide enough space between the SLB and the substrate to allow incorporation of functional transmembrane proteins. However, the structure of the PEG-SLB has not been characterized and important questions like whether the PEG brush is present on both sides of the membrane, its thickness, density and the kinetics of formation of PEG-bilayers have not been properly addressed. We present a comparison of the kinetics of PEG-SLB formation for different PEG molecular weights and densities as well as data on the location and thickness of the PEG brush.

METHODS: Large unilamellar lipid vesicles were prepared by extrusion through polycarbonate membranes with 100 nm pores from 1-Palmitoyl-2-Oleoyl-sn-Glycero-3-Phophocholine (POPC) lipids mixed with a 0-5 mol% of 1,2-Distearoyl-sn-Glycero-3-Phosphoethanolamine-N-

[Methoxy(Poly(Ethylene glycol)) MW550, 2000 or 5000] (PEG(MW)-PC) lipids. Adsorption kinetics of PEG-lipid vesicles and PEG-SLB formation were recorded by quartz crystal microbalance with dissipation monitoring (QCM-D, E4, Q-Sense, Sweden). Fluidity of PEG-SLB was also confirmed by fluorescence recovery after photobleaching (FRAP). Force-distance curves

were recorded with atomic force microscopy (AFM, Multimode, Digital Instruments, USA) equipped with 0.5 μm in diameter colloidal or standard tips with spring constant 0.12 N/m.

RESULTS: QCM-D measurements typically showed PEG-SLB formation following the general phases identified for pure POPC SLB formation (Fig. 1 (left)), but with the relative and absolute rate of the different phases affected by the PEG-lipid molar fraction and PEG molecular weight. Higher dissipation and mass was recorded for PEG-SLB than for normal SLB.

Force-distance measurements demonstrated that the thickness of e.g. a PEG(2000)-SLB layer is approximately 10-12 nm and follows first a de Gennes-type compression followed by linear compression and "jump-ins" signifying membrane rupture events (Fig. 1 (right)).

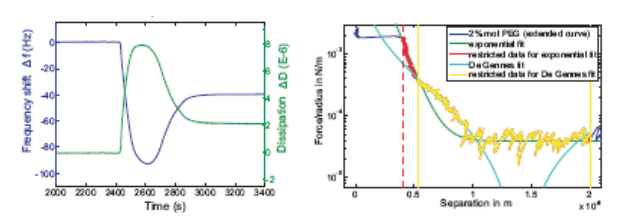


Fig. 1: QCM-D kinetics for formation of a PEG(2000)-SLB also confirmed by FRAP (left). Force-distance curve for compression of PEG(2000)-SLB with colloidal tip-AFM(right).

piscussion & conclusions: The QCM-D measurements indicate that a highly hydrated SLB is formed through a mechanism similar to POPC SLBs, but with higher barriers to vesicle adsorption and rupture, in particular the former. The thicknesses observed by AFM and the initial compliance to a behaviour typical for compression of a PEG brush strongly indicates that the PEG is only present on the distal leaflet of the PEG-SLB.

REFERENCES: ¹ M. Tanaka and E. Sackmann (2005) *Nature* **437**(7059):656-663. ² F. Albertorio, A.J. Diaz, T.L. Yang et al (2005) *Langmuir* **21**(16):7476-7482.

ACKNOWLEDGEMENTS: We thank the Swiss Competence Center for Materials Science and Technology (CCMX) for financial support and Dr S. Lee for support with the colloidal AFM measurements.

Biomedical Nanoparticle Interfaces Optical Sensing

A.Bezrukova

Faculty of Medical Physics and Bioengineering, St. Petersburg State Polytechnical University, St. Petersburg, 195 251, Russia

INTRODUCTION: Proteins, nucleoproteids, lipoproteids, liposomes, viruses, virosomes, lipid emulsions, blood substitutes and other nanoparticle systems can be considered as biomedical 3D disperse systems (DS) with nanoparticles as disperse phase in dispersive medium [1]. The experience [2-4] suggests that the set of optical parameters of so called "second class" is unique for each 3D DS. In another words each 3D DS can be characterized by n-dimensional vector in ndimensional space of optical parameters. Such presentation can serve as sensing platform and can provide further progress in biomedical 3D DS characterization and "on-line" or "in-situ" control in nanobiotechnology.

METHODS: Multiparametric optical analysis of 3D DS includes: a) simultaneous measurements of 3D DS by different compatible non-destructive optical methods such as refractometry, absorbency, fluorescence, light scattering (integral and differential, static and dynamic, unpolarized and polarized); and b) solution of inverse optical problem by different methods including technologies of data interpretation by information-statistical theory. For this purpose it is necessary to collect information about optical properties of different 3D DS.

RESULTS: Fig. 1 demonstrates the aggregated nanoparticles of rotavirus. One of the main problem for sensing biomedical 3D DS is the polymodality of particle size distributions. It is possible to find in dispersion the mixture of the original particles, their aggregates and fragments (debris), and different impurities. The analysis of experimental data for biomedical 3D DS by compatible optical methods allows draw the conclusion that there are three classes of parameters. The first class parameters are measured optical values, for example, intensity values of fluorescence or light scattering under certain conditions (installation conditions, conditions of object treatment, etc.). The second parameters can be calculated from experimental optical data without any "a priori" information about the nature, form and size distribution of particles. The third class parameters can be obtained after solution of inverse optical problem for experimental data.

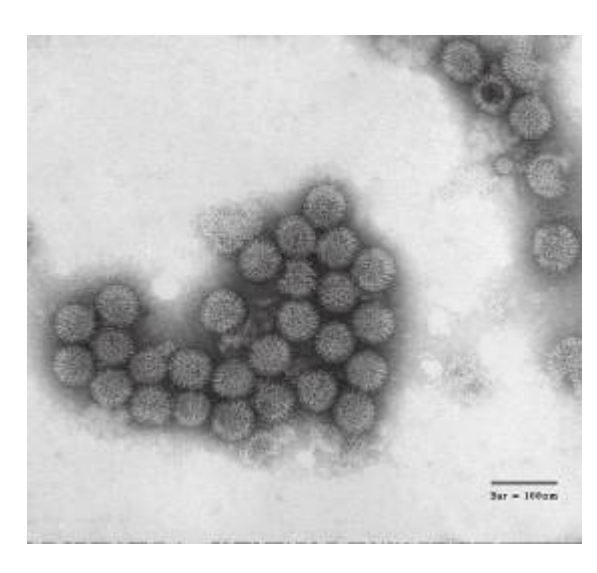


Fig. 1: Electron microscope photograph of Rotavirus nanoparticle aggregate.

be characterised and compared with another 3D DS by means of the second class optical parameters which set can reflect the most changes in the state of mixtures. Due to the fusion of various optical data it is possible to solve by information statistical theory the inverse physical problem on the presence of the component of interest in mixtures and in this case the polymodality of particle size distribution is not the obstacle.

REFERENCES: ¹V. Klenin (1999), *Thermodynamics of Systems Containing Flexible Chain Polymers*, Elsevier, 850 p. ²A. Bezrukova (2002), Proceedings of Material Research Society, Vol. 711, paper FF7.9. ³A. Bezrukova (2006), CD: 2006 Spring National Meeting Conference Proceedings, New York: AIChE. ⁴A. Bezrukova (2006), Proceedings of SPIE, V.6253, 62530C-1 - 62530C-4.

ACKNOWLEDGEMENTS: The author would like to thank Prof. Dr. Heinrich Hofmann from Powder Technology Laboratory (LTP) of Swiss Federal Institute of Technology in Lausanne (EPFL) and Prof. Dr. Marcus Textor from Department of Materials of Swiss Federal Institute of Technology in Zurich (ETHZ) for help in research and useful discussions.

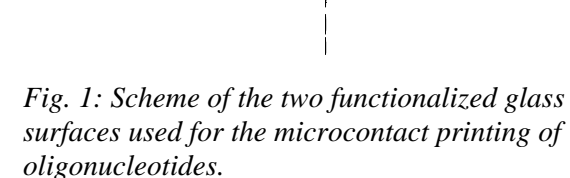
Microcontact Printing of DNA on Various Functionalized Monolayers

Martine Cantuel, Aldrik H. Velders, David N. Reinhoudt

Supramolecular Chemistry and Technology, University of Twente, Enschede, The Netherlands.

INTRODUCTION: Microcontact printing of DNA has been developped in the past few years, as a cheap alternative to the common techniques used in the fabrication of DNA microarrays. It has been successfully applied for the attachment of single strands of oligonucleotides on various surfaces, and the efficient hybridization has also been demonstrated on these systems [1,2]. Our goal is to further develop this method, in order to control precisely the printing process of oligonucleotides.

METHODS: Two different types of functionalized glass slides have been synthesized, using a first step of self-assembled monolayer formation. They possess either an isothiocyanato, either an aldehyde endgroup (see fig.1), which will allow the covalent attachment of amino-modified oligonucleotides.



The microcontact printing of 15 bases-length oligonucleotides has been conducted on these surfaces, using a PDMS stamp chemically modified with an amino-terminated dendrimer [3]. The inking and printing times, as well as the temperature of printing, have been varied in order to study their influence on the printing process. Finally, hybridization has been conducted directly onto the surfaces. The surfaces have been characterized with contact angle measurements, ellipsometry, XPS and fluorescence microscopy.

RESULTS & DISCUSSION: Figure 2 shows a microscopic fluorescence image of a glass slide which has been functionalized by microcontact printing with a single-stranded fluorescein-labeled oligonucleotide.

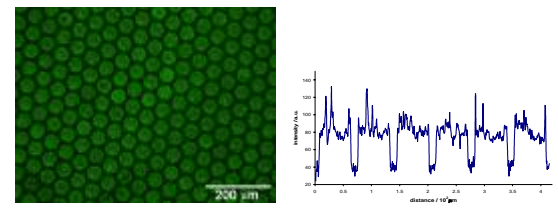


Fig. 2: Fluorescence image and associated intensity profile of a functionalized glass slide microcontact printed with fluorescein-modified ss-DNA.

Upon hybridization with an unlabeled complementary c-DNA, and depending on the conditions of the printing step, the intensity profile can be maintained. When the c-DNA is labeled with a Cy5 fluorophore, the corresponding red fluorescence image is obtained, demonstrating that the hybridization has occurred.

CONCLUSIONS: Microcontact printing of ss-DNA with covalent attachment has been successfully demonstrated on two different kinds of surfaces. In addition, work is conducted in order to quantify the amount of DNA transferred onto the surface, depending on the different printing conditions used.

REFERENCES: ¹ S. A. Lange, V. Benes, D. P. Kern, J. K. H. Horber, and A. Bernard, *Anal. Chem.* 2004, 76, 1641. ² C. Thibault, V. Le Berre, S. Casimirius, E. Trevisiol, J. Francois, and C. Vieu, *J. Nanobiotech.* 2005, 3, 7. ³ D. I. Rozkiewicz, B. J. Ravoo, and D. N. Reinhoudt, *J. Am. Chem. Soc.*, 2007, accepted.

ACKNOWLEDGEMENTS: This research was supported by a Marie Curie Intra-European Fellowship within the 6th European Community Framework Programme.

HIGH RESOLUTION MULTI-PROTEIN NANOPATTERNS

S. R. Coyer, ^{1,2} A. J. García², E. Delamarche¹

¹IBM Research GmbH, Zurich Research Laboratory, 8803 Rüschlikon, Switzerland. ²Woodruff School of Mechanical Engineering, Petit Institute for Bioengineering and Bioscience, Georgia Institute of Technology, Atlanta, GA 30332-0363

INTRODUCTION: The organization of proteins on surfaces is critical to the design of bioactive and biocompatible surfaces for implantable biomedical devices and in vitro studies of cell biology. In many cases, extracellular matrix composition and organization determine functionality, for example in stem cell localization, differentiation, and proliferation. Much attention has been given to developing methods to produce surfaces with biologically relevant modifications [1]. We report here a powerful yet simple method in which multiple proteins can be patterned simultaneously complex architectures with nanoscale resolution and high contrast [2].

METHODS: Nanotemplates were produced using standard electron beam lithography techniques. Poly(dimethylsiloxane) planar elastomers were made from Sylgard® 184. Atomic force microscopy (AFM) images were obtained using tapping mode. TRITC- and AlexaFluor 647-labeled goat anti-rabbit IgG were printed onto glass and visualized by fluorescence microscopy.

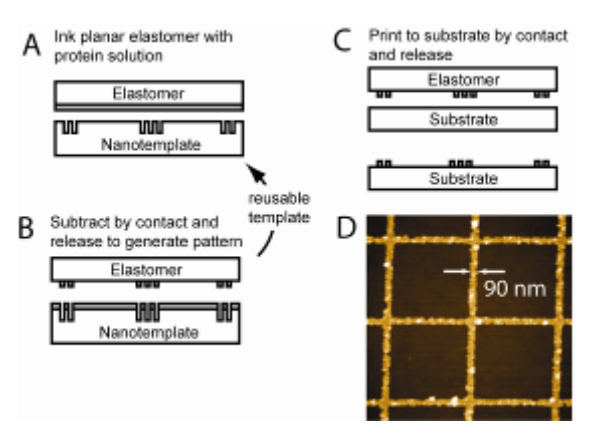


Fig. 1: (A-C) Experimental design to transfer patterns of proteins from a silicon nanotemplate to substrates using a planar elastomer. (D) Resulting pattern of proteins visualized by AFM.

RESULTS: Figure 1 presents the three steps in the "ISP" strategy: 1) a planar elastomer is inked (I) with a monolayer of fluorophore-labeled IgG and then brought into contact with the nanotemplate, 2) subtraction (S) occurs in regions of contact between the hydrophobic elastomer and hydrophilic nanotemplate, 3) the remaining protein pattern is printed (P) onto a final substrate. AFM visualization of the final substrate shows a pattern

of proteins with high resolution (90 nm) and high contrast. As shown in Table 1, the individual steps of the ISP strategy can be combined to produce a wide variety of protein patterns. Several geometries, sizes, and spacing between features can be produced. Spacing of up to 64 µm between nanoscale features is achieved. Multiple proteins can be printed simultaneously in either overlapping patterns or patterns that are intrinsically selfaligned.

Table 1. Combinations of the ISP Strategy produce unique protein patterns.

Protein	Patterning Steps	Results
В	$I_BS_BP_B$	
A then B	$I_{A}S_{A}P_{A}I_{B}S_{B}P_{B}$	* * * * * * * * * * * * * * * * * * *
A and B	$I_AS_AI_BS_BP_{AB}$	

DISCUSSION & **CONCLUSIONS:** The flexibility of the ISP strategy allows production of a wide variety of patterns with high resolution and high contrast. Single and multiple proteins can be printed in self-aligned patterns with precise control over feature geometry, size, and spacing. This technique is applicable to biological systems in which functionality is achieved through the combination of individual proteins into complex architectures. The ISP strategy provides a robust platform in which the role of individual components in the larger complex can be deduced through systematic variation of their organization.

REFERENCES: ¹S.J. Xiao, M. Textor, N.D. Spencer, H. Sigrist (1998) *Langmuir* 14 (19): 5507-5516. ²S.R. Coyer, A.J. García, E. Delamarche (in press) *Angew. Chem. Int. Ed.*

ACKNOWLEDGEMENTS: State Secretariat for Education and Research (SEC) within the framework of the EC-funded project NaPa (NMP4-CT-2003–500120). National Institutes of Health (R01-GM065918). Whitaker International Fellows and Scholars Program.

Novel Micro- and Nanopatterning Techniques for Biological Applications Using Particle Self-Assembly as Template

T.M. Blättler, A. Binkert, E. Thomasson, P. Senn, F. Rakusa, E. Reimhult, M. Textor, J. Vörös Laboratory for Surface Science and Technology, BioInterfaceGroup, ETH Zurich, Switzerland.

INTRODUCTION: Nanopatterns for bioapplications are increasingly popular because they provide novel tools to address biological problems. For example, protein nanoarrays not only enable molecular level statistics of binding events but also offer an increased sensitivity compared microarrays. Additionally, to nanopatterning plays a key role in cell studies, where cell-cell or cell-extracellular matrix interactions can be investigated. Particles arranged into 2D ordered structures can serve as a template for the fabrication of well-defined nanostructures. Certain novel applications, such as single molecule fluorescence studies, require nano-sized features in geometrically ordered patterns with a separation between the features in the low micrometer range in order to be able to detect individual nanostructures by optical microscopy.

METHODS: To achieve such patterns we have self-assembled micron sized latex particles by dipcoating and controlled drying in aqueous suspensions on silicon wafers and microscopy glass slides (sputter-)coated with 70 nm SiO₂ (intermediate layer) and 11 nm TiO₂ (overlayer). The latex particle patterns were then etched by reactive ion etching (RIE) to homogeneously reduce the size of the latex. Size and morphology of the latex features created after RIE strongly depend on the parameters, such as gas composition, forward power and chamber pressure, used during the RIE. The etched latex particle patterns can be used to create biologically active molecular assembly patterns by lift-off (MAPL) [1] or can serve as a mask to create an oxide contrast in the underlying substrate by RIE. The latter technique produces TiO₂ pillars in a SiO₂ background. With the selective molecularassembly patterning (SMAP) [2] technique the oxide contrast is translated into a biochemical contrast, by two simple dip-and-rinse processes. In short; alkane phosphates SAMs are created on the TiO₂ pillars by selective assembly and in a second step the SiO₂ background is passivated towards unspecific protein adsorption with poly(L-lysine)graft-poly(ethylene glycol) (PLL-g-PEG). SMAP patterns are then used for specific protein adsorption on the protein adhesive alkane phosphate SAM nanofeatures while background is protein resistant.

RESULTS: We will present results on SMAP nanopatterns as described above showing the crucial steps and parameters starting from the self-organized latex particle patterns to the RIE patterns (Fig. 1) all the way to the nano-sized protein patterns produced by the SMAP technique.

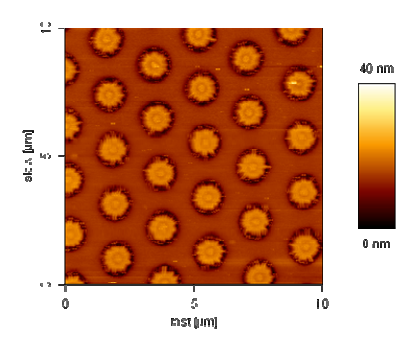


Fig. 1: AFM image of the etched oxide substrate after lift-off of the latex particles (1.9 μ m). The height of the pillars is ~15 nm.

DISCUSSION & CONCLUSIONS: We were able to produce nano-sized features of TiO_2 separated in the micron-range in a SiO_2 background and could successfully apply these patterns to SMAP patterns.

Future applications of our nanopatterned substrates include the study of cell-surface, vesicle/bilayer as well as protein-surface interactions.

REFERENCES: ¹D. Falconnet, A. Koenig, F. Assi and M. Textor (2004) *Adv. Funct. Mat.* **14** (8): 749-756. ²R. Michel, J.W. Lussi, G. Csucs, I. Reviakine, G. Danuser, B. Ketterer, J.A. Hubbell, M. Textor and N.D. Spencer (2000) *Langmuir* **18**:3281-3287.

ACKNOWLEDGEMENTS: This work, as part of the European Science Foundation EUROCORES Programme NanoSMAP, was supported by funds from the Swiss National Science Foundation (SNF) and the EC Sixth Framework Programme.

The authors would further like to thank Otte Homan from the Micro/Nanofabrication Lab (FIRST) at ETH-Hoenggerberg, Zurich for his helpful inputs regarding RIE.

Site-Specific Sorting of Proteoliposomes for High Density Parallel Screening of Membrane Receptor Function

K.Kumar¹, S.Kaufmann¹, M.Textor¹, E.Reimhult¹

¹ Laboratory for Surface Science and Technology, Department of Material Science, ETH Zurich, Zurich, Switzerland

INTRODUCTION: Membrane proteins have particularly high impact in drug discovery with at least 50% of all targets being membrane proteins [1]. As such, it would be ideal integrate membrane proteins on a sensor substrate to investigate their properties. Membrane protein function is strongly dependent on assuming the correct conformation within a cell membrane, resulting in that such a sensor should incorporate the membrane proteins within a lipidic structure, e.g. liposomes or planar lipid membranes. We propose to build a platform, which in addition to incorporating membrane proteins in a near native environment on a sensor substrate, will also be able to sort the membrane proteins according to their functionality. We here present the first steps towards this platform in terms of fabricating of fabricating micron to submicron wells and surface functionalization for selective adsorption of proteins and liposomes only inside the wells.

METHODS: First, a 350 nm layer of silicon nitride is deposited onto a Si wafer. High aspect ratio straight wells are etched through the silicon nitride using RIE with a chrome mask patterned by colloidal lithography. The well size can be tuned to between 50 nm and 1 μm depending on the requirement [2]. A PAAM-stamp "inked" with PLL-*g*-PEG will then be employed to passivate the top part of the sensor substrate [3]. Fibrinogen will then be used as a testbed subject to ensure that the substrate surface is non-fouling.

RESULTS: Wells were successfully etched into silicon nitride. Figure 1 shows the SEM top view of a silicon nitride surface where wells of 1 μ m diameter have been etched into the silicon nitride. Subsequently, the top part of the silicon nitride layer was successfully passivated against fibrinogen adhesion. Fibrinogen only adhered to the insides of the wells (Figure 2).

DISCUSSION & CONCLUSIONS: A porous substrate was successfully fabricated and initial tests with proteins indicated that this platform could also be used for the capture and subsequent investigation of proteoliposomes. Subsequent steps include backfilling the insides of the wells with PLL-g-PEG/Biotin or BSA/Biotin, and specific

adhesion of DNA strands to capture tagged proteoliposomes [4]. The proteoliposome adhesion will be studied using fluorescence microscopy and AFM.

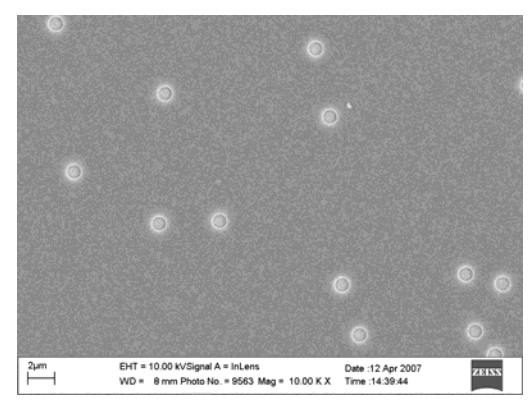


Figure 1: Wells of 1 μ m diameter were successfully etched into a silicon nitride layer.

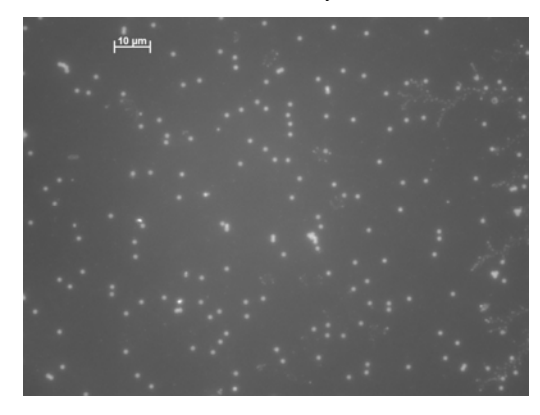


Figure 2: The top part of the sensor was passivated using PLL-g-PEG and the wells were backfilled with fibringen.

REFERENCES: ¹ A.D. Howard, et al., (2001) *Trends in Pharmacological Sciences* **22**(3): p. 132-140. ² E. Reimhult, K. Kumar, and W. Knoll, (2007) *Nanotechnology* **18**(27). ³ M. Ochsner, et al., (2007) *Lab on a chip* (Accepted). ⁴ B. Stadler, et al., (2004) *Langmuir*, **20**(26): p. 11348-11354.

ACKNOWLEDGEMENTS: National Science Scholarship (NSS PhD), Agency for Science, Technology and Research (A*STAR), Singapore and the Competence Centre for Materials Science and Technology (CCMX), Switzerland.

TOF-SIMS Analysis of Bio-Functionalized Surface Structures for Specific Cell Adhesion

H. Gliemann¹, S. Kalinina², A. Petershans^{1,3}, D. Wedlich², Th. Schimmel^{4,5}, S. Reichlmaier⁶, A. Lyapin⁶, G. Fisher⁷, S. Bryan⁷

¹ Institute for Technical Chemistry, Water Technology and Geotechnology Division, Forschungszentrum Karlsruhe GmbH, Karlsruhe, Germany. ² Zoological Institute II, University of Karlsruhe, Karlsruhe, Germany. ³ Zoological Institute I, University of Karlsruhe, Karlsruhe, Germany. ⁴ Institute of Nanotechnology, Forschungszentrum Karlsruhe GmbH, Karlsruhe, Germany. ⁵ Institute of Applied Physics, University of Karlsruhe, Karlsruhe, Germany. ⁶ Physical Electronics GmbH, Ismaning, Germany. ⁷ Physical Electronics USA, Chanhassen, MN, USA.

INTRODUCTION: Adhesive contacts between neighbouring cells and to the extracellular matrix play a crucial role in maintaining tissue integrity, cell differentiation and cell function as well as in understanding processes like bio-film formation [1, 2]. To achieve specific cell adhesion on inanimate matter (e.g. as substrates for tissue engineering) it is necessary to "mimic" the extracellular matrix by immobilizing extracellular matrix proteins - e.g. on the surface of a substrate - in a spatially well defined manner. This requires (1) the necessary extracellular matrix proteins, (2) a toolbox to prepare nano- and micro-patterned surfaces as well as (3) techniques for orientated immobilization of the proteins on the patterned surface. A common way to immobilize proteins or peptides by chemisorption is the coupling via aminofunctionalized surfaces which normally requires extensive chemistry with the risk of damage for the surface and/or the peptide [3].

METHODS AND RESULTS: Here we prepared - NH_2 -functionalized patterns on glass and a one-

step coupling mechanism of isothiocyanide-terminated peptides under mild experimental conditions. As model peptides we use synthesized isothiocyanide-terminated RGD-peptides. The amino acid sequence RGD is recognized by the integrin proteins of the extracellular matrix. The successful coupling to our amino-functionalized surface patterns is verified by cell adhesion assays.

TOF-SIMS analysis was carried out to follow all preparation steps. Spatially resolved chemical images from the sample surfaces verified the chemistry of the individual steps. These results will be discussed and used to derive future experiments.

REFERENCES: ¹ M.P. Sheetz, B.J. Dubin-Thaler, G. Giannone, G. Jiang, H.-G. Döbereiner (2005) *Cell Migration* (ed. D. Wedlich) ISBN: 3-527-30587-4. ² S. M. Pancera, H. Gliemann, D.F.S. Petri, Th. Schimmel (2006) *J. Phys. Chem. B* **110**: 2674. ³ U. Hersel, C. Dahmen, H. Kessler (2003) *Biomaterials* **24**: 4385-4415.

IMMOBILIZATION OF OLIGONUCLEOTIDES ONTO SUBSTRATES FOR CELL ADHESION STUDIES

J.Razumovitch¹, K. de França¹, N.Cottenye^{1, 2}, L.Ploux², W.Meier¹, C.Vebert¹

¹ Universität Basel, Basel, Switzerland. ²Institut de Chimie des Surfaces et Interfaces, Mulhouse, France.

INTRODUCTION: The of attachment biomolecules onto solid supports very significant for many biotechnological applications such as microchips or biosensors. There are several methods in the literature describing immobilization of oligonucleotides onto different substrates. The covalent immobilization provides stable, predictable and irreversible attachment of oligonucleotides to a surface. Unfortunately, physical chemistry investigations are still missing.

METHODS: We used the method of surface modification by silanizing with APTES using glutaraldehyde as a linker. This method has been reported to be well-suited for immobilization of oligonucleotides. Glutaraldehyde reacts via its aldehyde terminations with the amino groups of APTES, attached on a surface and the amino groups of modified oligonucleotides as well. Silicon wafers were cleaned ultrasonically in chloroform. The samples were activated in a UV/ozone chamber during 15 min. Silanization was done in toluene. The silanized wafers were incubated in a glutaraldehyde solution (pH 4, 24 h, RT).

Subsequence immobilization of the oligonucleotides

RESULTS: Each steps of the preparation were controlled by AFM, FT-IR, contact angle measurement and optimal conditions for these reactions were evaluated. Band position and mode assignments of the characteristic peaks of infrared spectra for the samples at each step of the preparation showed that sequential immobilization of species occurred. AFM images demonstrated the homogeneous coverage.

DISCUSSION & **CONCLUSIONS:** We optimized the method of silanization and glutaraldehyde coupling to get layers in preference covalently linked to the silicon surface. The data obtained showed that the oligonucleotides bind to

glutaraldehyde-modifed substrates with preservation of their functional properties. These oligonucleotides can be recognized by cells. The presented experiments are a first step in developing a comprehensive understanding of the role of the immobilized oligonucleotides in the mechanism of cell adhesion.

Table 1. Average ellipsometry and wettability results for each step of the preparation: silicon wafer before (A), after silanization with APTES (B), after glutaraldehyde binding (C) and after oligonucleotide deposition (D).

	A	В	С	D
Static contact angle	26.60°	67.15°	55.84°	29.50°
Thickness (theoretical)		0.8 nm	1.4 nm	10.1 nm
Thickness	2.9 nm	1.0 nm	0.7 nm	8.6 nm

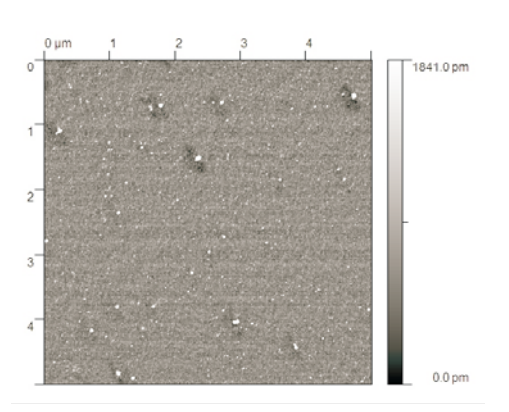


Fig. 1: AFM topographic image of the surface after oligonucleotide immobilization.

ACKNOWLEDGEMENTS: SNSF is greatly acknowledged for financial support

Effects of Optical Anisotropy on Waveguide Spectroscopy and its Measurement allows Elucidation of Conformational Changes in Supported Lipid Bilayers

A. Mashaghi¹, E. Reimhult¹, M. Swann², J. Popplewell² and M. Textor¹ ETH Zurich, Zurich, Switzerland. ² Farfield Scientific Ltd, Crewe, UK

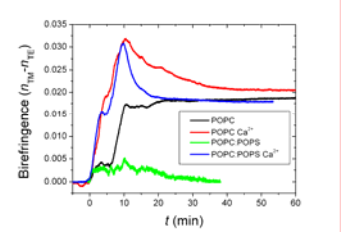
INTRODUCTION: Supported lipid bilayers (SLB) have recently received a high degree of interest for the functionalisation of biosensor interfaces and the importance of quantitatively investigating peptide-membrane interaction is increasingly appreciated.[1] Functionalisation of biosensor interfaces with SLB requires knowledge not only about their formation, but also about how the biosensor itself responds to the presence of a bilayer and conformational changes within it. Alignment of lipids orthogonal to the substrates, as in the case of SLB formation, significantly changes the effective refractive index of the lipids as probed by linearly polarised evanescent fields. The assumption of an isotropic SLB refractive index leads to incorrect determination of film thickness of lipid membranes and similarly how the estimated mass uptake will vary. Here these effects are investigated and quantified using the technique of Dual Polarisation Interferometry (DPI).[2]

METHODS: DPI measurements were done using Analight® BIO200 (Farfield Scientific Ltd., UK). By exciting the SiO_xN_y waveguide chip with two orthogonal polarisations, TE and TM waveguide modes, two separate measurements of fringe shifts were made as a function of time during liposome adsorption. DMPC, POPC and POPC:POPS (80:20 w/w) uni-lamellar vesicles, were prepared by extrusion through polycarbonate filters with 100 nm pore diameter in 10 mM HEPES, 150 mM NaCl with and without CaCl₂ (1mM and 2mM) at pH 7.4. The phase shifts were analyzed both using a standard one-layer model for isotropic films and modeled allowing for optical anisotropy within the film at a fixed thickness.

RESULTS: Larger phase responses are observed for DMPC liposomes layers than SLB (figure 1 (left)). SLBs formed with different protocols converge on similar phase change. SLB thickness resolved in a one-layer model for homogenous isotropic films yields a value up to 5 times the real value. In this case, thickness is a function of anisotropy (alignment/compression of the lipids). In case of POPC and POPC:POPS, regardless of lipid mixture, the SLB birefringence reaches a significant mean value of ~ 0.021 after SLB formation with a calculated average refractive index n ≈ 1.47 assuming a typically 4.7 nm thick SLB. Addition of 2 mM CaCl₂ to the buffer gives

rise to a pronounced maximum in the difference between TM and TE phase shifts during the liposome rupture phase (figure 2 (right)). Pronounced plateaus in the birefringence with increasing mass occur especially clearly for POPC without Ca²⁺ during infilling of first the vesicle layer before rupture and second the SLB before condensation of the

SLB to its final density and alignment increases the birefringence.



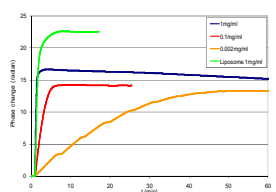


Fig. 1: TM phase changes for DMPC liposome and DMPC SLB depositions

(left). Effect of calcium on the kinetics of POPC and POPC:POPS SLB formation (right).

DISCUSSION & CONCLUSIONS: Allowing for optical anisotropy in the analysis of DPI data enables determination of birefringence of SLBs together with thickness or refractive index. This enables the molecular arrangement and distribution to be determined, which provides mechanistic details for the SLB formation process that are complimentary to what is obtained by other methods such as QCM-D.[3] Specifically, it was shown that addition of CaCl₂ has a pronounced effect on the SLB formation kinetics monitored with DPI, likely due to higher lipid alignment and deformation of liposomes before and during the rupture phase.

REFERENCES: ¹S. Daniel, F. Albertorio, P.S. Cremer (2006) *MRS Bulletin*, **31**(7): 536-540. ²N.J. Feeman, L.L. Peel, M.J. Swann (2004) *J Phys: Condens Matter* **16** S2493-S2496. ³E. Reimhult, M. Zäch, F. Höök et al (2006) *Langmuir* **22**(7):3313-9.

ACKNOWLEDGEMENTS: We thank the Swiss Competence Center for Materials Science and Technology (CCMX) for financial support.

Increasing the Sensitivity of Enzymatic Biosensors by Working at the Phase Transition Temperature

D. Grieshaber¹, E. Reimhult², J. Vörös¹

¹ Laboratory of Biosensors and Bioelectronics, Institute for Biomedical Engineering, ETH Zurich, Switzerland. ² Laboratory for Surface Science and Technology, Department of Materials, ETH Zurich.

INTRODUCTION: Biosensors highly are selective measuring tools due to the high substrate specificity of the enzymes. They offer the possibility of real-time analysis which is important for the rapid measurement of body analytes. Their potential application lies in the clinical analysis for health care [1]. Glucose biosensors have successfully been used in measuring the glucose level of diabetes patients. Other applications of enzymatic biosensors are in the field of monitoring environmental pollution. Α new possible application lies in multiplexed electronic detection systems for early cancer diagnostics. Based on the success of glucose sensors and ELISA assays [2] enzymatic biosensors are expected to play a keyrole in clinical, biochemical and biotechnological analysis. However, at present their application in cancer diagnostics is limited because of the low number of existing cancer markers and their insufficient sensitivity. In the current work we present an approach towards a highly sensitive enzymatic biosensor.

METHODS: Biotinylated poly(L-lysine)-graftedpoly(ethylene glycol) (PPB) was adsorbed to an indium tin oxide (ITO) surface. Subsequently, single stranded biotinylated DNA, coupled to neutravidin (NA/bDNA), was adsorbed. Vesicles, tagged with complementary cholesterol-DNA (vesicle/cDNA), were added in a last step. The enzyme glucose oxidase was incorporated into the vesicles. Glucose was used as a substrate. All measurements were carried out in either 100 mM potassium chloride (KCl) or in a 160 mM buffer consisting solution, 10 mMof hydroxyethyl)piperazine-1-ethanesulfonic acid and 150 mM NaCl, adjusted to pH=7.4.

Adsorption on ITO was observed with a Quartz Crystal Microbalance with Dissipation (QCM-D). This instrument measures changes in the frequency (f) and dissipation factor (D) of an oscillating quartz crystal upon adsorption of a viscoelastic layer [3]. Another technique to monitor in situ adsorption is the Optical Waveguide Lightmode Spectroscopy (OWLS). Thereby, changes in the incoupling angle were monitored; the adsorbed mass was calculated according to de Feijter's

formula [4, 5]. Furthermore, simultaneous optical and electrochemical measurements were performed in an electrochemical flowcell.

RESULTS: The buildup of our biosensor prototype is shown in Figure 1. The three steps correspond to the adsorption of PPB, NA/bDNA and vesicle/cDNA.

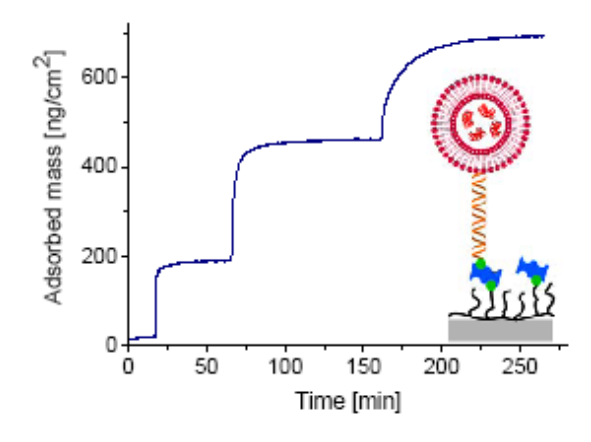


Figure 1: Adsorption curve of PPB, NA/bDNA and vesicle/cDNA. The insert shows a scheme of the biosensor that is built up.

Measurements at the phase transition temperature of the lipids showed a higher sensitivity. This is expected, because the coexistence of the two phases facilitates the diffusion of the substrate through the membrane.

DISCUSSION & CONCLUSIONS: We built a biosensor that allows for – with the currently used setup – detection of DNA hybridization. Once the sensitivity has been optimized, the next step will be to use an antibody/antigen system instead of the DNA-hybridization.

REFERENCES: ¹ A. Malhotra, *et al.* (2002) *Langmuir* **17**: 441-456. ² U.B. Nielsen *et al.* (2004) *J. of Immunological Methods* **290**: 107-120. ³ K. Marx (2002) *Bio Macromolecules*, **4**: 1090-1120. ⁴ J. Voros *et al.* (2002) *Biomaterials* **23**: 3699-3710. ⁵ J.A. De Feijter *et al.* (1978) *Biopolymers* **17**: 1759-1772

ACKNOWLEDGEMENTS: The authors would like to thank ETH Zurich for funding.

Biosensing and controlled interaction with cellular systems via structured interfaces

Mihaela Gheorghiu, Sorin David, Cristina Polonschii, Dumitru Bratu, Eugen Gheorghiu

International Centre of Biodynamics, Bucharest, Romania.

INTRODUCTION: Aiming to detect a wide range of target analytes, from low molecular weight compounds to whole cells we have considered the capabilities of structured metallic surfaces and combined electric and optical instrumentation as sensitive bioanalysis platforms able to provide real time monitoring of complex bio-interfaces (cell-"smart" substrates).

We will present some of our latest developments on harvesting the enhancing capabilities of nanogold plasmonics in conjunction with affinity compounds for biosensing, from platforms development to combined (electrochemical and optical) analysis set-up interfaced in small volumes.

METHODS: Multichannel, differential impedance spectroscopy (MDIS) in combination with SPR methods, (Surface enhanced) optical fluorescence assays are elaborated to develop, optimize and analyze specific nanostructured platforms (affine and cell based biosensors).

Surface functionalization and nanopatterning add the required selectivity and specificity to the otherwise nonspecific, yet powerful methods like electrochemical and SPR assays for biosensing.

RESULTS: We have developed a dual MDIS and SPR system, with integrated microfluidics with multiple channel detection capabilities. The capabilities of the system were investigated during bioaffinity reaction using modified gold sensors. The behavior of the dual system was evaluated during non specific protein adsorption, for specific detection of pathogen cells and low molecular weight target analyte.

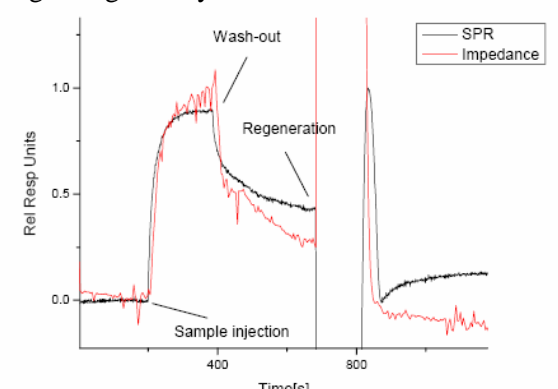


Fig. 1 Dual signal for protein adsorption (BSA 1 mg/ml on gold)

In the case of detecting a suspension of pathogen cells (E. coli) the attainable sensitivities, 10^5 - 10^6 cells/ml are better than the ones provided using bench top SPR instrumentation.

For a low molecular weight compound (gentamicin) we could achieve the required detection limits to comply with international regulations regarding the maximum residual limits.

The combined MDIS and SPR assay enables accurate assessment of recognition events (Ag-Ab) while eliminating the nonspecific influences, providing mutual validation and expanding the analyte detection range, from low molecular weight compounds to cells.

Preliminary results dealing with electro-optical characterization of (nano)functionalized interfaces for cell detection will be presented.

DISCUSSION & CONCLUSIONS:

Improvement in the sensitivity of the SPR sensors is an important issue for many applications, and we are investigating several alternative configurations such as combined electrical/SPR assays, Localised Surface Plasmon Resonance (LSPR) based on gold nanostructures or surface enhanced Total Internal Reflection Fluorescence microscopy.

Experimental verification of the concept has been achieved in designing immuno-affinity biosensing platforms for target analytes ranging from whole cells to low molecular weight compounds.

Preliminary data on exploring the influence of nanotopographies/nanopatterns, on cell attachment are presented. The proposed system combines the ultimate single molecule detection capabilities and high resolution on interfacial processes provided by SPR/TIRFM with the complementary virtues of impedance measurements to non-invasively appraise interfaces and non homogeneities.

REFERENCES: O.A. Sadik, E. Gheorghiu, H. Xu, D. Andreescu, C. Balut, M. Gheorghiu, D. Bratu, "Differential Impedance Spectroscopy for Monitoring Protein Immobilization and Antibody-Antigen Reactions", Analytical Chemistry, **74** (2002), 3142-3150.

ACKNOWLEDGEMENTS: This work was supported by the FP 6 projects CHARPAN and ROBIOS and National Project Nanoint.

Silane-dextran chemistry on polymer chips for point of care diagnostics

Christina Jönsson^{1,2}, Magnus Aronsson¹, Gerd Rundström¹, Christer Pettersson¹, Ib Mendel-Hartwig¹, Jimmy Bakker^{1,2}, Brian MacCraith², Ove Öhman¹, Jonas Melin^{1,2}
¹ Åmic AB, Uppsala, Sweden. ² Biomedical Diagnostics Institute, DCU, Dublin, Ireland.

INTRODUCTION: High performance point-of-care (POC) diagnostic devices, could substantially improve the prognosis for patients suffering from cardio vascular decease (CVD) by enabling early detection and treatment. Disposable plastic test chips, with integrated fluid handling and assay components, provide a platform for realizing such devices. The native hydrophobic nature of plastic surfaces does however require surface modifications to allow for proper fluid distribution and immobilization of affinity ligands.

We have developed a surface chemistry for cycloolefin polymer (COP) surfaces based on direct silanization of an oxidized plastic surface. The resultant amino terminated surface has further been functionalised with a surface-enlarging dextran matrix and used in an immunoassay for the inflammatory marker C-reactive protein (CRP).

METHODS: 4castchips were injection molded by Åmic AB (Uppsala, Sweden) in COP (Zeonor 1020R) and oxidized in oxygen plasma. The chips were immersed in a solution of 3% (3-Aminopropyl)Triethoxysilane (APTES) in 95:5 ethanol:water for 2h¹. The surface concentration of reactive amino groups was measured by confining an ~1 cm² area of the chip surface with a silicone frame. The cup defined by the chip surface and silicon walls was filled by 100 µl Alexa Fluor 647 succinimidyl ester dye (10 µg/ml, in 100 mM NaHCO₃) and incubated for 1 h. After extensive washing and sonication in 0.1% SDS and milliq-H₂O the signal was red out in a microarray scanner. APTES covered surfaces were immersed in 2% oxidized dextran solution for 2h and, rinsed in milliq-H₂O and further oxidized in 30 mM NaIO₄ for 2h. Capture Ab (αCRP, Mxxx,...) were spotted across the fluidic channel of the chip. CRP assays were carried out by sequential addition of: 15 µl of CRP-depleted serum spiked with a known concentration of CRP, 5 µl Alexa 647 labeled detection Ab (\alpha CRP, Mxxx,...) in serum and finally wash with 15 µl CRP-depleted serum. The signal intensities were recorded in a prototype lineilluminating fluorescence reader.

RESULTS & DISCUSSION: Upon oxidation OH-groups are formed on the COP surface which enables silanization. Reactive amino groups were found on APTES treated chips only (fig. 1). The

fluorescence intensity corresponds to a surface concentration of approximately 10^{13} aminogroups/cm², which is comparable to what has been shown for glass². Immobilization of dextran to the amine surface resulted in a low contact angle (~30°), which allowed for easy fluid distribution, and provided a high capacity matrix for antibody immobilization.

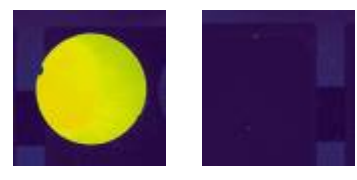


Fig. 1: Reactive amino groups on APTES treated (left) chip and negative control (right).

CRP was assayed with a limit of detection of 2 ng/ml and a dynamic range of 10^2 (fig. 2). The relative precision was about 15%, calculated from triplicate experiments.

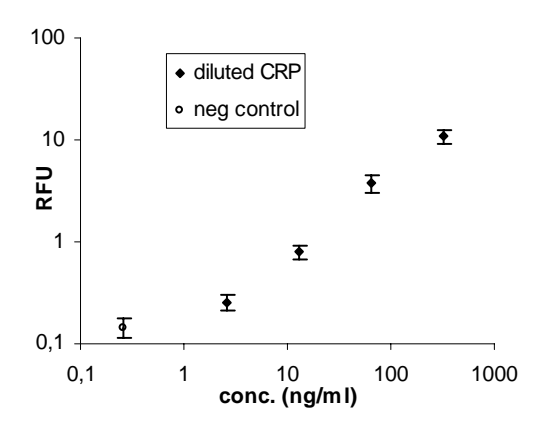


Fig. 2: CRP assay. Error bars indicate $\pm 1SD$.

CONCLUSIONS: We have demonstrated a straightforward and capable protocol for surface modifications of COP surfaces. The covalently formed amino layer functions as an anchor for covalent coupling of dextran and antibodies.

REFERENCES: ¹ Miksa, D. et al. (2006), *Biomacromolecules* **7**:557-564. ² Xing, Y., Borguet, E. *Langmuir* (2007) **23**:684-688.

ACKNOWLEDGEMENTS: This work was supported by Marie-Curie Fellowships and the Swedish Governmental Agency for Innovation Systems.

High resolution AFM as a tool for analysis of short-chain DNA structure and properties

J.Přibyl1, P.Skládal1, D.Renčiuk2, M.Vorlíčková2

¹ Masaryk University, Brno, Czech Republic. ² Institute of Biophysics ASCR, Brno, Czech Republic.

INTRODUCTION: Immobilization of biomolecules on surfaces while keeping the maximum conformational flexibility of molecules is one of the most important techniques for atomic force microscopy imaging. When the DNA molecules are studied with Atomic Force Microscope (AFM) either HOPG (Highly Ordered Pyrolytic Graphite) or freshly cleaved mica is used as s substrate because they show atomically flat surface. DNA molecule can be adsorbed to the graphite surface, however this kind of supporting material is very cost expensive. Mica also shows high flatness, unfortunately it can not be used for DNA immobilization without specific treatment¹, as both mica and DNA are negatively charged in standard buffer solutions. Scanning probe microscopies (SPM) are based on the ability to detect a local property of a surface by means of spatially controlled sensor or probe. Typically, the sensor is scanned over the area of interest so it s only transiently localized neighbourhood of a given point on the surface.

METHODS: The AFM images were taken in air as well as in liquid (buffered solution) using the AFM instrument from NT-MDT (Russia) equipped 'Scanning-by-sample' measuring allowing highly precise visualization of the surface profile. The whole system was stabilized by the dynamic vibration isolation system TS-150 (JRS Scientific Instruments, Germany). The DNA samples were immobilized to the solid surfaces showing high flatness. Mica and HOPG were used to this purpose. These materials are commonly used in current nanotechnology when biomolecules are needed to be visualized on a solid surface. Various methods were tested with regard to the possibility to capture DNA molecule to a solid support. A simple physical adsorption to HOPG is the simplest one. Efficiency of such process was improved by supporting of capillary forces, when the DNA sample was applied by pressure-print of flat silicon surface. Mica surface was treated in several ways. First, the use bivalent ions was used to make a bridge between DNA and mica surface having the same charge. 1 mM Mg²⁺ was used to capture DNA. However, such a complex is stable only in dry conditons. Nickelous ion of the same concentration were used in a similar way. This kind of ion is able to mediate the DNA-mica

interaction even in liquid. Moreover, silanization of the mica surface was employed too. APTES ((3-Aminopropyl)triethoxysilane) was employed to modify the mica surface in order to change its surface charge. Another silanization compound GOPS ((3-Glycidyloxypropyl)trimethoxysilane) was used for covalent attachment of the DNA molecule via formation of peptidic bond with the primary amino-group in the DNA structure.

RESULTS: Various approaches in modification of atomically flat surfaces were tested in order to determine not only efficiency of the binding of DNA molecule to such adapted materials but also to immobilize the biomolecules in a native state. It was found, that use of bivalent ions (Mg²⁺, Ni²⁺) is an effective method to capture long-chain DNA. On the other hand, short-chain DNA or even oligonucleotides can not be immobilized using such procedure, because of the DNA self-aggregation. The covalent binding of biomolecules should prefered in this case. Moreover, HOPG substrate was found as an easy-to-use, however very expensive support, showing false results due to breaks in its structure.

DISCUSSION & CONCLUSIONS: Even as the above mentioned methods are highly suitable for the DNA binding to solid substrates, there is a need to develop more sophisticated methods. Especially surface protection from non-specific adsorption is essential, e.g. in cases when the DNA molecules should be labelled with either a probe or antibody molecule.

REFERENCES: ¹ Lyubchenko, Y.L., Gall, A.A., Shlyakhtenko, L.S., Harrington, R.E., Jacobs, B.L., Oden, P.I., Lindsay, S.M. (1992) *J. Biomol. Struct. Dyn.* **10**:589-606.

ACKNOWLEDGEMENTS: The work was supported by the Junior Research Grant of Academy of Sciences of the the Czech Republic no. **KJB401630701** and grant of Ministry of Education, Youth and Sports no. **2B06056**.

Site-directed immobilization of antibodies on well-defined polymer brushes

R.Iwata¹, Y.Iwasaki², K.Akiyoshi¹

¹ Institute of Biomaterials and Bioengineering, Tokyo Medical and Dental University, Tokyo, Japan.
² Faculty of Chemistry, Materials and Bioengineering, Kansai University, Osaka, Japan.

INTRODUCTION: Surface characteristics for biosensor applications require both reducing nonspecific biofouling and enhancing specific recognition. Especially in the protein-chip technology, immobilization of proteins in proper orientation is necessary to maintain the biological We have reported activities. methacryloyloxyethyl phosphorylcholine (MPC) polymers synthesized as biomimetics biomembrane structures significantly reduce protein adsorption and cell adhesion¹. Furthermore, manipulation of protein and cell was well performed on well-defined poly(MPC) (PMPC) brushes produced by atom transfer radical polymerization (ATRP)². The block copolymer brushes consisting of PMPC and poly[glycidyl methacrylate (GMA)] were also recently prepared for engineered biomaterial surfaces³. We describe here about oriented immobilization of antibodies onto the polymer brushes for biorecognition surfaces.

METHODS: Polymer brushes consisting of PMPC and poly(GMA) (PGMA) were formed on silicon wafers by ATRP as described previously³. Pyridyl disulfide moieties were then introduced to the polymer brushes via epoxy groups in GMA unit. Fab' fragments (Goat anti-mouse IgG) solution was in contact with polymer brushes with pyridyl disulfide moieties and reacted at room temperature over night. After the immobilization of Fab' fragments and wash with buffer, 1% bovine serum albumin (BSA) was applied to surfaces and incubated for 1h at room temperature. isothiocyanate-Fluorescein (FITC-) labeled immunoglobulin (Mouse anti-rat IgG) was used as antigen. BSA solution was removed and antigen solution was in contact with polymer brushes with Fab' fragments for 1 h at room temperature. After wash and dried, the fluorescence intensity was analyzed.

RESULTS: Fab' fragment is one of the antibody fragments and has thiol group in the opposite side of antigen-binding domain. We can immobilize the Fab' fragments in ordered orientation via thiol-disulfide exchange between the thiol groups of Fab' fragments and pyridyl disulfide moieties in polymer brushes. To compare the amount of immobilized antibody, FITC-labeled Fab'

fragments were reacted with each surfaces and the fluorescence intensity was determined. We prepared the organosilane monolayer having epoxy groups (epoxysilane films) as a control surface. The amount of immobilized antibody increased with an increase in the length of GMA unit. PGMA brush immobilized largest amount of antibody. Fig. 1 shows the ratio of fluorescence intensity of each surface after contact with FITC-labeled antigen. The fluorescence intensity of polymer brushes was higher than that of epoxysilane. In PMPC-b-PGMA brushes, the fluorescence intensity increased with an increase in the thickness of PGMA.

DISCUSSION & CONCLUSIONS: The amount of immobilized Fab' fragments and subsequent reaction with antigen could be controlled by changing the thickness of polymer brushes. Although PGMA brush surface has larger amount of Fab' fragment compared with PMPC-b-PGMA brush with longer PGMA, the reactivity with antigen was similar on these surfaces (Fig. 1.). It is considered that the condition of immobilized Fab' fragments are different between PGMA brush and PMPC-b-PGMA brush which has biocompatible PMPC under PGMA. It was also shown that polymer brush surface for reaction with antigen was more effective than the epoxysilane films. The characteristics of PMPC and dense immobilization of antibodies in defined orientation are effective in high sensitive biorecognition.

REFERENCES: ¹S. Sawada, S. Sakaki, Y. Iwasaki, N. Nakabayashi, K. Ishihara (2003) *J Biomed Mater Res* **64A**:411-416. ²R. Iwata, P. Suk-In, V.P. Hoven, A. Takahara, K. Akiyoshi, Y. Iwasaki (2004) *Biomacromolecules* **5**:2308-2314. ³R. Iwata, Y. Iwasaki, K. Akiyoshi, A. Takahara (2005) *Trans. Mater. Res. Soc. Jpn* **30**:735-738.

ACKNOWLEDGEMENTS: The authors of this paper would like to thank Japan Society for the Promotion of Science for financial support of this research.

Defining cell shape in 3D

Mirjam Ochsner¹, Michael Smith², Michelle Grandin¹, Marcus Textor¹

¹ Department of Materials, Laboratory for Surface Science and Technology, BioInterfaceGroup.

²Laboratory for Biologically Oriented Materials, ETH Zurich, Switzerland

INTRODUCTION: In addition to substrate rigidity, matrix composition, and cell shape, dimensionality is now considered an important physical property of the cell microenvironment which directs cell behavior. However, available tools for the study of cell behavior in two-dimensional (2D) versus three-dimensional (3D) environments are difficult to compare, and no tools are available which provide 3D shape control of individual cells. ¹

METHODS: We have developed a set of tools combines 2-dimensional patterning with topographical microstructuring, thus presenting to the cells a controlled microenvironment that mimics the in vivo environment. The technique combines master fabrication in Silicon and replication techniques which result in polydimethylsiloxane (PDMS) chips that display defined microwells of various shapes and dimensions in the size range of single cells. By making use of different cross linking densities of the PDMS, substrate rigidity was also tuned over two orders of magnitude. Cell adhesion was limited to within microwells by passivation of the flat upper surface through an inverted microcontact printing technique of a non-fouling graft-co-polymer (PLL-g-PEG) onto the plateau and backfilling of the wells with either specific adhesive proteins or lipid bilayers.²

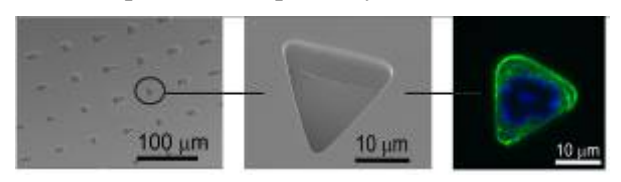


Fig.1: Microwell array with different shapes in the size of a singe cell (left), close up of a triangular microwell (middle), stained cell in a triangular shaped well with a blue nucleus and a green actin cytoskeleton (right).

RESULTS: Endothelial cells constrained within microwells were viable, although cell death was increased in very constrained microwells as has been reported for cells on flat substrates. In contrast to studies on 2D surfaces, actin stress fibers were present even within cells cultured in very constrained microwells, and in addition the

cytoskeleton exhibited 3D arrangement and was not only limited to the cell-substrate interface. ³

DISCUSSION & CONCLUSIONS: These observations demonstrate that microwells can be used to produce microenvironments for large numbers of single cells with 3D shape control and can be added to a repertoire of tools which are ever more sought after for both fundamental biological studies as well as cell-based assays for drug development and screening.

REFERENCES:

- ¹ M.R. Dusseiller, M.L. Smith, V. Vogel, M. Textor; *Biointerphases* (2006), 1, 1
- ² M.R. Dusseiller, D. Schlaepfer, M. Koch, R. Kroschewski, M. Textor, *Biomaterials* (2005), 26, 5917-5925
- ³ M. Ochsner, M.R. Dusseiller, H. M. Grandin, S. Luna-Morris, M. Textor, V. Vogel, M.L. Smith; *Lab on a Chip* (2007), In Press

ACKNOWLEDGEMENTS: We gratefully acknowledge the Swiss National Science Fundation (FN 205321-112323/1).

Selection of tuning PCL nanofiber non-wovens for muscle tissue engineering.

MN Giraud¹, D Keller¹, D Balazs², E Körner², T Humbert², H Tevaearai¹, G Fortunato²

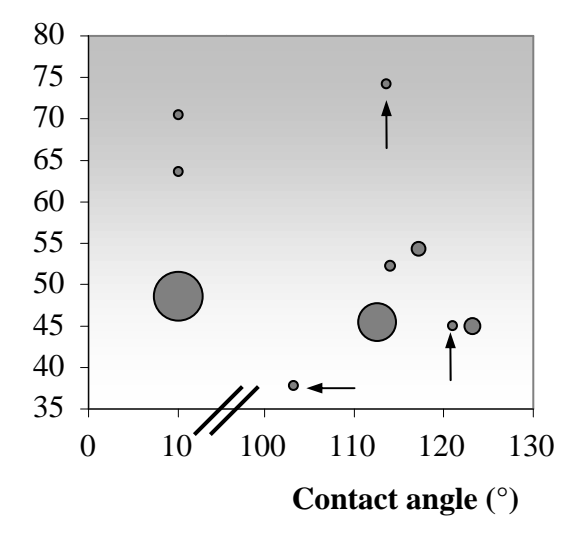
¹ Swiss cardiovascular Center, Bern, Switzerland, ²EMPA, Saint Gallen, Switzerland.

INTRODUCTION: Progress in tissue engineering is conditioned by the creation of a suitable environment in which cells can grow and organize themselves in a functional way. Electrospining offer the capability to design nano-fibrous scaffolds in the form of nonwonen structure that can biomimetic ECM found in the native tissue ¹. We addressed the role of nano- and micron-sized fiber structures in muscle cell proliferation, guidance and differentiation.

METHODS: The nano- and micron-sized nonwovens were prepared by an electrospinning procedure. Therefore, the biocompatible polymer polycaprolactone dissolved (PCL) was appropriate solvents and spun by applying a high voltage on a needle tip. Partial parallelisation of the nanofibers was obtained by using electrostatic lens systems and a fast rotating drum. Selected fiber patches were coated with a nitrogen-functionalized amorphous hydrocarbon coating (a-C:H:N), by performing RF plasma deposition using a gaseous mixture of ammonia and ethylene. Myoblasts cell lines (C2C12) and primary myoblast cell culture were seeded on the surface of biomaterials and cultured for up to 2 weeks in growth and differentiation media. We used MTT assay for cell proliferation and immunostaining differentiation.

RESULTS: The chemical and instrumental parameters used for the electrospinning procedure revealed a deep influence with respect to the PCL fiber diameters. Fibers with diameters from 100 nm to 2500 nm could be obtained. Main influencing parameters were the composition of the solvents used and the applied voltage.

Considering the factors such as fibers size, orientation (random or aligned) and wettability (contact angle) that may influence cell behaviors, we constructed a screening experiment to determine the optimal condition for muscle cell proliferation. The highest cell densities were obtained with aligned, 100 nm, hydrophobic PCL fibers and with 100 nm, randomly oriented, hydrophilic PCL fibers (Figure 1). Surface coating by plasma treatment of the biomaterials with the a-C:H:N provided an optimal cell adhesion that was increased by at least 20% with respect to non-coated patches. Interestingly, cell presented specific differentiation response with elongated and parallel myotubes (Figure 2).



DISCUSSION & CONCLUSIONS: Our results

Fig 1: Cell proliferation in response to electrospun PCL nano-fibrous scaffolds properties. Bubbles area represents fiber size from 100 to 2500 nm. Aligned fibers are indicated by arrow.

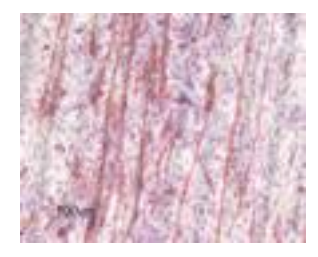


Fig.2. Aligned and elongated myotubes obtained from myoblast primary cell culture on a-C:H:N coated PCL (desmin immunostaining).

provide evidence that optimization of bioartificial tissue construct using nanofibers is challenged by biomaterials properties such as wettability, alignment and size of the fibers as well as specific coating. In addition parameters such as elasticity and porosity have to be considered for cell differentiation and the construction of a 3 dimensional bioartificial tissue.

REFERENCES:

1. Venugopal, J., S. Low, A. T. Choon, and S. Ramakrishna.(2007) Interaction of cells and nanofiber scaffolds in tissue engineering. *J Biomed Mater Res B Appl Biomater*, online..

In vivo evaluation of CaP produced nanocoating on laser macrostructured Ti6Al4V implants

M.D.Paz¹, S.Chiussi¹, P.González¹, J.Serra¹, B.León¹, J.I.Alava², I.Güemes³, F.M. Sánchez-Margallo³

INTRODUCTION: Titanium frequently used as dental and orthopaedic implant materials because of their excellent mechanical properties, chemical stability and biocompatibility. However, titanium and its alloys are non-bioactive after being implanted in bone. Thus, for further improvement of its bioactivity various implant surface modifications have been investigated (1). It has been a common practice to use primarily HA to coat metal implants for enhanced bioactivity and the PLD method became a promising technique in this field by producing films of pure and crystalline HA. HA is a calcium phosphate compound with similar composition to the mineral part of the bone⁽²⁾. It was found that osseoinduction was improved in surfaces with convexities (3) so a macrostructuration of the samples could benefit the bioactivity.

METHODS: The aim of this work was to evaluate in a sheep tibia model the effect of calcium phosphate nanocoatings on the bone regeneration at the interface between bone and implant of laser macrostructured titanium alloy samples.

Samples were Ti6Al4V cylinders of 10 mm long and 5 mm diameter with CaP coatings of 100 and 50 nm thick and their references without coating. Before coating, all samples, except the references, have been macrostructured with a Nd:YAG marking laser to achieve a regular pattern of craters. Thereafter, macrostructured samples have been coated with HA by using a 193 nm ArF excimer laser.

Before being implanted, the cylinders were sterilized in an autoclave.

Implantation took place into the tibia of 10 adult (Merina precoz) sheep. Four implants and a sham were implanted into one leg of each animal for 12 weeks.

Samples have been characterized with SEM and EDS before and after implantation. Microscopic evaluation using environmental scanning electron microscope (ESEM) was carried out directly on blocks of tissue embedded in resin, preceded by

sectioning and fine polishing using a JEOL JSM-59110LV electron microscope. The measurements of % BIC (Bone to Implant Contact) were performed using the Omnimet® image analysis system and were checked manually using a digital plan meter. The data was evaluated using double-blind statistical analysis of variance (ANOVA) and Student t-test for small samples (paired series).

RESULTS: SEM analyses show a continuous HA layer on the surface of the samples, EDS microanalyses of the interface between implant and resin show a little Ca/P peak in coated samples before implantation, this peak on the interface still appears after implantation in bone and its intensity is bigger than before. ESEM analyses of the coated samples show a better bone-implant interface than on the uncoated samples, and that the bone enters deeply into the craters of the macrostructure when the nanothin CaP coating was present.

DISCUSSION AND CONCLUSIONS: Superficial treatment of hydroxyapatite nanocoatings improves osseointegration and it seems that it gives a more integration than the laser macrostructuration without coating. Scientifically, this study has opened a new door for the "in vivo" studies on the interface between bone and implant and technically it opens the door for the study of an industrial application in dental implantation.

REFERENCES: ¹Mayor, B., Arias, J., Chiussi, S., García, F., Pou, J., León, B., and Pérez-Amor, M. (1998) *Thin Solid Films* **317**:363-366. ² Suchanek, W. and Yoshimura, M. (1998) *Journal of Materials Research* **13**:94-117. ³ Thomas, M. E., Richter, P. W., Crooks, J., and Ripamonti, U. (2001) *Key Engineering Materials* **192-195**:441-444

ACKNOWLEDGEMENTS: MAT2003-09277-C03-01, MAT IN94-0193, XUNTA DE GALICIA EXPTE:12/2006, INFRA PR405A2001/35-0, UNIVERSIDADE DE VIGO I418 122F 64102

 $^{^{\}it I}$ Applied Physics Department, University of Vigo, 36310 Vigo, Spain .

² Chemical Technology and Environment Department, INASMET, E-20009 Donostia, Spain.

³ Minimally Invasive Surgery Centre, 10071 Cáceres, Spain

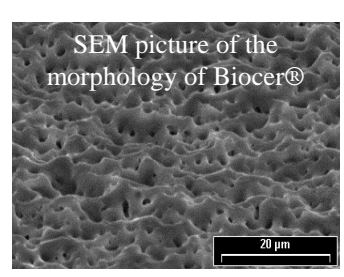
Biological responses of human osteoblasts to titanium coated by glow discharge anodisation

I. Gerber¹, J.C. Puippe², T. Wallimann¹

¹ ETH Zurich, Institute of Cell Biology; Zurich, Switzerland ² Steiger Galvanotechnique SA, Châtel-St-Denis, Switzerland; www.innosurf.ch

INTRODUCTION: The use of commercially pure titanium (cp Ti) and titanium alloys in the field of orthopedics and stomatology are widely accepted. Generally, for identification purposes, titanium implants are anodically colored as for instance by the proprietary "Biocoat blue" process. Further improvements in the biological performance can be achieved by surface modifications of these materials. The glow discharge anodisation Biocer® incorporating calcium and phosphate in a porous titanium oxyde coating has been investigated.

Thanks to its porous structure this coating is very suitable for a subsequent biofunctionalisation by grafting appropriated molecules. In this



study, we wanted first to compare the biocompatibility of Biocer® and Biocoat blue to cpTi and secondly to investigate the effects of Biocer® grafted with phosphocreatine (PCr). For both sets of experiments, human osteoblasts (HOB) are directly grown on these materials.

METHODS: HOB were isolated from bone chips from patients undergoing hip replacement surgery. In a first set of experiments, HOB were grown in direct contact with cp Ti, Biocer® and Biocoat blue. In a second set of experiments, HOB were grown on Biocer® grafted with PCr, uncoated Biocer® and on Biocer® with 1mM PCr in the growth medium. The standard cell culture polystyrene was used as a control. After 2 weeks, viability (quantification of neutral red uptake), metabolic activity (MTT assay), DNA content as well as bone forming parameters such as alkaline phosphatase activity (ALP) as well as C-terminal propeptide of collagen type I (CICP) and osteocalcin (OC) secretion were quantitatively assessed.

RESULTS: There were no significant differences found for HOB grown on cpTi, Biocer® and Biocoat blue concerning viability, metabolic activity, cellular CICP and OC secretion This was in contrast to the DNA content and ALP activity, where Biocer® had a significantly higher values

than cpTi (Fig. 1). Concerning ALP activity, Biocer® also was significantly higher than Biocoat blue.

Biocer® grafted with phosphocreatine. There was a significantly higher cellular osteocalcin secretion in the Biocer® groups, even though the number of cells was significantly lower than in the control groups (Fig. 2). All other parameters were similar. Furthermore, Biocer® grafted with PCr as well as Biocer® with 1 mM PCr in the growth medium had a significantly higher metabolic activity than the uncoated Biocer®.

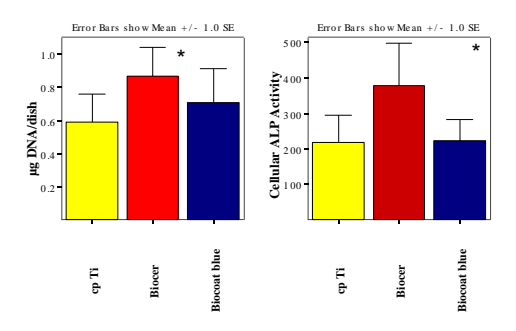


Fig. 1: DNA content (left) and ALP activity (right).

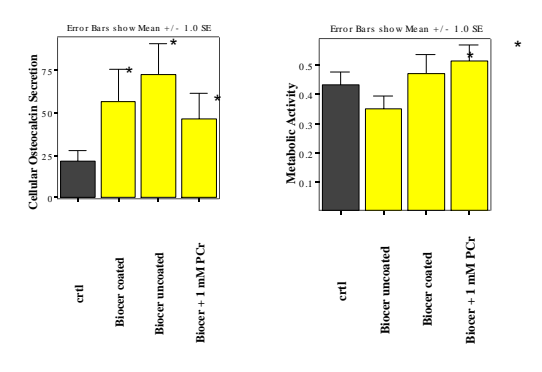


Fig. 2: Cellular OC secretion (left) and metabolic activity (right).

DISCUSSION & CONCLUSIONS: Biocer® and Biocoat blue show similar biological responses as cpTi for viability, metabolic activity, collagen and OC secretion, however Biocer® promotes cell grow and ALP activity over cpTi and even over Biocoat blue for ALP activity. Biocer® promotes differentiation by osteocalcin secretion as compared to the standard polystyrene cell culture dish. In addition, Biocer grafted with PCr significantly stimulates the metabolic activity of HOB.

Novel Neural Interface for Vision Prosthesis Electrodes: Neurite Outgrowth through Biomolecule Incorporation

R.A. Green¹, L.A. Poole-Warren¹ and N.H. Lovell¹

¹ Graduate School of Biomedical Engineering, University of New South Wales, Sydney, Australia.

INTRODUCTION: Epiretinal vision prostheses aim to restore vision to patients blinded by photoreceptor loss as a result of prevalent diseases retinitis pigmentosa (RP) and age related macular degeneration (AMD). Close apposition of retinal cells with implanted electrodes is critical to restoring vision¹. Conductive polymers, such as polyethylene dioxythiophene (PEDOT) coated on metal electrodes are proposed to improve the electrode interface by decreasing strain-mismatch and bi-layer capacitance that occurs between metal electrode surfaces and neural tissue. This study incorporating peptide proposes dopants conductive polymers to provide sites conducive to cell attachment. Several laminin peptides have been identified to target cell adherence (such as YIGSR and RGD) and neural growth or repair (YFQRYLI and SIKVAV)². This research explores two of these laminin peptides (YIGSR and YFQRYLI) combined with incorporation of nerve growth factor (NGF) into films. The aims were to assess the differentiation of cells on NGF incorporated films compared to differentiation of cells in NGF supplemented media and additionally to assess neurite cell adhesion on peptide doped films compared with laminin coated control films.

METHODS: Solutions of 0.1M EDOT doped with 0.05M pTS, $5\mu g/mL$ DCDPGYIGSR or $5\mu g/mL$ DEDEDYFQRYLI and supplemented with $1\mu g/mL$ NGF were produced in a solution of DI water and acetonitrile. The films were formed on platinum electrodes by galvanostatic electrodeposition at 2.0 mA/cm2 for 5 mins.

Films were washed with DI water for 12 h at 37 °C, disinfected by immersion in 70% EtOH and placed under UV for 1 hr. 5 μ g/mL laminin from murine sarcoma was coated on PEDOT/pTS controls. Fluorescent PC12s were plated at 20000 cells/cm², in 1% horse serum, RPMI. NGF was used as a media supplement at 50ng/mL in control films. Fluorescent images were taken at 96hrs and results were analysed using NeuronJ software. Average neurite length was used to assess cell differentiation and cell density was used as an indication of cell adherence.

RESULTS: Neurite outgrowth stimulated by NGF within the polymer film provided sufficient stimulus to result in neurites of comparable average length to those grown using NGF

supplemented media (see Fig 1). The average neurite length across all substrates was between $57\mu m$ and $75\mu m$, with no significant difference between the application types of NGF.

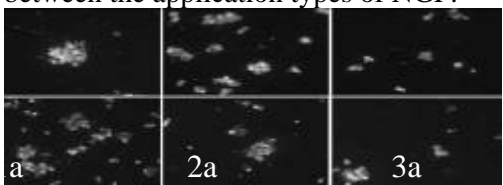


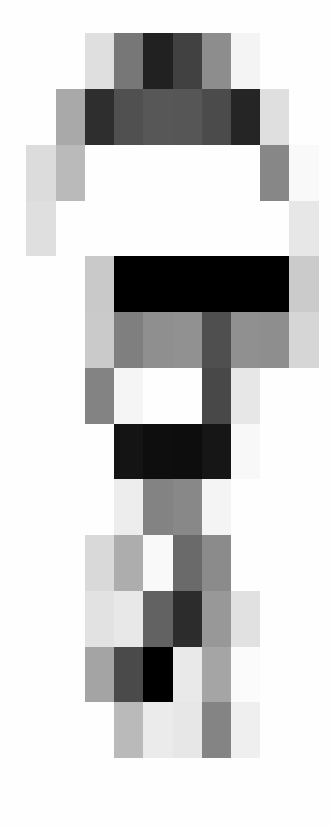
Fig 1: PC12s at 96hrs: 1.PEDOT/pTS; 2.PEDOT/DCDPGYIGSR; 3.PEDOT/DEDEDYFQ RYLI. a. NGF supplemented media and b. NGF incorporated into films.

Cell densities were much lower for films incorporating peptides indicating that exposure of adhesion peptides in doped films was less effective than in films coated with whole laminin (see Fig 2). However, films that incorporated peptides as the dopant grew neurites that were of similar length to those on laminin coated controls.

Fig 2: Cell density at 96 hrs.

polymer film can stimulate neurite outgrowth in PC12s. The use of laminin peptides as a dopant provided inferior adhesion of the PC12s than when the whole laminin molecule was used as a surface coating. This could be due to the laminin peptides being at a concentration that is too low, or accessibility of the peptides to cell receptors being limited by their restriction in the polymer matrix. Future studies will examine optimising presentation of peptide dopants.

REFERENCES: ¹Lovell, N.H., et al., Neural Engineering/Neuro-Nanotechnology, 2006. ²Nomizu, J., et al., J Bio. Chem; Vol. 27146; 2006.





Control of cell function on carbohydrate-immobilized phosphorylcholine polymer surfaces

Y.Iwasaki¹, U.Takami², Y.Shinohara², K.Akiyoshi²

¹ Kansai University, Osaka, Japan. ² Tokyo Medical and Dental University, Tokyo, Japan.

INTRODUCTION: We hypothesized that 2-methacryloyloxyethyl phosphorylcholine (MPC) polymer surfaces bearing carbohydrates might perform as biomembrane mimetic surfaces, which can interact with a specific cell. In this study, MPC copolymers with galactose residues have been synthesized and we present here the effectiveness of the surface in controlling cell/material interaction and preserving cell function.

METHODS: Poly[MPC-co-n-butyl methacrylate (BMA)] (PMB), poly[BMA-co-2-lactobionamidoethyl methacrylate (LAMA)] (PBL), and poly(MPC-co-BMA-co-LAMA) (PMBL) were synthesized by conventional radical polymerization¹.

Human hepatocellular liver carcinoma cell line (HepG2) cells and mouse fibroblasts (NIH-3T3) were purchased from RIKEN Cell Bank. The concentration of the cells was adjusted to 2.0 x 10⁴ cells/ml. The cells were seeded on the polymer surfaces and continuously cultured for specific periods. The polymer plates were then rinsed with PBS. The plates were soaked into Triton X-100 aqueous solution. The Triton X-100 solution was collected and the concentration of LDH from the adherent cells was measured.

Morphological observation of the HepG2 cells cultured on the polymer surfaces was performed by a confocal laser scanning microscope.

RESULTS: Figure 1 shows the time-dependent surface density of HepG2 and NIH-3T3 cells on a polymer surface after culture for given periods. On a PBMA surface, many HepG2 cells adhered and the density increased with an increase in culture time. In contrast, the cell adhesion was reduced on the PMB surface because adsorption of

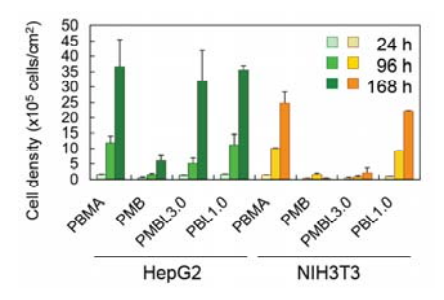


Fig. 1: Cell density on polymer surfaces.

the cell-adhesive protein on the surface could be reduced (data not shown). When the LAMA composition was 3% in PMBL, the density of adherent HepG2 cells was similar to that on PBMA for every culture period. NIH-3T3 cells adhered and proliferated as well as the HepG2 cells on the PBMA surface. On the other hand, the adhesion of NIH-3T3 cells was reduced on the polymer surfaces having MPC units.

Figure 2 shows confocal micrographs of HepG2 cells cultured on PBMA, PBL1.0, and PMBL1.0 for 168 h. On PBMA and PBL1.0 surfaces, monolayer cell adhesion was observed and each cell was spread. At the outline of the pseudopod formation of the adherent cells, actin was easily observed. In contrast, HepG2 cells cultured on PMBL1.0 formed spheroids with multilayer adhesion.

DISCUSSION **CONCLUSIONS:** Carbohydrate-immobilized phosphorylcholine polymers (PMBL) were newly synthesized to produce biomembrane mimetic surfaces, which perform selective recognition of proteins and cells. Surfaces coated with PMBL effectively reduced nonspecific interaction. and specific ligand/receptor interaction clearly was demonstrated. Changing the types carbohydrates enables changes in the types of biorecognition. The polymers have great potential for bioreaction, molecular separation, targeting, sensing, etc.

REFERENCES: ¹ Y. Iwasaki, U.Takami. Y.Shinohara, et al (2007) *Biomacromolecules*, in press.

ACKNOWLEDGEMENTS: We thank the New Energy and Industrial Technology Development Organization (NEDO) Japan for providing financial support.

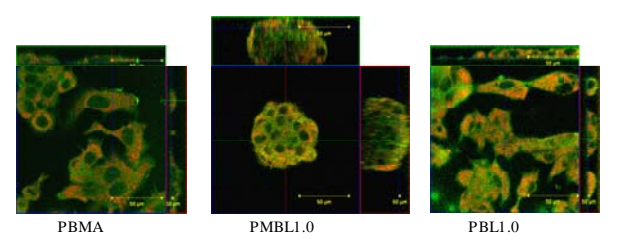


Fig. 2: Fluorescence micrographs of adherent cells.

Real Time Analyses of Myogenesis in Behaving Myoblasts

E. Thomasson¹, B. Staedler¹, T. Blaettler^{1,2}, J. Voeroes¹, A. Franco-Obregón¹

¹Laboratory of Biosensors and Bioelectronics, ETH Zurich, Switzerland. ²Laboratory for Surface Science and Technology, ETH Zurich, Switzerland.

INTRODUCTION: Effective Tissue engineering ultimately depends on understanding the interplay between the proliferation and differentiation stages of development. One of the best systems to examine these processes is myogenesis. Activated myoblasts first undergo many rounds of cell division. Depending on the needs of the cells, myoblasts may next withdraw from the cell cycle to fuse to form myotubes. Division and fusion are differentially modulated by mechanical stimuli transmitted to the cell's biosynthetic mechanisms via the actin-based cytoskeleton; Specifically cyclic stretch promotes proliferation and inhibits fusion.² By inference, the nature of cell attachment to the substrate should also influence transition through myogenesis. We therefore investigated the effect of the extracellular matrix on behaving cells undergoing either cytokinesis or fusion using atomic force microscopy (AFM) as well as confocal laser scanning microscopy (CLSM) in fluorescent mode.

METHODS: C2C12 muscle cells were seeded (5,000 cells/cm²) onto glass coverslips which had been coated with either Fibronectin or Laminin and maintained in growth media (20% Fetal Bovine Serum (FBS)) for two days in order to favour proliferation. Fusion was induced two days later with a switch to differentiation media (10% Horse Serum (HS)). Contractile competent myotubes were apparent 9 days after plating when grown on glass coverslips that had been patterned with lanes of extracellular matrix proteins. The topography of living myoblasts was analysed with an AFM (from JPK Instruments) in CO₂ independent media supplemented with 0.13% Glutamine and 20% FBS, or 10% HS, for cytokinesis and fusion studies respectively. The 2D organization of the actin-based cytoskeletal network was examined by CLSM after staining myoblasts with Rhodamine labelled Phalloidin. To distinguish between individual cells and to quantify the size of the myotubes, nuclei were stained with DAPI.

RESULTS: When compared to conventional confocal microscopy, our AFM analysis rendered more information concerning myoblast-myoblast and myoblast-substrate attachments. Whereas laminin promoted proliferation and cell migration, fibronectin was more permissive for tight

myoblast-myoblast contacts. Myoblast-myoblast adhesion was characterized by the expression of interdigitating membranous processes uniting groups of fusing myoblasts. The precise topography of the membrane tubules was most evident with the AFM. The same structures were also observed with CLSM and revealed that these membrane tubules were built upon a scaffold of actin filaments. Similar membrane processes were less evident during cytokinesis.

DISCUSSION & CONCLUSIONS: These results suggest that the substrate is of importance for myoblast behaviour during myogenesis. Since myoblasts interact with laminin and fibronectin via distinct integral membrane protein complexes (dystroglycan and integrins, respectively) these results suggest that distinct extracellular matrixbinding complexes differentially govern transition through myogenesis. Membrane tubules were observed in the fusion process and therefore we believe that, in accordance with recent findings in the drosophila system³, the nucleation of actin filaments initiates the fusion process. Actin could then in myoblast fusion, as in the drosophila system, be responsible for a transportation of vesicles to the cell membrane. These would then in turn constitute the active part of the fusion process.

REFERENCES: ¹ T. Hawke, et al. **J. Appl. Physiol.** (2001) *Myogenic satellite cells:* physiology to molecular biology, 91:534-551. ²U. Cheema, et al. **J. Cell. Phys.** (2005) *Mechanical Signals and IGF-I Gene Splicing In Vitro in Relation to Development of Skeletal Muscle*, 202:67-75. ³S. Kim, et al. **Developmental Cell** (2007) A Critical Function for the Actin Cytoskeleton in Targeted Exocytosis of Prefusion Vesicles during Myoblast Fusion, 12:571-586

ACKNOWLEDGEMENTS: This project is supported by a grant from the Swiss National Science Foundations, SNF K-32K1-116532.

The cell adhesion process and apoptosis monitored with the piezoelectric sensor \underline{Z} . Fohlerová \underline{I} , \underline{P} . Skládal \underline{I} , \underline{J} . Turánek \underline{I}

¹Masaryk University and ²Veterinary Research Institute, Brno, Czech Republic.

INTRODUCTION: The cell adhesion process was studied due to its relevant role in many biological research areas. The complex view into the mechanism of the cell adhesion can be obtained using the quartz crystal microbalance technique (QCM). This approach enables to record a shift in the resonant frequency and/or resistance of the sensor during the cell attachment and spreading on the surface. QCM responses are markedly different according to the cell type and number, adhesion power and vitality. Several ECM proteins were tried as coatings improving cell attachment on the gold surface. Finally, apoptosis due to the effect of drugs was monitored with QCM as well.

METHODS: The 10 MHz quartz crystal with gold electrodes on both sides was placed on the bottom of the thermostated measurement chamber. For different experiments the electrodes were used uncoated and pre-coated either with laminin (2 μg/cm²), fibronectin (10 μg/cm²) or vitronectin (0.1 μg/cm²). Two cell lines such as rat epithelial cells (WB F344) and lung melanoma cells (B16F10) were cultured for the comparison and seeded on the sensor at the appropriate density. The shifts of the resonant frequency and resistance were monitored in real-time over the 1 day cultivation. Next, the presence of cells on the sensing surface was detected using the fluorescent microscope (MitoTracker Red CMXRos staining). The apoptosis was initiated with the addition of α -TAM (derivate of vitamine E) at 300 µM to the established confluent layer of cells simultaneously microscopically compared with the standard microplate experiment.

RESULTS: Fig.1 shows the typical and expected result of the cell adhesion process on the vitronectin-modified surface. The resonant frequency was decreasing and resistance increasing because of viscoelastic properties of the adhering cells. Similar results were achieved with the bare electrode and fibronectin coated surface as well. The different result was obtained with laminin. This surface was promoting cells attachment but the electrochemical signal was contrary to the surfaces mentioned previously. A marked change was also between two cell lines. A steeper decrease in resonant frequency and a larger increase in resistance were obtained with B16F10 cells compared to WB F344 cells. Regarding the QCM

response of cells after the drug addition the frequency sloped down and the resistance was slightly increasing.

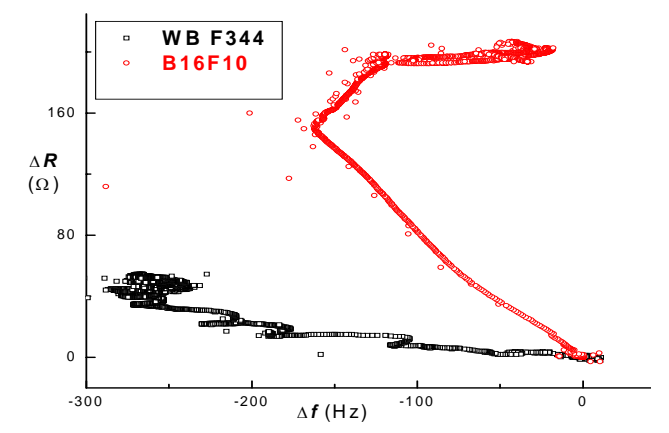


Fig. 1: Dependence of the resistance on the resonant frequency during cells attachment process on the vitronectin coated sensing surface.

biscussion & conclusions: Piezoelectric sensor is a suitable device for monitoring of adherent cells on modified surfaces. Real-time monitoring of cellular processes allows to achieve more detailed information compared to standard microplate-based cultivation techniques. The tested cell lines were successfully combined with modified sensing surfaces, thus obtained cell-based biosensors are promising for convenient testing of physiologically active compounds as novel drugs, which modify either metabolic activity or morphologic properties of the attached cells

REFERENCES: ¹C. Fredriksson, S. Khilman, B. Kasemo, J. Mater. Sci.: Materials in Medicine 1998, 9: 785-788. ²J. Wegener, A. Janshoff, H. Galla, Eur. Biophys. J., 1998, 28: 26-37. ³T. Zhou, K. Marx et al., Biotechnol. Prog., 2000, 16:268-277. ⁴K. Marx, T. Zhou, A. Montrone et al., Biosens. Bioelectron., 2001, 16: 773-782

ACKNOWLEDGEMENTS: This work was supported by grants CZ-MZE 0002716201, CZ-MSM 0021622413, and EU-QLK3-CT-2001-00244 (CELLSENS).

THE CELLHESION - QUANTIFYING ADHESION FORCES BETWEEN SINGLE CELLS

K. Poole, G.Behme², H. Haschke³, R. Owen

JPK Instruments AG, Bouchéstr. 12, 12435 Berlin, Germany

The CellHesion Development Kit has been designed to allow reproducible and quantitative analysis of cell-cell and cell-substrate binding forces. Using a combination of light microscopy and force spectroscopy, single cells can be selected, attached to a flexible cantilever and subsequently allowed to adhere to a second, specific cell or region of substrate. The instrument allows precise control of the force the cells are subjected to during a user-defined binding period. The bound cells can then be separated at a specific speed, to a distance of up to 100 µm. By monitoring the bending of the sensor during the retraction process a force-distance curve can be plotted. From this force-distance curve it is possible to calculate the amount of work and maximal force required to separate the two cells. Additionally, analysis of sub-features of the forcedistance retraction curve allows the determination of the force required for the unbinding of single protein-protein interactions at the cell surface. The design of the CellHesion allows a combination of this AFM force spectroscopy with phase contrast, DIC and epifluorescent microscopy or confocal imaging. Such capabilities not only enable the selection of specific cells within a culture for binding measurements, but also the monitoring of multiple additional cellular processes that may occur on binding, such as changes to actin structure, calcium flushes, distribution of labelled proteins, or morphological changes.

Interaction of Osteoblasts with the Surface Structure of Different Oxide Layers on Titanium Substrate

<u>A. Ochsenbein</u>^{1,2}, <u>F. Chai</u>³, <u>S. Winter</u>¹, <u>M. Traisnel</u>², <u>H.F. Hildebrand</u>³, <u>J. Breme</u>¹

¹Saarland University, Department of Metallic Materials, Saarbrücken, Germany. ²PERF, Villeneuve d'Ascq, France. ³GRB, Lille, France.

INTRODUCTION: Titanium is the material of choice for many biomedical applications. Its potential as a biomaterial and especially its biocompatibility can be explained by its native surface oxide layer of TiO₂ with a thickness of 2-6 nm. In our recent works, investigations have been carried out to determine to what extent a reinforcement or a change in the chemical composition of the native oxide layer could even improve the biocompatibility of cp-Ti.

METHODS: Oxide layers consisting of TiO_2 , Nb_2O_5 , SiO_2 and TiO_2 - SiO_2 have been produced by the Sol-Gel process and have been deposited on mirror-like polished substrates of cp-Ti by spin-coating. The physical and chemical properties have been characterized by spectroscopic ellipsometry, by atomic force microscopy (AFM) for topography, by scanning electron microscopy (SEM) and by contact angle measurements (sessile drop method).

MC3T3-E1 osteoblasts have been used for biological tests: cell proliferation by cell counting, cell vitality with Alamar blue dye, cell morphology by SEM observations and cytochemical immunelabelling of actin and vinculin.

RESULTS: Oxide layers with a thickness of 100-130 nm had been produced. The morphology investigations revealed a nanoporous structure of the TiO₂ and Nb₂O₅ (Fig. 1) layers whereas the SiO₂ and TiO₂-SiO₂ layers appeared compact and very smooth.

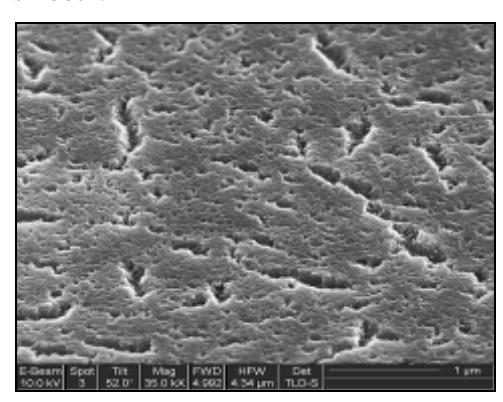


Fig. 1: SEM micrograph of the nanoporous surface of a Nb_2O_5 layer on a cp-Ti substrate with a subsequent drying and annealing at 450 °C for 1 hour.

The roughness values Ra, determined by AFM, ranged from 0.36 nm to 3.46 nm. The contact angle measurements indicate that the SiO_2 layer surfaces are very hydrophilic with contact angles of about 22° towards water whereas TiO_2 , Nb_2O_5 , SiO_2 and TiO_2 - SiO_2 layers are more hydrophobic with contact angles between 52° and 56° .

The proliferation rates for all samples tested were higher than for the polystyrene control. The results for the TiO_2 , TiO_2 - SiO_2 and cp-Ti layers were about the same, the results for the Nb_2O_5 layer were slightly worse. The SiO_2 layer revealed the poorest results.

Cell vitality tests proved a good biocompatible behavior of all layers tested. For Nb_2O_5 and cp-Ti a significantly increased cell activation has been noted.

DISCUSSION & CONCLUSIONS: The SiO₂ layer showed the poorest cell proliferation and vitality results. This may be caused by its high hydrophility. The TiO₂ layer did not improve the cells response compared to the native oxide layer on cp-Ti. The TiO2-SiO2 layer showed a better proliferation than the Nb₂O₅ layer whereas both revealed a good vitality and cell spreading. Both layers showed about the same contact angle whereby the TiO2-SiO2 layer has a smooth appearance whereas the Nb₂O₅ layer appears porous and rough-textured. A special interest is given to the Nb₂O₅ layer that induced the most favourable cell spreading with normal actin stress fibres and a well developed network of focal adhesion contacts as revealed by SEM and cytochemical labelling, respectively.

REFERENCES: ¹ E. Eisenbarth et al (2002) *Interactions between cells and titanium surfaces* Biomolecular Engineering **19**:243-249.

ACKNOWLEDGEMENTS: The authors wish to thank the Deutsche Forschungsgemeinschaft for their kind support.

Adhesion, proliferation and differentiation of primary keratinocytes on chemically functionalized nano- and microstructured surfaces

P.Schweizer¹, K.Borchers¹, D.Wojciukiewicz¹, D.Riester¹, M.Weimer¹, G.Tovar², H.Mertsching¹

¹ Fraunhofer Institute for Interfacial Engineering- and Biotechnology Fh-IGB. Nobelstraβe 12, 70569 Stuttgart, Germany. ² University Stuttgart, Institute for Interfacial Engineering, Nobelstraβe 12, 70569 Stuttgart, Germany

INTRODUCTION: Tissue Engineering is an interdisciplinary research field with the goal to manufacture *in vitro* tissues and organs. But so far only a few 3D-tissues have been successfully developed. Culture of primary cells is challenging, since especially most human cells are fully differentiated in the adult organism and can therefore be poorly proliferated *in vitro*. They are prone to loss of function or initiation of apoptosis during isolation and cultivation. Therefore, new cell culture systems have to be created, featuring structurally and functionally tailored substrates that meet the needs of primary cells^{1,2,3}.

To gain basic insight into the impact of non-biological features on cells' behaviour, primary keratinocytes were cultured on chemically functionalized substrates with planar, nano- and microstructured surfaces. Adhesion, proliferation and differentiation have been evaluated by immunohistochemical staining and scanning electron microscopy (SEM).

METHODS: Glass-slides were modified with ultra-thin coatings of polyelectrolyte-films resulting in planar surfaces displaying positive and negative surface-charges as well as different organic functionalities e.g. amino-, carboxyl- and sulfuric groups. Additionally, amino- and carboxyl modified nano- and microparticles were deposited, to gain functionalized nano- and microscopic rough surfaces. For analyzing the percentage of surface coverage by particles the program "analySIS" from Soft Imaging System GmbH was used.

Cells were isolated from human skin and cultured at 37°C and 5% CO₂. Adhesion, proliferation and differentiation of primary keratinocytes on various surfaces were evaluated e.g. with microscopic examinations and immunohistochemical staining against specific Cytokeratins.

RESULTS: The polyelectrolyte-films were verified by ellipsometry and a surface coverage with particles between 70% and 90% was achieved. The kind of differentiation of primary keratinocytes range between progenitor-like and late differentiated depending on structural and functional modification of the substrate. Also

strong distinctions in cell's spreading time were noticed. Surface adhesion properties were illustrated by staining the actin-cytoskeleton of primary keratinocytes. Direct interaction of filopodia-like structures and nanoparticles was observed with SEM (Fig.1).

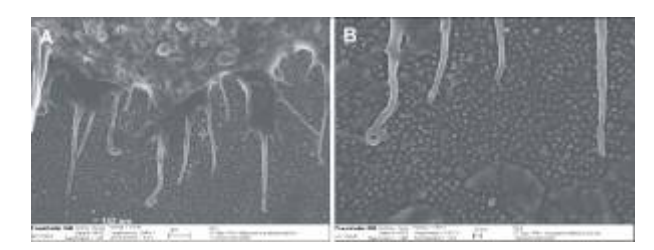


Fig. 1: A) With SEM filopodia-like structures of primary keratinocytes can be illustrated. B) Direct interaction of these filopodia-like structures with nanoparticles.

DISCUSSION & CONCLUSIONS: Long term objectives of these studies are to cope with crucial points of Tissue Engineering: effective isolation of primary cells, long term cultivation of stem cells, selective differentiation and functional cultivation of primary cells.

Insight into the cells' preferences concerning structure and chemical functionality of the substrate helps to built up improved cell-culture systems, optimized biomaterials and tailored surfaces for implants without the use of cost-intensive biological components.

REFERENCES: ¹M.M. Stevens and J.H. George, (2005) *Exploring and engineering the cell surface interface*, Science **310**, 1135-8. ²M.P. Lutof and J.A. Hubbell (2005) *Synthetic biomaterials as instructive extracellular microenvironments for morphogenesis in tissue engineering*, Nat Biotechnol **23**, 47-55. ³B.C. Isenberg and J.Y. Wong (2006) *Building structure into engineered tissues*, Materialstoday, **9**, pp 54-60.

ACKNOWLEDGEMENTS: The authors kindly the Peter und Traudl Engelhorn Stiftung and the Fraunhofer Gesellschaft for funding this project.

C1q and C-reactive Protein (CRP) Modulate Platelet Activation on Adsorbed Immunoglobulin G and Albumin

1. Skoglund^{1, 2*}, J. Wetterö³, T. Skogh³, C. Sjöwall³, P. Tengvall¹ and T. Bengtsson^{1, 2}

INTRODUCTION: Blood platelets have for long been recognized during hemostasis but are now also emerging as key actors during inflammation following implantation of a biomaterial, as well as in diseases with an inflammatory component such as atherosclerosis. A material in contact with blood will adsorb plasma proteins within milliseconds, e.g. immunoglobulin G (IgG) and albumin. Surprisingly, little is known regarding how protein adsorption regulates the platelet activation and their subsequent impact on other cells. C-reactive protein (CRP) is an acute phase protein which is elevated during inflammation and tissue injury, and represents a powerful predictor of coronary artery disease ¹. Although the physiological role of CRP is incompletely understood, we and others have shown that CRP binds to C1q and activates the classical complement pathway, although limited to the initial stages of the complement system, i.e. no membrane attack complex is formed.

The aim of this study was to characterize the CRP, C1q and adsorbed plasma protein interaction with respect to platelet activation.

METHODS: IgG albumin and were spontaneously pre-adsorbed to methylated inorganic supports, and CRP and Clq were allowed prior humoral interaction before surface exposure. Protein adsorption was analyzed by ellipsometry, combined with polyclonal antibody detection. Surface-triggered platelet activation was investigated using a static platelet adhesion assay, where adherent platelets were stained for F-actin and visualized in a fluorescence microscope. phosphatidylserine Furthermore, platelet expression was evaluated by annexin-V-binding, and thromboxane B2 was measured as a marker for platelet secretion.

RESULTS: CRP alone did not associate with the adsorbed IgG, but when preincubated with C1q,

both C1q and CRP were detectable on the surface. Ellipsometry also confirmed that C1q bound to the adsorbed IgG, and also suggested that both C1q and CRP may bind to pre-adsorbed albumin, a protein regarded to blunt inflammation. The platelet count and the cell morphological examination showed extensively more activated platelets on IgG surfaces in reference to albumin surfaces. Interestingly, the addition of C1q or CRP reduced the adhesion to IgG, HSA and methylated matrices. Furthermore, preincubation of C1q and CRP was the most effective in reducing platelet adhesion to the adsorbed IgG. It was also observed that C1q triggered an incomprehensive platelet activation morphology, for all surfaces. The inhibitory effects of CRP and C1q were also seen with platelet phosphatidylserine expression.

DISCUSSION & CONCLUSIONS: Platelet adhesion to adsorbed plasma proteins is inhibited by complement protein C1q as well as by the acute-phase protein CRP. It is possible that C1q facilitates the binding of CRP to IgG and thereby modulate platelet activation. We suggest that this regulatory role of CRP may be important in preventing the potential harmful side effects of inflammation at artificial surfaces, e.g. extensive platelet activation.

REFERENCES: ¹ C. Sjöwall, J. Wetterö, (2007) Clin Chim Acta **378**: 13-23.

ACNOWLEDGEMENTS: Agneta Askendal is acknowledged for valuable laboratory assistance. This study was supported by the strategic research area "Materials in Medicine" (Linköping Council University and the County Östergötland), the Swedish Fund for Research Animal Experiments, Trygg-Hansa Research Fundation, Swedish Society for Medicine and the Goljes minne and Magn Bergvall research foundations.

¹ Materials in Medicine, Division of Applied Physics, Department of Physics, Chemistry and Biology, Linköping University, Linköping, Sweden

² Cardiovascular Inflammation Research Center, Division of Pharmacology, Department of Medicine and Health Sciences, Linköping University, Linköping, Sweden

³ Division of Rheumatology/Autoimmunity and Immune Regulation unit (AIR), Department of Clinical and Experimental Medicine, Linköping University, Linköping, Sweden * Corresponding author: carsk@imv.liu.se

Glycopolymer-engineered biodegradable microparticles as vaccine against Leishmaniasis

N. Csaba¹, G. Coullerez², X. Liu³, M. Textor², P.H. Seeberger³, H.P. Merkle¹

¹ Drug Formulation and Delivery Group, ² Laboratory for Surface Science and Technology. ³ Laboratory of Organic Chemistry, ETH Zurich, CH-8093 Zurich, Switzerland.

INTRODUCTION: This work aimed at engineering the surface of biodegradable PLGA microparticles with a glycopolymer for the delivery of synthetic Leishmania antigen promoting T cell mediated specific immune responses. Microparticulate carriers coated with the poly(L-lysine)-graft-poly(ethylene glycol) (PLL-g-PEG) brush copolymers reduce their non-specific phagocytosis while polymers functionalized with ligands allows for specific recognition.^{1,2} Herein, a mannose containing synthetic tetrasaccharide, derived from a lypophosphoglycan expressed on the cell surface of Leishmania donovani, was conjugated to the PLL-g-PEG, which was then adsorbed to poly(D,L lactic-co-glycolic acid) (PLGA) microparticles. The microparticles were also loaded with a model protein to enhance the immunogenicity and characterized with regard to physico-chemical properties, protein encapsulation and release.

METHODS: Leishmania tetrasaccharide terminated with a mercapto propyl linker at the reducing end was synthesized as previously described³ and conjugated to the polycationic PLL-g-PEG graft copolymer in a ratio ca 20% of PEG-antigen as determined by ¹H-NMR. The PLGA microparticles optionally loaded with 5% w/w ovalbumin, were prepared by static multilamination micromixer technology.⁴ Surface coating was carried out by incubation of the particle suspensions with the polymer solutions in a thermomixer.² Protein loading and release was measured by fluorimetry. Availability of the sugar epitope for biorecognition of a mannose binding lectin Concanavalin A (ConA) was quantified by optical waveguide lightmode spectroscopy (OWLS) on flat surfaces and by FACS analysis on particles using ConA-Alexa Fluor® 488 dve.

RESULTS: OWLS analysis showed specific recognition of the lectin ConA to the glycopolymer while at the same time the surface resisted nonspecific adsorption of proteins from human serum. The PLGA microparticles were produced in a size range of $1-10~\mu m$. Surface modification was confirmed by the change of the zeta potential values from initial negative charge to neutral or slightly

positive values after incubation with the copolymer. Availability of the antigen on the particles surface was confirmed by FACS analysis showing ConA binding (Figure 1). While PLL-g-PEG coated PLGA microparticles were protein resistant, ConA adsorbed on their surface in the presence of the sugar. Ovalbumin was incorporated within the formulation with an efficiency of 30%. Extent of lectin binding varied with the presence of the protein in the particles (both uncoated and carbohydrate tagged particles). Nonspecific binding might be due to a burst release of the protein during the assay.

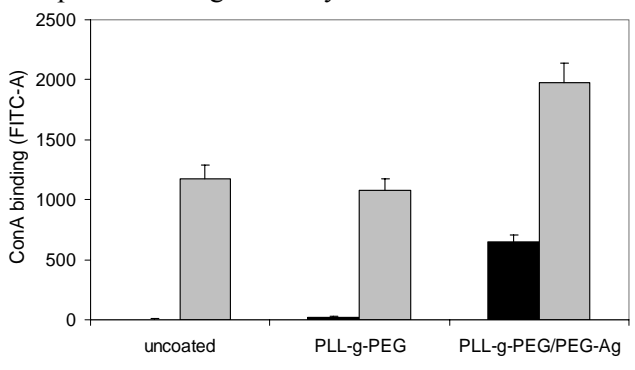


Figure 1. Effect of protein encapsulation and particle coating on ConA binding. (**m**) PLGA microparticles without protein, (**m**) ovalbumin-loaded PLGA microparticles (standard deviation below detection limit for PLL-g-PEG coated particles)

Nevertheless, ConA adsorption was increased on polymer tagged with the antigen indicating specific binding also on the microparticles.

DISCUSSION & CONCLUSIONS: The assembly of a carbohydrate antigen onto PLGA microparticles is feasible through its chemical conjugation to a PLL-g-PEG brush copolymer. These surface modified microparticles could be potentially used as antigen carriers to the immune system.

REFERENCES

¹Faraasen, S. et. al; (2003) Pharm Res, **20**(2), 237-46. ²Wattendorf, U. et. al (2006) Biointerphases, **1**(4), 123-133. ³Hewitt, M.C. and P.H. Seeberger (2001) Org Lett, **3**(23), 3699-702. ⁴Fischer, S. et. al (2005) J Control Release, **111**(1-2) 135-144.

PLL-g-PEG/PEG-mannose functionalized nanogels for cell-receptortargeted drug delivery application

C. Perrino, N. Csaba, G. Coullerez, G. Gorodyska, S. Bravo, H.-P. Merkle, M. Textor

¹ Laboratory for Surface Science and Technology, ² Drug Formulation and Delivery Group, ETH Zurich, CH-8093 Zurich, Switzerland

INTRODUCTION: Polymeric nanoparticles are receiving considerable attention for several biomedical applications, including delivery of therapeutic drugs and gene delivery. They hold a large potential in medicine, especially if biofunctionalities can be linked to their surface. The purpose of this work is to develop sugarfunctionalized nanoparticles for targeted drug/gene delivery mediated via C-type lectin receptors, e.g. DC-SIGN or mannose binding lectins, known to recognize oligosaccharides.

METHODS: Nanoparticles were prepared from a polycationic graft copolymer poly(L-lysine)-graftpoly(ethylene glycol) (PLL-g-PEG) through electrostatic interactions with negatively charged gelling crosslinkers, eg. hyaluronic acid. The ratio of the cationic polymer to the crosslinker was varied in order to obtain series of nanogels with different sizes. Graft copolymers with different lysine to PEG grafting ratios (g) were also used to vary PEG density, molecular weight and the positive charge density of the copolymer. Functional nanogels were then prepared using PLL-g-PEG conjugated with mannosides. The particles were characterized with regard to their size distribution and surface properties by means of dynamic laser light scattering and laser-Doppler anemometry, respectively. The size and particle morphology were also measured by atomic force microscopy (AFM).

RESULTS: The developed nanoparticles were in the size range of 100-500 nm. The zeta potentials were positive (between 10 and 30 mV) decreasing as the concentration of the hyaluronic acid was increased in the nanocomposites. The PEG grafting ratios of the copolymer influenced the zeta potential values, with the particles prepared from polymers with higher degree of PEGylation being less positive than the more open-structure ones. These results were also supported by AFM measurements that revealed the morphology of the particles to have a dense crosslinked central core (Figure 1). The stability of the nanoparticles was studied in water and in CaCl₂ for 2 weeks and 2 months after preparation. Cytotoxicity tested with macrophages in vitro decreased with increasing

PEG density demonstrating that the PLL charges become shielded by a PEG corona.

In the same way mannose functionalized nanogels were produced. The availability of the carbohydrate ligand for controlled cell uptake will be carried out via specific interaction with a model plant lectin and using different cell lines. Potential applications of DNA loaded particles for gene transfection are currently investigated.

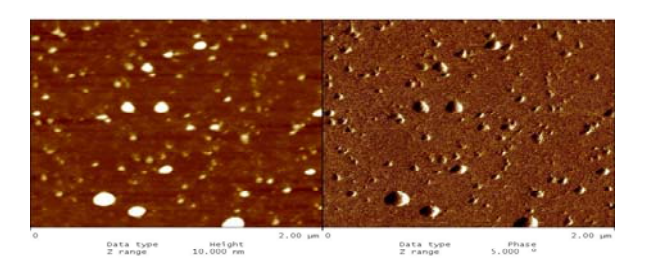


Fig.1 AFM micrograph $(2 \times 2 \mu m^2)$ of PLL-g[18.1]-PEG based nanogels crosslinked with hyaluronic acid (3/1 ratio).

DISCUSSION & **CONCLUSIONS:** The PLL-g-PEG/PEG preparation of based nanocomposites is feasible in a controllable and reproducible fashion. The methodology for the preparation of nanogels is straightforward, and would open up simple ways to design drug and gene delivery carriers or for the delivery of antigens to mediate specific immune response. The potential application of the platform using mannoside-functional polymers to target cell receptors on various human monocyte cell lines for gene delivery is currently under evaluation.

REFERENCES: ¹L. L. X. Yuan, A. Rathinavelu, J. Hao, M. Narasimhan, M. He, V. Heitlage, L. Tam, S. Viqar, M. Salehi, *J. Nanosci. Nanotech.* 6, 2821-2828 (2006). ²A. A. S. Patnaik, S. Nimesh, A. Goel, M. Ganguli, N. Saini, Y. Singh, K.C. Gupta, *J. Controlled Release* 114, 398-409 (2006). ³C. R.-L. P. Calvo, J.L.Vila-Jato, M.J.Alonso, *J. Appl. Polym. Sci.* 63, 125-132 (1997). ⁴F. C. F. Qian, J. Ding, C. Yin, *Biomacromolecules* 7, 2722-2727 (2006). ⁵A. R. S.T. Reddy, H.G. Schmoekel, J.A. Hubbell, A. Melody, *J. Controlled Release* 112, (1), 26-34 (2006). ⁶S. P. J.M. de la Fuente, *Biochim. Biophys. Acta* 1760, 636-651 (2006).

Cell Biological Investigations on Bioactive Surfaces

¹F. Lüthen, ¹C. Bergemann, ²B. Finke, ²K. Schröder, ²A. Ohl, ¹J. Rychly

¹University of Rostock, Medical Faculty, Dept. of Cell Biology, Rostock, Germany.

²Institute of Low Temperature Plasma Physics (INP), Greifswald, Germany.

INTRODUCTION: The surface properties of an implant material influence strongly the cellular behavior at the interface. The general goal is the control of the tissue physiology by creating bioactive surfaces [1]. In our study we examined differently modified surfaces for the stimulation of human mesenchymal stem cells (hMCS) to differentiate to osteoblastic cells in vitro. Polished titanium dishes were functionalized by amino (-NH₂) or carboxyl (-COOH) groups assuming that the different surface charges affect the cellular response.

METHODS: Polished titanium discs (Ti-P) (grade 2, R_a 0.19µm) were coated with an about 50-100 nm thin layer of plasma polymerized allylamine (Ti-PPA, NH₂-group) or acrylic acid (Ti-PPC, COOH-group). These films prepared by pulsed low pressure microwave discharge plasma (2.45 GHz, 500 W, p=50Pa and 700 W, p=20 Pa, respectively). hMSC (6000 cells/cm², Lonza) were plated on the modified titanium surfaces and cultivated in MSCBM medium under basal and osteogenic conditions. Spreading (cell area in µm²) of PKH26-stained cells [3] was measured using confocal microscopy (LSM 410, Carl Zeiss). Quantitative real time RT-PCR assays were performed for alkaline phosphatase (ALP), collagen 1 (Col), bone sialo protein (BSP), osteocalcin (OCN), Runx2, and monitored in triplicate using an ABI PRISM® 7500 Sequence Detection System. Gene expression values were calculated by the comparative $\Delta\Delta C_{T}$ method and normalized to Ti-P.

RESULTS:

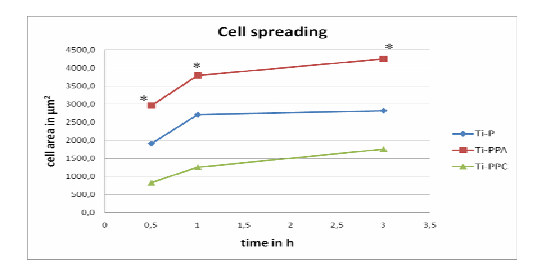


Fig. 1: Initial spreading phase of hMSC in basal medium (0,5-3 h). Cells spread significantly faster on Ti-PPA compared to Ti-P and Ti-PPC (n=40/time, U-test, * $p\le0,01$).

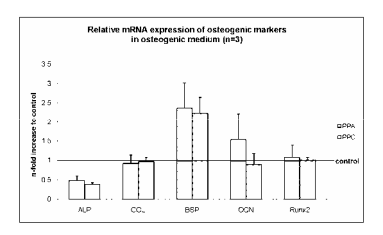


Fig. 2: mRNA expression for osteogenic differentiation markers after 3d, compared with cells on Ti-P. Note the increase of BSP and OCN.

Amino-functionalization of titanium (Ti-PPA) considerably improves cell spreading as an initial cellular effect (Fig. 1). In osteogenic medium the mRNA expression of BSP rises on both the PPA-and PPC-surfaces, whereas OCN increases on PPA only (Fig. 2). Under basal conditions the mRNA expression of ALP and Col is increased 2-fold and of Runx2 1,5-fold after 3 days on Ti-PPC compared to Ti-PPA (Data not shown).

DISCUSSION & CONCLUSIONS: The bioactivation of titanium with positively charged amino-groups improves initial steps of the cellular contact to the material surface. Concerning the stimulation of osteogenic differentiation both surfaces are able to affect the expression of osteogenic markers, depending on the culture conditions. Negatively charged functional groups appear to stimulate early mRNA differentiation markers under basal conditions, whereas osteogenic stimulation advances late differentiation markers, like BSP and OCN, after 3 days (Fig.2).

REFERENCES: ¹R. Langer, D.A. Tirrell (2004) *Nature* **428**:487-92. ²B. Finke, A. Ohl, K. Schröder B. Nebe, C. Bergemann, K. Liefeith, J. Rychly, F. Lüthen (2006) Biomol. Eng. *in press.* ³F. Lüthen, R. Lange, P. Becker, J. Rychly, U. Beck, B. Nebe (2005) *Biomaterials* **26**:2423-40.

ACKNOWLEDGEMENTS: The investigations were supported by the Government of the State Mecklenburg-Vorpommern, the Helmholtz Association and the European Union (UR 04 022 10). We appreciate technical support of DOT GmbH Rostock.

RESPONSE OF ENDOTHELIAL CELLS TO POLYETHYLENE TEREPHTHALATE SURFACES ACTIVATED BY IRRADIATION

S.Pezzatini¹, C. Satriano², G. Marletta², M. Ziche¹, L. Morbidelli¹

¹ Pharmacology section, Dept Molecular Biology, University of Siena, Siena, Italy ² Laboratory for Molecular Surfaces and Nanotechnologies and CSGI, Dept. of Chemical Sciences, University of Catania, Catania, Italy

INTRODUCTION: Important factor implicated in the cardiovascular graft failure is the lack of endothelial cells lining the lumen of the vessel. In the last few years several biomimetic approaches have been developed, in order to immobilize short peptide sequences, such as RGD, onto various surfaces, and produce biofunctional materials. Moreover, ion beam irradiation of polymer surfaces has been shown to induce the formation of a drastically modified altered layer, strongly affecting the cell-surface interaction [1]. The aim of this study was to investigate the *in vitro* response of endothelial cells grown onto PET surfaces modified by low energy Ar-irradiation (50 keV) and/or RGD and FBS adsorption.

METHODS: Polyethylene terephthalate (PET, Aldrich) was deposited as thin films by spin coating onto monopolished silicon wafers. The ion irradiation of samples was performed under vacuum of about 7.0 x 10⁻⁷ mbar at room temperature, with an ion fluence of 1x10¹⁵ ions/cm². After irradiation the samples were aged in controlled laboratory atmosphere for a period of two weeks before surface characterization. peptide/protein adsorption and cell adhesion experiments. The peptide sequence Arg-Gly-Asp (RGD) was dissolved in deionized water (2.9 mM), while FBS was diluted in PBS solution (10% v/v). The immobilization of RGD or FBS onto PET surfaces was obtained by spontaneous adsorption for 1 h. The surface coverage and chemical structure of the ad-layers was investigated by XPS and AFM. Endothelial cells isolated from postcapillary venules (CVEC, coronary venular endothelial cells) were used in the study [2]. Subconfluent cells were plated onto the various PET surfaces. Cell morphology and the interaction endothelial cells, among biomaterials extracellular matrix components were evaluated after 4 days by scanning electron microscopy (SEM) and immunofluorescence techniques [2].

RESULTS: The physico-chemical characterization of irradiated PET surfaces showed that ion irradiation induces a modification of the chemical structure of the outermost surface layers, while the

AFM analysis evidenced that Ar⁺ irradiation did not affect significantly the morphology and roughness of PET surfaces. The efficiency of biofunctionalization of PET by immobilization of RGD or FBS was estimated by XPS quantitative When CVEC were cultured analysis. unirradiated PET, they appeared retracted with altered morphology showing poor adhesion (Fig. 1A). On the contrary, when cell were grown onto irradiated PET, either biofunctionalized or not with RGD or FBS, the typical endothelial cell morphology was maintained over prolonged time, showing well-being status (Fig. 1B). Moreover, the endothelial cells preserved their ability to produce cytoskeletal protein (α-tubulin, Fig 1) and extracellular matrix proteins, such as fibronectin and laminin.

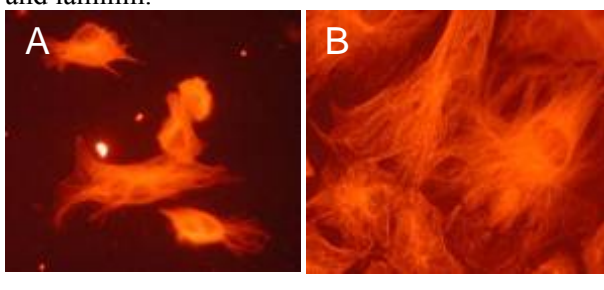


Fig. 1: α -tubulin fluorescence images. Original magnification 40x.

DISCUSSION & CONCLUSIONS: The results show the endothelialization of the biomaterial. In fact, the altered layer produced by ion irradiation of PET is in itself able to promote enhanced CVEC adhesion, spreading and proliferation, irrespectively of the surface biofunctionalization.

REFERENCES: ¹G. Marletta and C. Satriano (2004) *NATO Science Series, II: Mathematics, Physics and Chemistry*; 152: 7. ²S. Pezzatini et al. (2006) *J Biomed Mater Res A*.;76(3):656-63

ACKNOWLEDGEMENTS: Support by ITS-LEIF (Ion Technology and Spectroscopy at Low Energy Ion Beam Facilities) and MIUR-FIRB project n° RBNE01458S 007.

Micropatterned hydrogel layers for Tissue Engineering

A.Sala^{1,3}, M.Ehrbar¹, D.Trentin², J.Vörös³, F.E.Weber¹

¹ Section Bioengineering and Department of Cranio-Maxillofacial Surgery, US Zurich, Switzerland. ²Laboratory for Surface Science and Technology, Department of Materials, ETH Zurich, Switzerland.³ Institute for Biomedical Engineering, Laboratory of Biosensors and Bioelectronics, ETH Zurich, Switzerland

INTRODUCTION: One of the main challenges in the field of Tissue Engineering is the construction of functional and well organized 3-D tissues. For this purpose, distribution of cells, as well as biological cues involved in tissue formation, must be tightly controlled.

We propose to pattern synthetic hydrogels with cell-instructive motifs, such as growth factors (e.g.: VEGF) and peptides sequences known to activate specific signaling pathways (e.g.: RGD), in order to control cell differentiation and function into the desired cell phenotype. First, we want to create patterned surfaces in order to study cell behaviour in a simplify 2-D model.

To create such cell instructive surfaces, fibrin-like synthetic Poly(ethylene glycol) hydrogels^{1, 2}, which allow simultaneous incorporation of biomolecules during gel formation, are used. The hydrogel crosslinking mechanism is based on a transglutaminase, called Factor XIII, that catalyzes an acyl-transfer reaction between two substrates: TG and Lys (Fig. 1), resulting in an isopeptide bridge. In a first approach, we pattern on a non-fouling PLL-g-PEG background the TG domain, which has been previously grafted to PLL-g-PEG (PLL-g-PEG-TG), by Molecular Assembly Patterning by Liftoff $(MAPL)^3$. This technique has been successfully used to pattern RGD³ on a nonfouling background. The TG domain at the end of the PLL-g-PEG could be used as a liker to selectively bind Lys-modified molecules (e.g.: 8 arm Lys-PEG), which could be further used to bind TG-modified molecules (e.g.: TG-VEGF).

METHODS: First, PLL-g-PEG-TG (Fig.1) was immobilized on a Nb₂O₅ wafer (60μm x 60μm) previously patterned with a photoresist. After removal of the photoresist, PLL-g-PEG was used as back fill. In a second step, 8-arm Lys-PEG was bind in presence of FXIIIa (10 U/ml) and Ca²⁺ (50 mM) to the TG domain tether to PLL-g-PEG. Afterwards, TG-VEGF was linked to 8-arm Lys-PEG. Presence of VEGF was detected with a first anti-VEGF antibody and a FITC-labelled secondary antibody (Fig.2).

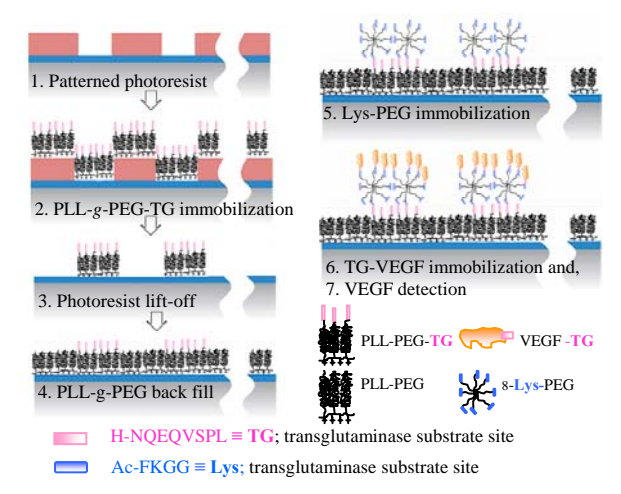


Fig. 1: Schematic figure of the patterning approach.

RESULTS & DISCUSSION: In Fig. 2 we can see the expected pattern. In green, TG-VEGF is detected in areas where PLL-g-PEG-TG was immobilized. The black pattern corresponds to ares where PLL-g-PEG was used as back fill. However, further studies are needed to demonstrate; 1) a pattern of PLL-g-PEG-TG on a PLL-g-PEG background, 2) selective linkage of Lys-PEG to the TG domain on the PLL-g-PEG-TG molecule, and 3) covalent linkage of TG-VEGF to 8-arm Lys-PEG.

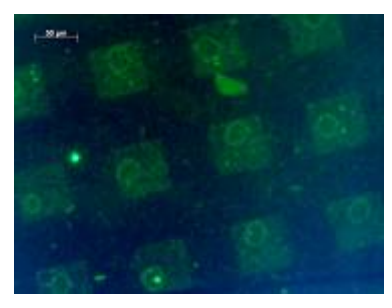


Fig. 2: TG-VEGF pattern on 60µm x 60µm Nb2O5 wafer.

REFERENCES: ¹ M. Ehrbar *et al.* (2007), Biomaterials **28**: 3856-3866. ² Ehrbar *et al.* (2007), In Press. ³ D. Falconnet (2005) Molecular Assembly patterning by lift-off at the micro- and nanoscale for applications in the biosciences, dissertation submitted to ETH.

ACKNOWLEDGEMENTS: The authors acknowledge the CCMX-MatLife for supporting this work.

EVALUATION OF SUPPORTED PHOSPHOLIPID BILAYER PERSISTANCE AND MOBILITY IN CELL CULTURE

N.Tymchenko, D.Thid, J.Gold

Department of Applied Physics, Chalmers University of Technology, Göteborg, Sweden

INTRODUCTION: The use of supported synthetic lipid membranes as cell culture substrates is an increasingly popular approach to investigate cell-molecular interactions, as well as to model cell-cell interactions in a controlled manner. Whilst unmodified phosphocholine (POPC) membranes are inert to protein adsorption and cell adhesion, they may be functionalised with ligands in order to present cells with specific cues for attachment, or for signalling of proliferation, differentiation, or apoptosis.

The present study is an assessment of supported POPC bilayers over 10 days in culture with adult rat-derived hippocampal progenitor (AHP) cells. The aims were to (1) investigate stability, morphology and fluidity of the POPC membranes with or without the attachment-promoting IKVAV peptide, and (2) identify any interactions between the cells and the fluorescently labelled bilayer.

METHODS: Cell experiments were performed on borosilicate glass cover-slips incubated with sterile-filtered solutions of 30 nm POPC vesicles doped with 1-5% (n/n) NBD-DHPE, with or without 3% maleimido-EG₂-POPE lipid. Cysteine-terminated IKVAV peptide was covalently bound to the maleimide terminated lipids^{1,2}.

Quartz crystal microbalance with dissipation monitoring (QCM-D) analysis showed characteristic bilayer formation from vesicle adsorption onto silicon oxide. The bound peptide was stable upon rinsing and binding behaviour was as expected^{1,2}.

Fluorescence recovery after photobleaching (FRAP) was used to assess the mobility of bilayers every day for 10 consecutive days. FRAP measurements and cell imaging was performed on live cultures. Images were acquired at various intervals after a 15s bleach.

RESULTS: POPC bilayers were largely cell resistant, supporting in general few, often very large, sedimented clusters (lack of cell processes). The IKVAV-functionalisation promoted AHP attachment followed by growth in clusters. At later time points, cells grew out forming an interconnecting network between clusters. AHP growth morphology on these surfaces was as previously reported².

With time, we observed losses in fluorescence intensity and lateral mobility of both IKVAVfunctionalised and non-functionalised bilayers, indicating that the integrity of the bilayers was compromised. This occurred more rapidly (within 48 hours) for the functionalised bilayers than for POPC (day 7). Bilayers on the back side of the cover-slips remained as mobile as on day 1, out to day 6-8. Bilayer recovery was observed at early time points under sedimented/non-spread cells (Fig 1.), whereas in other cells there was loss of fluorescence and/or reduced mobility in areas under, as well as immediately surrounding, cells and their processes. We have also observed fluorescent cells on both bilayers already from day 1. Fluorescence intensity was both diffuse as well as specifically located to certain regions of the cell, eg. processes.

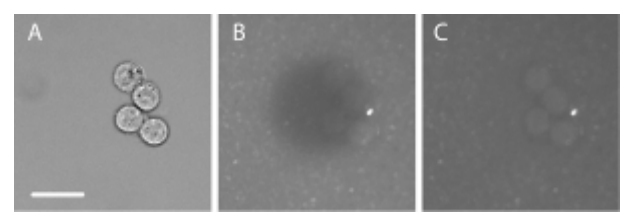


Fig. 1: POPC (1%NBD) Bilayer mobility under cells after 24 hours in culture. Bright field (A) Bleach spot (B) Recovery after 5 minutes (C). Scale bar indicates 20 micrometers.

DISCUSSION & CONCLUSIONS: We report a more rapid loss in lateral mobility for a bilayer supporting cell spreading/extension of processes compared to those without specific attachment. Furthermore, uptake of fluorescent lipid from the underlying bilayer into cells was observed. Loss of bilayer fluorescence under and around cells might be a direct result of this uptake, and/or an indication of bilayer destruction in these regions. Chemical analysis of bilayers in cell culture is needed to clarify the loss of fluorescence and changes in composition with time.

REFERENCES: ¹S Svedhem et al, Langmuir, 2003; ²D Thid et al, JBMRA, 2007.

ACKNOWLEDGEMENTS: Financial support was received from the Swedish Foundation for Strategic Research (SSF), the Swedish Council for Research (VR), and the Chalmers Bioscience Initiative

CELL RESPONSE ON SILK FIBROIN SCAFFOLDS WITH VARYING TOPOGRAPHIES

A. Wandrey¹, M. Garcia-Fuentes¹, M. Mattotti¹, V. Vogel², L. Meinel¹, H.P. Merkle¹

¹ Drug Formulation and Delivery, ETH Zurich, CH-8093 Zurich, Switzerland. ² Biologically oriented Materials, ETH Zurich, CH-8093 Zurich, Switzerland.

INTRODUCTION: Micro- and nanopatterning through soft lithography is an established technology for the fabrication of topographies suitable for oriented tissue engineering purposes. As a technically and economically more attractive alternative we focus here on the preparation of silk fibroin (SF) scaffolds with aligned nanofiber orientation by the technique of electrospinning. Application of electrospun scaffolds for oriented tissue engineering was evaluated with the use of human mesenchymal stem cells (hMSC).

METHODS: An aqueous solution of SF was blended with polyethylene oxide to improve processability during electrospinning¹. Random electrospun scaffolds were collected on a cylindrical target (d = 4 cm) rotating at 200 min⁻¹. To produce aligned scaffolds, the rotating speed of the cylindrical target (d = 14 cm) was increased from 1000 to 4000 min⁻¹. Low relative humidity (RH) was maintained during electrospinning to ensure the deposition of uniform, bead-free fibers. SF nanofibers were examined for their architecture using scanning electron microscopy (SEM). Cell response to the different scaffolds was monitored by SEM and confocal laser scanning microscopy (CLSM) after fluorescent labeling of cell membranes.

RESULTS: As determined by SEM, maintaining a low relative humidity (< 30% RH) during electrospinning was a critical process factor to obtain uniform, bead free fibers. Control of fiber network anisotropy was by the rotational speed of the cylindrical target, with no alignment at the lowest and nearly complete SF fiber alignment achieved at the highest speed examined.

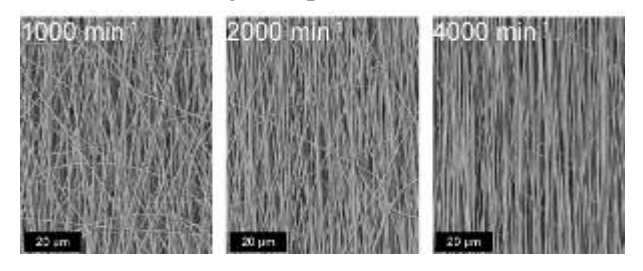


Fig. 1: Effect of rotational speed of cylindrical target during electrospinning on SF nanofiber deposition: increasing fiber orientation with increasing rotational speed (from left to right).

Upon cell seeding, different cell morphologies were observed depending on SF fiber orientation. hMSC adopted an elongated and spindle shaped morphology when cultured on aligned fibers, with the alignment of the cells being parallel to the prevailing fiber direction. This finding was in contrast to random electrospun fibers with no preferential cell orientation.

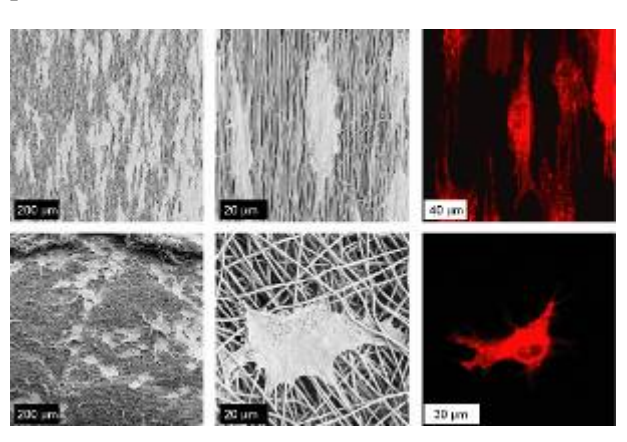


Fig. 2: SEM and CLSM micrographs showing hMSC on aligned (top row) and random SF nanofibers (bottom row).

DISCUSSION & CONCLUSIONS: Highly uniform SF aligned and scaffolds manufactured by electrospinning under controlled conditions (relative humidity, rotational speed of cylindrical target). Anisotropic topography by fiber alignment allowed to control hMSC morphology and cell/tissue orientation mimicking the oriented architecture of the extracellular matrix in native tissue such as tendon or ligament, implications for tissue engineering. Further studies will be dedicated to detail the impact of surface structure on the genomic profile of hMSC during attachment and differentiation.

REFERENCES: ¹ H.J. Jin, S.V. Fridrikh, G.C. Rutledge, et al. (2002) *Biomacromolecules* **3**(6):1233-9.

ACKNOWLEDGEMENTS: We thank the group of Prof. Gauckler (ETH Zurich) for access to their SEM and Trudel Inc. (Zurich, Switzerland) for the supply of silk cocoons.

Live-cell monitoring tools for cell-surface interaction investigations

A.-K. Born*, M. Rottmar*, Miriam Pleskova, K. Maniura-Weber, A. Bruinink

Laboratory for Materials-Biology Interactions, Empa, Materials Science and Technolgy, Lerchenfeldstrasse 5, 9014 St. Gallen, CH

INTRODUCTION: The optimal interaction between cells and implant surfaces is of key importance for the clinical success of implants. Latter interaction can be described as a sequence of time dependent processes. The common biochemical analysis of the biological response taking only mean total culture values and only one or a few time points into account enables only a rough estimate of the latter response. For more detailed description new single cell based tools have to be developed.

One aspect of cell –surface interaction is the adhesion and spreading behaviour of cells. Cell shape and regulation of biological processes such as proliferation and differentiation are to a large degree connected^{1,2,3,4}.

Cell spreading requires a firm contact with the underlying substrate, with focal contacts (FC) being the primary sites of adhesion. They consist of a large number of clustered transmembrane proteins (integrins). FC integrins connect the cell cytoskeleton with the cell substratum. The gradual process of osteogenesis can be followed by different proteins being expressed at various time points, comprising early (e.g. runx2) and late (e.g. osteocalcin) genes.

The aim of our project is to develop new tools to live monitor cell functional states and differentiation of single cells for the investigation of cell – surface interactions.

METHODS: We used gene constructs containing the genetic information for the focal adhesion proteins vinculin and vinexin (pEGFP-vinculin, pGFP-vinexin) fused to red or green fluorescence for nucleofection of human bone marrow cells. This method allows fluorescently tagged functional proteins to be visualised and monitored during FC formation and disintegration. Nucleofection allows the delivery of the gene of interest directly into the nucleus and cellular distribution of fluorescence was verified after 1-4 days. In addition cells were transfected with a gene construct reporting for osteogenesis, e.g. osteocalcin.

RESULTS: Adult human stromal cells (HBMC) transfected with the fluorescent-labeled vinculin or vinexin showed the expected accumulation of fluorescence signal at focal adhesion sites. The correct localisation of the vinculin was confirmed by staining against endogenous vinculin, suggesting that the tagged protein is correctly synthesized. GFP expression regulated by osteogenesis specific promoters could be detected in differentiated HBMC osteoblastic cells.

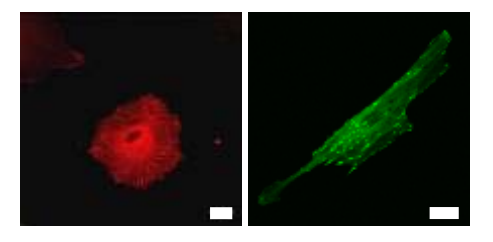


Fig. 1: Transfection of human cells with proteins vinculin (left) and vinexin (right) fused to red and green fluorescent protein. [Scale bar 20 µm] Cells showed the expected accumulation of fluorescence in focal adhesion sites.

DISCUSSION & CONCLUSIONS: Our primary results suggest that transfection of human cells with the present fluorescent-labelled adhesion proteins is efficient and therefore qualified for live cell monitoring.

REFERENCES:

¹ F.M. Watt, et al, (1988) *Proc Natl Acad Sci USA* **85**, 5576–5580

² C.D. Roskelley, at al (1994) *Proc Natl Acad Sci USA* **91**, 12378–12382 ³ R.S. Carvalho, et al (1998) *J Cell Biochem* **70**, 376–390

⁴ R. McBeath, et al. (2004) *Developmental Cell* 6: 483-495

ACKNOWLEDGEMENTS: The present study is supported by the European Commission through the specific targeted research project CellForce (Contract N° : NMP4-CT-2005-016626) and CCMX Matlife.

* shared first author

Aragonite Crystalline Biomaterials as Bioactive and Instructive Microenvironments for Neural Development

Danny Baranes^{1,2}, Hagit Peretz^{1,2}, Razi Vago³

¹Department of Life Sciences, ²National Institute for Biotechnology in the Negev (NIBN), and ³Department of Biotechnology Engineering, Ben-Gurion University of the Negev, Beer-Sheva 84105, Israel

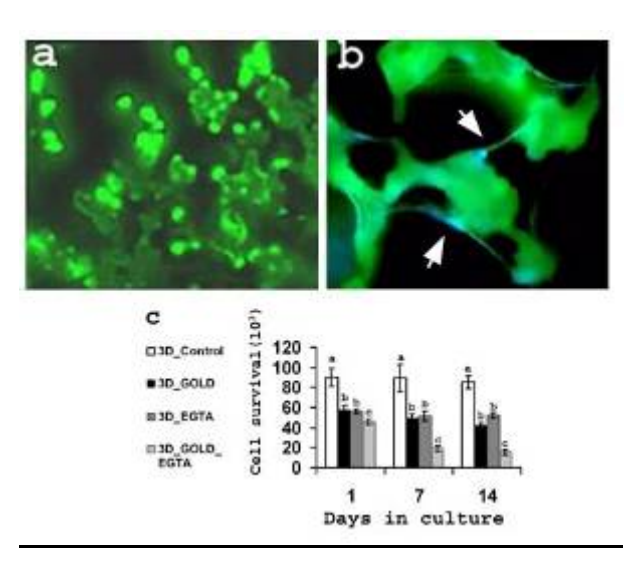
INTRODUCTION: scaffolds Identifying supporting in vitro reconstruction of active neuronal tissues in their three-dimensional (3D) conformation is a major challenge in tissue engineering. We have previously shown that aragonite coral exoskeletons support development of neuronal tissue from hippocampal neurons and astrocytes[1-4]. Here we investigated the cues that sustain the unique cell-material interactions between the coral skeleton and hippocampal cells, with focus on two causative factors: 1) the 3D architecture and 2) the surface chemistry of the scaffold, i.e. - the ability of the cells to exploit the calcium of the scaffold biomaterial.

METHODS: Experiments were performed in the following steps: (i) underwater cloning and fabrication of microcolonies of the hydrozoan *Millepora dichotoma*, (ii) incubation and labeling with calcein and $^{45}Ca^{2+}$, (iii) seeding of neural cells from rat postnatal 1-2, (iv) calcium uptake measurements (calcein by fluorimetry and immunofluoresence microscopy, and $^{45}Ca^{2+}$ by radioactivity.

RESULTS: To check for aragonite-derived calcium incorporation by the cells we exposed cloned hydrozoan species Millepora dichotoma to calcein or ⁴⁵Ca²⁺ which were incorporated into the organism's growing skeleton, and thereby available for the cultured cells. We found that hippocampal cells took up aragonite-derived calcium, with the uptake being enhanced when the availability of extracellular calcium ions was reduced (chelated with EGTA). When the cells were cultured on coral skeletons that had been coated with gold, a mean to dissect out the role of the 3D surface architecture from its chemistry, cell survival was reduced but not arrested, suggesting a role for matrix 3D architecture in neural survival. Hence, the durability of cultures on coralline aragonite matrices is due both to its 3D porous surface and its function as a calcium nurturing scaffold.

DISCUSSION & CONCLUSIONS: Here we show that although, three dimensional architecture is an important factor for tissue growth and durbaility, the aragonite biomaterial itself is acting

as an extremely bioactive vehicle by a unique way of providing the cells with calcium ions, enhancing neuronal survival. We posit that the translocation of calcium from the biomaterial to the cells activates a variety of membrane-bound signaling molecules, which affect the subsequent cell behavior. Such cell-material interactions hint at the potential of porous aragonite matrices in the fabrication of advanced biomaterials for neural tissue engineering applications.



Coralline aragonite matrices support neuronal survival by calcium nurturing and 3D scaffolding. (a) calcein uptake by the matrix. (b) uptake of matrix-derived calcein by cells (arrows). (c) cell survival is only partially reduced when cell were cultured on gold coated matrices, even in the absence of extracellular calcium.

REFERENCES: ¹Shany, B., Vago, R., and Baranes, D. Growth of primary hippocampal neuronal tissue on an aragonite crystalline biomatrix. Tissue Eng. 11, 585, 2005. ²Baranes, D., Cove, j., Blinder, P., Shany, B., Peretz H., and Vago, R. Interconnected network of ganglion-like neural cell spheres formed on hydrozoan skeleton. Tissue Eng. 13, 473, 2007. ³Peretz, H., Talpalar, A., Vago, R., and Baranes, D. Superior survival and durability of neurons and astrocytes on 3-dimensional aragonite biomatrices. Tissue Eng. 113, 461, 2007.

ACKNOWLEDGEMENTS: Partially supported by the NIBN and Binational Science Foundation.

Monitoring and analysis of cell migration

J.-P. Kaiser and A. Bruinink

Materials – Biology Interactions Laboratory, Materials Science and Technology (Empa), Lerchenfeldstrasse 5, CH-9014 St. Gallen, Switzerland

INTRODUCTION: Cell migration plays a key role in normal physiological processes. Cell behaviour is influenced by the substrate characteristics such as chemical and structural properties. The observation and monitoring of cell behaviour such as cell shape, cell orientation, cell migration direction and migration velocity as well are therefore of key importance to elucidate the mechanisms behind cell-surface interactions and to make statements about the critical surface features that are influencing and steering cell behaviour.

METHODS: Cells (3T3 fibroblasts) were labelled before starting the migration experiments with a fluorescent dye (DiI). The structured surfaces with the labelled cells were placed in a special incubation chamber with a cover glass lid. This chamber allowed the on-line observations of the migrating cells with a confocal laser scanning microscope (CLSM) under cell culture conditions. Cell migration was monitored for several days by taking a picture each 15 minutes from the same previously selected areas of interest. Based on the obtained sequence of pictures of each cell, the migration pathway (trajectory), cell shape, migration direction and migration velocity were calculated by special image analysis software.

Cell migration was analysed on a titanium alloy sample with a plane surface and 10 different micromaschined structures (grooves/ridges). The width of the ridges and grooves as well as the inter ridge/groove distance was in the range of 5-40 μ m. The structured surfaces can be divided in V-shaped surfaces, U-shaped surfaces and \cap -shaped surfaces. Cell migration was monitored on all types of surfaces at the same time [1].

RESULTS and DISCUSSION: The fibroblast cells were strongly affected by the surface structures and the extent was structure dimension dependently.

The frequency of cells with a circular shape was higher on the plane surface, than the amount of cells with round shape found on the structured surfaces. No significant difference in the frequencies of a certain type of cell shape was found among the different structured surfaces.

On structured surfaces the fibroblasts significantly preferred orientating themselves parallel to the axis of the grooves/ridges within a sector $\pm 10^{\circ}$. Cell

orientation occurred also on larger grooves/ridges with dimensions up to 30 μm . Among all structured surfaces, structures with shallow grooves/ridges (5 μm width) and large plane sections between the grooves/ridges exhibited the lowest number of cells orientated parallel to the structures.

Cells migrating on the plane surface showed a migration direction respectively migration angle, which was evenly distributed in all directions. Cells, which were seeded on the structured surfaces, migrated preferentially parallel to the grooves/ridges. Depending on the dimensions of the grooves/ridges and on the width of the plane tracks between the grooves/ridges no or only a few cells were switching from one track to the neighbouring track. Cells migrating on tracks with shallow grooves on the sides of the tracks were able to over cross the shallow grooves. However, switching of tracks was not only depending on the dimensions of the grooves/ridges but also on the width of the tracks in between on which the cells were migrating. On larger tracks the cells did not have the tendency to switch the tracks as often as they do, when they migrate on narrow tracks.

On the various structured surfaces different mean migration velocities were observed. 3T3 fibroblasts cells migrating on the plane surface were by far not migrating with the lowest velocity. Cells migrating on structures with large plane tracks between the grooves, respectively large flat areas between the ridges exhibited the highest mean migration velocity. Structuring of the surface resulted in an increase in cell migration velocity parallel to the grooves/ridges compared to the overall mean velocity on that certain surface. The comparison of the migration velocities between 3T3 fibroblasts migrating parallel to the structures (± 10°) and cells migrating perpendicular to the structures (± 10°) revealed that the migration velocity of perpendicular migrating cells was significantly lower than the migration velocity of cells migrating parallel to the structures.

REFERENCES: ¹ J.-P. Kaiser, A. Reinmann and A. Bruinink (2006) The effect of topographic characteristics on cell migration velocity, *Biomaterials* **27**: 5230-5241.

Dynamic observation of axonal growth on textile fibres

S.Weigel¹, L.Yao², M.Halbeisen¹, A.Pandit², A.Bruinink¹

¹ Empa, St. Gallen, Switzerland. ² NCBES, Galway, Ireland.

INTRODUCTION: In the current century, one of the most challenging issues of neuroscience is the regeneration of injured nerves. Today, critical nerve defects are bridged using hollow conduits with or without supporting cells or materials. Approaches using structured textile materials are promising for enhancing their functionality. Usually the success of neurite regeneration is evaluated at one or a few time points. The dynamic processes of growth cone translocation (outgrowth and retraction) can hardly be elucidated in that way. By real time observation additional decisive information can be obtained to optimize neuroregeneration supportive materials.

METHODS: *Cell culture:* Chicken embryonic motoneurons were isolated at stage 28 [1]. Reaggregates were formed by shaking and placed near the fibres. On-line CLSM monitoring was started after an equilibrium period of 16 hours. [2].

Plasmid: Cells were transfected with a modified RFP-plasmid vector either *in ovo* after breeding the eggs for 70 hours at 37 °C [3] or using the Amaxa Nucleofector II after dissociating the cells.

Textile fibres: To correlate fibre characteristics (chemistry, structure, diameter) with neurite outgrowth different fibres were evaluated: fibres of a diameter of 18-22μm Polyethylenterephthalat (PET), Polylactid (PL), and the Polyamides (PA) 6 and 6.6, PET fibres with a diameter of 50μm and Triacetate and Viscose fibres, which have a natural longitudinal structure and PET fibres with laser-induced artificial groove.

Data collection and analysis: Growth cone behaviour was analysed by comparing subsequent pictures taken every 5 min. Growth cones that could be tracked for at least 3 hours were manually marked in each picture in analogy to Adams and co-workers [4]. Migration (velocity and direction) was quantified using Visiometrics software as previously described [2].

RESULTS: The dynamics of axonal growth like outgrowth and retraction can be monitored using fluorescent protein labelled motoneurons. Comparing growth cone behaviour on various textile fibres and plane surfaces we observed that fibres were not seen by the neurite as equivalent substratum to grow on. Migration velocity on the plane surface and the various fibres was not

significantly different. However, the movement along the fibre axis differed depending on fibre characteristics. It was especially evident that the application of a groove to the fibre was able to align neurite outgrowth (Fig 1 & 2).

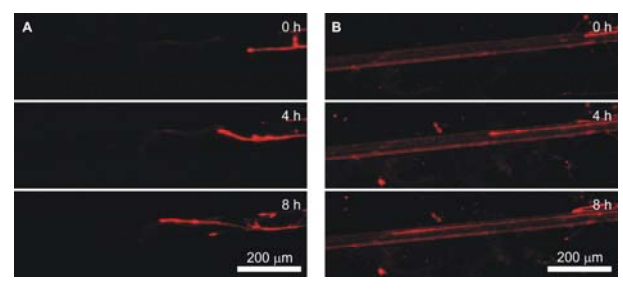


Fig. 1: Neurite growth on (A) unstructured PET fibres and on laser structured PET fibres (B) at different time points.

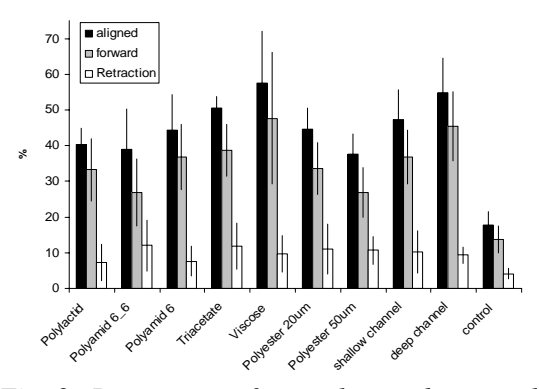


Fig. 2: Percentage of axonal growth steps aligned to the fiber direction.

DISCUSSION & **CONCLUSIONS:** By observation RFP labelled neurons using a CLSM we can monitor the dynamics of axonal growth like outgrowth and retraction. In addition to classical end-point observation we demonstrated that neurite outgrowth is usually not straight but can be influenced by fibre surface structure.

REFERENCES: ¹ T.B. Kuhn (2003) Growing and working with spinal motor neurons *in Methods in cell biology*, 67-87. ² J.P. Kaiser, A. Reinmann, A. Bruinink (2006) *Biomaterials* **27(30)**:5230-41. ³ V. Pekarik, et al (2003) *Nat. Biotechnol.* **21**, 93-96. ⁴ D.N. Adams, et al (2005) *J. Neurobiol.* **62**, 134-147.

ACKNOWLEDGEMENTS: We thank U. Tobler for technical assistance. The RFP-vector was a kind gift of Prof. J.-C. Perriard (ETHZ, CH).

Adhesion Energy Balance at the Cell-Matrix-Substrate Interface

T.Pompe, S.Glorius, C.Werner

Leibniz Institute of Polymer Research, Max Bergmann Center of Biomaterials, Dresden, Germany.

INTRODUCTION: Cell adhesion on artificial substrates is triggered by the physical and chemical characteristics of the supporting material. It is well known that cells react via outside-in and inside-out signalling pathways to environmental cues of the extracellular support like ligand concentration, substrate stiffness, conformation of adhesion ligands, and ligand-substrate interaction strength. In previous work we demonstrated the reaction mechanism of adherent cells to variations in the interaction between the substrate and extracellular matrix components in regulating the formation of focal and fibrillar adhesions¹. Starting there we aimed now to quantify the involved adhesion forces and interaction energies and to dissolve the coupling between cellular signalling events related to substrate-matrix interaction and substrate stiffness.

METHODS: Polyacrylamide hydrogels with different elastic modulus E in the range of 0.8 to 3 kPa were surface modified by coatings of different maleic acid copolymer layers, namely poly(styrene-alt-maleic acid) (PSMA), poly-(propene-alt-maleic acid) (PPMA), and poly-(ethylene-alt-maleic acid) (PEMA). Because of the differences in protein-copolymer interaction subsequently adsorbed fibronectin layers exhibit different adhesion strength to the substrate surface. Endothelial cells were grown for 50 min on top of these substrates. Cellular traction fields and strain energies were determined by analysing displacement vectors of hydrogel-incorporated fluorescent beads with subsequent calculations using Fourier Transform Traction Cytometry².

RESULTS: The quantitative measurements of cellular tractions revealed a dependence of the maximal exerted traction fields T_{max} on fibronectin-substrate interaction (Fig. 1). This observation can be accounted to cellular signalling pathways (i.e. Roh-Rac) and force-sensitive elements (i.e. integrins) coupled to adhesion sites and the cytoskeleton. It goes in hand with earlier results on the formation of fibrillar fibronectin matrix structures¹.

The determination of strain energies U of adherent cells revealed an interesting dependence on the elastic modulus of the substrate. The energy exerted by the cells to the substrate decreased with

increasing stiffness. The correlation can be nicely fit to a dependence of $U \sim 1/E$ (Fig. 1). Furthermore, the slope of correlation $U \sim 1/E$ for the different copolymers surfaces exhibits an increase with increasing fibronectin-substrate interaction strength.

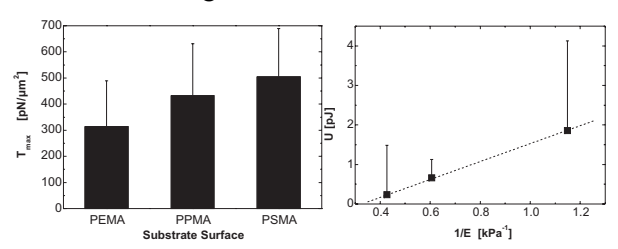


Fig. 1:LEFT: Maximum traction field T_{max} exerted by adherent cells to hydrogel substrates with different maleic acid copolymer coatings RIGHT: Strain energy U exerted by adherent cells to PSMA coated hydrogel substrates with different elastic modulus E.

DISCUSSION & **CONCLUSIONS:** The observed dependence of $U \sim 1/E$ can interpreted as energy optimisation mechanism correspondence to the substrate characteristic as proposed recently³. Obviously the non-covalent attachment of adhesion ligands to the substrate allows to control the force, which the cells exert at single adhesion sites leading to an almost constant force level for a certain surface characteristic of stiffness. independently substrate phenomenon is in contrast to the well-known increase of cellular traction forces with increasing stiffness for covalently attached adhesion ligands. It can be concluded, that the substrate-matrix interaction strength governs the force level applied by the cellular adhesion apparatus, while at the same time the cell optimises its adhesion energy in respect to substrate stiffness.

REFERENCES: ¹ T. Pompe, L. Renner, C. Werner, (2005) Biophys J **88**:527-34.; T. Pompe, K. Keller, C. Mitdank, C. Werner, (2005) Eur Biophys J **34**:1049-56. ² N. Wang, I.M. Tolić-Nørrelykke, J. Chen, et al, (2002) Am J Physiol Cell Physiol 282:C606-16. ³ I.B. Bischofs, U.S. Schwarz (2003) Proc Natl Acad Sci USA **100**:9274-9.

ACKNOWLEDGEMENTS: This work was supported in part by the German Science Foundation.

Engineering strontium-containing titanium implant surfaces

M. Schnabelrauch¹, A.R. Kautz¹, J. Weisser¹, J. Schmidt¹, A. Henning¹, C. Schrader¹, U. Bayer¹, F. Schlottig²

¹<u>INNOVENT Technologieentwicklung e. V.,</u> Jena, Germany. ²<u>Thommen Medical AG</u>, Waldenburg, Switzerland.

INTRODUCTION: Titanium and its alloys are well-established implant materials because of their known inertness and biocompatibility. However this rather biopassive behavior may result in slower healing processes and a weaker implant fixation compared to bioactive materials like bioglass or calcium phosphates. A promising approach to promote implant osteointegration represents the modification of implant surfaces with bioactive agents able to stimulate bone formation. Based on several studies during the last years [1,2], there is growing evidence that strontium ions locally administered at a defined dose have the potential to both inhibit bone resorption and enhance bone formation.

In this context we studied the preparation and characterization of strontium-containing coatings on titanium implant materials using a plasmachemical oxidation process. In first *in vitro* experiments the influence of these coatings on osteoblast-like cells was examined.

METHODS: Samples of TiAl6V4 and TiNb alloy were coated in a galvanostatic mode at room temperature using varying aqueous electrolyte mixtures of phosphate, strontium, and calcium salts, both the latter ones chelated with ethylenediamine tetraacetic acid. After coating, the samples were rinsed with distilled water and dried in air. Scanning electron microscopy (SEM) in combination with energy dispersive X-ray analysis (EDX), Xray photoelectron spectroscopy (XPS) and FT-IR spectroscopy were used to characterize the chemical composition and the topography of the coating. Dissolution experiments were performed in phosphate buffer saline (PBS) at 37 °C for 21 days and liberated strontium amounts were determined by inductively coupled plasma optical emission spectrometry (ICP-OES). Cell culture experiments were performed with pig primary osteoblasts seeded onto the layers using an osteoinductive cell culture medium. Protein content and alkaline phosphatase (AP) activity were determined after 1, 2, and 3 weeks of culture from cell lysates by standard techniques.

RESULTS: Microporous coatings of about 7 μm thickness with satisfying substrate adhesion to the

titanium alloy and varying contents of strontium and calcium ions have been prepared. Based on the performed structure analysis (EDX, XPS, FT-IR spectroscopy) of the strontium-containing coatings, the presence of amorphous strontium phosphate besides titanium oxide within the coatings can be assumed. In the dissolution experiments it was found that during the measured time period small amounts of strontium ions are released from the coatings. Measured strontium concentrations in the surrounding medium were in a range between 2 and 4 mg/l.

AP activity of osteoblasts cultured on the different surfaces increased continuously, but at 21 days AP activity of cells grown on strontium-containing surfaces were about twice as high as grown on uncoated titanium alloy surface and even on coated surface generated from a calcium and phosphate salt-containing, but strontium-free electrolyte.

DISCUSSION & CONCLUSIONS: New strontium-containing coatings have been prepared by a plasma-chemical oxidation process. Although the formed coatings do not show a microscopically detectable degradation in PBS medium over several weeks, small amounts of strontium ions are released resulting in a distinct increase in the AP activity of osteoblasts.

Based on these first results, the incorporation of slowly releasable strontium ions into titanium surfaces seems to represent a promising method to improve the bioactivity of these valuable implant materials. Further investigations including an *in vivo* study will be conducted to prove these hypothesis.

REFERENCES: ¹ P.J. Marie, P. Ammann, G. Boivin, C. Rey (2001) *Calcif Tissue Int* **69**:121-29. ² C Wu, Y. Ramaswamy, D. Kwik, H. Zreiqat (2007) *Biomaterials* **28**:3171-81.

ACKNOWLEDGEMENTS: The authors thank M. Frigge, R. Linke, and R. Sokoll (all INNO-VENT) for performing surface analytics.

Characterization of RGD-functionalized gold substrate and monitoring of cell adhesion process using QCM-D

L. Sandrin, L. Coche-Guérente, D. Boturyn, P. Labbé, P. Dumy

Département de Chimie moléculaire (DCM), UMR CNRS-UJF 5250, ICMG FR_2607, Université Joseph Fourier-Grenoble 1, BP 53, 38 041 GRENOBLE CEDEX 9

INTRODUCTION: Molecular conjugate vectors that are capable of in vivo cells targeting and breaching the membrane barrier represent a challenge for future diagnosis and therapeutic applications. The present work aims at studying the immobilization of molecular conjugate vectors onto the surface of transducers in order to evaluate the targeting properties of peptidic ligands using quartz crystal microbalance with dissipation monitoring (QCM-D) by the way of cell adhesion experiment. In this context, we have devised a very selective and effective $\alpha_v \beta_3$ integrin targeting system based on the multivalent presentation of the conformationally constrained RGD-containing cyclopeptide, c[-RGDfK-], by RAFT molecule, a regioselectively addressable cyclodecapeptide scaffold developed by Prof. Dumy's team [1]. The functionalized group at the lower face of the RAFT(c[-RGDfK-])₄ vector (Fig. 1A) is devoted to the grafting onto the transducer surface.

METHODS: In order to prevent the adsorption of protein or the attachment of cells on gold surface, we use self-assembled monolayers (SAMs) of alkanethiolates terminated in short oligomers of the ethylene glycol group ($[OCH_2CH_2]_nOH$ n = 4 - 6) SAM-OEG [2]. The strategy developed in this work to graft the targeting ligand on gold-coated transducer, uses streptavidin as a linker between a biotin-containing mixed **SAM-OEG** biotinylated RAFT(c[-RGDfK-])₄ to produce biomolecular assembling with high packing density. Several techniques have been performed to characterize the biomolecular assembly allowing complementary informations on the adsorbed layers. These techniques include quartz crystal microbalance with energy dissipation monitoring (QCM-D), spectroscopic ellipsometry electrochemistry.

RESULTS: The build up of the multilayered surface architecture has been characterized on gold coated quartz transducer using QCM-D. The experimental results indicate that each layer behaves as a thin rigid film, which in turn allowed us to apply the Sauerbrey equation to assess the mass uptake per unit area. The electrochemical reductive desorption of thiol monolayers in

alkaline solution lead to the calculation of a surface concentration corresponding to a densely packed monolayer of alkanethiolate. The layer thickness has been measured in buffer solution using ellipsometry.

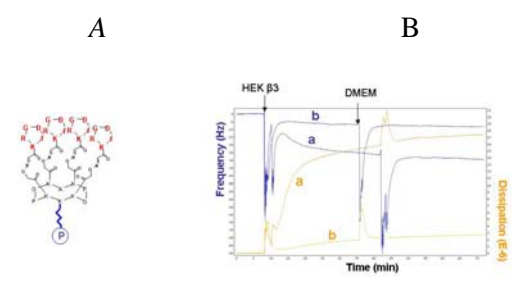


Fig. 1: A: Schematic representation of RAFT(c[-RGDfK-])₄ (P represents the grafting precursor group); B: Typical f and D responses (for the 5th overtone) to HEK β_3 cells of RAFT(c-[-RGDfK-])₄ (a) and SAM-OEG without RGD ligand (b) grafted onto a quartz crystal resonator.

The quartz crystal microbalance with dissipation (OCM-D) is an attractive and versatile in vitro method for real-time characterization of cell adhesion and spreading [2]. In order to evaluate the specificity of the $\alpha_v \beta_3$ -RGD recognition, we performed QCM-D experiments onto biomolecular assemblies with living cells (HEK β_3). We show that HEK β_3 cells lead to large shifts in frequency and dissipation (fig. 1Ba) when very low shifts have been observed with cells devoid of $\alpha_v \beta_3$ receptors (HEK β_1). In addition, a surface coated with SAM-OEG exempt of targeting functions shows also very low signals (fig.1Bb). The QCM-D results have been correlated to the imaging of the quartz surface using optical microscopy showing a large surface density of cells spreading onto the quartz surface coated with RAFT(c-[-RGDfK-])₄. These observations confirm the adhesion potency of the grafted ligand to $\alpha_v \beta_3$ expressing cells and validate the immobilization methodology of molecular conjugate vectors.

REFERENCES: ¹ P. Dumy, M.C. Favrot, D. Boturyn, J.L. Coll PCT/FR2003/002773; WO 2004/02894. ² G. Nimeri, C. Fredriksson, H. Elvoing, L. Liu, M. Rodahl, B. Kasemo, *Colloids and Surfaces B: Biointerfaces* **1998**, 11, 5805.

PHOTOCHEMICALLY FUNCTIONALIZABLE SURFACES FOR NERVE REGENERATION

Tessa Lühmann, Hans Sigrist*, Christian Hinderling[§] and Heike Hall

Cells and BioMaterials, Department of Materials, ETH Zurich, Switzerland; *arrayon biotechnology, SA, Switzerland, §CSEM, Neuchâtel, Switzerland.

INTRODUCTION: OptoDex is a dextran-based polymer with photoactive side groups. Proteic and carbohydrate guidance cues can be used to modify the surface of OptoDex either as single components or in combination to direct neurites along preformed structures. In this study, recombinant L1Ig6, the 6th immunoglobulin-like domain of cell adhesion molecule L1, represents a specific ligand for ανβ3 integrins, also found in the peripheral and central nervous system [1-2]. It is used as a substrate immobilized on different OptoDex materials. A carbohydrate guidance cue is also used: poly sialic acid (PSA). PSA is a linear glycopolymer consisting of α2, 8-linked N-acetylneuraminic acid. In the developing nervous system, PSA is attached to neural cell adhesion molecules (PSA-NCAM). Recent findings suggest that PSA acts sterically by introducing negative charges between adjacent cells therefore reducing cell-cell contacts [3]. The aim of the project is to investigate OptoDex materials as tool to immobilize guidance cues such as L1Ig6 and PSA for nerve guiding on 2D surfaces.

METHODS: OptoDex materials (A/K) were functionalized with L1Ig6 or PSA in two concentrations by one step photo activation.

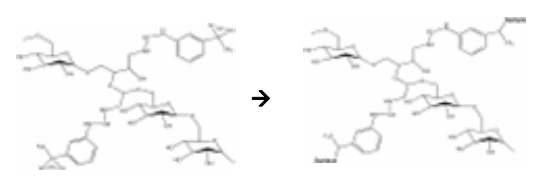


Fig. 1: The diazirines groups in OptoDex are photo activated at 350 nm, forming covalent bonds between the surface and the immobilized ligands.

Neural ND7/23 cells were cultured for 2 days on native OptoDex A or OptoDex K (exposing 22.5 kDa PLL). In addition, OptoDex A and K surfaces were modified with L1Ig6 or PSA at 1 and 10 $\mu g.$ L1Ig6 and PSA adsorbed on TCPS were used as controls. Cell viability was determined by fluorescein diacetate and ethidium-bromide stains and compared between all substrates.

RESULTS: ND7/23 cells poorly attached and survived on native or OptoDex A surfaces modified with 1 μg L1Ig6 or PSA, respectively. Cell viability remained at 40 % (Fig. 2). L1Ig6-immobilized to OptoDex A at 10 μg increased cell viability to 60 % (Fig. 2). On OptoDex K exposing

22.5 kDa PLL underneath L1Ig6 or PSA, cell viability was found to be between 60 and 80 % (Fig. 2). No increase in cell viability was observed after immobilization of L1Ig6, whereas a slight increase in cell viability was observed when increasing amounts of PSA were immobilized on OptoDex K (Fig. 2). This might be due to compensatory charge effects as negatively charged PSA seems to partially neutralize positively charged OptoDex K surfaces.

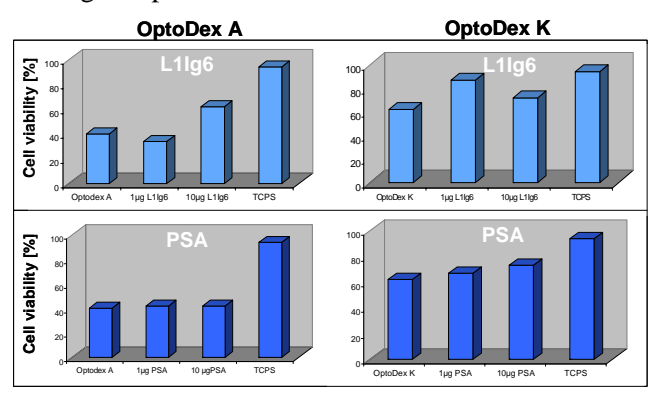


Fig.2: ND7/23 cells were cultured for 2 days on native and L1Ig6 or PSA-functionalized OpotoDex A and K surfaces. Cell viability was determined.

ND7/23 cells adhered, survived and extended neurites on L1Ig6 adsorbed to plain TCPS (Fig. 3).

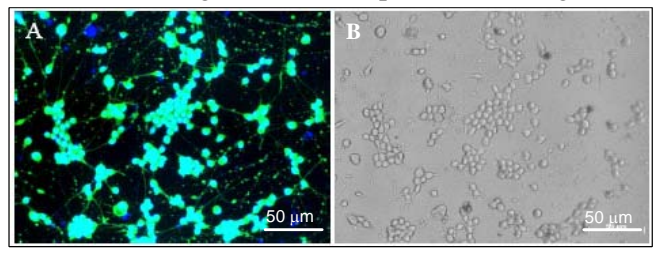


Fig. 3: ND7/23 cells cultured for 2d on 1µg L1Ig6 adsorbed to TCPS. Green fluorescence is shown by living cells (Al. Phase contrast image indicates neurite extension (B). Scale bar: 50 is µm.

DISCUSSION & CONCLUSIONS: Surface-functionalization of OptoDex A and K with neural guidance cues L1Ig6 or PSA are currently optimized towards increased cell viability and neuronal differentiation (Fig. 3).

REFERENCES: ¹ Horsch et al., 2000, Mol. Cell. Neurosci. **15**. 1-10. ² Blaess et al., 1998, J. Neurochem., **71**. 2615-25. ³ Bruces et al., 2001, Biochimie **83**. 635-643.

European Cells and Materials Vol. 14. Suppl. 3, 2007 (page 93) **ACKNOWLEDGEMENTS:** This work was kindly supported by CCMX.

ISSN 1473-2262

Surface Modification of Silk Fibroin with Ferulic Acid

S. Wang^{1,2} XJ. Lian¹ XM. Chen¹ EL.Li¹ HS. Zhu².

¹School of Material Science and Engineering, Beijing Institute of Technology, Beijing,

²Research Centre of Material Science, Beijing Institute of Technology, Beijing, 100081, China

INTRODUCTION: Silk is a natural protein and has been used as surgical sutures for centuries. Silk fibroin (SF) is the main component of silk and was found to maintain the strength of silk. However, the surface of SF materials should be modified to improve hemocompatibility when used in bloodcontacting materials. Ferulic Acid (FA, 3methoxy-4-hydroxyl-cinnamic acid) is an active ingredient of many Chinese herbal medicines such as Ligusticum chuanxiong Hort, Angelica sinensis Diels [1], which have been used to treat cardiovascular disease by Chinese physicians for thousands of years. In this paper, we modified the SF surface with FA and discussed the materials' antithrombogenicity, stability in water as well as mechanical properties.

METHODS: The FA derivative, 3- methoxy-4acryloyloxy-cinnamic acid (I) was synthesized via the reaction of FA with allyl chloride, and then was grafted onto SF cloth surface by uncatalyst polymerization according to the method described by ref [2]. The micrographs of the modified SF (mSF) were made by using a microscopy. The relative amount of surface coverage of the FA derivative onto SF is expressed as a ratio of C/N measured using XPS. The samples' stability in water was studied in an oscillating chamber at 37 for 17 days. The mechanical property was measured by a YG004N electronic single fiber strength tester. The anticoagulant activity in vitro evaluated by the activated partial thromboplastin time (APTT), the thrombin time (TT) and the whole blood coagulant time (WBCT).

RESULTS: FA was introduced to the SF surface through polymerization with **I** and a dark red mSF was obtained (Fig 1). The result of XPS showed that the ratios of C/N on the mSF surfaces are much larger than the untreated one (Table 1). The mSF samples were immersed in water for 17 days and no free FA was released, this indicates the high stability of the sample. However, mSF showed a relatively weaker strength and smaller elongation than the pure SF. The mSF cloth with holes about $100\mu m^2$ was placed on the PS cells and then measured the coagulant time. The test results showed that the APTT, TT and WBCT of mSF are much longer than that of pure SF (Table 2). We further prepared a series of mSF samples covered

with FA in different degrees and found the coagulant times are prolonged with the increase in C/N ratio.



Fig. 1: Micrographs of SF (left) and mSF (right)

Table 1. The results of XPS analysis

Sample	C %	O %	N %	C/N
SF	62.21	34.19	3.59	17.3
mSF	65.09	34. 07	0.83	78.4

Table 2. The coagulant times in vitro of samples

sample	APTT(s)	TT(s)	WBCT(min)
PS^1	39.8±0.4	12.6 ± 0.2	5.5 ± 0.0
SF	40.9±0.3	12.8±0.1	6.0±0.7
mSF	$>150^{2}$	>60 ²	10.5 ± 3.3^3

¹The samples' substrate. ²The maximum measured by the apparatus. ³The data from another mSF sample with C/N of 37.0

DISCUSSION & CONCLUSIONS: First, we tried to graft FA directly to the surface of SF due to its acrylate structure, however this was unsuccess-ful. With the parmacodynamics studies we found that FA still has bioactivity after its side chains were modified. Thus we chose to react –OH of FA with ClCO- of allyl chloride to form I, then graft I to the SF surface. The resulting mSF showed a better antithrombogenicity and a good stability in water. This indicates that FA modified SF may be a promising anticoagulant biomaterial. The modify-cation of SF film with FA is under investigation.

According to the theory of Chinese medicine the disease treatment needs the synergetic effect of the components from herbs. Our further research will focus on selecting other right active components from Chinese herbs to graft them onto SF and study their anticoagulant performance and correlation.

REFERENCES: ¹ Zh. Wang, et al (1988) Chinese J. Pharmacology 9(5):430-38. ²J.H. Liu, et al (1994) Journal of Fudan University 33(4):371-376. **ACKNOWLEDGEMENTS:**The work is financed by '973' project in China No. 2005CB623906.

Investigation of a unique nanostructured dental implant surface

<u>U.Pieles¹</u>, <u>T.Bühler¹</u>, <u>B von Rechenberg²</u>, <u>K. Voelter²</u>, <u>D.Snetivy³</u>, <u>F. Schlottig³</u>

¹FHNW Hochschule für Life Sciences Gründenstrasse 40CH, Muttenz, Switzerland; ²MSRU, University of Zürich, Winterthurerstrasse 260, Zürich, Switzerland; ³Thommen Medical, Hauptstrasse 26d, Waldenburg, Switzerland

INTRODUCTION: The use of osseointegrated dental implants is a predictable and successful treatment method for functional restoration of the fully or partially edentulous patient. A satisfactory clinical outcome relies on primary stability for load bearing immediately following implantation. This requires osseointegration within a short healing time. One of the most important surface properties is the topography of the surface. Topographical modifications enhance shortand longterm may osseointegration. Different treatment methods aiming at a nanostructural topographical respective chemical change and claiming to promote stronger and faster bone in-growth and healing^{1,2}.

METHODS: Titanium dental implants with a nanostructured titanium surface were manufactured with a subtractive plasma etching process. After sandblasting and oxygen cleaning plasma treatment the implants were reactive etched with a mixture of BCl₃ and Cl₂. Afterwards a final oxygen plasma cleaning step was performed to remove any surface hydrocarbon contamination. The topography of the implant surface was characterized with SEM.

The implants were tested *in vivo* in a sheep model (pelvis). The implants were inserted in both sides of the pelvis in sheep. Following sacrifice, macroscopic, radiographic and histomorphometric evaluations were conducted.

RESULTS: The SEM photomicrograph of the implant surface shows the macroroughness caused by sandblasting (Fig 1). The plasma etching process leads to a nanostructured, pincushion like surface structure (Fig 2). The needles have a diameter of less then 0.5 μ m and a length between 1–3 μ m.

In vivo: all implants were well integrated in the bone. Within the trabecular thread area the bone to implant contact (BIC) was 71.1±15.7% after 4 weeks and 61.4±13.7% after 8 weeks.

There were no significant differences between the implantation time points. Typical histological sections are shown in Fig. 3 and Fig. 4.

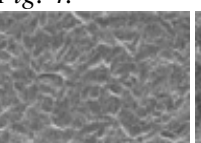




Fig.1 and 2 SEM photomicrographs of the implant surface showing the macroroughness and the nanostructure of the surface





Fig. 3 and 4: Histological sections after 4 weeks and 8 weeks of implantation with old (light blue) and new bone (dark blue)

DISCUSSION & CONCLUSIONS: Different *in vivo* studies have examined the effect of the implant surface on bone healing showing significantly greater percentage of bone-to-implant contact for microrough titanium surfaces compared with machined or polished titanium surfaces. The plasma etched surface shows similar but no better results compared to sandblasted and acid etched dental implant surfaces regarding published BIC³. Further experiments will be performed to optimize the plasma etching process and in vitro experiments will be performed.

REFERENCES: ¹Ellingsen JE et al (2004) *Improved retention and bone-to implant contact with fluoride-modified titanium implants.* Int J Oral Maxillofac Implants 19(5):659-66, ²Vanessa C et al (2006) *Discrete Calcium Phosphate Nanocrystals Render Titanium Surfaces Bone Bonding*, Canadian Biomaterials Society, 25th Annual Meeting; ³ Buser D. et al (2004) *Enhanced Bone Apposition to a Chemically Modified SLA Titanium Surface* J Dent Res 83(7):529-533

ACKNOWLEDGEMENTS: Thanks to J.Langhoff for all his help regarding the animal study.

Engineering surfaces for blood deheparinization using an

heparin-binding peptide

M.C.L. Martins¹, S.A. Curtin², S.C. Freitas^{1,3}, P. Salgueiro¹, B.D. Ratner² and M.A. Barbosa^{1,3}

¹ Instituto Eng. Biomedica, Div. Biomateriais, R. Campo Alegre, 823, 4150-180 Porto, Portugal.

² Dep. Bioengineering and Dep. Chemical Engineering, Univ. of Washington, Seattle, USA

³ Universidade do Porto, Fac. de Engenharia, Dep. Eng^a Metalúrgica e Materiais, Porto, Portugal

INTRODUCTION: Thrombus formation is one of the major complications associated to medical devices for cardiovascular applications. Heparin is the most widely used drug to prevent blood clotting. However, the use of heparin has been associated with a high incidence of hemorrhagic complications [1]. In the case of haemodialysis, where heparin is injected in the extracorporeal circuit before the dialyser, the use of a filter to remove heparin after the dialyser should avoid this problem.

The main objective of this work is to design surfaces, at molecular level, with capacity to selectively bind heparin from blood. A heparinbinding peptide, composed of L-lysine and L-leucine (pKL), was synthesized and immobilized onto SAMs terminated with tetra (ethylene-glycol) (EG4 SAMs). This terminal group was chosen because of its known capacity to resist non-specific protein adsorption.[2] pKL was synthesized based on the consensus sequences present in heparinbinding proteins. These sequences are composed of basic amino acid and uncharged or hydrophobic amino acid clusters [3].

METHODS: SAMs with different functional groups were prepared by immersion of gold slides into 0.1mM of 11-mercaptoundecyl tetra (ethylene glycol) (EG4) in ethanol. Incubation was performed at room temperature over 24 hours under a nitrogen environment. After incubation, the monolayers were washed three times with fresh ethanol and dried with a stream of pure argon.

pKL, with a molecular weight around 8500 Da was synthesized using the N-carboxyanhydride method. Peptide immobilization was performed using N,N'-carbodiimidazole (CDI) in a two-step reaction. During the first step, the EG4-SAMs hydroxyl groups were activated with CDI in anhydrous tetrahydrofuran. In the second reaction step, some activated OH groups reacted with the amine group of the polypeptide. Surface characterization of surfaces was performed using x-ray photoelectron spectroscopy (XPS), ellipsometry, contact angle measurements and infrared reflection absorption spectroscopy (IRAS). Heparin adsorption studies

(in PBS and in plasma) were assessed using IRAS and N-sulphonate-³⁵S-heparin.

RESULTS: Activation of EG4-SAMs with CDI was followed by the increase of the thickness of the monolayer, the water contact angle, and the amount of nitrogen. pKL immobilization was characterized by an increase of the thickness of the monolayer and also by the presence of nitrogen and carbon with binding energies characteristics of peptides.

The presence of pKL increases heparin adsorption to EG4-SAMs, even in the adsorbed state. The amount of heparin adsorbed does not increase with higher pKL concentrations. However, the selectivity to heparin was successfully reached only for low concentrations of pKL.

DISCUSSION & CONCLUSIONS: In the present work, an heparin-binding peptide (pKL) was successful synthesized and immobilized on EG4-SAMs in different concentrations.

The results demonstrated that the presence of pKL increases heparin adsorption to EG4-SAMs, independently of the pKL concentration and the nature of binding (adsorption or covalent binding). In addition, the selectivity to heparin was successfully reached for low concentrations of pKL. The selectivity can be explained because at high concentrations, pKL may not expose a large number of amino acid sequences, either due to a hindrance effect of closely packed chains or because high degrees of CDI activation can bind several lysines of pKL, thus reducing the number of selective adsorption sites to heparin.

ACKNOWLEDGEMENTS: POCI/CTM/55644//2004 and EPARIMED project finaced by *Agência de Inovação*.

Professor Ratner acknowledges support from UWEB (NSF grant EEC-9529161).

REFERENCES: ¹Nephrol Dial Transplant. 2002;17 (suppl 7):63-71. ²Mrksich M, Whitesides GM. Poly(Ethylene Glycol) ACS SYMPOSIUM SERIES 680: 1997. p 361-373. ³Cardin AD and Weintraub HJR. Arteriosclerosis 1989;9:21-32.

Platelet adhesion and activation modulated by selective adsorption of proteins to self-assembled monolayers

<u>I.C. Gonçalves</u>^{1,2}, M.C.L. Martins¹, M.A. Barbosa^{1,2}, E. Naeemi³, B.D. Ratner³

¹ Instituto Eng. Biomedica, Div. Biomateriais, R. Campo Alegre, 823, 4150-180 Porto, Portugal ² Universidade do Porto, Fac. de Engenharia, Dep. Eng^a Metalúrgica e Materiais, Porto, Portugal ³ Dep. Bioengineering and Dep. Chemical Engineering, Univ. of Washington, Seattle, USA

INTRODUCTION: When a biomaterial contacts blood, the first event to occur is protein adsorption. Following contact with the layer of adsorbed proteins on the surface, platelets will either adhere or "bounce off", depending on their state of activation and the ligands present at the interface. Platelet adhesion on surfaces is mediated by GPIIb/IIIa via adsorbed fibrinogen (HFG), but interaction between GPIb/IIa and von Willebrand Factor (vWF) can also occur.[1]

Since albumin-coated surfaces have been found to reduce platelet adhesion to synthetic materials [2], research has been conducted to create surfaces that attract and bind albumin from the bloodstream in a selective way.

Based on the approach of selectively binding albumin (HSA) to free fatty acids, tetra (ethylene-glycol)-terminated self-assembled monolayers with different percentages of C18 ligands on the surface were prepared. Selective and reversible adsorption of HSA to these surfaces was studied and related to the adhesion and activation of blood platelets.

METHODS: Preparation of EG4-C18 SAMs comprises two steps: (1) preparation of 11-mercaptoundecyl tetra (ethylene glycol) on gold (EG4 SAMs); (2) reaction of the OH groups from the EG chains with the isocyanate group of a compound with 18 carbons (0-10% C18 solutions).

Protein adsorption to EG4-C18 SAMs was performed using ¹²⁵I-HSA. Competition tests were made comparing adsorption from pure HSA solutions with mixtures of HSA with fibrinogen (HFG) or 1% plasma. Exchangeability of adsorbed ¹²⁵I-HSA for HSA or HFG was also evaluated.

The effect of protein adsorption on platelet adhesion and activation was studied by preimmersing the EG4-C18 SAMs in PBS, HSA or plasma before incubation in a platelet concentrate $(3x10^8 \text{plt/ml})$. The number of platelets adherent to the surfaces and their degree of activation was analyzed by Glutaraldehyde Induced Fluorescence Technique.

RESULTS: There is an increase of HSA adsorption as surface becomes more hydrophobic due to the increase of C18 ligands.[3] Regarding

competitive adsorption between HSA and HFG, EG4 and 2.5%C18 SAMs are selective for HSA but 5% and 10%C18 SAMs adsorb some HFG. However, in the presence of plasma, except for EG4 SAMs, all the surfaces adsorb other plasma proteins. Concerning exchangeability of adsorbed ¹²⁵I-HSA, SAMs prepared from solutions with 2.5%C18 replaced 85% of the adsorbed radiolabed HSA by HSA in solution, but not by HFG. EG4 SAMs also have a reversibility of ca. 80% but, in opposite to the former, they exchange the preadsorbed HSA by either HSA or HFG in solution, showing a lack of selectivity.

Following the trend observed in adsorbed proteins, there is an increase of platelet adhesion as the % of C18 ligands increases. Moreover, the morphology of platelets changes from round to spread as they contact more hydrophobic surfaces. However, when a pre-immersion of HSA is performed, there is an 80% decrease in the number of platelets, and the few ones that adhere are not activated. When SAMs are pre-immersed in plasma, the only surface that shows a reduction in the number of adherent platelets is 2.5%C18 SAMs. Regarding the other surfaces, while EG4 SAMs maintain adhesion and activation of platelets after pre-immersion in plasma, SAMs with 5% and 10%C18 increase it.

DISCUSSION & CONCLUSIONS: One of the surfaces (2.5% C18 SAMs) shows some selectivity towards albumin adsorption from plasma, exchanging almost all the adsorbed radiolabeled HSA by HSA in solution, but not by HFG. This behaviour is associated with minimum adhesion and activation of platelets.

REFERENCES: ¹Gorbet MB, Sefton MV. *Biomaterials* 2004;25:5681-5703 ²Kottkemarchant K et al *Biomaterials* 1989;10:147-155 ³Gonçalves IC et al. *Biomaterials* 2005;26:3891-3899.

ACKNOWLEDGEMENTS: Portuguese Blood Institute and FCT (grants: SFRH/BD/18337/2004 & DFRH/BPD/14890/2004 and project POCTI/CTM/55644//2004. Professor Ratner acknowledges support from UWEB (NSF grant EEC-9529161).

Cell Spreading in Response to Adhesive Microenvironments

S. A. Johnston, ¹ Chun L. Yeung, ¹ J. Bramble, ² S.D. Evans, ² J.A. Preece, ¹
P. M. Mendes, ¹ L. M. Machesky ¹

¹University of Birmingham, UK. ²University of Leeds, UK.

INTRODUCTION: Developing an understanding of cell migration has been limited by the lack of good experimental models. In this context, microscale engineered material surfaces are expected to be excellent candidates as *in vitro* model systems to gain valuable insight into the role of several factors in cell migration [1]. Here we report the use of microcontact printing [2] to fabricate micropatterned features of fibronectin on glass surfaces for the study of filopodia [3] — actin filament bundles that guide cell migration.

METHODS: In order to visualise the patterns by fluorescence microscopy, we labelled fibronectin with the fluorophore Cy3 and confirmed that mouse embryonic fibroblasts (MEFs) were able to spread normally on this substrate. For the production of patterns, unlabelled fibronectin was doped with Cy3 fibronectin in a 4:1 ratio. Microcontact printing stamps were made from poly(dimethylsiloxane) (PDMS) by curing liquid prepolymers of PDMS on a photolithographically prepared master. Stamps were inked for between 5 and 40 minutes, washed and placed in contact with glass. In order to block uncoated areas of the pattern, the surfaces where coated with heat denature bovine serum albumin (BSA) for 1 hour as cells are unable spread on or lay down endogenous fibronection on BSA [4].

RESULTS & DISCUSSION: In serum free conditions, MEFs were able to attach and spread to 10 µm stripes of fibronectin. The velocity of spreading was approximately halved compared to an unpatterned substrate but this behaviour is probably due to the reduced area of total activating substrate. Cells only spread on stripes that they initially make contact with on settling down and within the 2 hours observed did not move to new stripes. Cells can be seen to produce filopodia that make contact with BSA surface within the gaps of the pattern (solid arrows Figure 1) but do not produce persistent protrusions, like those seen on the fibronectin stripes (hollow arrows Figure 1). MEFs formed normal mature adhesions on stripes, visualised with antibody against the adhesion protein vinculin. Other vinculin labelling in filopodia is much weaker and independent of surface.

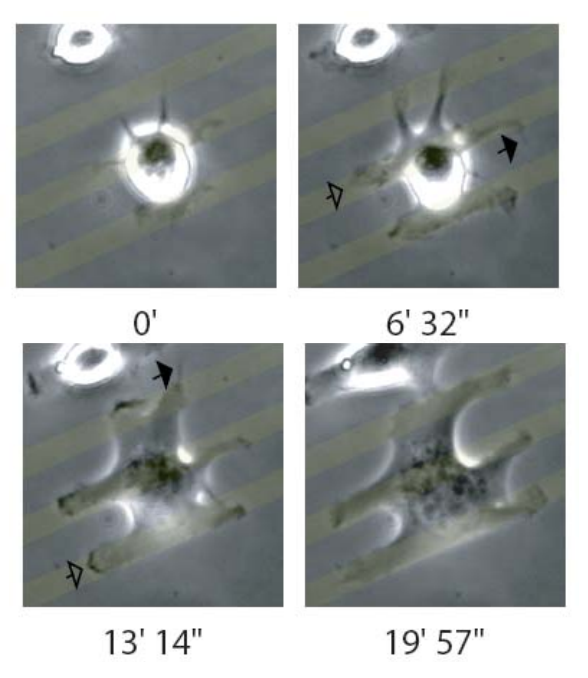


Fig. 1: Images are single frames from a timelapse of a MEF spreading on 10 µm fibronectin stripes. The position of the stripes is shown by the yellow overlay that was added in Adobe Photoshop.

CONCLUSIONS: We have produced patterned substrates consisting of stripes of fibronectin on glass in order to investigate how cells with an active cytoskeleton are able to interact with non-adhesive surfaces and how they make new contacts on adhesive surfaces. It has been found that cells extend filopodia into non-adhesive areas but do not move into them. This result support the hypothesis that filopodia function in the sensing of the cell environment.

REFERENCES: ¹M. P. Sheetz, D. P. Felsenfeld, and C. G. Galbraith, Trends Cell Biol. **8** (2), 51 (1998). ²Amit Kumar and George M. Whitesides, Appl. Phys. Lett. **63** (14), 2002 (1993). ³J. Faix and K. Rottner, Curr. Opin. Cell Biol. **18** (1), 18 (2006). ⁴F. Grinnell and M. K. Feld, Cell **17** (1), 117 (1979).

ACKNOWLEDGEMENTS: The authors acknowledge support of this work through a Birmingham Interdisciplinary Bridging in Engineering, Medicine & Science (BIBEMS) award.

Alignment of mammalian cells on laser nanostructured polystyrene

E.Rebollar, I.Frischauf, T.Peterbauer, M.Olbrich, C.Romanin, J. Heitz

Institute of Applied Physics, Johannes Kepler University Linz, Austria. Institute of Biophysics, Johannes Kepler University Linz, Austria. Department of Pharmacology and Toxicology, University of Vienna, Austria.

INTRODUCTION: Biomaterial surface chemistry and nanoscale topography are important for many potential applications in medicine and several areas of biotechnology as they strongly influence cell function, adhesion and proliferation [1-3]. In this work we present the periodic surface structures generated by KrF laser light (248 nm) on polystyrene (PS) foils. The ripples have a periodicity of 200-430 nm and a depth of 40-100 nm depending on the angle of incidence of the laser beam. We show that the laser modification enhances the proliferation of human embryonic kidney cells (HEK-293). Furthermore, we report on the alignment of HEK-293 cells, Chinese hamster ovary (CHO) cells and rat skeletal myoblasts along the direction of the ripples when the periodicity is larger than a critical value.

METHODS: The experiments were performed at PS foils of a thickness of 25 μm. Irradiation was carried out in air with a linearly polarized KrF laser beam (248 nm, 10 Hz) at a fluence in the range from 7.1 up to 8.9 mJ/cm and at different angles of incidence. The modifications induced by the laser irradiation were studied by atomic force microscopy (AFM), contact angle measurements, Fourier-transform infrared spectroscopy using an attenuated total reflection device (ATR-FTIR) and X-ray photoelectron spectroscopy (XPS).

For the experiments we used the standard expression cell line HEK-293, the CHO cell line LDL-A7 and rat skeletal myoblasts. Optical analysis was performed and additionally CTB cell viability assay was carried out for HEK-293 cells.

RESULTS: Laser irradiation induced the formation of ripples with a periodicity of 200, 270, 340 and 430 nm and structure depths of 40, 70, 80 and 100 nm respectively, by changing the angle of incidence.

After irradiation there is an increase in the surface hydrophilicity due to the introduction of oxygen containing groups, together with some nitrogencontaining groups, as shown by contact angle measurements, ATR-FTIR and XPS.

Proliferation assay performed for HEK-293 cells shows that the cell population densities are significantly higher on the irradiated PS foils in

comparison to the untreated PS, 4 days and 8 days after seeding.

HEK-293 cells are observed to align along the ripples 24 hours after seeding when the periodicity of the structures is equal or above 270 nm, but for untreated foils and ripples with a periodicity of 200 nm, cells are randomly oriented. CHO align along ripples with a periodicity equal or above 340 nm, they align weakly along ripples with a periodicity of 270 nm, and are randomly oriented on untreated foils and for lower periodicities. Rat myoblasts align well along ripples of 430 nm periodicity, but are randomly oriented for narrower structures (Fig.1).

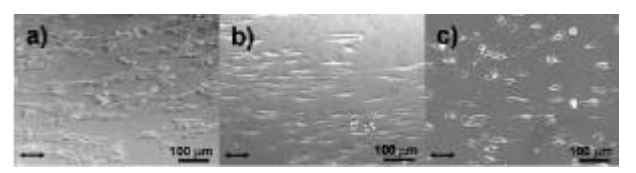


Fig. 1: Cells on 430 nm ripples: a) HEK-293 24 hours after seeding, b) CHO cells 27 hours after seeding, c) Rat myoblasts 24 hours after seeding...

presented here show that physicochemical properties of the substrates affect cell proliferation and orientation. Laser irradiation of PS foils induced surface chemical changes and topographical modifications. Due to the chemical changes mainly consisting on the introduction of oxygen-containing groups, cell proliferation is enhanced. We also show that different kind of cells align along the ripples and most importantly, this alignment takes place when the periodicity of the structures is above a critical value which depends on the cell type.

REFERENCES: ¹J.H. Lee, J.W. Lee, G. Khang, et al (1997) *Biomaterials* **18**:351-58. B. Zhu, Q. Lu, J. Yin, et al (2004) *J Biomed Mater ResB* **70**: 43-48. A. Thapa, T.J. Webster, K.M. Haberstroh (2003) *J. Biomed. Mater. Res. A* **67**:1374-83.

ACKNOWLEDGEMENTS: This work was supported by the Austrian NANO initiative under contract number N102-NAN and by Austrian Science Fund FWF under contract number W1201-N13.

Label free biosensor assay on the kinetics of cell-substrate interactions

E. Madarasz¹, I. Levkovets¹, K. Erdelyi², I. Szendro²

¹Institute of Experimental Medicine of Hungarian Academy of Sciences, Budapest; ² MicroVacuum Ltd., Budapest, Hungary

INTRODUCTION: Selective cell adhesivity is a biological principle, which provides mechanisms for inevitable processes including phagocytosis or the construction of multicellular organisms. Cell-to-substrate adhesion is an active initiated by receptor-ligand process interactions between the molecules of the cell surface and the extracellular environment. Initial cell surface reactions trigger multiple responses (cytoskeletal activation, recruitment of adhesion molecules, activation of signal pathways, secretion of extracellular matrix molecules), which will decide on spreading or detachment. The cell-type specific molecular interactions at the adhesive loci, however, are largely unknown. As a novel approach, we combined traditional time-lapse video-microscopy(1), molecular techniques and optical waveguide light spectroscopy (OWLS)(2) to study the initial phases of cell attachment.

METHODS: Suspensions (10^6 cells/ml; 100μ l) of neural stem or MDCK epithelial cells in proteinfree, artificial cerebro-spinal fluid were introduced into a temperature-controlled (37°C) cuvette of OWLS 120 instrument (MicroVacuum, Hungary) tightened to the optical grating coupler waveguide sensor (OW 2400) chip. By varying the incidence angle of polarized light (632.8 nm), a mode spectrum was obtained and the effective refractive indices (N) were calculated for electric and magnetic modes. A four-layer waveguide model was used for real-time monitoring the events at the sensor surface, and the adsorbed mass (ng/cm²) was calculated. Cell-substrate interactions were monitored up to 80 - 120 min. The sensor surface was coated with different cell-adhesive molecules. "attachment" of The cells treated Cytochalasin B, fixed (4% paraformaldehyde), or cooled (+4 °C) was also analyzed. The modulations of the cell shape were followed by time-lapse microscopy, and cell-secreted material evaluated by cell-blotting technique.

RESULTS: The ΔN *versus* time function clearly distinguished active cell attachment from passive sedimentation. The records revealed characteristic differences in the adhesive behavior of neural stem and epithelial cells. Neural stem cells showed a biphasic material deposition: a passive sedimentation phase was followed by active adhesion. Active cell attachment started with a latency period, with a

length depending on the adhesive property of the surface. The active phase could be prevented by cooling (Fig.1) or fixing the cells, or by blocking their cytoskeletal activation. Cell-blotting assays indicated that a massive amount of secreted proteins was deposited to the sensor surface at the time of establishing direct cell to surface contacts.

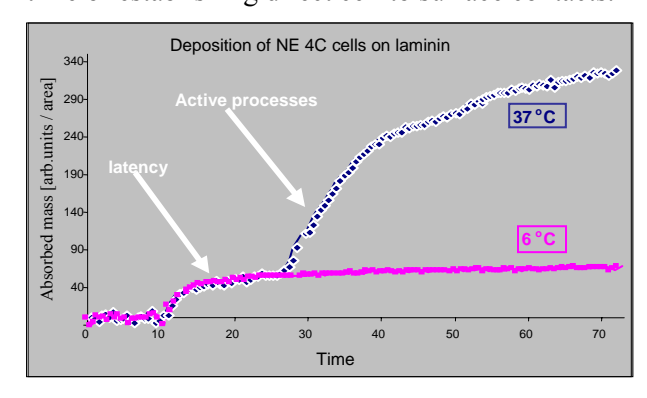


Fig.1. Passive (cooled to 6 °C) and active (37 °C) adhesive "behavior" of NE-4C neural stem cells(3) as recorded by OWLS.

DISCUSSION & CONCLUSIONS: OWLS assays allowed quantifying the deposition of cellderived material in a thin (<150 nm) layer above the solid sensor surface. In terms of cells, it could provide data on secreted proteins, focal contacts and adhesion sites, while the rest of the cellular mass remained out of the field of detection. OWLS provided techniques for rapid evaluation and quantification of cell - surface interactions In the course of active cell attachment two "types" of material have been deposited onto the solid substrate: the contacting cell surface-material, itself, and a relatively large fraction of proteins secreted by the cells. As the length of the preadhesion latency period reflects the adhesivity of the solid surface, OWLS assays could be used to select appropriate adhesive surfaces for attachment of different types of cells.

REFERENCES: ¹ Környei Z, Czirók A, Vicsek T, Madarász E. (2000) *J Neurosci Res.* **61**:421-429 ² Voros J, Ramsden J J, Csucs G, Szendro I, De Paul S M, Textor M, Spencer N D. (2002) *Biomaterials* **23**:3699–3710 3 Schlett K, Madarasz E. (1997) *J Neurosci Res* **47**: 405-415

ACKNOWLEDGEMENTS: This work was supported by Natl.Science & Devl. Prog. NKFP 1A-060/2004 and NKFP 3A-058/2004.

Enhancement of cell growth on SU-8 by O₂ Plasma activation

Ferdinand Walther¹ and Marc Hennemeyer¹, Sandra Kerstan², Polina Davidovskaya¹, Katrin Schürzinger², Alexander M. Gigler¹, Steffen Maßberg², Robert W. Stark¹

¹ Department for Earth and Environmental Sciences, Munich, 80333 Germany. ² German Heart Centre, Technical University Munich, Munich, 80636 Germany

INTRODUCTION: In order to mimic biological systems by building artificial microstructures, SU-8 proved to be an advantageous polymer being highly chemically inert and hydrophobic. Besides this, spin coated SU-8 exhibits a smooth surface with an RMS roughness of 0.1 nm. Since protein adhesion and cell growth behaviour appears to be dependent on surface roughness, wettability, and surface charge, ^{1,2} O₂ plasma treatment is a useful process for altering these parameters³. Depending on the plasma dose, the surface is rendered ultrahydrophilic and its RMS roughness is increased to more than 10 nm.³ In order to evaluate the effect of this surface alteration on cell growth, proliferation assays were performed on SU-8.

METHODS: SU-8 10 was processed on a soda lime wafer following the manufacturer's recommendations. The effect of 0.75 kJ and 6 kJ plasma on the contact angle and RMS roughness was determined by contact angle goniometry and AFM measurements. Chips of this wafer (1x1 cm²) were separated into sets of 4 each. Two sets were then activated by plasma at different doses, while a third set remained untreated. Afterwards, the chips were autoclaved, rinsed with PBS solution, and then seeded with the same amount of MRC-5 cells (human fibroblast-like cells from fetal healthy lung tissue, commonly used in quality assurance of cell culture devices). After three days of cultivation, the cells were fixed with 4 % paraformaldehyde. The number of cells per mm² was assessed using an optical microscope and statistically evaluated by a one-way analysis of variance (Holm-Sidak, pvalue = 0.05).

RESULTS & DISCUSSION: The goniometry and AFM measurements of the plasma treated surfaces revealed a strong activation, and a roughness exceeding that of glass (see Table 1). The proliferation assays revealed that on untreated SU-8 surfaces as well as on glass, cells loosely covered the substrate after three days of cultivation. In contrast, the number of cells on plasma treated SU-8 chips significantly increased. Plasma etched SU-8 surfaces exceeded the performance of glass plates and crude SU-8 chips. Figure 2 shows representative optical micrographs acquired in phase contrast mode with 10x magnification of cell proliferation on the different

surfaces and a quantitative cell proliferation assay.

		crude	SU-8	SU-8
	Glass	SU-8	0,75kJ	6kJ
contact angle	<5°	78.5°	15.6°	7.7°
day 0		±0,9°	±2.3°	±0.5°
RMS rough-	0.8	0.1	0.4	2.3
ness (nm)	±0.2	±0.05	±0.1	±0.2

Table 1: RMS roughness and contact angle of ultra pure water on SU-8 after plasma treatment.

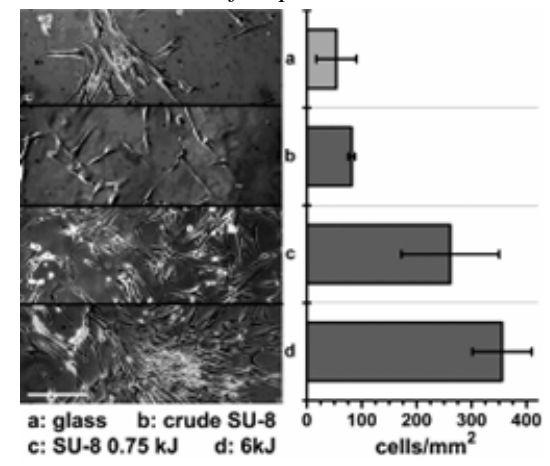


Figure 1: Representative optical micrographs of cells (scale bar $100\mu m$) (left) and cell proliferation statistics (right). The number of cells is significantly increased on oxygen plasma treated SU-8 surfaces compared to glass and crude SU-8.

In both illustrations, the increase of cell proliferation on plasma treated SU-8 is clearly visible. As the used glass as well as the 6 kJ SU-8 has an RMS roughness of less than 1 nm, the changed surface chemistry seems to prevail the increased roughness. The enrichment of antimony, which has been reported previously³, did not affect the growth of the selected cell culture to a measurable amount.

CONCLUSIONS: This study shows a strong improvement of cell proliferation on plasma treated SU-8. Furthermore, the data indicate that besides the increase of roughness, the change of the surface chemical properties has a predominant influence on cell growth. A negative influence of antimony on the cell culture could not be verified.

REFERENCES: ¹M. Stangegaard, *et al.*, Molecular BioSystems 2, 421 (2006). ²M. Winkelmann, et al. Biomaterials 24, 1133 (2003). ³F. Walther, *et al.*, Journal of Micromechanics Microengineering 17, 524 (2007).

The influence of the surface topography of Titanium implants on the behaviour of adhesive osteoblastic cells – statistical correlations

R.Lange¹, F.Lüthen², B.Nebe², <u>U.Beck¹</u>

¹ University of Rostock, Faculty of Computer Science and Electrical Engineering, 18051 Rostock, Germany. ² University of Rostock, Faculty of Medicine, Ernst-Heydemann-Str. 6, 18057 Rostock, Germany.

INTRODUCTION: For mathematical modelling of the biomaterial-cell contact it is necessary to find both parameters characterizing physical and chemical properties of the material surface and also such describing the reaction of the adhering cells. The aim of this paper is to present results of physical/chemical and biological investigations made on differently modified rough titanium implant surfaces in order to find out only the correlating parameters. Furthermore we want to discuss several ways to apply statistical methods to the correlation problem. [1]

METHODS: The surface structure of cp-titanium samples was modified in a range of roughness average Ra from 0.07 µm to 7 µm by several modification methods (polishing, machining, etching and blasting with glass balls and corundum particles). For the physical characterization of the surface morphology both standardized roughness parameters (ISO 4287) and additional parameters like fractal dimension D_f and topothesy K were calculated from the surface profile. Furthermore electrochemical parameters were determined by methods Linear Sweep Voltammetry, Chronoamperometry Electrochemical and Impedance Spectroscopy. [2]

Cellular investigations were carried out with MG-63 osteoblastic cells. Cells were cultured in DMEM with 10% fetal calf serum (FCS) and 1% gentamycin (Ratiopharm GmbH, Ulm, Germany) at 37°C and in a 5% CO2 atmosphere. In general, cells were seeded with a density of $3x10^4$ cells/cm² onto the titanium materials and into control dishes. Following cellular parameters were investigated: Adhesion, spreading, integrin expression, and length of integrin contacts. [3]

Correlation between material and biological parameters was made by means of the statistical program SPSS presuming a linear dependence. For every combination between material and cell biological parameters the pearson's correlation coefficient R was calculated based on N=7 material modifications. Furthermore we used the resampling method of bootstrapping to increase statistical accuracy. Bootstrap analysis (n=1000)

was made by means of the statistics toolbox of the software MATLAB.

RESULTS: For every combination between material and cellbiological parameters we got the pearson's correlation coefficient R shown in figure 1 instancing the cellbiological parameter length of $\beta 1$ integrin contacts. From bootstrap analysis we also got a mean and standard deviation of the pearson's correlation coefficient, shown in fig.1.

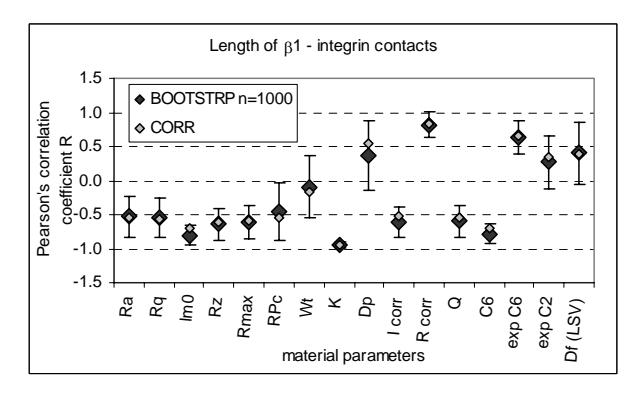


Fig. 1: Correlation between the biological parameter length of βl integrin contacts and all investigated material parameters, represented by the Pearsons correlation coefficient R.. Comparison between the results of the conventinal correlation analysis (CORR) and bootstrap method (BOOTSTRP n=1000).

DISCUSSION & CONCLUSIONS: We found in our studies that the fractal structure parameter topothesy K and the corrosion resistance R_{corr} have influence on the spreading behaviour of the osteoblastic cells and on the length of the $\beta 1$ integrin contacts. On the other hand it seems that there is no appreciable influence of material parameters on the integrin expression and only few influence on cell adhesion.

REFERENCES: [1] Anselme K, Bigerelle M (2006) *Biomaterials* 27, 8, 1187-1199; [2] Kirbs A, Lange R, Nebe B, Rychly J, Müller P, Beck U (2003) *Materials Science and Engineering* C23, 413-418; [3] Lange R, Lüthen F, Beck U, Rychly J, Baumann A, Nebe B (2002) *Biomolecular Engineering* 19, 255-261

ACKNOWLEDGEMENTS: We thank the DFG for financially supporting and the DOT GmbH for providing the titanium samples.

Exploiting lymphatic transport and complement activation in nanoparticle vaccines

Sai T. Reddy¹, André J. van der Vlies¹, Eleonora Simeoni¹, Conlin P. O'Neil¹, Melody A. Swartz^{1,2}, & Jeffrey A. Hubbell^{1,2}

¹Institute of Bioengineering and ²Institute of Chemical Sciences and Engineering, École Polytechnique Fédérale de Lausanne (EPFL), CH-1015 Lausanne, Switzerland

INTRODUCTION: The development of vaccine technologies has emerged as a forefront healthcare initiative, especially technologies for use in developing countries, posing severe economic and logistic constraints. One must develop antigen targeting and adjuvant schemes that respectively facilitate delivery of antigen to dendritic cells (DCs) and elicit their activation. Here we engineered antigen-bearing nanoparticle vaccines with two novel features: lymph node-targeting and in situ complement activation. intradermal injection, interstitial flow transported our ultra-small nanoparticles (25 nm) highly efficiently into lymphatic capillaries and their draining lymph nodes, targeting half of the DCs there, whereas nanoparticles even 100 nm large were only 10% as efficient. Furthermore, the surface chemistry of our nanoparticles activated the complement cascade, which spontaneously generated a danger signal in situ and potently activated DCs. With the model antigen ovalbumin conjugated to the nanoparticles, we demonstrated humoral and cellular immunity in mice in a highly and complement-dependent size-dependent manner.

METHODS: *Nanoparticle synthesis.* Pluronic-stabilized PPS nanoparticles with diameters of 25 and 100 nm were synthesized by inverse emulsion polymerization as described elsewhere¹.

Fluorescence microlymphangiography. A constant pressure infusion of fluorescently labelled nanoparticles was performed as previously described¹⁹ in order to visualize the lymphatic capillary network in the tail skin of mice.

C3a detection. A C3a sandwich ELISA was performed to measure complement activation in human serum following incubation with polyhydroxylated- or polymethoxylated-nanoparticles.

OVA antibody titers. A direct ELISA against OVA was performed to detect presence of anti-OVA IgG in mouse serum.

RESULTS: Ultra-small nanoparticles accumulate in lymph nodes after subcutaneous injection, while slightly larger ones do not. Polyhydroxylated nanoparticle surfaces activate complement to much higher levels than do polymethoxylated-

nanoparticles. Lymph node-targeting, complement-activating nanoparticles induce DC maturation *in vivo*. Lymph node-targeting, complement-activating nanoparticles induce antigen-specific adaptive immune responses. Humoral and cellular immunity was observed with antigen bearing nanoparticles.

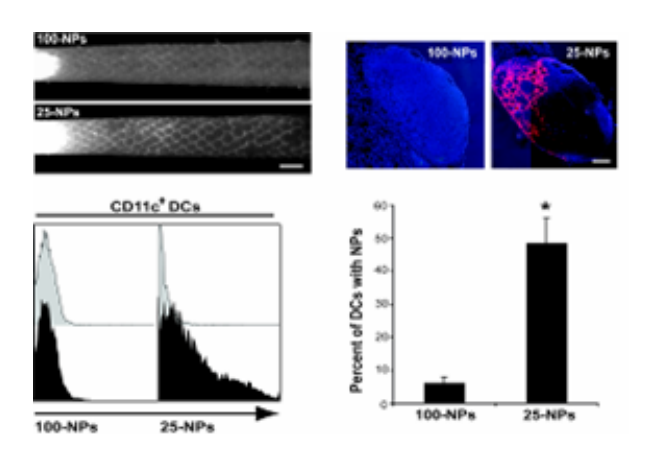


Fig. 1: NP uptake into lymphatic vessels and lymph node retention.

DISCUSSION & CONCLUSIONS: Our results highlight two potentially interesting alternative strategies: harnessing interstitial-to-lymphatic flow to deliver antigen and adjuvant to lymph noderesident DCs and using in situ complement activation to mature them. While we present the nanoparticle system here as one implementation to explore these concepts, we do note its interesting features of ease of fabrication and antigen conjugation, high stability and attractive affordability. Nevertheless, many questions remain to be addressed to demonstrate the reported system as more than an implementation to explore these two strategies, including questions of toxicity, elimination, and molecular interactions of complement with DCs.

REFERENCES: ¹ A. Rehor, J.A. Hubbell, N. Tirelli (2005) *Langmuir* **21**:411-417.

² S.T. Reddy, A.J. van der Vlies, E. Simeoni, et al (2007) *Nature Biotechnology* (in press).

THE NEURON-TO-CHIP INTERFACE ANALYZED BY FIB-MILLING

A. G. Bittermann¹, C. Burkhardt², F. Greve³, A. Hierlemann³, H. Hall⁴

¹ ZMB, Center for Microscopy and Imaging Analysis, University of Zurich, Switzerland, ² NMI Reutlingen, Germany, ³ PEL, Physical Electronics Laboratory, Department of Physics, ETH Zurich, Switzerland, ⁴Cells and BioMaterials, Department of Materials, ETH Zurich, Switzerland.

INTRODUCTION: Electrophysiological activities of neuronal networks can be analyzed by means of extracellular microelectrode arrays (MEAs). In order to obtain measurements with high signal-to-noise ratio, a tight coupling between MEA-surfaces and cells is required. This study aimed at designing the interface between dorsal root ganglion neurons and the MEA after adsorption of the neurite-growth-promotion protein laminin-111. The neuron-to-chip interface was characterized by SEM and TEM, and SEM after in situ focused-ion-beam (FIB) milling. The physical thickness of the adsorbed protein layer was determined by QCM-dissipation measurements (not shown). Moreover this study aimed at exploring FIB/SEM as a new technique to analyze cell-to-material interfaces in situ.

METHODS: CMOS chips (0.8 µm-CMOS process provided by austriamicrosytem) or glass surfaces were sputter-coated with Pt and then, laminin-111 was adsorbed. DRG neurons from 10day old chicken were cultured for 2d in EAGLE's MEM, 10% FBS, 5% chicken serum, 1% ABAM and 50 ng/ml NGF. 0.4 µM Ara C was added. For SEM, TEM and FIB/SEM cells were fixed in PFA and GA, followed by OsO₄. After incubation with uranyl acetate, cells were dehydrated and for SEM and FIB/SEM critical-point dried. 5 nm Pt was sputter-coated onto the samples, and the images were recorded. FIB/SEM was operated with Gallium ions at beam currents of 0.1 - 1 nA and an acceleration voltage of 30 keV. The sample stage was tilted to 54° obtain cross sections by life milling. For TEM, DRG neurons were fixed dehydrated and embedded in Epon 812 (Fluka). Ultra thin sections were cut and stained with uranyl acetate and Raynold's lead acetate. Images were recorded.

RESULTS & DISCUSSION: Different microscopic techniques were compared to analyze the neuron-to-substrate interface. TEM images elucidate only a spatially very restricted area (Fig. 1). Moreover, neither cell type nor cellular subregions can be identified. SEM images provide an overview and allow for selecting specific cells or sub-regions (Fig. 1). Unfortunately, the cell-to-substrate interface is invisible, even when the

sample is tilted. Therefore, *in situ* cross-sections were produced by FIB milling. This technique enables the selection of specific areas (Fig. 2), and

in situ milling allows investigation of the cell-to-substrate interface at submicron resolution. On laminin-111, the ventral cell membrane formed tight contacts of 20-30 nm, alternating with areas of up to 1 μ m distance. This finding suggests that the neuron-to-chip interface is only partially influenced by the physical thickness of the adsorbed protein layer (laminin-111: \sim 70 nm). Moreover, the biological properties of a neurite-promoting protein also determine characteristics and morphology of a neuronal network (data not shown).

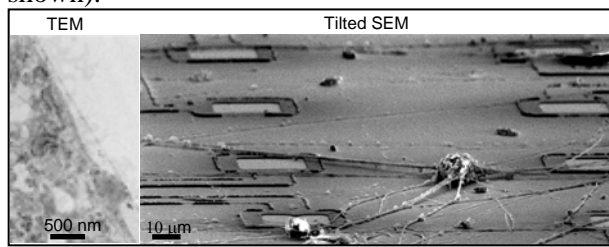


Fig. 1: Neuron-to-substrate interfaces analyzed by TEM and SEM. DRG neurons were cultured on Pt sputtered and laminin-111-adsorbed glass- (TEM) and MEA- (Tilted SEM) surfaces.

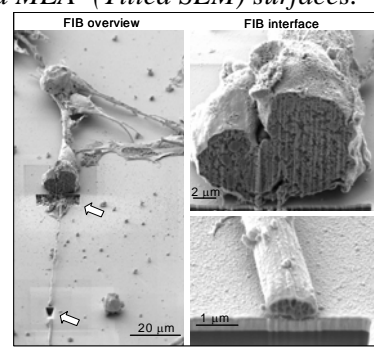


Fig. 2: Neuron-to-substrate interfaces analyzed by FIB/SEM after in situ FIB milling. DRG neurons were cultured on Pt-sputtered glass-surfaces adsorbed with laminin-111)

CONCLUSION: FIB/SEM allows detailed *in situ* analysis of biological structures on/in 2D or 3D-scaffolds independent of the material properties. The method offers a great potential for the characterization of tissue-to-materials interfaces. **ACKNOWLEDGEMENTS:** ETH Zurich for

financial support from grant TH-0108.

INFLUENCE OF SURFACE ROUGHNESS OF TITANIUM SUBSTRATES ON WETTABILITY AND HUMAN BONE CELL ADHESION

S. Giljean¹, M. Bigerelle², K.Anselme¹

¹ ICSI UPR 9069, 15 Rue Jean Starky, BP 2488, 68057 Mulhouse cedex, France, ² Laboratoire Roberval, UTC, Centre de recherche Royallieu 60205 Compiègne cedex, France

INTRODUCTION: The objective of this study is to determine the relative influence of surface roughness and surface chemistry on human bone cell response. For the first time, a wide range of 22 different roughnesses was prepared on titanium substrates (Ra from 1 to $21\mu m$). Human bone cell adhesion was characterized thanks to image analysis. The influence of surface roughness on wettability was also studied.

METHODS: Titanium plates were electro-eroded using different electrodes and voltage (diameter 20mm and thickness 4mm). Finally 22 samples with different roughnesses were obtained with Ra=1.19µm to Ra=20.96µm. Roughness evaluation was assessed by a 3D tactile profilometer. Using home-made software, 101 roughness parameters (amplitude, frequency, hybrid and fractal parameters) were calculated at different evaluation scales from 0.2µm to 8 mm with 0.2µm steps. Wettability measurements were performed with one liquid and two liquids phase method with 2µ1 drops. Several cleaning protocols were tested. Contact angle was measured without cleaning, after chemical cleaning (acetone and cyclohexane combined with ultrasonics) and after chemical cleaning combined with an argon plasma cleaning. To separate the chemical and the roughness effects on the contact angle value, polyelectrolyte multilayers were used in order to control the surface chemistry. Three bilayers of polystyrene sulfonate/poly allylamine (PSS/PAH) were adsorbed on a layer of poly ethyleneimine (PEI) and dried before contact angle measurement (one liquid phase method). Further, coated and uncoated samples were used for cell culture.

Cell culture was performed using human bone osteoprogenitor cells (HOP), with a density of 1.0×10^4 cells/cm². After 2 days of culture, the actin cytoskeleton was labeled by phalloidin-FITC or TRITC, and nucleus by DAPI. Fluorescence micrographs were used to perform a statistical image analysis in order to determine the number of cells and cell spreading. Alternatively S.E.M was also used to characterize cell spreading in particular on rougher substrates.

RESULTS: With two liquids phase method, contact angle value was around 140°-150° without

cleaning,. This value was reduced to 120-140° with chemical cleaning and to 40-120° with chemical cleaning combined with argon plasma cleaning. With one liquid phase method, the contact angle values onto dried polyelectrolyte multilayers increased when roughness increased in first stage. Then a transient stage with heterogenous values was observed. Finally a third stage appeared with contact angle values decreasing when roughness increased, with a significant drop in values with first stage. Concerning cell culture, Figure 1 shows that the cell covering percentage decreases when roughness increases. The cell number doesn't follow the same behavior and remains quite stable.

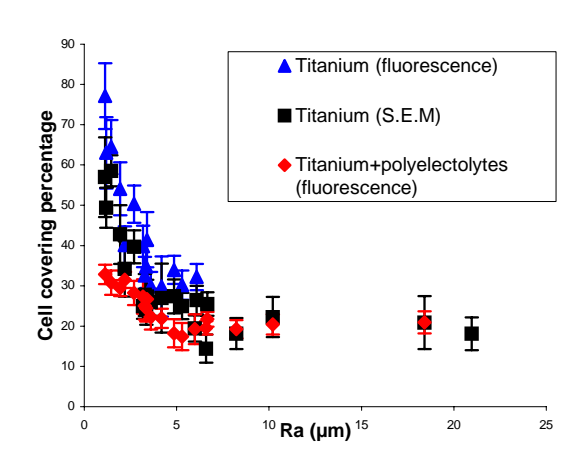


Fig. 1: Cell covering percentage onto original titanium and polyelectrolyte coated titanium.

DISCUSSION & CONCLUSIONS: Whatever the cleaning method used, contact angles values cannot be linked to the conventional Wenzel or Cassie-Baxter laws. After polyelectrolyte deposition, the first stage could be linked to Cassie-Baxter law and third stage to Wenzel law. The cell culture results are very significant since a very wide Ra range was studied with the same surface morphology. Statistical modelling is currently under calculation in order to determine what are the best evaluation scale and the best relevant roughness parameters for describing roughness influence on cell behaviour. Finally, results of a global analysis are expected for the conference for correlating roughness, wettability and cell behaviour.

PROANGIOGENIC EFFECT OF HYDROXYAPATITE NANOCRYSTALS ON MICROVASCULAR ENDOTHELIUM

<u>S.Pezzatini¹</u>, R. Solito¹, E. Boanini², A. Bigi², <u>M.Ziche¹</u>, A. Giachetti¹

¹ Pharmacology Section, Dept. Molecular Biology, University of Siena, Siena, Italy. ² Chemist Dept. "Ciamician", University of Bologna, Bologna, Italy

INTRODUCTION: Angiogenesis includes migration, proliferation and differentiation of endothelial cells to form new capillaries from preexisting vessels. Angiogenesis is prerequisite for osteogenesis [1] and its proper evolution is required for successful reconstructive substitutive orthopaedic surgery with synthetic biomaterials. Among the synthetic biomaterials for bone repair, hydroxyapatite (HA) attracts great interest due to its similarity with the bone mineral phase. Synthesis of HA crystals in nanometric scale has been proposed to improve its likeness to bone apatite, thus favouring compatibility. The aim of this study was to investigate cell functions of microvascular endothelium following exposure to HA nanocrystals.

METHODS: HA nanocrystals were synthesized by reaction between Ca(NO₃)₂ and (NH₄)₂HPO₄ in aqueous solution at 90°C, pH 10, under N2 flow [2]. Post-capillary venular endothelial cells (CVEC) were isolated and characterized as previously described [3]. Endothelial migration was performed by the use of modified Boyden Chamber. The activity of enzyme linked to migration (Matrix Metalloproteinases, MMP, and Focal Adhesion Kinase, FAK) was measured by gelatine zymography and western blotting, respectively. Cell proliferation was quantified by MTT test in subconfluent cells (10.000 cells/well in 48 multiwell plates) incubated with increasing concentration of nanocrystals of HA (2-10 µg/ml). Expression of $\alpha v\beta 3$ integrin was evaluated by immunofluorescence [2].

RESULTS: Nanocrystalline HA (5-500 μ g/ml) induced cell migration in a concentration dependent manner. Endothelial cell migration was accompanied by induction of metalloproteinase (MMP-2) and focal adhesion kinase (FAK) activity. These data document the ability of HA nanocrystals to stimulate capillary endothelium toward an angiogenic phenotype. Long term exposure (4 days) to nanostructured HA increased by 30% endothelial cell survival and proliferation and maintained positive labelling/subcellular localization of $\alpha\nu\beta3$ integrin (Fig. 1).

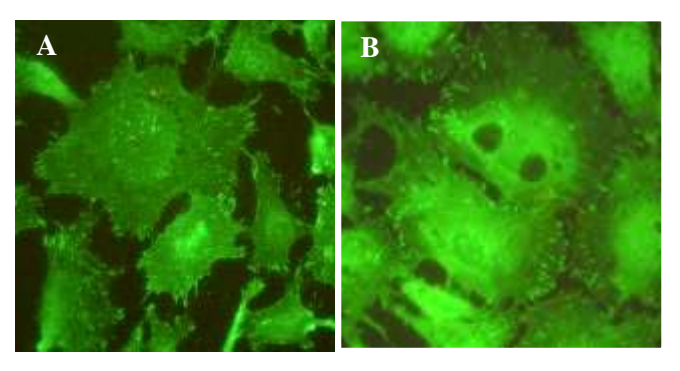


Figure 1: $\alpha v \beta 3$ integrin expression and localization in control (A) and HA treated cells (B). Original magnification 40x.

DISCUSSION & CONCLUSIONS: The results obtained indicate that HA synthesized in nanometric scale favours endothelial cell migration concentration dependent manner. Microvascular endothelial cells demonstrate high compatibility to HA nanocrystals over long term exposure, as indicated by the increase in their survival maintenance and their adhesive/migration behaviour as well as the typical biochemical markers (avß3 integrin, FAK). It is concluded that nanocrystalline HA favours endothelial cell functions occurring during angiogenesis and suggests their potential use as proangiogenic biomaterial.

REFERENCES: ¹H.P. Gerber, N. Ferrara (2000) *Trends Cardiovasc Med* **10**: 223-8. ²S. Pezzatini, L. Morbidelli, R. Solito, et al (2007) *Bone* doi:10.1016/j.bone.2007.06.016. ³M. Ziche, L. Morbidelli (2002) *Methods Enzymol* **352**:407-21.

ACKNOWLEDGEMENTS: Supported by MPS Foundation (grant 2007) and Lima Lto S.p.A..

NANOCRYSTALLINE HYDROXYAPATITE PROMOTES ANGIOGENESIS IN VITRO BY UP-REGULATION OF FGF-2

S.Pezzatini¹, R. Solito¹, L. Morbidelli¹, A. Bigi², M. Ziche¹

¹ Pharmacology Section, Dept. Molecular Biology, University of Siena, Siena, Italy. ² Chemist Dept. "Ciamician", University of Bologna, Bologna, Italy

INTRODUCTION: During bone repair angiogenesis precedes osteogenesis, as newly formed vessels drive the orientation of bone microcolumns. In reconstructive orthopaedic surgery adequate blood supply is necessary for proper biomaterial/tissue interaction. Thus for a successful surgery outcome, the biomaterial should favour the cellular and molecular events of angiogenesis. In the bone growth plate, the production of fibroblast growth factor -2 (FGF-2), and of vascular endothelial growth factor (VEGF), drive neovascularization and osteogenesis [1,2]. The aim of the study was to assess the effect of hydroxyapatite (HA) crystals synthesized in nanometric scale on angiogenesis in vitro and growth factors expression angiogenic functions.

METHODS: HA nanocrystals were synthesized by reaction between Ca(NO₃)₂ and (NH₄)₂HPO₄ in aqueous solution at 90°C, pH 10, under N₂ flow [3]. Post-capillary venular endothelial cells (CVEC) were isolated and characterized as previously described [4]. Cell proliferation was quantified by MTT test in subconfluent cells (10.000 cells/well in 48 multiwell plates) incubated with 2-10 µg/ml of HA nanocrystals. eNOS (endothelial nitric oxide synthase) activity was measured by conversion of [3H]L-arginine in [³H]L-citrulline [4]. COX-2 (cyclooxygenase-2), eNOS and FGF-2 expression was evaluated by immunofluorescence and western blotting. Cell spreading and formation of capillary-like structures were monitored by the use of endothelial cell covered microbeads embedded in 3D fibrin gel.

RESULTS: Endothelial cells exposed to HA were more responsive to VEGF increasing their survival. Investigation of key signalling pathways in angiogenesis, such as eNOS and FGF-2 demonstrated that low concentrations (2-10 μ g/ml) of HA increased their expression above control (p<0.001). HA nanocrystals did not modify COX-2 expression. When HA nanocrystals were embedded in 3D fibrin gels, they promoted endothelial cell organization and differentiation into capillary-like structures (Fig.1).



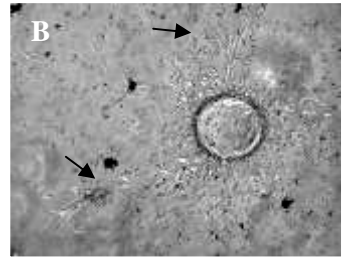


Fig. 1: Microcarrier beads covered with CVEC were embedded in 3D fibrin gels containing 5 µg/ml HA (B). The arrow indicates the capillary-like structures in the presence of HA compared to control condition (A). Original magnification 20x.

DISCUSSION & CONCLUSIONS: These results document the ability of nanocrystalline HA to phenotype stimulate proangiogenic microvascular endothelium. HA nanocrystals improve endothelial cell proliferation biochemical signalling pathways (eNOS and FGF-2 expression) required in angiogenesis and osteogenesis. HA nanocrystals prime endothelial cells response to VEGF action, but did not activate pro-inflammatory signals. Embedding nanocrystalline HA in 3D matrices with fibrin, promotes vascular network formation. It is concluded that HA nanocrystals are strong promoter of angiogenesis by up-regulation of FGF-2 expression.

REFERENCES: ¹H.P. Gerber, N. Ferrara (2000) *Trends Cardiovasc Med* **10**: 223-8. ²R.A.D. Carano, E.H. Filvaroff (2003) *Drug Discovery Today* **8**: 980-9. ³S. Pezzatini, L. Morbidelli, R. Solito, et al (2007) *Bone* doi:10.1016/j.bone.2007.06.016. ⁴M. Ziche, L. Morbidelli (2002) *Methods Enzymol* **352**:407-21.

ACKNOWLEDGEMENTS: Support by the EU project EICOSANOX FP6 funding (LSHM-CT-2004–0050333).

Effect of ultrasound stimulation on the biosynthetic activity of chondrocyte in cell-seeded matrices

Gulnara Hasanova, Sandra Noriega, Joseph Turner and Anuradha Subramanian Department of Chemical and Biomolecular Engineering, Lincoln, Nebraska, U.S.A

INTRODUCTION: The cellular component of the articular cartilage, chondrocytes, have long been recognized as strain-sensitive cells, and this straininduced biological response of chondrocytes has been exploited to facilitate chondrocyte culture in in vitro systems and examples include the application of hydrostatic pressure, dynamic compression, hydrodynamic shear and application of low-intensity pulsed ultrasound (US). In the present study a continuous ultrasound wave for predetermined time intervals was employed, as opposed to pulsed-ultrasound used in previous studies, to stimulate chondrocytes seeded in 3-D scaffolds. Both the frequency of application as well the effect of the US signal intensity on the biosynthetic activity of chondrocytes was studied.

METHODS: Chondrocytes seeded in 3-D scaffolds were subjected to stimulation by US as follows: 1.5-MHz for 161 seconds, 5.0-MHz for 51 secs and 8.5-MHz for 24 secs and the US signal was applied twice in a 24-hour period. Non-US stimulated scaffolds served as the control. Both control and US stimulate groups were maintained in culture for 10 days and at the conclusion of the culture period chondrocytes were assayed for the total DNA content, morphology, and cartilage specific gene expression by RT-PCR.

RESULTS: Chondrocytes stimulated by US (1.5, 5.0 and 8.5-MHz) had 1.2 to 1.4 times higher viabilities as determined by the MTT assay (data not included). When compared to control, no increase in hydroxyproline content was observed in cells stimulated with 1.5-MHz US signal, whereas cells stimulated by US at 5.0-MHz and 8.5-MHz had 1.2- times to 1.5 times higher hydroxyproline, respectively, when compared to controls. Dead cells, stained red, were found on most surfaces, however the appearance of dead cells were observed more on control scaffolds and scaffolds stimulated with the 8.5 MHz US signal. We have analyzed the expression of select cartilage specific genes at day-10 in human articular chondrocytes cultured on 3-D scaffolds subjected to US stimulation. At day-10, type-II collagen and aggrecan mRNA was significantly higher in US stimulated samples than in the control group, in addition expression was significantly higher in 5.0 and 8.5 MHz stimulated samples, respectively¹. Thus US signal of 5.0 MHz was selected for all future experiments, where the frequency of US stimulation was studied. The mRNA expression levels of collagen type II and aggrecans are shown in Figure 1.

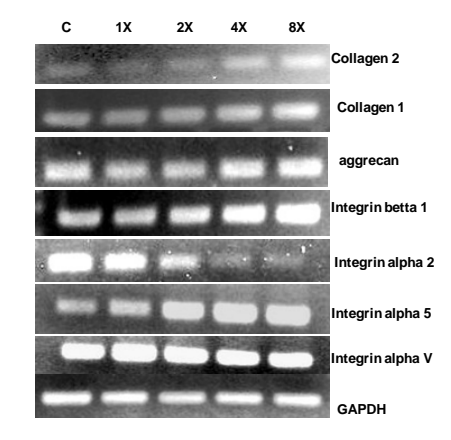


Figure 1: RT-PCR analysis. Total RNA was extracted from liquid nitrogen-frozen chondrocytes using Trizol method and treated with DNA-ase. DNA-depleted RNA preparations were used for synthesis of the first-strand cDNA with random hexamers primer using the SuperScript First-Strand Synthesis System kit (Invitrogen). PCR amplification was performed using primers specific to the sequences of interest genes and GAPH gene as loading control. C:control; 1X to 8X:indicate frequency of US stimulation per day at 5.0 MHz for 31 secs.

DISCUSSION & CONCLUSIONS: Our results¹ show that chondrocytes when stimulated with continuous US for predetermined time intervals, possessed 1.2 to 1.4times higher cellular viability than control and had higher levels of type-II collagen and aggrecan mRNA expression when compared to controls. Furthermore it appears that US stimulation impacts the "inside-out" expression of cell-surface integrins and the gene expression of integrins α_5 , α_2 , α_V and β_1 was found to vary with the frequency of US stimulation. While $\alpha 5$ and $\beta 1$ were up-regulated, $\alpha 2$ was significantly inhibited at higher application frequency of US stimulation. Based on our results, we hypothesize that role for integrin-dependent, protein-phosphorylation in the activation of the signaling cascade in human articular chondrocytes in response to US stimulation.

REFERENCES: ¹ S. Noriega (2006) Tissue Engineering. Vol 13(3). 2007.

Cell Patterning Using Nanostencil Lithography: An Alternative to Micro-Contact Printing

K. Pataky¹, M. Cordey², J. Brugger¹, M. Lutolf²

¹ Microsystems Laboratory 1, EPF Lausanne, Lausanne, Switzerland. ² Laboratory of Stem Cell Bioengineering, EPF Lausanne, Lausanne, Switzerland.

INTRODUCTION: In this work, we present the use of nanostencil lithography for the patterning of cell adhesions on a variety of substrates. Unlike conventional lithography, nanostencil lithography is a one-step shadow-mask technique with sub-100 nm resolution. This resolution makes it of particular interest in patterning cell adhesions because it is theoretically possible to limit the size of adhesions to smaller than 1 µm in diameter – the minimum size of focal adhesions reported in literature [1]. As it is a shadow-mask technique, it can theoretically be applied to the patterning of nearly any material deposited on nearly any substrate without requiring major process development time. In this work, cells are localized to Au patterns produced by nanostencil lithography and a simple surface modification procedure.

METHODS: All nanostencils with silicon nitride membranes were prepared using the methods described in the literature [2]. A 5 nm Ti adhesion layer and a 50 nm Au layer were deposited through the stencils onto various substrates by electron beam evaporation. The substrates used were Si wafers, Si wafers with 500 nm wet oxide (SiO2), polystyrene, and Silastic PDMS. To render the Au adhesive to cells, patterned substrates were immersed in a solution of a thiolated poly-peptide (2.4 mg/mL) presenting an RGD group (Ac-GCGYGRGDSPG-NH₂). The substrates were then immersed in a 30 mg/mL solution of BSA in PBS to back-fill the surrounding areas. An overview of the process is given in *Figure 1* below.

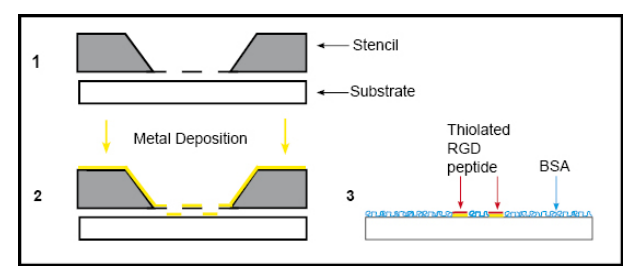


Fig 1: Process outline of stencil patterning and surface modification.

GFP+ breast cancer cells and primary epidermal fibroblasts were plated on the substrates and cultured under standard conditions.

RESULTS: The confinement of cells to the patterned regions of Au was good on both the SiO2 surface and the polystyrene. In the case of Si, cells spread but were not confined, indicating ineffective backfilling possibly due to the weak lower of the native oxide layer. In the case of PDMS cells grew everywhere and were rounded up on the surfaces. A significant Si signal observed in XPS measurements of large Au patterns on the PDMS suggested that unbound PDMS oligomers had migrated onto the surface of the Au patterns, interfering with the thiolation [3]. Successful localization of cells on polystyrene is displayed in *Figure* 2.



Fig. 2: GFP+ breast cancer cells localized on an Au pattern (1mm² array of 2 µm squares with a 4 µm pitch). The pattern was produced by nanostencil lithography on a polystyrene substrate. Fluorescence is indicated in red.

DISCUSSION & CONCLUSIONS: Nanostencil lithography can be used to create cell adhesive patterns to sub-micron dimensions from a variety of materials on a variety of substrates with very little process development time. Future work will focus on using this technique for studying sub-micrometric cellular adhesions, as well as patterning flexible substrates to study mechanosensitive gene expression.

REFERENCES: ¹ B. Geiger, et al (2001) *Nature Reviews Molecular Cell Biology* **2:** 793 – 805. ² G.M. Kim, et al (2003) *Microelectronic Engineering* **67-68**: 609 – 614. ³ J.N. Lee, et al (2003) *Anal. Chem.*, **75(23)**: 6544 – 6554.

ACKNOWLEDGEMENTS: This project is funded by the Swiss National Science Foundation.

The Application with Danshen to Improve cell affinity on Silk Fibroin Surface C.Su¹, S.Wang^{1,2}, X.Lian¹, Z.Gao¹, H.Zhu², J.Bei², S.Wang²

¹School of Material Science and Engineering, Beijing Institute of Technology, Beijing, China.

² Research Centre of Material Science, Beijing Institute of Technology, Beijing, China.

INTRODUCTION: As a natural biopolymer, silk fibroin (SF) has unique mechanical properties and good biocompatibilities. Several works have been done to improve the properties of silk fibroin to meet application's demand □ but the modification with Chinese medicine hasn't been reported. Studies showed that Chinese medicine have multiple pharmacological modes of actions. Danshen (Radix Salviae Miltiorrhizae) is one of the traditional Chinese medicines, which has been used clinically in the treatment of cardiovascular diseases for more than 2000 years. It was studied that the water-soluble ingredients of Danshen(DS) are mainly responsible for its pharmacological activity[1]. In this study we have modified silk fibroin with DS and protocatechualdehyde(PCA)□ one dissolvable ingredient of DS. We have found that the modified SF surface has better cell affinity to SF. The further research of the correlation between structure and biological function is still being done on the way.

METHODS: Two modified SF membranes were investigated. Blend membranes were prepared by mixing aqueous solutions of SF and DS at different ratios and then drying them at 50 . Modified SF with PCA were prepared by immersing SF membranes in PCA aqueous solution of 1% for 10 min, then the samples were washed with distilled water to remove weakly adherent PCA on SF. The absorbance was measured at 310 nm using a UV spectrometer to evaluate the amount of PCA immobilized on SF membrane.

Human umbilical vein endothelial cell (HUVEC), named ECV-304, were kindly provided by the Academy of Military Medical Sciences of China, and routinely cultured in our lab with DMEM-high glucose in a humidified air with 5% CO₂ at 37 . The medium was supplemented with 10% BCS. After ECV-304 (200 $\mu l, 10^4$ cells/well) was cultured in 96 pore plates coated with SF and modified SF substrates for 3 days, the relative cell viability was evaluated by MTT. The relative strength of cell adhesion on material surfaces was evaluated by a parallel-plate flow chamber[2]. ECV-304 were cultured on glass plate coated with SF and modified SF substrates with a density of $5{\times}10^5$ cells/ml for 3 hours at 37 . The fraction of adherent cells with

time was obtained by counting the number of cells at different times using the image processing software.

RESULTS:: The results of MTT assay show that the SF/DS blend has higher cell viability than the pure SF membrane. Fig.1 shows UV spectra of the modified SF film with PCA, pure PCA and pure SF. Fig.2 shows the cell adhesiveness on pure SF film and on the modified SF film with PCA. Obviously, the latter shows the stronger cell adhesion strength.

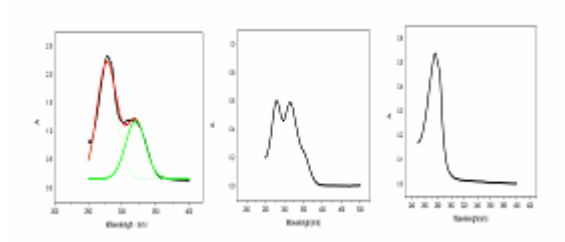


Fig. 1: UV spectra of SF coated with PCA(left), PCA(middle) and pure SF membrane(right).

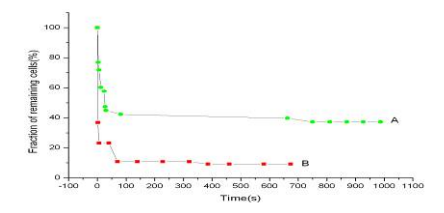


Fig. 2: Fraction of remaining cell vs .time for a pure SF membrane(low) and modified SF with PCA (top).

DISCUSSION & CONCLUSIONS: Danshen was introduced to SF film and increased cell viability on SF surface. One of the possible explanations is that PCA, an active ingredient of DS, adsorbed on SF and strengthened the cell-SF surface adhesion.

REFERENCES: ¹ R.Xu, B.Yang, et al (1990) *Danshen-Biology and Application*, Academic Press, pp 114–25. ²Y.Wan, J.Bei, S.Wang, et al (2003) *Biomaterials* **24** 3757–64.

ACKNOWLEDGEMENTS: This work was financed by the '973' project in China (No. $2005CB623906\Box$.

ELECTRODEPOSITIONAL IMMOBILIZATION MANNERS OF POLY(ETHYLENE GLYCOL) ON TITANIUM

Y. Tanaka¹, Y. Tsutsumi¹, H. Doi¹, T. Yoneyama² & T. Hanawa¹

Institute of Biomaterials and Bioengineering, Tokyo Medical and Dental University, Japan.

Department of Dental Materials, Nihon University School of Dentistry, Japan.

INTRODUCTION: In the design of bloodcontacting metallic devices such as catheters and bioaffinity sensors, it is important to generate biofunctional surfaces that are able to prevent or drastically reduce proteins adsorption. major challenge to achieve the biofunctional surfaces by an immobilization of poly(ethylene glycol), PEG. In this study, PEG terminated at both terminals with amine was immobilized onto a titanium surface with electrodeposition in an attempt to control the orientation of PEG easily and to apply for all metals and morphological materials. A thin PEG immobilized layer on the titanium surface was characterized using X-ray photo-electron spectroscopy, XPS, and Fourietransform infrared spectrometer with reflection spectrometry, FTIR-RAS, absorption discharge optical emission spectroscopy, GD-OES.

METHODS: Both terminals of PEG were terminated with amine, NH₂-PEG-NH₂ (MW=1000), because the terminals of PEG are positively charged, from NH₂ to NH₃⁺, for electrodeposition. 2mass%PEG was dissolved in a 0.3 mol L⁻¹ NaCl solution, and electrodeposition was carried out at 310 K with -5 V for 300 s. The pH of the solution with PEG was 11. A cp-Ti (grade 2) disk was metallographically polished and ultrasonically rinsed in acetone. Chemical bonding states at the interface and orientation of PEG molecules electrodeposition immobilized with characterized using XPS, GD-OES, and FTIR-RAS. For comparison, cp-Ti was immersed in a solution containing NH₂-PEG-NH₂ for 2 h and 24 h without any electric charge.

RESULTS & DISCUSSION: The GD-OES results shown in Figure 1 are expressed with the emission lines plotted against acquisition time. Depth profiles of Ti have a change in slope of the curve as shown on a dotted line. This point is assumed as the interface between PEG layer and TiO₂. Therefore, the N signal in left side of this point is originated from PEG molecules and increased in the direction of the interface from outersurface in electrodeposition. FTIR-RAS results revealed that NH₂-PEG-NH₂ were oriented in a direction perpendicular to TiO₂ in electro-

deposition. Also, $\mathrm{NH_3}^+$ and NHO peaks in N 1s XPS spectrum led to the bonding state in the interface between PEG layer and $\mathrm{TiO_2}$. The $\mathrm{[NHO]/[NH_3^+]}$ ratio shown in Figure 2 was larger in electrodeposition than in immersion.

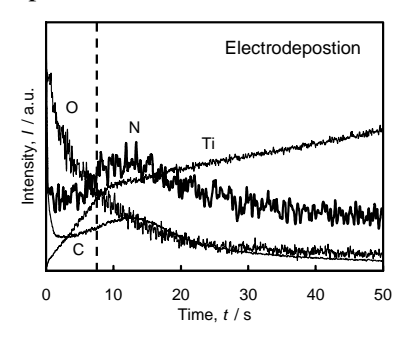


Fig. 1: Depth profile of NH₂-PEG-NH₂ layer immobilized onto titanium with electrodeposition.

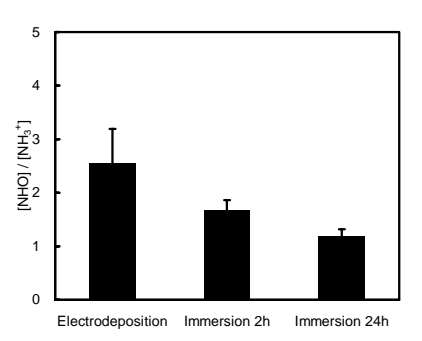


Fig. 2: Ratio, $[NHO]/[NH_3^+]$, obtained from the deconvoluted N 1s electron energy region peak.

CONCLUSIONS: Amines in terminals locate inside of the NH_2 -PEG- NH_2 layer and combine mainly with TiO_2 as stable NHO by electrodeposition, while amines randomly exist and show mainly unstable bonding with TiO_2 by immersion, as shown in Figure 3.

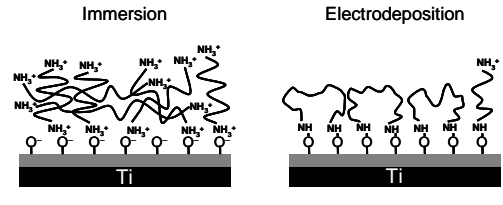


Fig. 3: Schematic immobilization manners of NH₂-PEG-NH₂ on titanium surface with immersion and electrodeposition.

Improved Cyclodextrin-Based Receptors for Camptothecin by Inverse Virtual Screening

A. Steffen¹, <u>C. Thiele</u>², S. Tietze³, C. Strassnig², A. Kämper¹, T. Lengauer¹, G. Wenz², J. Apostolakis³

¹ Max-Planck-Institute for Informatics, Saarbrücken, Germany. ² Organic Macromolecular Chemistry, Saarland University, Saarbrücken, Germany. ³ Institute for Informatics, Ludwig-Maximilians University, Munich, Germany.

INTRODUCTION: We report the computer-aided optimization of a synthetic receptor for a given guest, based on inverse virtual screening of receptor libraries.¹ A library of β-cyclodextrin (β-CD) 1 derivatives was generated, docked against camptothecin and ranked according to the predicted binding affinity. The most promising subsequently molecules are submitted to experimental validation. De Jong et al.² reported the identification of novel ligands for a given synthetic receptor by application of the docking tool Dock. In this work we address the opposite problem of looking for synthetic receptor that bind a given guest with high affinity, since this task is highly relevant for the complexation and controlled delivery of drugs.

METHODS: A virtual library of 6-O-mono- and 6-O-hepta-substitued β -CD derivatives was generated from β -CD core and thiol building blocks. We performed an inverse docking in which the receptor conformation was optimized in the field of the rigid ligand. The virtual screening was performed through the use of two docking tools, namely Autodock and Glamdock.

β-CD derivatives were synthesized by nucleophilic displacement reaction. The binding constant K and the corresponding binding free energies $ΔG^0$ of all complexes with camptothecin (CPT) were determined with the solubility method described by Kang.²

RESULTS: In principle the predicted binding free energies correspond to the experimental data with a correlation coefficient for Glamdock of 0.82. The predicted affinity scores for hepta-substituted derivatives were generally more favorable than for the corresponding mono-substituted derivatives with both docking programs.

Nine hepta-substitued derivatives were synthesized, four of them were insoluble in water. Therefore we also synthesized the corresponding mono derivatives. The remaining five out of nine synthesized hepta derivatives exhibit binding constants between 3134M⁻¹ and 7496 M⁻¹ and are

clearly superior to native β -CD. Heptakis- [6-deoxy-6-(2-sulfanylethanesulfonic acid)]- β -CD (2) showed the highest value of K with $7496M^{-1}$. The mono derivatives are generally in the range between 370 M^{-1} and 641 M^{-1} . Mono-[6-deoxy-6-(6-sulfanyl-9H-purine)]- β -CD (3) is an exception and shows the strongest binding affinity with 3629 M^{-1} , which is in the range of the hepta-substituted derivatives.

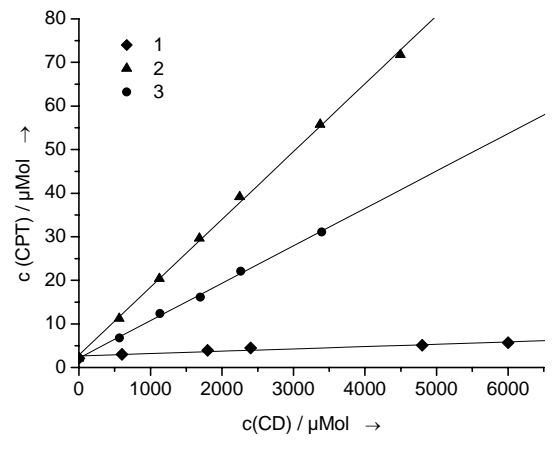


Fig. 1: Dependence of the solubility of camptothecin (CPT) on the concentration of the β -CD derivatives.

DISCUSSION & CONCLUSIONS: Our results indicate that inverse virtual screening can support the identification of improved receptors for a given ligand significantly. Applications for the controlled delivery of camptothecin are conceivable. This approach is not limited to CD derivatives and can be expanded to other host-guest systems.

REFERENCES: ¹ A. Steffen, C. Thiele, C. Strassnig et al. (2007) *Chem. Eur. J.* DOI: 10.1002/chem.200700661 ² M. R. de Jong, R. M. A. Knegtel, P. D. J. Grootenhuis, et al (2002) *Angew. Chem. Int. Ed.* **114**: 1046-1050 ³ J. Kang, V. Kumar, D. Yang, et al (2002) *Eur. J. Pharm. Sci.* **15**: 163-170

Nanogel-Inorganic Hybrid: Synthesis and Characterization of Polysaccharide-Calcium Phosphate Nanomaterials

S. Yamane^{1, 2}, K. Akiyoshi^{1, 2}

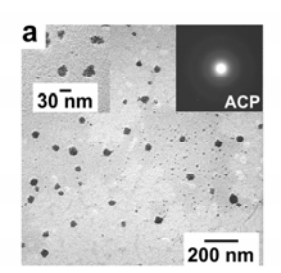
¹ Institute of Biomaterials & Bioengineering, Tokyo Medical & Dental University, Tokyo, JAPAN.

² Center of Excellence Program for Frontier Research on Molecular Destruction and Reconstruction of Tooth and Bone, Tokyo Medical & Dental University, Tokyo, JAPAN.

INTRODUCTION: The organic-inorganic hybrid materials have attracted growing attention for drug delivery system (DDS). Calcium phosphate that is a main inorganic component of teeth and bone shows excellent biocompatibility. We developed hydrogel nanoparticles by self-assembly of cholesterol-bearing polysaccharides. The nanogels hydrophobic drugs and proteins hydrophobic interaction and they are widely applied to DDS¹. Hybrid materials between calcium phosphate and the nanogels are expected to use as novel nanobiomaterials. In our previous work, cholesterol-bearing pullulan (CHP) nanogel acted as a template for mineralization of amorphous calcium phosphate (ACP) nanoparticles by pH-gradient method². Here we report synthesis of calcium phosphate hybrid material using cholesterol-bearing anionic mannan (CHM) nanogel³ as a template. CHM, which has phosphodiester linkage, acted as an effective template for mineralization of calcium phosphate. The preparation of hybrids of CHM-protein nanogels with calcium phosphate and also the controlled-release property of the proteins from the hybrid nanomaterials were investigated.

METHODS: CHM was substituted with 1.0 cholesteryl groups per 100 mannose units of the mannan from Saccharomyces cerevisiae (2.7 phosphorous per 100 mannose units, $M_{\rm w} = 5.5 \times$ 10⁴). The average hydrodynamic diameter of the nanogels was 29 nm. The nanogels trapped FITC labeled insulin (FITC-Ins) by just mixing at 37 °C for 12 h. The CHM nanogels or CHM nanogels trapped FITC-Ins were added to hydroxyapatite (HAp) solution which was prepared by bubbling with CO₂ gas. The mixture was stirred for 8 h at 25 $^{\circ}$ C (CHM = 0.5 mg·mL⁻¹). After the addition of BSA (5 mg·mL⁻¹), the released FITC-Ins from the nanoparticles was evaluated by size-exclusion chromatography (SEC) with UV detector at 494 nm.

RESULTS: In the presence of CHM nanogels, dispersed inorganic nanoparticles were observed in the transmission electron microscope (TEM, Fig.1). Energy-dispersive X-ray spectroscopy confirmed that obtained materials contain Ca and P.



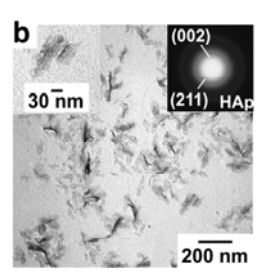


Fig.1: TEM images of CHM nanogel-calcium phosphate nanoparticles. Insets show magnification and electron diffraction pattern of nanoparticles. The concentration of Ca^{2+} ; a) 0.8 mM, b) 2.0 mM.

In the dilute HAp solution ($[Ca^{2+}] = 0.8 \text{ mM}$), ACP nanoparticles were obtained (Fig.1a). When the concentration of Ca²⁺ was 2.0 mM, dispersed HAp nanoparticles were obtained (Fig.1b). Under the same condition ($[Ca^{2+}] = 2.0$ mM), HAp was precipitated in the presence of nonionic CHP nanogels. Dispersed FITC-Ins-trapped CHM nanogel-HAp nanoparticles were also obtained $([Ca^{2+}] = 2.0 \text{ mM})$. From the hybrid nanoparticle, FITC-Ins was not released at all before the addition of BSA. The 89% and 31% of FITC-Ins were released from non-mineralized CHM nanogels and hybrid nanoparticles respectively after incubation with BSA for 0.5 h. The continuous release of FITC-Ins from hybrid nanoparticles was observed up to 12h.

DISCUSSION & CONCLUSIONS: By pH-gradient method, well-dispersed CHM nanogel-calcium phosphate nanoaprticles (both ACP and HAp nanoparticles) were obtained. Anionic property of mannan, derived from phosphodiester linkage, should affect the formation of calcium phosphate. The initial burst of FITC-Ins from CHM nanogels was prevented by the mineralization with calcium phosphate. These nanohybrids can be used as biocompatible drug carriers with controlled-release properties.

REFERENCES: ¹N. Morimoto et al. (2006) Nanogel Engineered Designs for Polymeric Drug Delivery in *Polymeric Drug Delivery Volume II* (eds S. Svenson) ACS pp.88-101, ²A. Sugawara, S. Yamane, K. Akiyoshi (2006) *Macromol. Rapid Commun.* **27**:441-446, ³E. Akiyama, N. Morimoto, P. Kujawa et al. (2007) *Biomacromolecule* In press

C₆₀ Sputter Depth Profiling of Drug-Loaded Poly(lactide)

AG. Shard¹, S. Westall², R. Ogaki², IS. Gilmore¹, MR. Alexander², MC. Davies²

¹ National Physical Laboratory, Teddington UK. ² LBSA, School of Pharmacy, University of Nottingham, UK.

INTRODUCTION: Cluster ion sources are finding increasing use in the surface analysis of organic and biological materials. The high sputtering yields enable the depth profiling of organic materials without the accumulation of high levels of damage. With the development of C_{60}^{n+} ion sources [1] there is substantial expectation that the approach will be useful for measuring the distribution of organic materials in surface layers. This will be of benefit in the engineering of drug delivery systems and potentially useful for the imaging of tissues and cells. Indeed, SF_5^+ ions have previously been employed to demonstrate both lateral and vertical phase separation in drug loaded polymers [2].

METHODS: Depth profiles were carried out using an TOFSIMS IV time of flight mass spectrometer (IONTOF Gmbh, Muenster, Germany). Samples consisted of poly(lactide): drug solutions spin-coated in a variety of concentrations onto silicon wafers. Model drugs included bupivacaine and codeine. Sputtering was performed using 10 keV C_{60}^+ ions and the centre of the sputtered area analysed with a focussed Bi_3^+ ion beam. In this manner, three-dimensional datasets of secondary ion intensity could be obtained.

RESULTS: Films of pure polylactide of up to 700 nm thickness could be readily depth profiled (Fig. 1). After a rapid initial accumulation of chemical damage [3], manifested by a drop in secondary ion intensity, a steady state is achieved until the film is completely removed. The depth resolution at the interface is approximately 50 nm. In drug-loaded films, protonated drug molecules could be detected as intense secondary ions during depth profiles of ~250 nm thick films (Fig. 2).

DISCUSSION & CONCLUSIONS: The steady state achieved during depth profiling of pure poly(lactide) films indicates that there is a constant sputtering rate for these materials. Both the steadiness of the sputtering rate and the good depth resolution imply that poly(lactide) does not roughen during C_{60}^+ ion bombardment. A depth scale, proportional to ion dose, can therefore be readily applied to these materials. Codeine is found to be evenly distributed throughout poly(lactide), except for a thin surface layer with very low codeine content. Bupivacaine appears to phase

separate from poly(lactide) to form a stratified system (Fig. 2). These results demonstrate that determination of the spatial distribution of drugs in poly(lactide) is possible using C_{60}^{+} ion sputtering.

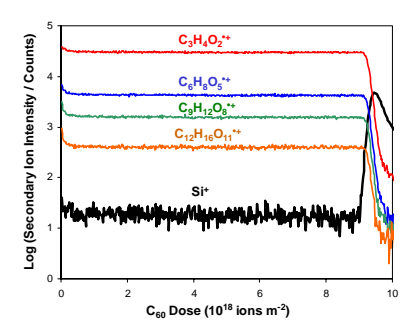
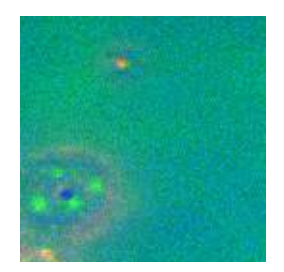


Fig. 1: Depth profile of a 700nm thick polylactide film on silicon, showing the intensities of secondary ions typical of the organic film and the substrate.



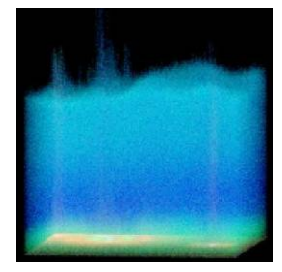


Fig. 2: Left: Composite image (160 µm × 160µm) of components in a ~250nm thick drug-loaded polymer film; sodium contamination (red), bupivacaine (green), silicon substrate (blue). Right: Height-corrected side view showing mixed bupivacaine and polymer at surface (cyan), intermediate polymer-rich layer (blue) and bupivacaine-rich layer at interface (green).

REFERENCES: ¹ D. Weibel, S. Wong, N. Lockyer, et al (2003) *Anal. Chem.* **75**: 1754. ² C.M. Mahoney, D.V. Patwardhan, M.K. McDermott (2006) *Appl Surf Sci* **252**: 6554. ³ A.G. Shard, P.J. Brewer, F.M. Green, I.S. Gilmore (2007) *Surf Interface Anal* **39**: 294.

ACKNOWLEDGEMENTS: This work forms part of the Measurements for Emerging Technologies programme supported by the National Measurements System Policy Unit of the UK Department of Trade and Industry.

Peptide nanoparticles for drug delivery applications

C.Fraysse-Ailhas¹, A.Graff-Meyer¹, Per Rigler², C.Mittelhozer¹, S.Raman¹, U.Aebi¹, P.Burkhard³

¹ M.E. Müller Institute for Structural Biology, University of Basel, Switzerland. ² Department of Chemistry, University of Basel, Switzerland. ³ Alpha-O Peptides AG, Allschwil, Switzerland

INTRODUCTION: Bio-nanotechnology opened a wide range of applications for drug delivery systems and cancer therapy. In particular, it is possible to design new systems able to deliver in a specific and non-cytotoxic manner a therapeutic compound that would normally be rapidly degraded in the blood plasma [1]. A lot of studies [2, 3] have been performed on systems like lipids or polymer nanoparticles. Due to the nanometer size of such cargos, the transportation of therapeutic compounds in the blood stream is increased in terms of time circulation. Nevertheless, their surface functionalization, to improve drug-targeting properties is usually complicated and rather ineffective. We recently designed a novel type of functional nanoparticles with regular icosahedral symmetry, mimicking small and rigid viral capsids. These particles have a diameter of about 22nm and self-assemble from single polypeptide chains.

METHODS: These nanoparticles are formed by a specific peptide sequence consisting of a pentameric coiled-coil domain from the Cartilage Oligomerization Matrix Protein (COMP) (ref) and a de novo designed minimal trimeric coiled-coil domain, which are joined by a two-glycine residue linker segment. At either end, the peptide chain can be extended by peptide sequences with a specific function (targeting peptides, cell penetration peptides). In addition, drugs or molecular markers (radionuclides, fluorescent probes, etc.) can be covalently attached and hence be presented at the particles surface (see Fig.1). For nanoparticles large-scale production and for efficient functionalization, the peptides are produced using a recombinant protein expression system (E. coli).

RESULTS: After production and purification, the peptide quality was monitored on SDS-Page gel, and showed the presence of monomers as well as trimers. The nanoparticles assembly properties were analyzed by various techniques like: transmission electron microscopy (TEM), fluorescence correlation spectroscopy (FCS) and light scattering (DLS). dynamic DLS investigations of nanoparticles without ligand, after refolding by stepwise dialysis, showed a hydrodynamic radius of 27nm. In the case of TEM measures, the radius measured was around 13nm. The difference, between these two techniques can be explained by electrostatic interactions, which are higher in solution for DLS measurements. In the case of nanoparticles modified with the fluorescent label Alexa-488, FCS was performed and showed a diffusion time of 500ms, corresponding to particles with a radius of 10nm. Extension of the nanoparticles with somatostatin, induced a small increase of the particles size, as expected.

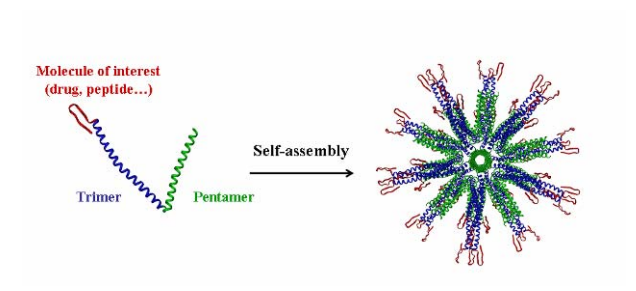


Fig. 1: Functionalized nanoparticles (right) formed by self-assembly of peptides (right). The trimeric domain can be modified by a ligand or by a drug.

DISCUSSION & CONCLUSIONS: The main objective was to develop a prototype of selfassembling peptide nanoparticles, which can be functionalized to be used as a drug targeting and delivery system for cancer treatment. According to the computer design, we obtain nanoparticles with predicted biophysical characteristics. The addition of peptide ligands or fluorescent probes does not interfere with the nanoparticles assembly behavior. The high ligand density on the particle surface will increase the avidity for the specific receptor due to cooperativity of binding. As a consequence the drug dose can be decreased and the side effects can be reduced. The next step will be to make nanoparticles functional studies in vitro and in vivo conditions.

REFERENCES: ¹ M.L Thakur (1995) *Nuclear medicine communications* **16**:724. ²D.D.Lasic (1996), *Drugs and the Pharmaceutical Sciences* **73**:297-328. ³Y.P.Zhang, B.Ceh, D.D.Lasic (2002) *Polymeric Biomaterials* (2nd Edition), pp 783.

ACKNOWLEDGEMENTS: This work was supported by grants of the KTI, of the Swiss Nanoscience Institute (Argovia) and the M.E. Mueller Institute for Structural Biology (MSB).

Haemocompatibility studies of novel anti-infective vascular grafts

F.D. Matl^{1, 2, 3}, S. Repmann¹, M. Kiokekli³, A. Obermeier^{1, 3}, W. Friess² and A. Stemberger^{1, 3}

¹Institute of Medical Engineering, Technische Universität München, Garching, Germany.

²Department of Pharmacy-Pharmaceutical Technology and Biopharmaceutics, Ludwig

Maximilians-Universität, München, Germany.

³Institut für Experimentelle Onkologie und Therapieforschung, Klinikum r. d. Isar, München, Germany.

INTRODUCTION: Biocompatibilty and haemocompatibility are important characteristics of alloplastic implants¹. Contact between biomaterials and blood leads to increased thrombogenicity and activation of the complement system. The specific task of this work was to study the effect of novel, alloplastic vascular grafts on the activation of blood coagulation and the complement system.

METHODS: Commercially available ePTFE grafts (Alpha Graft® PTFE) were equipped with different anti-infective coatings. Grafts were coated with gentamicin and teicoplanin incorporated in four different lipid-like carriers under aseptic conditions in a dipping process. acid, tocopherol acetate, Poly-D, L-lactic Dynasan® 118 and Softisan® 649 served as drug carriers. In order to examine thrombogenious characteristics of individual coatings, haemocompatibility studies were carried out. Sample and reference grafts were incubated for eight minutes in four milliliter human whole blood. Plasma was generated and different coagulation factors were assessed in order to get information about a modified coagulation. Citrated blood plasma was examined with an amidolytic substrate assay for factor XIIa-like activity (UnitestTM FXIIA) as well as for plasma F1+2 values (Enzygnost F1+2 micro) by a monoclonal enzyme immunoassay. EDTA blood plasma was proved for C3a-desArg (Complement C3a-desArg ELISA). Thromboelastographic studies for whole blood were carried out with a roTEG Coagulation Analyser (Pentapharm GmbH).

RESULTS: Haemocompatibility of individual coatings could be confirmed by conducted studies. Assays of factors F1+2, XIIa as well as complement factor C3a and thromboelastography

studies of individual lipid-like coatings show comparable results to established uncoated PTFE grafts.

Table 1. Sample groups of PTFE coatings consisting of individual drug carriers with

incorporated gentamicin sulfate (G) or teicoplanin

(1)		
Drug carrier	Gentamicin	Teicoplanin
	sulfate	
PDLLA	G1	T1
Tocopherol acetate	G2	T2
Softisan® 649	G3	Т3
Dynasan® 118	G4	T4

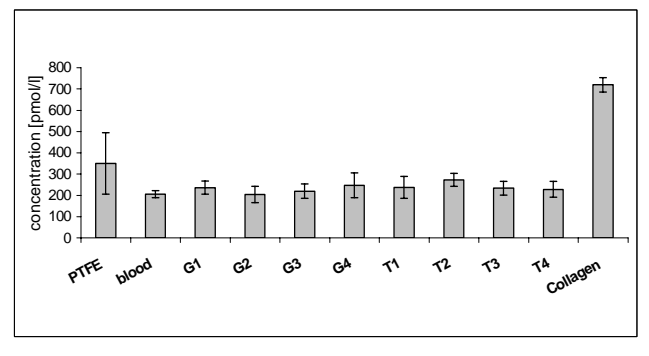


Fig. 1: Human prothrombin fragment concentrations activated by individual lipid-like coatings on PTFE prostheses. Uncoated prostheses served as reference, collagen as positive control.

DISCUSSION & CONCLUSIONS: Antiinfective vascular graft coatings are a highly effective protection from biomaterial-associated bacterial infections. In this study we could demonstrate the development of a drug eluting system consisting of lipid-like polymers with incorporated chemotherapeutics and confirm at least comparable haemocompatible characteristics to already established uncoated ePTFE grafts in surgery.

REFERENCES: ¹ A. Bolz, M. Schaldach (1993) *Haemocompatibility optimisation of implants by hybrid structuring*, Med. Biol Eng Comput., 31 Suppl: p.123-30.

ACKNOWLEDGEMENTS: This study was kindly supported by the Arbeitsgemeinschaft industrieller Forschungsvereinigungen (AiF).

Surface Functionalization of Nanoparticles For Cell-Targeted Drug Delivery

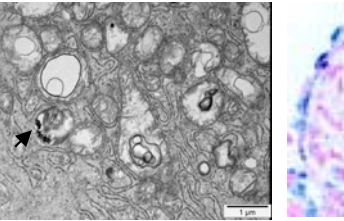
F. Cengelli¹, J. Grzyb², F. Tschudi-Monnet³, X. Montet⁴, A. Montoro¹, H. Hofmann⁵, S. Hanessian², L. Juillerat-Jeanneret¹

¹University Institute of Pathology, University of Lausanne, Lausanne, Switzerland; ²Department of Chemistry, University of Montreal, Montreal, Canada; ³Institute of Physiology, University of Lausanne, Lausanne, Switzerland; ⁴Department of Cell Physiology and Metabolism and Medical Radiology, University of Geneva, Geneva, Switzerland; ⁵EPF Lausanne, Lausanne, Switzerland.

INTRODUCTION: SuperParamagnetic Iron Oxide Nanoparticles (SPIONs) with a core size of 9-10 nm diameter and a polymer coating such as polyvinyl alcohols (PVA) [1] may be useful both for selective disease detection by MRI and targeted drug delivery provided that their polymer surface is functionalized with therapeutic drugs and/or cell-targeting molecules. Our objectives are to develop surface-functionalized-SPIONs and to evaluate their biocompatibility, uptake by specific cells and cellular localization in cells and organs, and their therapeutic efficacy.

METHODS: The cell uptake of surfacefunctionalized-SPIONs was evaluated using either 2-dimensional cell cultures or 3-dimensional tumor cell spheroids or brain cell aggregates. SPIONs were injected i.v. in normal mice and organs were examined for their SPIONs content. To evaluate the cell and tissue uptake of SPIONs we combined detection of their fluorescent coating by confocal microscopy and of the iron oxide core by prussian blue detection and transmission electron microscopy. To determine their biocompatibility and their potential for chemotherapy, we evaluated cell survival by measuring metabolic activity and DNA synthesis.

RESULTS & **DISCUSSION:** Using dimensional cell cultures the presence of amino groups on the SPIONs coating was shown to be mandatory for cell uptake, and this uptake did not modify cell proliferation. SPIONs uptake by cells was increased in the presence of an external magnetic field. The polymer coating and the iron oxide core of SPIONs were internalized by cells in vitro (Fig. 1 and [2]). In 3-dimensional cell culture models SPIONs were found associated with cells, being able to invade tumor spheroids (Fig. 2 and [3]) but not differentiated brain aggregates [2]. In vivo amino-functionalized-SPIONs were found in the spleen and the liver but not the brain and kidneys [3]. SPIONs functionalized by therapeutic drugs such as 5-fluorouridine, displayed anti-tumor activity (Fig 2 and [4]).



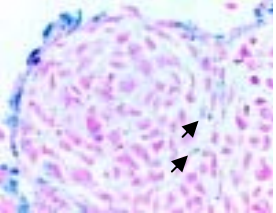


Fig. 1: Transmission electron and light microscopy of functionalized-SPIONs (arrow) in human melanoma cells and in human melanoma cell spheroids [3].

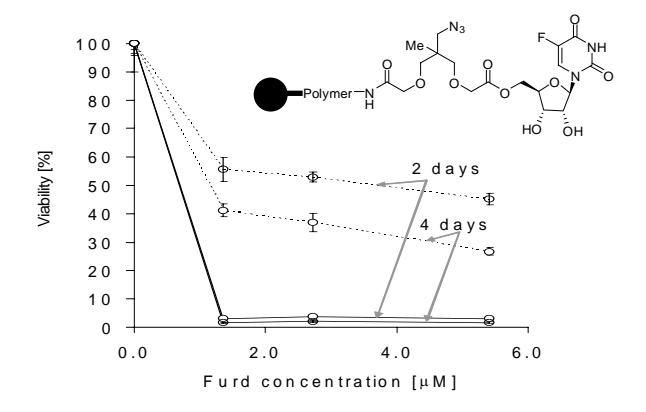


Fig. 2: Structure of drug-functionalized-SPIONs (5-fluorouridine, Furd) and their effects on human melanoma cell metabolic activity (dotted lines) or DNA synthesis (solid lines)[4].

CONCLUSIONS: These approaches gave a proof of concept of the feasibility of using drug functionalized-SPIONs in biological systems for targeted cell-delivery of therapeutic agents and of their potential to be selectively taken up by living cells in 3-dimensional structures.

REFERENCES: [1] Petri-Fink A, Chastellain M, Juillerat-Jeanneret L, *et al* (2005) *Biomaterials* 26:2685-2694; [2] Cengelli F, D. Maysinger D, Tschudi-Monnet F, *et al* (2006) *JPET* 318:108-116; [3] Cengelli F, *et al.*; [4] Hanessian S, *et al.*, *submitted*

ACKNOWLEDGMENTS: This work was supported by the Swiss National Scientific Research Foundation (Grant 3152A0-105705) and the Swiss Society for Multiple Sclerosis.

Surface delivery of siRNA for implants

M. Ø. Andersen^{1,2}, J. V. Nygaard¹, K. A. Howard^{1,2}, R. Bak¹, S. R. Paludan³, M. Raarup⁴, F. Besenbacher¹, J. Kjems^{1,2}

¹Interdisciplinary Nanoscience Center (iNANO), ²Department of Molecular Biology, ³Institute of

¹Interdisciplinary Nanoscience Center (iNANO), ²Department of Molecular Biology, ³Institute of Medical Microbiology and Immunology, ⁴Stereology and Electron Microscopy Research Laboratory, University of Aarhus, 8000 Aarhus C, Denmark

INTRODUCTION: Using short interfering RNAs (siRNAs) we can shut down the production of any cellular protein specifically. This has many potential applications in implant and tissue engineering technology. One could for example use it to direct the differentiation of stem cells (i.e. by targetting a transcription factor or a repressor thereof) or to reduce the local immune response (i.e. by targetting an inflammatory cytokine). But for a siRNA formulation to be used together with an implant they need to be interfaced. Here we present a surface delivery system for siRNAs which can be coated onto 2 and 3 dimensional structures. The system is based on a lyophilized formulation of biocompatible nanoparticles

METHODS: siRNA particles were formed with chitosan or TransIT-TKO. Particles were added sucrose or gelatine and used to coat various surfaces including cell culture wells and PCL scaffolds which were then lyophilized. The particles released from the dried coat were studied by native PAGE, dynamic light scattering and laser doppler velocimetry. Macrophages, epithelial cells and mesenchymal stem cells were grown upon the surface and uptake and activity studied using microscopy, ELISA, flow cytometry and RT-PCR

RESULTS: We show that sucrose protects the particles during the coating process and that we can tune the release rate and localisation of the particles using gelatine. We also show that the delivery system can deliver the siRNAs into cells growing on and nearby the coated surface and silence a cellular target in these cells. Specifically we have targeted TNF- α in macrophages grown on a siRNA coated 2d surface and eGFP in epithelial cells and mesenchymal stem cells on 2D and 3D surfaces.

DISCUSSION & CONCLUSIONS: We have developed a system that could be used to silence a wide range of proteins in cells growing on surfaces. This system will advance the field of

implant technology by making them more immunocompatible and capable of directing differentiation of stem cells.

ACKNOWLEDGEMENTS: The authors are grateful to Claus Bus and Rita Rosendahl Hansen for helpful and valuable technical work.

Reductively degradable PEG-nanoparticles for DNA delivery

M. Gengler, H.Hall, JA.Hubbell²

D-MATL, ETH Zurich, Zurich, Switzerland. ² EPF Lausanne, Lausanne, Switzerland.

INTRODUCTION: The aim of this project was to develop a novel, biodegradable drug delivery system for cancer therapy. Polymeric nanoparticles for the use as drug- and gene-delivery vehicles have been developed by using multi-arm poly-(PEG)-thiol macromers ethylenglycol biocompatible and stealth providing polymer. Disulfide-reduction of the thiols that formed the nanoparticles was explored as a natural. intracellular degradation method, to release complexed plasmid DNA for in vitro transfection.

METHODS: Nanoparticles were prepared in an inverse (glycine buffer in hexane) emulsion, using a mix of Span80 and Tween80 as surfactants. Radical polymerization of multi-arm PEG-thiol macromonomers was initiated using APS/TEMED. Active substances could be either added to the polymerizing solution (e.g. entrapment of plasmid DNA into the nanoparticles) or covalently linked to unreacted (average of 2.5 % of initial) thiols after formation of the particles. Nanoparticles were purified using a simple extraction method, followed by extensive dialysis. The particle size was determined using Dynamic Light Scattering.

Uptake into cells (HeLa, Cos7, 293T) was characterized by using fluorescein-labelled nanoparticles. Potential cytotoxicity of internalized nanoparticles was evaluated through cell viability (live/dead) and -activity (WST) assays in HeLa cells. pEGFP-N1, a plasmid encoding for green fluorescence protein entrapped was nanoparticles and used as a model for in vitro plasmid delivery and gene expression in HeLa cells. Intracellular pathways of the nanoparticles were investigated by monitoring fluoresceinlabelled nanoparticles. The nanoparticels were colocalized with marker proteins for early – and late endosomes. The cell number was determined by Hoechst nuclear stain.

RESULTS: Nanoparticles could be formed by inverse emulsion polymerization of multi-arm-PEG thiols. The size was found to be between 120 - 200 nm. The diameter depended on the emulsion parameters and type of encapsulated molecules. For DNA-plasmid entrapment the diameter was 200 nm. Particles showed no cytotoxicity and were well uptaken by cells (up to 1000 ug/ml). Colocalization studies of nanoparticles with early and late endosomal marker proteins (fig. 2) showed no

indication of nanoparticles in the endosomal However. nanoparticle-associated pathway. fluorescence was detected in the perinuclear zone, suggesting accumulation of nanoparticles or their degradation products. Fig. 1 shows in vitro transfection of HeLa cells with pEGFP-containing nanoparticles. The transfection efficiency was 2.5% as compared to DEAE-Dextran. In vitro transfection by these reductively degradable PEGpolymer nanoparticles required three days until transfected cells showed detectable expression. These findings suggest that the DNAcontaining nanoparticles are very stable and DNA is only slowly released intracellularly.

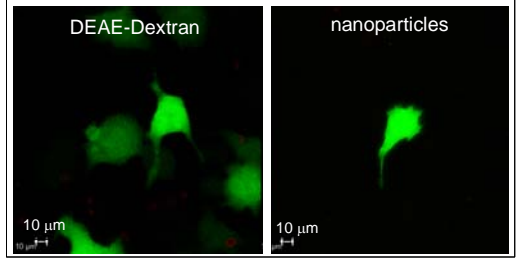


Fig. 1: In vitro transfection of HeLa cells after 3 days: DEAE (left) and pEGFP-N1-containing nanoparticles particles (right).

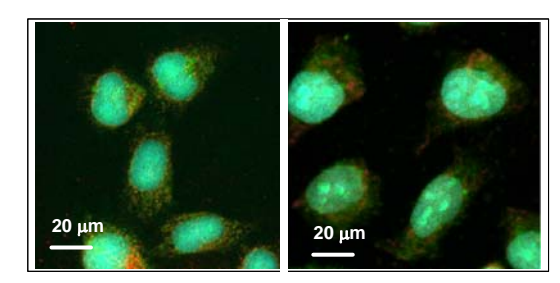


Fig. 2: Colocalization of fluorescein-labelled nanoparticles (green) in HeLa cells with early endosomal marker proteins (red, left image) or late endosomal marker proteins (red, right image).

DISCUSSION & CONCLUSIONS: PEGdisulfide nanoparticles were found to be taken up into HeLa cells however, the mechanism of uptake remains unclear. *In vitro* transfection with a plasmid entrapped within the nanoparticles is 2.5%. The slow appearance of green fluorescent protein and accumulation of the nanoparticles in the perinuclear zone of transfected cells indicate that the nanoparticles are very stable within the cell and that the release of the plasmid is very slow. This feature might be interesting for DNA-delivery in long-term *in vivo* applications.

Block copolymer based vesicles as carriers and biological membrane mimetics

M.Grzelakowski¹, C.Fraysse¹, P.Riegler¹, W.Meier¹

¹ Department of Chemisty University of Basel, Basel, Switzerland

INTRODUCTION: Amphiphilic block copolymers aggregate in water forming different morphologies [1]. The interest in vesicular structures arises from the potential applications in different fields like delivery-release, biomineralization or nanoreactors [2].

METHODS: By combination of different techniques like NMR, GPC, DLS, FCS, LB, BAM, TEM, cryo-TEM and light microscopy we investigated the ABA block copolymers

(A–polyoxazoline, B-polydimethylsiloxane) concerning the composition and self-assembly of into vesicular and giant vesicular structures. The major aim of this study was to obtain quantitative information on membrane properties, in particular, the intramembrane lateral diffusion (polymer chain mobility). Such observations are feasible with the fluorescence correlation spectroscopy after the polymer chains had been covalently labeled with a fluorescent marker [3]. This approach will be further applied to investigate protein-reconstituted polymer membranes [4] to understand the structural details of such a matrix perturbed by a thickness-mismatch like a membrane protein.

RESULTS: Successful synthesis of well defined ABA block-copolymers: forming vesicular aggregates, stable membranes, activating membrane proteins, capable of encapsulation of desired content (carrier) and enabling immobilization platform

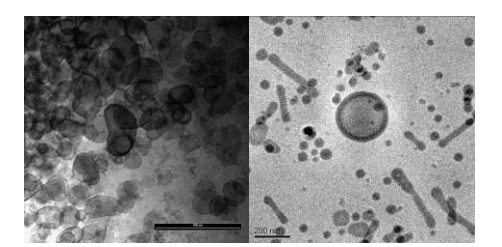


Fig. 1:TEM (left) and cryo-TEM(right) picture of vesicles

DISCUSSION & CONCLUSIONS: This poster will present the synthesis, purification and characterization of the amphiphilic ABA triblock copolymers library, as well as self assembly into planar and spherical membranes. Systematic studies on the polymer diffusion in membranes depending on the polymer chain lengths and block ratio will be discussed.

REFERENCES: [1] A. Taubert, A. Napoli, W. Meier, Current Opinion in Chemical Biology 8, 598-603 (2004). [2] K. Kita-Tokarczyk, J. Grumelard, T. Haefele, W. Meier, Polymer, 46, 3540-3563 (2005).

- [3] L. Luo, J. Tam, D. Maysinger, A. Eisenberg Bioconjugate Chem.; 2002; 13(6) pp 1259 - 1265;
- [4] W. Meier, C. Nardin and M. Winterhalter, Angew. Chem. 112, 4747 (2000). Angew. Chem. Int. Ed. 39, 4599 (2000).

ACKNOWLEDGEMENTS: This work is supported by National Center of Competence in Research (NCCR) and Swiss National Science Foundation (SNF).

Nucleo-copolymers: oligonucleotide-based amphiphilic diblock copolymers

F. Teixeira Jr. 1, C. Cattin 1, M. Ledergerber 1, A.H.E. Müller 2, C. Vebert-Nardin 1

¹ Chemistry Department, University of Basel, Basel, Switzerland. ² Macromolecular Chemistry, University Bayreuth, Bayreuth, Germany.

INTRODUCTION: Nucleo-copolymers are amphiphilic copolymers which have as hydrophilic segment an oligonucleotide sequence¹. These copolymers take advantage of the high specificity and functionality presented by nucleic acid sequences, which may be considered as negatively charged polymers, in order to build functional macromolecular nanostructures. These nanostructures are also capable of undergoing noncovalent, yet highly specific interaction by basepairing, as well as being recognized by biological systems^{2,3}.

METHODS: The synthesis of these nucleocopolymers was performed using different 12nucleotide long sequences, namely, Guanosine (G_{12}) , Cytidine (C_{12}) and Guanosine-Adenosine (A₅G₇), bearing a terminal carboxylic group, coupled to amino-terminated polybutadiene (PB, $Mw = 2000 \text{ Da})^4$. The synthesis was performed by solid phase synthesis on phosphoramidite (CPG). Purification was achieved through Size Exclusion Chromatography (SEC) after cleavage of the material from the surface. The copolymers were characterized by FT-IR and their self-assembly into vesicular structures in dilute aqueous solution was studied and described through several Microscopy techniques and Dynamic Light Scattering (DLS). Preliminary biological studies using macrophages were also carried out.

RESULTS: FT-IR analysis showed that the synthesis of the nucleo-copolymers was successful in all three cases. This is reinforced by the fact that in dilute aqueous solution these copolymers feature self-assembly. spontaneous into structures. These vesicles were well-characterized using different microscopy methods and DLS, resolving the morphology to determining the size of the self-assemblies (Fig. 1), respectively. The dynamics ruling the formation and stability of the vesicles along larger time periods were observed as well, showing modifications in size. Biological studies with macrophages were also carried out. Using labelled nucleo-vesicles, Confocal Laser Scanning Microscopy (CLSM) showed that the self-assembled structures were internalized and demonstrated very good stability upon cellular uptake process (Fig. 2).

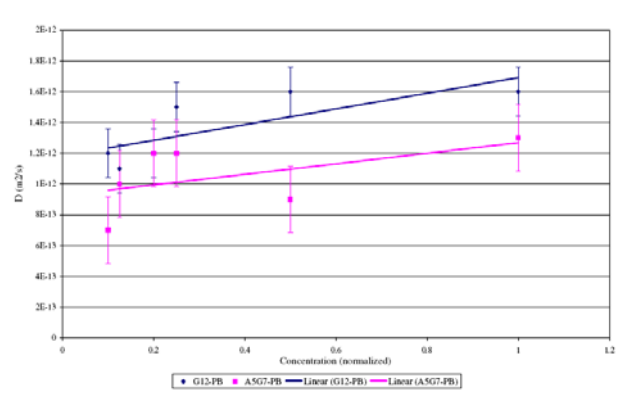


Fig. 1: DLS determination of the hydrodynamic radius (R_h) of G_{12} -PB and A_5G_7 -PB in PBS.

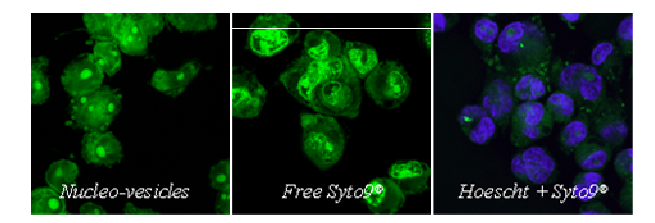


Fig. 2: CLSM micrographs of the uptake of the nucleo-vesicles by macrophages.

DISCUSSION & CONCLUSIONS: The vesicular structures formed by nucleo-copolymers synthesised present a very good stability, but the presence of charges in the copolymer seem to drive the dynamics of the self-assembling process along with time. The fact that this system presents a great environmental response and the possibility of tunning the oligonucleotide sequence, in order to achieve specific cell recognition, gives this material a great range of possible applications.

REFERENCES: ¹ F. Teixeira Jr., P. Rigler, C. Vebert-Nardin, *Chem. Commun.* **2007**, 1130-1132. ² R. A. Chandra, E. S. Douglas, R. A. Mathies, C. R. Bertozzi, and M. B. Francis, *Angew. Chem. Int. Ed.* **2006**, *45*, 896-901. ³ P. Broz, S. M. Benito, C. Saw, P. Burger, H. Heider, M. Pfisterer, S. Marsch, W. Meier, and P. Hunziker, *J. Controlled Release* **2005**, *102*, 475-488. ⁴ S. Nosov, H. Schmalz, A.H.E. Müller, *Polymer* **2006**, *47*, 4245-4250.

ACKNOWLEDGEMENTS: We acknowledge Prof. Dr. Axel Müller for kindly providing us with material and support, SNSF for funding and all the people involved in this project.

Surface Modified Microparticles As Carriers For Nucleic Acid Vaccines And Immunopotentiators

N. Csaba¹, S. Fischer¹, G. Gorodyska², M. Textor², H.P. Merkle¹

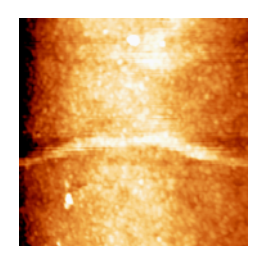
¹Drug Formulation and Delivery Group, ²Laboratory for Surface Science and Technology. ETH Zurich, CH-8093 Zurich, Switzerland.

INTRODUCTION: The main objective of the present work was the development of nano-scale surface modifications of poly(D,L lactic-coglycolic acid) (PLGA) microparticles for the delivery of nucleic acids. As a first approach, PLGA microparticles were surface modified with cationic polymers (chitosan or protamine) in order to facilitate the electrostatic assembly of plasmid DNA or messenger RNA to the particles. Furthermore, with the aim of increasing loading efficiency and providing better protection for the associated DNA/RNA, the possibility of forming multiple layers on the particle surface was investigated. The feasibility of similar systems incorporating these antigen encoding nucleic acids vaccination in combination immunostimulatory sequences such as CpG oligonucleotides or poly (I:C) as adjuvants was also studied.

METHODS: Microparticles of PLGA were prepared by static multilamination micromixer technology [1]. The development of the coating layers was carried out by incubating of particle suspensions with optimized concentrations of cationic polymers or nucleic acids under mixing. Particle size was determined by light scattering. Efficiency and stability of the coatings were analysed by zeta-potential measurements. The amount of the coating polymer in the particle composition was determined by fluorescent labelling using fluorescamine as described previously [2]. Nucleic acid loading was analysed by using PicoGreen/RiboGreen dyes and gel electrophoresis. Surface characteristics and particle morphology were studied by atomic force microscopy.

RESULTS: PLGA microparticles were in the size range of 1-10 μ m, with negative surface charge and spherical shape. Incubation of the particles with chitosan or protamine led to an inversion of the surface charge to positive values, showing efficient surface modification of the particles. The quantification of the cationic polymers on the particles also indicated the development of a thin coating layer. Nucleic acid association led again to a significant reduction of the surface charge to negative values. DNA and RNA association

efficiencies were dependent on the type of the cationic coating, being protamine more efficient in associating high amounts nucleic acids to the particles surface (over 90% association efficiency). Results of atomic force microscopy analysis further confirmed the above findings, showing the development of a continuous granular coating layer on the particles surface upon their incubation with the cationic polymers. Moreover, we could observe the deposition of an additional mesh-like network upon the incubation of the coated particles with nucleic acids (Fig. 1.), being the network density dependent on the type of the underlying cationic layer (chitosan vs protamine).



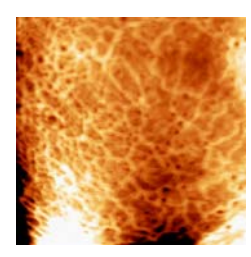


Fig. 1: Chitosan-coated PLGA microparticles without/with associated plasmid DNA.

The addition of a further cationic layer converted again the zeta potentials to highly positive values and the surface morphology to a continuous granular pattern. Analogously, the stable deposition of subsequent layers consisting of either pDNA, mRNA or immunostimulatory CpG or poly(I:C) sequences, alternating with cationic polymers, could also be confirmed.

DISCUSSION & CONCLUSIONS: Surface modification of biodegradable PLGA microparticles with cationic polymers allows the efficient surface assembly of nucleic acids. This technique provides a possibility for the development of stable multilayer compositions for increased DNA/RNA loading, and for the combination of antigen encoding and adjuvant nucleic acids within the same delivery system.

REFERENCES: ¹ S. Freitas, H. Merkle and B. Gander. (2005) *J Control Release* **102**:313-332. ² S. Fischer, C. Foerg, S. Ellenberger et. al. (2006) *J Control Release* **111**:135-144.

Surface active poly(ethylene glycol) (PEG) catechol derivatives on metal oxide surfaces: influence of pH, pK_a and isoelectric point on adsorption kinetics and adlayer stability

B.Malisova¹, K.Gademann², S.Zürcher^{1,3}, S.Tosatti^{1,3}, M.Textor¹

¹ Laboratory of Surface Science and Technology,

Department of Materials, ETH Zürich Switzerland

² Chemical Synthesis Laboratory, Institute of Chemistry and Chemical Engineering, EPF Lausanne, Switzerland

³ SurfaceSolutionS GmbH, Zürich

INTRODUCTION: A commonly used method to prevent surfaces from non-specific adsorption of proteins relies on chemical immobilization of poly(ethylene glycol) (PEG) e.g. bound via thiol or silane [1]. However most of the proposed techniques showed limitations in terms of substrate choice due to very specific molecule-surface interactions. Within this project a new binding chemistry for PEG based on catechol derivatives was used [2]. Catecholic hydroxy groups presented in these polymers have the special property of being much more acidic than other hydroxy groups e.g. present in alcohols or sugars and therefore are already dissociated at physiological pH [3]. The reactivity of such deprotonated molecules towards metal oxides and other materials is supposed to be higher than the reactivity of protonated molecules. The aim of this work is to achieve a deeper insight and a better understanding of the binding mechanism of different functionalized catechol derivatives on selected metal oxides. For this purpose the influence on the adsorption and stability of the polymers of parameters such as assembling solution pH or acidity (pKa) of the catechol protons in relationship with the isoelectric point (IEP) of the substrates, was investigated.

METHODS: The molecules 1-5 (fig. 1) were investigated in terms of adsorption behavior and subsequent resistance against serum adsorption, using variable angle spectroscopic ellipsometry (VASE) and X-ray photoelectron spectroscopy (XPS). For polymer adsorption standard conditions were defined as follows: 0.1 mg/ml of polymer dissolved in cloud-point buffer, adsorption at 50°C for 4 hours. Adsorptions were done on TiO₂ resp. Nb₂O₅ and SiO₂ coated silicon wafers.

These results will provide the basis for a novel surface modification platform, which can be used

for the functionalization of biomaterials and

biosensors.

RESULTS: Our results show that the charge of catechol PEG conjugates, together with the pK_a of the catechol protons and the IEP of the substrates, have an influence on polymer adsorption and stability (fig. 2).

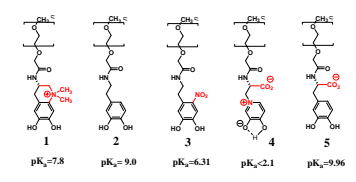


Fig. 1: PEG conjugate derivatives and the pK_a values of their hydroxy groups.

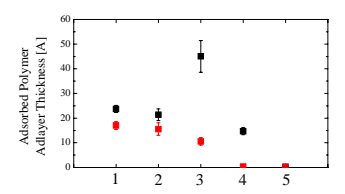


Fig. 2: Adlayer thickness of compounds 1-5 directly after adsorption close to cloud point conditions [4h, 50° C, 1.2 M ionic strength, pH=6.0] (black squares) and after immersion in physiological buffer solution [24 hours, RT, 0.15 M ionic strength, pH=7.4] (red squares).

DISCUSSION & CONCLUSIONS: The charge of a binding group combined with the acidity of hydroxy catechol groups effect the adsorption and stability, however it is hard to distinguish between these parameters. We will further try to characterize their contributions together with the influence of other parameters, such as pH.

REFERENCES: [1] a) J. Rundqvist, J. H. Hoh, D. B. Havilland, Langmuir 2005, 21, 2981. b) A. E. Moser, C. J. Eckhardt, Thin Solid Films 2001, 382, 202. [2] a) J. L. Dalsin, L. Lin, S. Tosatti, J. Vörös, M. Textor, P.B. Messersmith, Langmuir 2005, 21, 640. b) S. Zuercher, D. Waeckerlin, Y. Bethuel, B. Malisova, M. Textor, S. Tosatti, K. Gademann, J. Am. Chem. Soc. 2006, 128, 1064. [3] T. Ishimitsu, S. Hirose, H. Sakurai, Chemical & Pharmaceutical Bulletin 1978, 26, 74.

PEG-BASED SAMS ONTO TITANIUM OXIDE SURFACES: EFFECT OF PEG MOLECULAR WEIGHT

S.Bozzini¹, P.Petrini¹, S.Zürcher², S. Tosatti², M.C.Tanzi¹, G.Bianchi³, P.Robotti³

¹Dept. of Bioengineering, Politecnico di Milano, Italy . ²SuSoS AG, Wolfgang-Paulistrasse 10, CH-8093 Zurich, Switzerland. ³ Eurocoating Spa, via Al Dos De La Roda, 60 I-38057 Ciré-Pergine, Trento Italy.

INTRODUCTION: The deposition monomolecular adlayers based on poly(ethylene glycol) (PEG) chemistry may contribute to a strategical control of the none-specific protein adsorption. The present work aimed to study a new monomolecular PEG-based adlayer system and its protein resistance properties, by exploiting the spontaneous formation of alkane phosphate selfassembly monolayers (SAMs) on titanium oxide [1] and their capability of tailoring the surface physico-chemical properties in a relatively simple and controlled way. The effect of PEG chain lenghts (2kD and 5kD molecular weight) on the surface compositions and the protein resistance properties was also evaluated.

METHODS: Mixed SAMs of methoxy-PEGmaleimide-11-thio-undecyl-phosphate (PEGmal-S-UDPO₄) and hydroxy-dodecyl-phosphate (OH-DDPO₄) were prepared on titanium substrates (20 nm PVD on silicon wafer) and waveguides (8 nm TiO2 layer on 200 nm-thick Si_{0.25}Ti_{0.75}O₂) in order to achieve different PEG surface density, as described in [2]. The chemical composition of modified surfaces were analyzed by X-ray Photoelectron Spectroscopy (XPS) with a SAGE100 system (Specs, Berlin, Germany), by using a non monochromatized Al Ka radiation at 320 W (13 kV). SAMs thickness and protein adsorbed (20 min human incubation) were measured by a Variable Angle Spectrometric Ellipsometer (VASE) M-2000F (L.O.T. Oriel GmbH, Darmstadt, Germany). The adsorbed serum mass was quantified by Optical Spectroscopy, OWLS Waveguide Lightmode (BIOS-1 integrated optical scanner, monochromatic, polarized beam Microvaccum Ltd., Budapest, Hungary)

RESULTS: The PEG presence can be revealed by XPS C-O/C-C intensity ratio: the ratio increases with the mole fraction increase of PEGmal-S-UDPO4 $\chi_{PEGmal-S-UDPO4}$. The same tendency is observed for thickness values, confirming the lowest value (16 Å) for $\chi_{PEGmal-S-UDPO4}$ =0 and the highest one (30 Å) for $\chi_{PEGmal-S-UDPO4}$ =1: the same thickness values are detected for both PEG molecular weights at the same molar fractions. The

protein resistance properties are PEG surface density dependent, revealing a decrease either in term of protein adlayer than protein mass adsorbed with the mole fraction increase. The different molecular weight (2kD and 5kD) does not seems to affect the protein resistance properties at least in term of protein adlayer adsorbed on the surfaces: a similar decrease trend is observed with the two different chain lenghts.

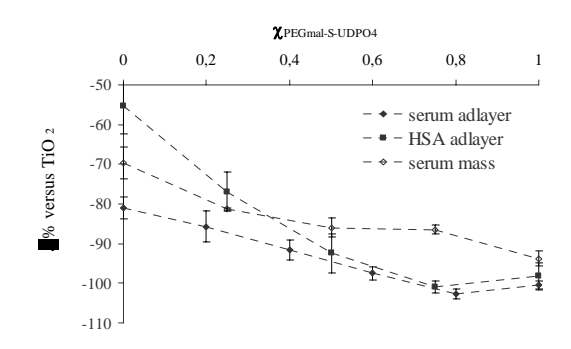


Fig. 1: Percentage variation versus TiO_2 of the human serum (\blacklozenge) and human serum albumin (\blacksquare) adlayer tichkness and of the adsorbed serum mass (\diamondsuit) at different molar fractions $\chi_{PEGmal-S-UDPO4}$.

DISCUSSION & CONCLUSIONS: PEG-based alkane phosphates have been shown to adsorb spontaneously onto titanium oxide surfaces from aqueous solution to form SAMs. The PEG surface density can be simply tailored by coadsorption with a non pegylated phosphate changing its molar fraction in solution, leading to surfaces with controllable protein resistance. Preliminary studies reveal the surface properties, SAM composition and protein resistance, can be retained by using either 2kD than 5kD PEG molecular weight.

REFERENCES: ¹ S. Tosatti et al., *Langmuir* 2002, 18, 3537-3548]. ² S. Bozzini, "Organic functionalisation of titanium oxides surfaces", PhD Thesis Politecnico di Milano 2005.

Non-fouling hydrogel coatings on polymer substrates

N.M.Graf¹, J.Möller², V.Vogel², A.Mühlebach³, W.Rutsch³, M.Textor¹, R.Konradi¹

¹ Laboratory of Surface Science and Technology and ² Laboratory for Biologically Oriented Materials, ETH Zürich, Switzerland. ³ Ciba Specialty Chemicals, Switzerland.

INTRODUCTION: Bacterial contamination can cause severe problems such as patient infection in clinical environments or food spoilage in food industry. An effective method to render surfaces bacteria-repellent is to graft polyethylene glycol (PEG) onto them¹. Most studies have dealt with the PEGylation of metal oxide or noble metal surfaces by rather thin adlayers². We present a facile approach to render polymeric substrates biopassive by covalently grafting PEG-hydrogels. The adlayer thickness can be readily adjusted via process parameters.

METHODS: We aim to graft polymeric foils with PEG-diacrylate (PEG-DA) and simultanously crosslink the layers by UV-Illumination.

In order to work with a simple and well defined substrate, model surfaces were created as follows (Fig. 1). Silicon wafers (or glass coverslips for bacteria tests) were covered with a polystyrene (PS) layer (24 nm) by spin coating. Then, PS was activated by O₂ plasma, followed by spin coating of a mixture of PEG-DA and PEG-photoinitiator onto the activated PS. The surfaces were then exposed to UV-light and rinsed with deionized water in order to remove any unbound material.

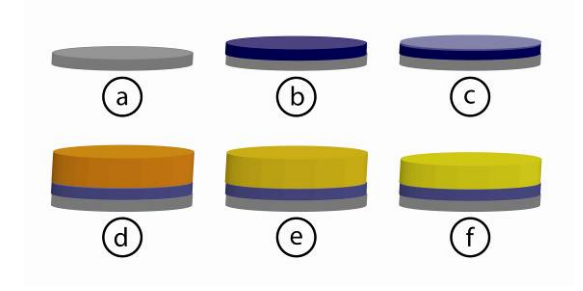


Fig. 1: Model substrates: First, a Si-wafer (a) was spin-coated with PS (b). After O₂-plasma activation (c) PEG-DA was added (d), crosslinked (e) and then rinsed with water (f).

RESULTS & DISCUSSION: Figure 2 shows the layer thickness of two samples spin coated with different solutions of PEG-DA in isopropanol. The layer thickness increased with increasing PEG-DA concentration. Additionally, the layer thickness could be varied by spin coating speed (data not shown). The layers appear very stable since the thickness is not remarkably reduced after exposure of the samples to water (10'), soap solution (20')

and ultrasonic cleaning (10' in water, data not shown).

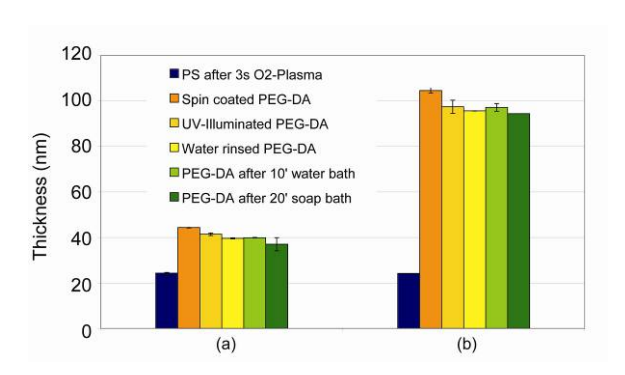


Fig. 2: The layer thickness can be adjusted by the concentration (a: 1wt%, b: 3wt%). The layers ramain stable upon stability tests.

PEG-DA hydrogel covered surfaces were exposed to a suspension of E.Coli (ELT 115) bacteria in HEPES 2 buffer (Fig. 3). Bacterial adhesion is strongly reduced after 20 minutes bacteria incubation as compared to the blank PS surface. The grooved PEG-DA surface seems to be due to the high crosslinking density.

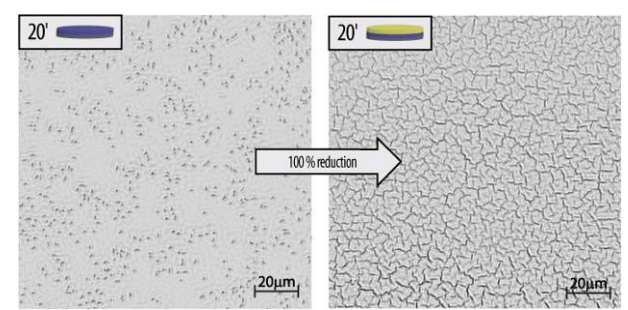


Fig. 3: Reduction of bacterial adhesion by grafting PEG-DA onto a PS surface. (a) blank PS surface, (b) with PEG-DA.

The presented model system shows that the PEG hydrogel layer thickness is readily variable by spin coating speed and concentration. The layers are stable under practically relevant conditions and strongly reduce bacterial adhesion. The next step will be to reduce the crosslinking density by mixing the PEG-diacrylate with a monoacrylate.

REFERENCES: ¹ J. M. Harris, *Plenum Press*, (1992), *ACS Washington D. C.* 489pp, ² N. D.Spencer, et al. (2000), *Journal of Physical Chemistry*, **104**, 3298 -3309

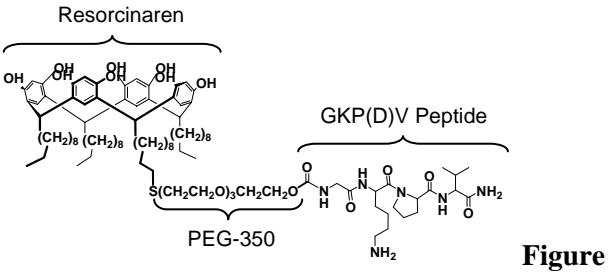
Evaluation of Anti-Inflammatory and Antimicrobial Resorcinarene-Peptides for Biomaterial Modification

M. Charnley¹, K. Fairfull-Smith², N.H. Williams², C. W. I. Douglas³, S. L. McArthur¹, J.W. Haycock¹.

¹Department of Engineering Materials, Sheffield University, U. ²Department of Chemistry, University of Sheffield, UK. ³Department of Oral Pathology, University of Sheffield, UK.

INTRODUCTION: There is an increase in the use of implantable medical devices for the repair of soft and hard tissue. Many such devices can initiate acute inflammation, or become infected when implanted, resulting in device failure. α-Melanocyte-stimulating hormone (MSH) is a potent anti-inflammatory hormone¹, which also possesses antimicrobial properties², produced in the body with very short peptide sequences that make it amenable for easy laboratory synthesis. The aim of this work is to immobilise short MSH peptides onto medical device surfaces using molecules called resorcinarenes, which are known to attach to a wide variety of material surfaces. This is being approached by synthesizing MSHresorcinarene molecules with the aim of being able to 'dip and dry' treat medical devices with an antiinflammatory and antimicrobial 'coating'.

METHODS: Surfaces were coated with two compounds, resorcinarene-PEG-OMe, without the peptide moiety, and resorcinarene-PEG-GKP(D)V in varying molar ratios (0% to 100%), and characterised using XPS.



1: Schematic diagram of the GKP(D)V peptide attached to the resorcinarene compound via a PEG-350 tether, which is then coated onto glass.

The ability of the immobilized peptide to inhibit inflammatory signaling was determined by culturing RN22 Schwann cells upon the treated surfaces and measuring NF-κB/p65 inflammatory transcription factor activation.

RESULTS: *Surface Characterisation*; XPS indicated that the GKP(D)V peptide was immobilized onto the glass surface.

NF-κB Activation; Unstimulated cells exhibited predominately cytoplasmic labelling stimulation of the cells with LPS (100 ngml⁻¹) caused rapid translocation, and therefore activation, of NF-κB to the nucleus. Culturing cells on resorcinarene-monoPEG-OMe coated surfaces had no effect on NF-κB activity. In contrast cells culturing on resorcinarene-monoPEG-GKP(D)V coated surfaces inhibited stimulated NF-κB activation by up to 28.2±4.0% (p<0.001). Levels of inhibition were comparable to those observed when cells were co-stimulated with GKP(D)V at 10⁻⁹ M and LPS (38.9±3.3%; p<0.001) (Fig 2).

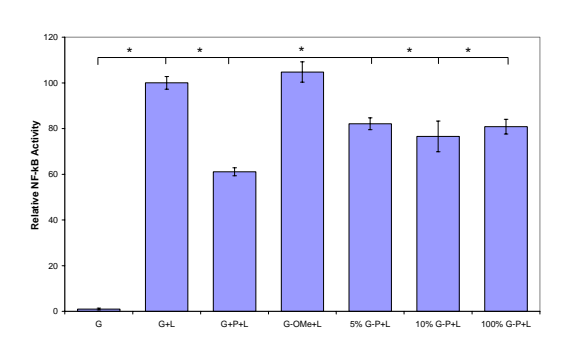


Figure 2: Immobilised GKP(D)V inhibits NF-κB activity. G, glass; L, LPS; P, GKP(D)V peptide; G-OMe, resorcinarene-monoPEG-OMe; G-P, resorcinarene-monoPEG-GKP(D)V; n=3, *p≤0.05

CONCLUSIONS: Results indicate the GKP(D)V peptide has been immobilised onto glass using resorcinarene chemistry and retains anti-inflammatory properties. Future work involves the investigation of the antimicrobial properties of KP(D)V peptide, and related melanocortin peptides, in solution and when immobilised.

REFERENCES: ¹R. P. Hill, S. MacNeil, and J.W. Haycock, (2006) *Peptides* **27**; 421-430. ²M. Cutuli, S. Cristiani, J. M. Lipton, A. Catania, (2000) *J. Leukoc Biol* **67**; 233-239.

ACKNOWLEDGEMENTS: We would like to thank the BBSRC and EPSRC for funding this work.

Combining Devices and Drugs by Synthetic Natural Product Hybrids

S. Bonazzi¹, J.-Y.Wach¹, K. Gademann²*

¹Chemical Synthesis Laboratory (SB-ISIC-LSYNC), ²EPF Lausanne, Lausanne, Switzerland

INTRODUCTION: Natural products contain the evolutionary wisdom of ages and only synthetic organic chemistry can unlock their full potential. Hybridization of natural products by combining fragments with different bioactivity presents an appealing strategy to modify and to leverage given properties. Traditional approaches to natural product hybridization involve the combination of two natural pharmacophores by a covalent linker without impacting the biological activity of each fragment. Moreover, higher order hybrids can be obtained by linking several components together, either covalently or by self-assembly. In this communication, we demonstrate the preparation of quaternary natural product hybrids.

METHODS: Recently, a biomimetic linker for ultramild surface functionalization was introduced, relying on powerful catechol metal oxide interactions.² This linker has been used to render surfaces resistant to fouling,² a serious problem in many areas ranging from water technology to medicine.³

RESULTS: We have prepared through organic chemistry a series of complex ternary hybrids linking the anachelin chromophore as biomimetic linker via a PEG spacer to various biologically active natural products. In addition, these compounds were hybridized to surfaces thus generating unique quaternary hybrids (Fig. 1).

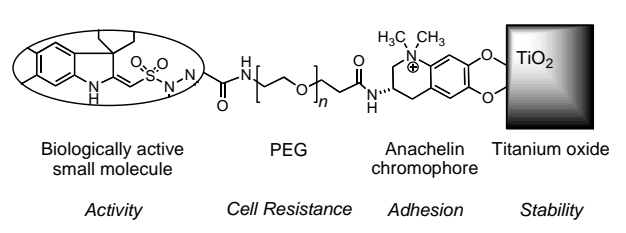


Fig. 1: Quaternary natural product hybrids linking a surface such as a metal oxide (stability) via the linker (adhesion) and a PEG spacer (providing cell resistance) to a natural product with powerful biological activity.

approach for the generation of bioactive surfaces is presented. The utilization of natural product hybrids is very promising, as distinct features of each component can be hybridized and their properties leveraged. The quaternary hybrids are thus merging properties such as stability, surface adhesion, protein/cell resistance, and pronounced biological activity for the generation of antimicrobial surfaces or antifungal surfaces. Therefore, devices and drugs can be combined through synthetic natural product hybrids.

REFERENCES: ¹ K. Gademann (2006) *Chimia* **60**:841-845. (fulltext).

- ² S. Zuercher, D. Waeckerlin, Y. Bethuel, B. Malisova, M. Textor, S. Tosatti, K. Gademann (2006) *J. Am. Chem. Soc.* **128**:1064-1065. (fulltext).
- ³ K. Gademann (2007) *Chimia* **61**:373-377. (fulltext).

Covalent Immobilization of Antibacterial Furanones via Photochemical Activation of Perfluorophenylazide

S. Al-Bataineh¹, M. Textor¹, M. Yan²

¹ ETH Zurich, Zurich, Switzerland. ² Portland State University, Portland, USA.

The Australian marine red algae Delisea pulchra produces fimbrolides, a class of compounds comprising a five-membered lactone ring and halogen substituents. They reside in vesicles on the surface of the algae and provide a defense against fouling of algal surfaces by marine organisms. Compounds of particular interest are the brominated furanones, as a number of naturally occurring halogenated furanones as well as synthetic analogues have shown interesting antimicrobial properties such as interference with the quorum sensing process in biofilm formation of many bacteria including human pathogens [1,2]. Given the often severe consequences of nosocomial medical device infections and the present lack of successful long-term preventative strategies, these compounds have attracted growing recent interest as promising antibacterial molecules for use in human health care. To ensure effectiveness, as an antibacterial coating for medical devices, for extended periods of time, they must be immobilized covalently onto a device surface; this was done via a photoactive heterobifunctional crosslinker due to its simplicity and versatility.

In this study, a silane functionalized perflourophenylazide (PFPA-silane) [3,4] is used as crosslinker to covalently immobilize furanone molecules on silicon oxide or glass substrates, Fig. 1.

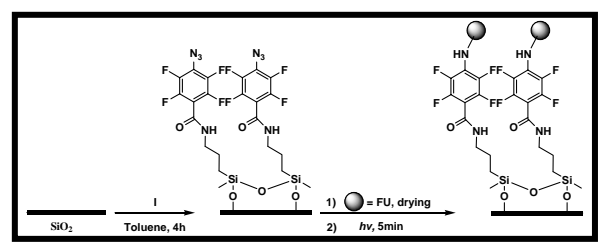


Fig. 1: Covalent immobilization of furanone molecules on PFPA-functionalized surface.

This approach is based on the photochemistry of the perflourophenylazide molecules. Upon irradiation, perflourophenylnitrenes are generated and undergo efficient C-H and/or N-H insertion reactions with the neighboring molecules. Because the insertion reaction occurs at the interface between substrate and furanone molecules only a

monolayer of furanone molecules is covalently immobilized after the un-attached molecules are removed by solvent extraction. This method is simple and easy to perform; it involves coating of the material on a photolinker followed by UV irradiation. Because the immobilization chemistry is based on C-H/N-H insertion reaction therefore. there is no need to functionalize furanone molecules to be immobilized as long as they possess C-H or N-H bonds. Additional advantage to this method is that it can be used to selectively modify desired areas using a photomask. One goal of this study was to vary the density of fursanone molecules immobilized on the surface in order to study how that reflects on the activity of these surfaces against bacterial adhesion. This was done by preparing diluted concentrations of PFPA-silane solution.

The functionalized surfaces were characterized by XPS, ellipsometry, IR and contact angles. The results showed successful surface modification and that we were able to control the density of PFPA-silane on the surface, thus immobilized furanone molecules.

REFERENCES: ¹M. Manefield, T.B. Rasmussen, M. Henzter, et al (2002) *Microbiology 148*: 1119-1127. ²R. de Nys, P. D. Steinberg, P. Willemsen, et al (1995) *Biofouling 8*: 259-271. ³J. F. W. Keana and S. X. Cia (1990) *J. Org. Chem.* 55: 3640-3647. ⁴M. Yan and J. Ren (2004) *Chem. Mater.* 16: 1627-1632.

ACKNOWLEDGEMENTS: This research was supported by Dr. h.c. Robert Mathys Foundation, Switzerland.

EFFECT OF CONCENTRATION OF ACTIVE HYDROXYL GROUPS ON THE IMMOBILIZATION OF POLY(ETYLENE GLYCOL) ONTO METALS

T. Hanawa¹, Y. Tanaka¹, H. Saito², Y. Matsuo², Y. Tsutsumi¹ & H. Doi¹

¹ Institute of Biomaterials and Bioengineering, Tokyo Medical and Dental University, Japan.

Department of Materials Science, Shibaura Institute of Technology, Japan.

number of active hydroxyl groups. A thickness of NH₂-PEG-NH₂ layer on each metal was determined by an ellipsometer (DVA-36Ls, Mizojiri Optical, Co., Ltd., Japan).

INTRODUCTION: The hydroxyl groups on metal surface oxide film play an important role in some surface modifications because they are the initiation sites for chemical reactions in the surface modification process. Previous studies reported that poly(ethylene glycol) terminated with amines at both terminals, NH2-PEG-NH2, immobilized onto titanium oxide offered several biofunctions, such as the prevention of proteins adsorption [1]. In this study, NH2-PEG-NH2 is immobilized on commercially pure titanium, cp-Ti, 316L austenitic stainless steel, SS, and cobalt-chromiummolybdenum alloy, Co-Cr-Mo, with electrodeposition. The concentrations of active hydroxyl groups of cp-Ti, SS, and Co-Cr-Mo were determined with a zinc-complex substitution technique and their effects on the immobilization of NH₂-PEG-NH₂ onto the metals investigated.

METHODS: The concentrations of active hydroxyl groups were determined with the following zinc-complex substitution technique. An ammonium chloride solution (4.0 mol L^{-1}) was mixed with a zinc chloride (0.4 mol L^{-1}) solution. Specimens were immersed in 30 mL of the resultant solution for 0.3 ks. During immersion, one zinc complex was formed with two hydroxyl groups, as shown in Fig. 1. Then, the specimens were immersed in 2.5 mol L^{-1} nitric acid for 0.6 ks to release zinc ions into the nitric acid solution (Figure 1).

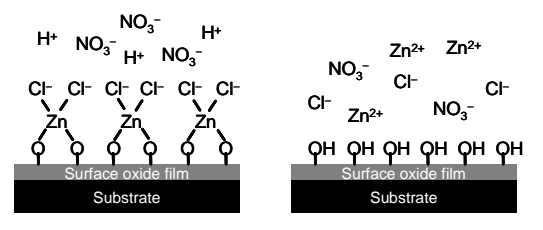


Fig. 1: Formation (left) and decomposition (right) of the zinc complex by the reaction of active hydroxyl groups (OH).

The concentrations of zinc ions per unit surface area of each metal, $N_{\rm Zn}$ were determined using an inductively coupled plasma atomic emission spectrometer (ICP-AES: PS-3000UV, Leeman Labs, Inc., Lowell, MA). Twice $N_{\rm Zn}$ equals the

RESULTS & DISCUSSION: The concentrations of the active hydroxyl groups in Co-Cr-Mo were significantly larger than those in cp-Ti and SS, but no difference was observed between cp-Ti and SS. The thicknesses of the NH₂-PEG-NH₂ layer immobilized with electrodeposition were the largest in Co-Cr-Mo, as shown Figure 2. This relationship corresponds to that of the active hydroxyl groups on the surface oxide film. These results revealed that the active hydroxyl groups played an important role in the electrodeposition of NH₂-PEG-NH₂, while they did not in the immersion. In case of immersion, the thickness of PEG on the SS oxide film was significantly larger than those on cp-Ti and Co-Cr-Mo in Fig. 2. The thickness of PEG immobilized on each oxide film with immersion is in inverse proportion to the relative permittivity of each oxide film.

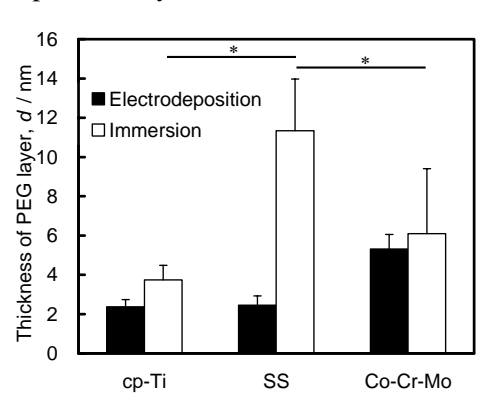


Fig. 2: Thickness of the NH_2 -PEG- NH_2 layer on cp-Ti, SS, and Co-Cr-Mo. The bars represent statistically significant differences ($p \le 0.05$).

CONCLUSIONS: The relative permittivity of surface oxides was a predominant factor for the immobilization of PEG with immersion, while the concentrations of the active hydroxyl groups were the predominant factor in the immobilization with electrodeposition.

REFERENCES: ¹ Y. Tanaka, H. Doi, Y. Iwasaki, S. Hiromoto, T. Yoneyama, K. Asami, H. Imai and T. Hanawa (2007) *Mater Sci Eng C* **27**: 206-12.

Anti-microbial coatings for urological applications

A. Franken, E. E. M. van den Bosch, O. Crespo-Biel, J. A. Loontjens and A. A. Dias

Performance Materials Chemistry and Technology, DSM Research, P.O. Box 18, 6160 MD, Geleen, The Netherlands

Keywords: urinary tract infections, Foley catheter, lubricity, silver

The US Centre of Disease Control has attributed nosocomial infections as the fourth leading cause of deaths after heart disease, cancer and stroke. 80% of these infections are due to indwelling medical devices such as catheters and cost the health care industry approximately \$3000 / infection or an average of 1.2 billion a year (US data, 2002). As a result, preventive measures have been attempted, including the application of antimicrobial coatings to catheters. This approach has been shown to be more effective than the systemically administered antibiotics. Antimicrobial catheters have been found to reduce blood stream infections (central venous catheters) by 15 times and catheter associated urinary tract infections (CAUTI; urological catheters) by 3 times (Frost & Sullivan, 2003). CAUTI account for 40% of the device related nosocomial infections and Foley catheters account for 85% of them. While there are various coatings developed or in development, there remains a need for antimicrobial coatings for Foley catheters.

The bacterial infection of catheters was studied on two levels; the implant-anatomical level and the surface-biomaterial level. This resulted in the development of a lubricious hydrophilic silver coating. Lubricious coatings and hydrophilic coatings both have shown to reduce the damage to the mucosal lining caused by the insertion/removal of urological catheters (Vaidyanathan et al., 1994; Vapnek et al., 2003). Mucosal lining damage is recognised as an initial nidus of infection. Moreover, a lubricious hydrophilic coating is suggested to reduce the adhesion of bacteria due to the surface bound water that contributes to the smooth and slippery surface. Silver is the antimicrobial compound of choice, due to its multimodal action (Holt & Bard, 2005; Sondi & Salopek-Sondi, 2004). Silver ions exhibit biocidal activity toward the broad spectrum of bacteria and fungi found in CAUTI (Zachariadis et al., 2004). Other advantages are its low toxicity to mammalian cells (Gosheger et al., 2004) and in contrast with antibiotics, silver does not easily provoke microbial resistance (Percival et al., 2005).

A dual coating consisting of a primer layer and a topcoat is developed. Both layers are applied to the catheter tubing by a dip coating procedure involving UV radiation curing. The topcoat is PVP-based and contains a cross-linker and silver. Friction tests show that this coating is lubricious, exhibits good wear resistance and is characterised by a dry-out time of about 10 min. Moreover, the coating is uniform and the coating process is reproducible as revealed by optical microscopy. These properties are not found with the current silver coated Foley catheters that are commercially available. Preliminary results of anti-microbial activity tests under various conditions confirm that the DSM lubricious silver coating reduces the adhesion of bacteria and is bacteriocidal.

- Frost, & Sullivan (2003). US Antimicrobial Devices Market, A433-54.
- Gosheger, G., Hardes, J., Ahrens, H., Streitburger, A., Buerger, H., Erren, M., Gunsel, A., Kemper, F.H., Winkelmann, W., & von Eiff, C. (2004). *Biomaterials*, 25, 5547-5556.
- Holt, K.B, & Bard, A.J. (2005). *Biochemistry*, 44, 13214-13223.
- Percival, S.L., Bowler, P.G., & Russell, D. (2005). *J. Hosp. Infect.*, 60, 1-7.
- Sondi, I., & Salopek-Sondi, B. (2004). *J. Colloid Interface Sci.*, 275, 177-182.
- Vaidyanathan, S., Soni, B.M., Dundas, S., & Krishnan, K.R. (1994). *Paraplegia*, 32, 493-500.
- Vapnek, J.M., Maynard, F.M., & Kim, J. (2003). *J. Urol.*, 169, 994-998.
- Zachariadis, C.P., Hadjikakou, S.K., Hadjiliadis, N., Skoulika, S., Michaelides, A., Balzarini, J., & de Clercq, E. (2004). *Eur. J. Inorg. Chem.*, 7, 1420-1426.

Poly(2-methyl-2-oxazoline): Protein-like Polymer for the Fabrication of Functional Non-Fouling Surface Coatings

R. Konradi, B. Pidhatika, Q. Li, M. Textor

Laboratory for Surface Science and Technology, Department of Materials, ETH Zürich, Switzerland.

INTRODUCTION: We are investigating poly(2methyl-2-oxazoline) (PMOXA) as an alternative polymer to poly(ethylene glycol) (PEG) for the fabrication of functional non-fouling surface coatings. Like PEG this polymer is nonionic and hydrophilic having a biomimetic 'protein-like' structure. Unlike PEG, however, it does not comprise of any ether bond that is prone to autoxidation. Moreover, functional initiators, terminal groups and monomers can be readily included in the synthesis of PMOXA making it much more versatile for the construction of sophisticated functional surface coatings. We designed comb copolymers consisting of a poly(Llysine) backbone grafted with PEG or PMOXA side-chains (PLL-g-PEG or PLL-g-PMOXA) and are currently striving to equip them with functions in order to biologically active specifically control the interfacial biological response on a bioinert polymeric support (Fig. 1).

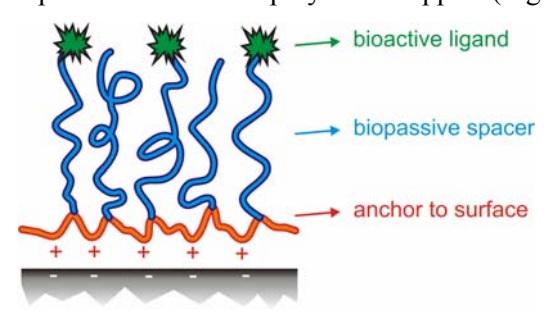
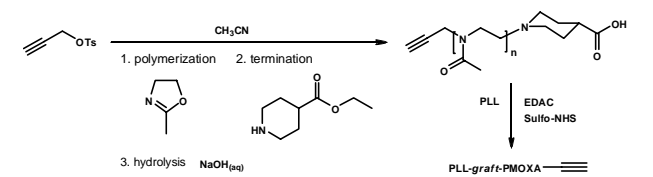


Fig. 1: Schematic illustration of biofunctional PLL-g-PMOXA self-assembled onto a negatively charged substrate

METHODS: α ,w-heterobifunctional PMOXA was synthesized by initiating the living cationic polymerization of 2-methyl-2-oxazoline with an alkynyl-functional initiator and terminating with a carboxy-functional piperidine derivative. The w-carboxy group was coupled to the PLL backbone using water soluble carbodiimide chemistry. The propargyl α -function will allow for the copper(I)-catalyzed cycloaddition of azide-functionalized biological moieties via 'click chemistry' (Scheme 1).



Scheme 1: Synthesis of alkynyl-functional PLL-g-PMOXA

RESULTS: Surfaces coated with unfunctional PLL-*g*-PMOXA reduced full human serum protein adsorption quantitatively to the same level as for PLL-*g*-PEG (< 2 ng/cm² as determined by optical waveguide lightmode spectroscopy; data not shown). First alkynyl-functional PMOXA and PLL-*g*-PMOXA have been synthesized and characterized by NMR and Maldi-Tof MS. The exact absolute mass and a low PDI of the PMOXA sidechains were confirmed by Maldi-Tof MS and successful grafting was corroborated by NMR (Fig 2).

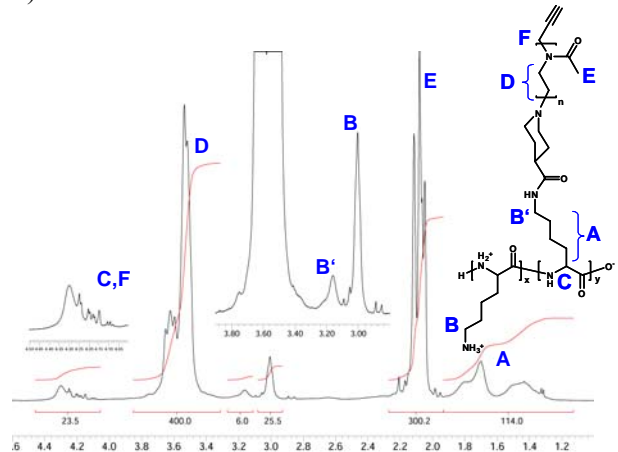


Fig. 2:¹H- NMR spectra of alkynyl-functional PLL-g-PMOXA

DISCUSSION & CONCLUSIONS: Based on the highly bioinert properties of PLL-g-PMOXA modified surfaces we have now incorporated terminal bio-conjugation sites for the attachment of various biological cues. These comb copolymers will next be tested for protein resistance and functionalized with bioactive ligands.

ACKNOWLEDGEMENTS: Financial support by SNSF (Swiss National Science Foundation) is gratefully acknowledged.

Biofilm formation on mcl-polyhydroxyalkanoates: relevance of purity grade and pre-conditioning

Mauclaire L., Bünger J.-D., Lübben J., and M. Zinn

Swiss Federal Laboratories of Material Testing and Research, St. Gallen, Switzerland

INTRODUCTION: Polyhydroxyalkanoates (PHAs) are a class of polyesters produced as reserve materials by many archae and eubacteria. Only the production of PHA in microorganisms guarantees the complete stereospecificity, which is essential for biodegradability and biocompatibility. PHAs are suitable for a broad range of applications in medicine and industry. Research on elastomeric 3-hydroxyalkanoate mcl-PHAs (containing monomers ranging from C6 to C14) has been intensified the last years. Poly-(4hydroxybutyrate) has been approved by FDA for applications as suture material. A major task in the downstream processing is the avoidance of pyrogenic impurites. The use of an optimized procedure leads to production of mcl-PHA which complies with the endotoxin requirements of the FDA for biomedical applications such as implants and drug delivery systems¹ (Furrer et al., 2007). In addition to the presence of impurities, the bacterial antifouling properties of mcl-PHAs is a major issue for its use in medicine because infection is the most common cause of biomaterial implant failure, the most common infecting organisms being Staphylococcus aureus and Escherichia coli.

METHODS: This study was designed to provide an in vitro evaluation of the potential biofilm development on mcl-PHAs in an environment mimicking physiologic conditions. We compare the development of S. aureus and E. coli PHL628 biofilms on two mcl-PHAs (C8 and C11). evaluating the impact of purity grade (yellow and for low- and high- purity grade, respectively). Microarchitecture of the coating was investigated using atomic force microscopy (AFM). The degree of hydrophobicity and zetapotential were used to characterize surface properties. When the mcl-PHAs are place in the body, the host of molecules interact with the to form a conditioning film. surface discriminate the influence of impurities versus conditioning film, the mcl-PHAs were tested in presence and absence of human plasma.

RESULTS & DISCUSSION: Pre-conditioning with human plasma increased the hydrophilicity of the material (e.g. contact angle $93^{\circ} \pm 3^{\circ}$ and $68^{\circ} \pm 2^{\circ}$ for pure C8 in absence and presence of human

plasma, respectively). Under all tested conditions, E. coli was always a better biofilm former than S. aureus. AFM observations of the two bacterial species revealed that their stiffness were quite similar but their adhesion forces differed by one order of magnitude. Figure 1 shows that the degree of purity of mcl-PHAs had a significant impact on E. coli biofilm growth depending on media composition. In absence of human plasma, the purification procedure had a significant influence in case of both polymers, the purest ones showing the most antifouling property. However, the beneficial effect of purification grade disappeared when coatings were conditioned with human plasma. Furthermore, the conditioning with human plasma inhibited biofilm formation especially for S. aureus (data not shown). The antifouling activity of plasma conditioning film was probably due to the pattern and conformation of proteins adsorbed onto the material surface potentially altering interaction with bacterial surface.

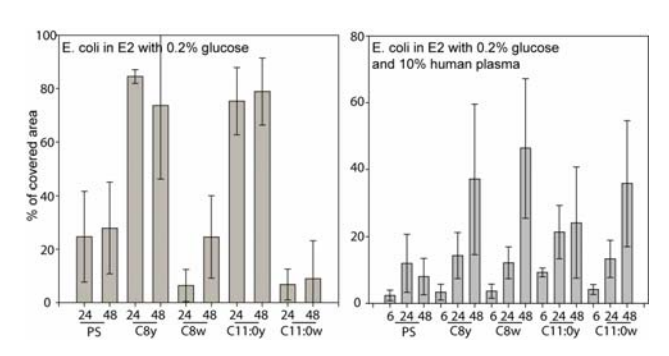


Fig. 1: Percentage of surface covered by E. coli biofilms at 6, 24 and 48 hours for the different media and different coated surfaces. PS (polystyrene), y (yellow), w (white). Average and standard deviation (n=3 without human plasma, n=5 in presence of human plasma). Percentage of covered area was evaluated by epifluorescent microscopy and automated image analysis

CONCLUSIONS: Purified mcl-PHAs did not enhanced biofilm formation compared to polystyrene controls. This result is encouraging in the perspective of developing antifouling biopolymer by covalently linking antifouling agent to mcl-PHAs.

REFERENCES: ¹ Furrer P. et al. (2007) J Chromatography **1143**: 199-206.

ACKNOWLEDGEMENTS: This research was granted by ESA-MAP 15200/01/NL/SH.